

UNCLASSIFIED

AD NUMBER

AD366003

CLASSIFICATION CHANGES

TO: unclassified

FROM: confidential

LIMITATION CHANGES

TO:
Approved for public release, distribution unlimited

FROM:
Distribution authorized to DoD only; Test and Evaluation; 30 NOV 1955. Other requests shall be referred to Army Ordnance Missile Command, Redstone Arsenal, AL.

AUTHORITY

USAMC [USAMICOM] ltr, 26 Mar 1981; USAMC [USAMICOM] ltr, 26 Mar 1981

THIS PAGE IS UNCLASSIFIED

UNCLASSIFIED

AD NUMBER
AD366003
CLASSIFICATION CHANGES
TO
confidential
FROM
secret
AUTHORITY
30 Nov 1967, DoDD 5200.10

THIS PAGE IS UNCLASSIFIED

AD- 308003

SECURITY REMARKING REQUIREMENTS

DDO 5200.1-R, DEC 78

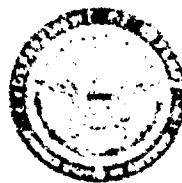
REVIEW ON 30 NOV 75

UNCLASSIFIED

AD 366003

CLASSIFICATION CHANGED
TO: UNCLASSIFIED
FROM CONFIDENTIAL
AUTHORITY: USAMC

1 Tr, 26 March 81



UNCLASSIFIED

THIS REPORT HAS BEEN DELIMITED
AND CLEARED FOR PUBLIC RELEASE
UNDER DOD DIRECTIVE 5200.20 AND
NO RESTRICTIONS ARE IMPOSED UPON
ITS USE AND DISCLOSURE.

DISTRIBUTION STATEMENT A

APPROVED FOR PUBLIC RELEASE;
DISTRIBUTION UNLIMITED.

SECURITY

MARKING

The classified or limited status of this report applies to each page, unless otherwise marked.

Separate page printouts MUST be marked accordingly.

THIS DOCUMENT CONTAINS INFORMATION AFFECTING THE NATIONAL DEFENSE OF THE UNITED STATES WITHIN THE MEANING OF THE ESPIONAGE LAWS, TITLE 18, U.S.C., SECTIONS 793 AND 794. THE TRANSMISSION OR THE REVELATION OF ITS CONTENTS IN ANY MANNER TO AN UNAUTHORIZED PERSON IS PROHIBITED BY LAW.

NOTICE: When government or other drawings, specifications or other data are used for any purpose other than in connection with a definitely related government procurement operation, the U. S. Government thereby incurs no responsibility, nor any obligation whatsoever; and the fact that the Government may have formulated, furnished, or in any way supplied the said drawings, specifications, or other data is not to be regarded by implication or otherwise as in any manner licensing the holder or any other person or corporation, or conveying any rights or permission to manufacture, use or sell any patented invention that may in any way be related thereto.

PLATO

ANTI-MISSILE MISSILE PROGRAM XSAM-19

PHASE TWO QUARTERLY REPORT NO. 8

REPORTING PERIOD: JULY 1 - SEPTEMBER 30, 1955

ARMY ORDNANCE CONTRACT DA 30-069-ORD-1166

This document contains information affecting the national defense of the United States within the meaning of the Espionage Laws, Title 18, U.S.C., Sections 793 and 794. Its transmission or the revelation of its contents in any manner to an unauthorized person is prohibited by law.

November 30, 1955

Approved

Edwin D. Schriber

Manager

SYLVANIA ELECTRIC PRODUCTS INC.
MISSILE SYSTEMS LABORATORY
WALTHAM, MASSACHUSETTS

SECRET

57AA

40128

AD 366003

CONFIDENTIAL

TABLE OF CONTENTS

SECTION		PAGE NO.
I.	OBJECTIVE	1
II.	SUMMARY	3
III.	EVALUATION STUDIES	7
	3.1 System Optimization	7
	3.1.1 The Radius of Ground Damage From Enemy Warhead Burst	8
	3.1.2 The Interceptor Midcourse Flight- Time Characteristics	8
	3.1.3 Total Time of Flight Available.	13
	3.1.4 Volumetric Coverage of the Acquisition Radar	18
	3.1.5 The Intercept-Point Prediction Accuracy at Launch.	22
	3.1.6 Conclusions	26
	3.2 System Effectiveness	29
	3.2.1 Counter-Battery Fire	29
	3.2.1.1 ESTIMATION OF LAUNCH SITE.	29
	3.2.1.2 LAUNCH SITE COUNTERMEASURES.	32
	3.2.2 Salvo Vs. Ripple Fire	32
	3.2.3 Intercept Altitude.	36
	3.2.4 System Vulnerability	39
	3.2.4.1 POSSIBILITY OF ENEMY ATTACK ON PLATO	39
	3.2.4.2 ATTACK BY SHORT RANGE MISSILES	39
	3.2.4.3 ATOMIC WEAPONS ATTACK.	40
	3.2.4.3 ATTACK BY LOW-FLYING AIRCRAFT.	41
	3.2.5 Nature of Ground Installations	41
	3.2.5.1 INTRODUCTION	41
	3.2.5.2 TACTICAL UNIT SIZE	41
	3.2.5.3 TACTICAL UNIT PROXIMITY	42
	3.2.5.4 MODEL TACTICAL AREA.	42
	3.2.5.5 DEFENSE OF CITIES	48

CONFIDENTIAL

57AA

40128

CONFIDENTIAL

TABLE OF CONTENTS (Cont)

SECTION	PAGE NO.
3.2.6 Technique of Enemy Attack.	53
3.2.6.1 ENEMY TACTICS	53
3.2.6.2 PROBABILITY OF DEFENSE.	57
3.2.6.3 FUTURE WORK	58
3.2.7 Available Warning Time for Passive Defense.	58
IV. ENGINEERING STUDIES	63
4.1 Acquisition Radar	63
4.1.1 General	63
4.1.2 Radar Parameters and System Optimization	63
4.1.2.1 PRESENT POSITION MEASUREMENT ACCURACY.	64
4.1.2.2 ERRORS IN RADAR ANGLE MEASURE- MENT DUE TO ERRORS IN BEAM SELECTION	64
4.1.2.3 COORDINATE TRANSFORMATION ERRORS	68
4.1.2.4 THE RADAR SCAN INTERVAL (T_s). . .	68
4.1.2.5 THE MAXIMUM RANGE OF DETECTION (r_0)	68
4.1.2.6 RADAR LOCATION AND VOLUMETRIC COVERAGE.	73
4.1.2.7 BLENDING OF RADAR DATA.	73
4.1.3 Engineering Studies.	75
4.1.3.1 TARGET FLUCTUATION.	75
4.1.3.2 SURVEY OF RF POWER SOURCES. . . .	76
4.1.3.3 ANTENNA MECHANICAL DESIGN STUDY	80
4.2 Precision Tracking Radar.	83
4.2.1 General.	83
4.2.2 Tracking Radar Performance and System Optimization	83

CONFIDENTIAL

TABLE OF CONTENTS (Cont)

SECTION	PAGE NO.
4.2.3 Engineering Studies.	85
4.2.3.1 PENCIL BEAM TRACKER MECHANICAL STUDIES.	85
4.2.3.2 ANALYSIS OF VARIOUS TRIANGULA- TION SYSTEMS.	88
4.2.4 Countermeasures.	89
4.3 The Track Initiation Computer and the Prediction Computer.	91
4.3.1 Track Initiation	91
4.3.2 Extraneous Alarms.	96
4.3.2.1 ALARMS TYPICAL OF THOSE HANDLED BY THE ACQUISITION RADAR.	96
4.3.2.2 ALARMS TYPICAL OF THOSE HANDLED BY THE TRACK INITIATION COMPUTER.	97
4.3.3 The Prediction Computer.	97
4.3.3.1 THE TIMING CYCLE.	98
4.3.3.2 INFORMATION FLOW.	99
4.3.3.3 MATHEMATICAL PROCEDURE FOR THE TRAJECTORY FITTING PROCESS.	103
4.4 Guidance Studies: Extension to Three Dimensions.	109
4.4.1 The Midcourse Guidance System.	111
4.4.1.1 PROGRAMMED PATH COEFFICIENT COMPUTER.	113
4.4.1.2 ERROR COMMAND COMPUTER.	113
4.4.1.3 PROGRAMMED PATH CURVATURE COMPUTER.	120
4.4.1.4 VELOCITY VECTOR COMPUTER.	121
4.4.1.5 PROGRAMMED GAINS.	121
4.4.1.6 DIGITAL STABILIZERS	121
4.4.1.7 COORDINATE TRANSFORM AND ORIENTATION COMPUTER.	122
4.4.1.8 TIME-TO-GO CLOCK.	122

CONFIDENTIAL

TABLE OF CONTENTS (Cont)

SECTION	PAGE NO.
4.4.2 The Terminal Guidance System.	122
4.4.3 Discussion on Transition From Midcourse to Terminal Guidance.	127
4.5 Interceptor.	127
4.5.1 Interceptor Performance Optimization.	127
4.5.2 Aerodynamics.	139
4.5.2.1 TRAJECTORY STUDIES	139
4.5.2.2 AERODYNAMIC HEATING.	141
4.5.2.3 CONTROL SURFACE EVALUATION	142
4.5.2.4 LAUNCH PHASE AERODYNAMIC COEFFICIENTS	145
4.5.3 Dynamics.	146
4.5.3.1 AUTOPILOT	151
4.5.3.2 LAUNCH PHASE	156
4.5.4 Design.	158
4.5.5 Structures.	160
4.5.6 Interceptor Reference System.	161
4.5.6.1 TYPES OF REFERENCE SYSTEM.	163
4.5.6.2 SYSTEM PERFORMANCE DESCRIPTION	164
4.5.6.3 CONCLUSIONS.	167
4.5.7 Command System.	167
4.5.7.1 SYSTEM ASPECTS	167
4.5.7.2 PERFORMANCE REQUIREMENTS	169
4.6 Ground Communications Network.	169
4.6.1 System Aspects.	170
4.6.1.1 GROUPING OF GROUND EQUIPMENT	170
4.6.1.2 ANTENNAS	172
4.6.1.3 PROPAGATION.	173
4.6.1.4 DATA ENCODING.	173
4.6.2 Performance Requirements.	173

CONFIDENTIAL

TABLE OF CONTENTS (Cont)

APPENDICES		PAGE NO.
I	STATEMENT OF WORK.	175
II	BIOGRAPHICAL SKETCHES OF TECHNICAL PERSONNEL . . .	179
III	CONFERENCES	185
IV	LIST OF PLATO INTERIM TECHNICAL REPORTS.	187
V	LIST OF SYMBOLS	191
VI	INTERCEPTOR TURNS.	193
VII	EVALUATION OF DISTANCE AND VELOCITY IN HORIZONTAL PORTIONS OF FLIGHT.	199
VIII	DERIVATIONS OF VELOCITY RELATIONSHIPS DURING INCLINED STRAIGHT FLIGHT	203

CONFIDENTIAL

SECRET

SECTION I

OBJECTIVE

The objective of Phase I of Project PLATO was to estimate the characteristics of ballistic missiles likely to be used by an enemy in the event of war and to propose a guided anti-missile missile system or other countermeasure, making full use of the experience of previous efforts in this direction. This work was completed April, 1955, and is described in the PLATO Phase I Final Report.

The objective of Phase II of Project PLATO is to refine and optimize the proposed design of the guided anti-missile system and to prepare a program that will lead to the design of a prototype system.

The complete statement of work appears in Appendix I.

SECRET

1

SECRET

SECTION II

SUMMARY

The factors which determine the defended area have been identified and quantitative inter-relationships between some of these parameters and the defended area have been worked out. This information is being developed in the form of equations and curves which will be used to evaluate the effects of varying the system design and then in determining the relationship between cost and the defended area. It has been determined that the high elevation angle enemy trajectories place the severest restrictions on the distance which can be defended behind the launch site and that the low angle trajectories limit the defense in the forward direction. Equations relating the limits of the defended area to the geometry of the radar coverages and equations relating the defended area to interceptor midcourse flight capability and the intercept point prediction accuracy at the time of launching have been developed. Partial numerical results have been worked out. Work is in progress on obtaining relationships between the defended area and the radar tracking accuracy and missile flight capability during the terminal phase of interception. Since changes in system design may cause a change in the factor which limits the defended area, it will not be possible to specify defense envelopes until this work is completed.

Equations describing survival probability as a function of raid size, system capacity and system reliability have been developed. The results of these studies will be combined with the system optimization studies described above to obtain survival probability - cost curves.

Although it appears that it will be possible to design the system to obtain a single shot kill probability close to unity, it may not be possible to obtain such a high probability of reliable operation. It may, therefore, be necessary to fire more than one interceptor missile to obtain a near unity engagement kill probability. If these multiple defensive missiles are used in ripple fire, it will be necessary to have a spacing which will prevent the detonation of the first warhead from incapacitating the later missiles. It is estimated that this spacing between interceptors would have to be at least 5,000 ft. Since only one of these spaced interceptors can be fired at the optimum time, it is apparent that the effectiveness of the early and late missiles may be somewhat reduced; the early interceptors tending to meet the target at very high altitude where their maneuverability is inadequate and the late interceptors allowing the target to get too near the defended installation. By sacrificing defended area, the kill probabilities of all of these interceptors can be kept close to unity. On the other hand if the multiple defensive missiles are fired to arrive at the target simultaneously, it will be necessary to have all

SECRET

of them within lethal distance of the target at the same time and to fire the warheads essentially simultaneously; otherwise the first interceptor to explode will destroy the others. These conditions require that the interceptors arrive at the target within about 0.1 sec. of each other and that the warheads be detonated with a timing accuracy of the order of one microsecond. It is doubtful that either condition can be met. However, since the causes of low single shot kill probability are likely to be missile equipment failure and inability of the interceptor to close out the observed miss distance during the last two or three seconds of flight, it will be possible to fire only those warheads which are in a position to obtain kills.

Consideration of the vulnerability of the PLATO system to other methods of attack has led to the conclusion that the greatest threat lies in low flying aircraft attacks using conventional weapons. Nuclear weapons carried by aircraft would most likely be used against the prime targets rather than the defense system and defenses such as Nike can be expected to be effective against aircraft at high altitude.

The ability of the PLATO system to locate the enemy launch site has been examined. The uncertainty in enemy launching and guidance procedures during powered flight appears to introduce the greatest error, the uncertainty being of the order of 1 nautical mile. If the enemy designs his ballistic missile system with the expectation that retaliatory attack will be promptly made, it is not clear that he will be forced to accept significant losses of equipment and personnel even if a direct hit can be made on the site from which his missile was launched.

In order to provide information for system optimization, studies have been made of the effect on interception point prediction accuracy of changes in the acquisition radar parameters such as power and scan rate and also the effect of improving angular accuracy by beam interpolation. The magnitude and nature of the errors to be expected are being studied.

A survey of transmitter tubes suitable for use in the acquisition radar indicates that suitable klystrons can be developed and that a suitable beam power tetrode will be available within the next few months.

A study of the effects of variation in geometry of the range triangulation system on the tracking accuracy is in progress and a comparison of the performance of this type of system with that of a triangulation system using angle measurements is partially finished.

A study by Steel Products Engineering Company of the mechanical problems associated with a pencil beam precision tracking system indicates that the weight of the mount and antenna system to meet the PLATO requirements

SECRET

will be of the order of 25 tons. The mechanical tolerances specified for this study were substantially those used for the Nike system. Based on the Nike I field tests, these tolerances should result in an overall system angular tracking accuracy which would match the PLATO system requirements.

Study of the feasibility of the use of rods as countermeasure decoys has indicated that a few pounds of metal in the form of quarter-inch rods could produce an echo equal to that of a ballistic missile. Round steel rods would lag a streamlined missile by about half a mile at 175,000 ft. and would therefore be resolved from the target by the radar, but might seriously confuse the tracking. An attempt is being made to analyse the type signal fluctuations to be expected from missiles and possible decoys to see if the fluctuations can be used to distinguish the target.

Additional details of the logical design of the track initiation and prediction computers have been worked out. Also a mathematical method for target trajectory prediction which uses all past tracking information but eliminates the necessity for storing all past points on the track has been developed.

The mathematical design for the midcourse and terminal guidance computer has also been worked out. The midcourse guidance utilizes a polynomial equation for the trajectory and for the terminal guidance, a linear prediction equation. A study of the polynomial trajectories indicates that a seventh order polynomial gives reasonable flight performance without exceeding the maneuvering capability of the vehicle.

For targets impacting behind the launch site, the defended area may be limited by air frame maneuvering capabilities. It has been determined that maximum rearward coverage can be obtained with a wing loading (W/S) between 25 and 45#/ft.², the upper limit representing the smallest wing area that will still result in rearward flights which terminate in the inverse trajectory at 60,000 ft., the lower limit representing an optimum based on structural weight considerations. Using the S-3 interceptor characteristics, the maximum rearward coverage for an intercept with at least 5 g. capability is 30 nm against a 45° target trajectory. If the target trajectory is shallower, the intercept range must be reduced, but ground defended area remains much the same because the target impact point moves to the rear thus compensating for the decrease in intercept range.

A study of the interceptor control surface problem indicates that balanced flaps should be used and that a flap area of about 10% of the exposed wing area will provide adequate control.

The transfer functions and response characteristics of the autopilot described in the 7th Quarterly Report have been computed. It has been

SECRET

possible to obtain a response to a step input which achieves 90% of the full lateral acceleration in 1/4 second and never exceeds the commanded lateral acceleration.

Some of the requirements for the ground-to-air command link and the ground communication network have been determined.

SECRET

SECTION III EVALUATION STUDIES

3.1 SYSTEM OPTIMIZATION

The portion of the optimization study investigating the technical aspects related to the size of the defended area is discussed in this section. This portion of the optimization study will be composed of two parts:

- (1) The specifications for the major components of the system are to be derived based upon providing a well-integrated and well-balanced system which will defend the maximum ground area within the present state of the art.
- (2) The specifications for the major components of the system are to be derived based upon providing a well-integrated and well-balanced system which will defend the optimum size of ground area where the optimum size is determined from the cost and the operational aspects of the system.

The first part of the study may be further divided into the derivation of the maximum size of defended area for a unit system and for a multiple component system. The unit system is defined as one containing one acquisition radar, one triangulation radar, and one launch site (each including the necessary associated computing equipment). The multiple component system is defined as one containing multiple installations of any of the major components. The maximization study of the defended area for a unit PLATO system is over fifty percent complete and is discussed in this section.

The basic factors in the PLATO system which impose limitations on the size of the defended area are:

- (1) The radius of ground damage from enemy warhead blast.
- (2) The interceptor midcourse flight-time characteristics.
- (3) The total time available after detection to effect an intercept.
- (4) The volumetric coverage of the acquisition radar.
- (5) The intercept-point prediction accuracy at launch.
- (6) The intercept-point prediction accuracy during the terminal phase.
- (7) The interceptor terminal guidance characteristics.

SECRET

7

SECRET

Simplified mathematical models are being derived for each of these limitations. Models already have been derived for the first five limitations upon the defended area size.

3.1.1 THE RADIUS OF GROUND DAMAGE FROM ENEMY WARHEAD BURST

A study of the ground damage resulting from the burst of the enemy warhead has been made. The results of this study are being reported in Section 3.2.3 of this report and therefore will not be repeated here. The portion of those results which are of particular importance here defines the radius of ground damage resulting from a near-ground burst. For an enemy warhead of 3 MT, a 7-2/3 n.m. radius of 10 cal/cm² or more damage results. If this radius of damage is symbolized as r_{DG} , then X_{DR} the radius of the defended area for a rearward impact, can be defined as follows:

$$X_{DR} = \text{distance defended rearward} = X_R - r_{DG}$$

where X_R is the distance to the ground impact-point of the target which falls just outside of the rearward range of the defenses. The corresponding expression in the forward situation is

$$X_{DF} = X_F - r_{DG}$$

3.1.2 THE INTERCEPTOR MIDCOURSE FLIGHT-TIME CHARACTERISTICS

The interceptor flight path between its launch site and an interception with the target is one factor determining the most limiting or most distant target trajectory that can be intercepted from a given launch site. The basic mathematical models for optimum midcourse trajectories were derived in the 7th PLATO Quarterly Progress Report in Sections 3.1.1.1 and 3.1.1.2.

Typical values have been chosen for the variables involved in order to obtain an idea of the size of the resulting defended area.

$h_m = 0.8$ n.m. = minimum altitude before the interceptor starts a maneuver.

$R_1 = 0.5$ n.m. = radius of the first turn.

$R_2 = 4$ n.m. = radius of the turn onto the inverse trajectory.

$t_{45} = 10$ sec. = time spent on the inverse trajectory prior to intercept.

$V_i = 0.5$ n.m./sec. = average velocity of the interceptor.

$\gamma = 30^\circ, 45^\circ, 60^\circ, 90^\circ$ = angle of target impact with the ground.

SECRET

$R_t = 1000, 800, 600, 200, 100$ n.m. = ground range of target.

$t_f = 40$ sec., 90 sec. = interceptor time of flight.

$r_{DG} = 7-2/3$ n.m. = radius of damage of the target warhead.

These data are used for calculating intercept points forward and rearward of the launch site and are plotted in Figures 3-1 and 3-2 respectively. In the forward case, two types of trajectories were considered:

- (1) The intercept altitude h_1 was fixed at 10 n.m. and an R_1 of the necessary size was used.
- (2) The radius R_1 was set at its minimum value of $1/2$ n.m. and the resulting altitude was accepted.

In the forward case, these low altitude intercepts are necessary to prevent target missiles from "sneaking" under the 10 n.m. high umbrella. Based upon these low-altitude-intercept trajectories, the time of flight can be plotted as a function of the size of the defended area forward of the launch site assuming various average values of interceptor velocity. These data are plotted in Figure 3-3.

Trajectories for intercepts rearward of the launch site are plotted in Figure 3-2. In the rearward case, the alternatives of flying an optimum trajectory (i.e. normal to the limiting cone as discussed in Section 3.1.1.1 and 3.1.1.2 in the 7th PLATO Quarterly Progress Report) or of simply flying a horizontal trajectory must be considered. For a 40-second time of flight, either might be flown, but with a 90-second time of flight, the optimum trajectories cause the intercept point to vary in altitude from 4 n.m. to 33.5 n.m. This is well beyond the altitude capabilities of an aerodynamically controlled interceptor.

Another consideration depends upon the difference between the impact point of the 80° and 45° target trajectory which can just be intercepted with an optimum interceptor trajectory. For example, the optimum interceptor trajectory makes it possible to intercept a 45° , 1000 n.m. target impacting the earth 52 n.m. from the launch site. However, an 80° , 1000 n.m. target can get in as close as 37.5 n.m. from the launch site. (See Figure 3-2, optimum trajectory intercept loci.) The important point is that there is no advantage in designing the system specifically for intercepting targets launched at lower angles which impact the earth outside this limiting target trajectory.

Now a comparison between an optimum interceptor trajectory and a horizontal interceptor trajectory can be made by comparing the ground distance from the launch site to the ground impact point for the limiting 80° target

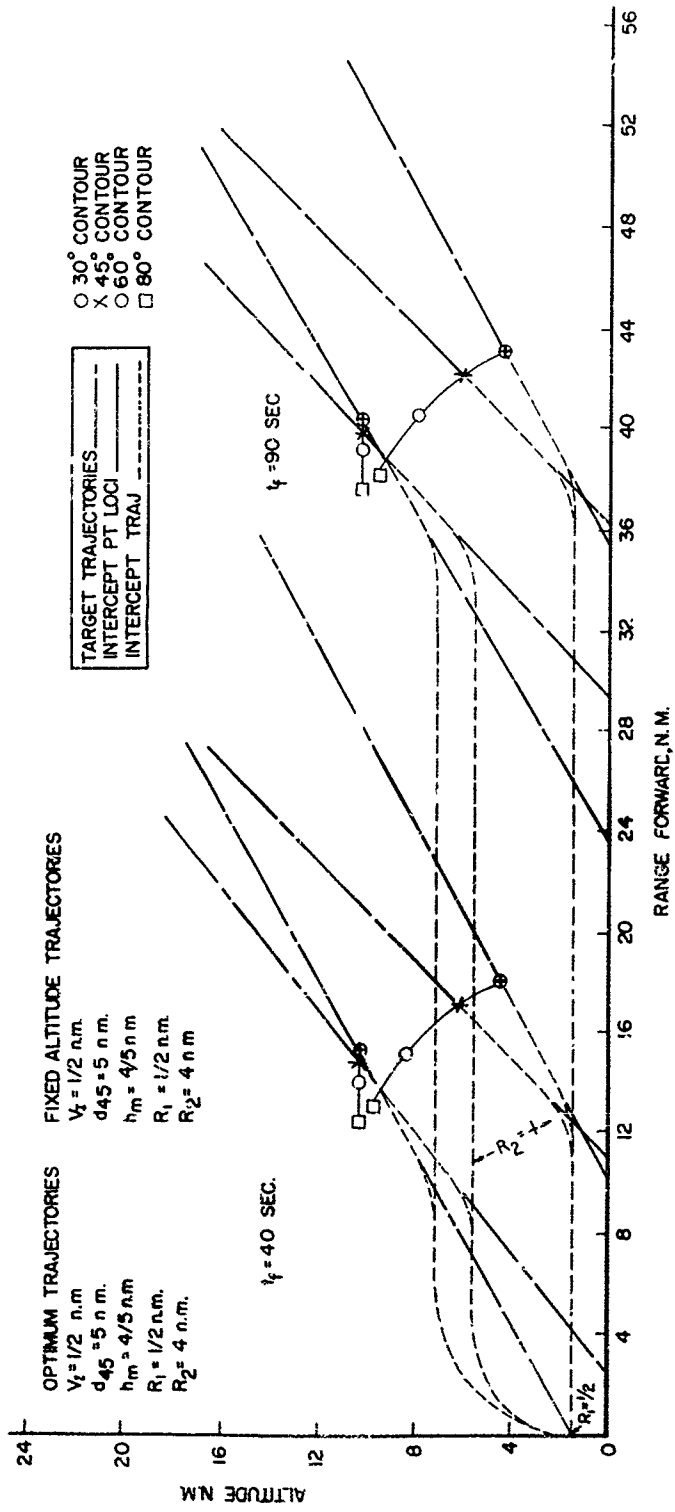


FIGURE 3-1. FORWARD TRAJECTORIES

SECRET

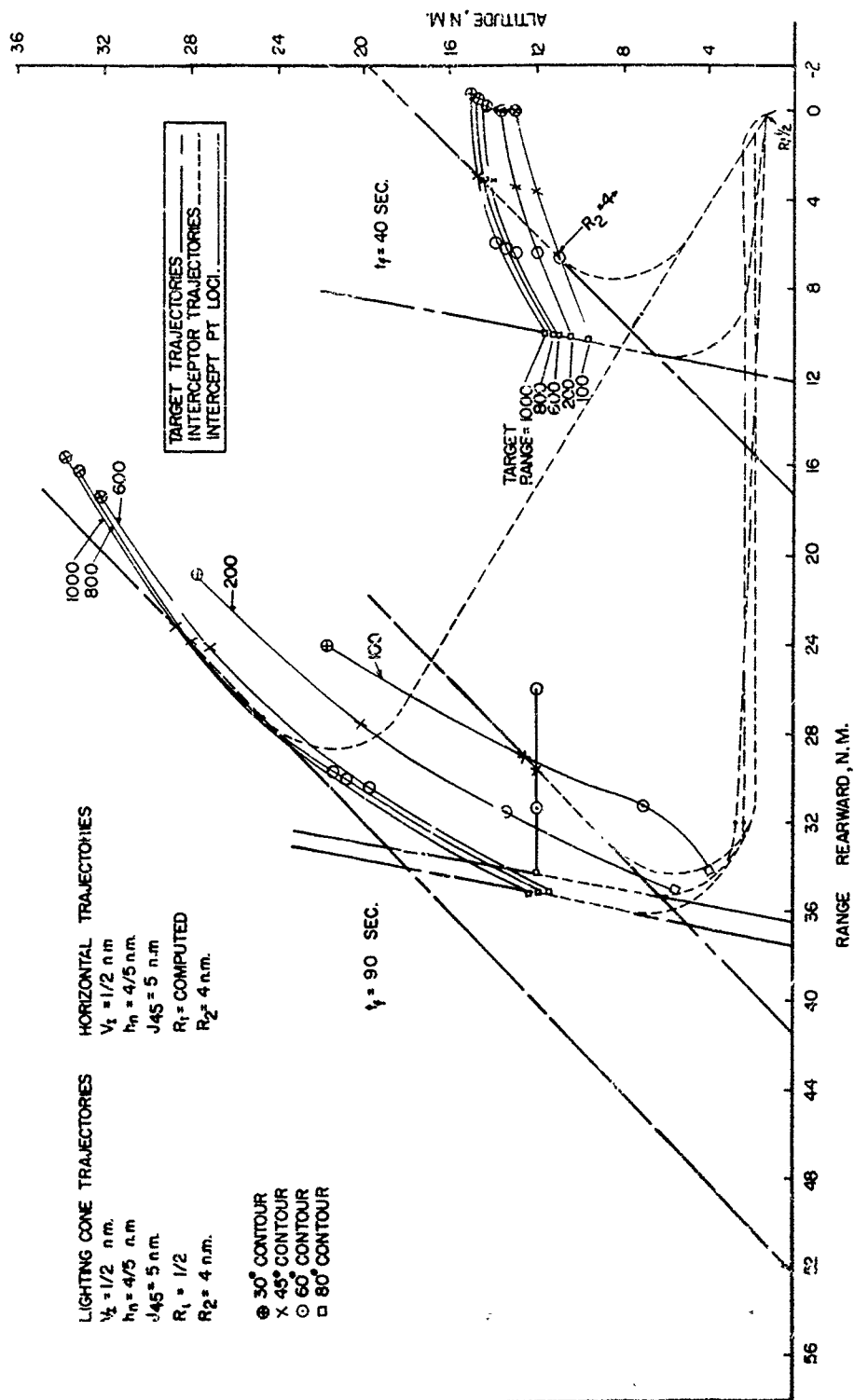


FIGURE 3-2. REARWARD TRAJECTORIES

SECRET

SECRET

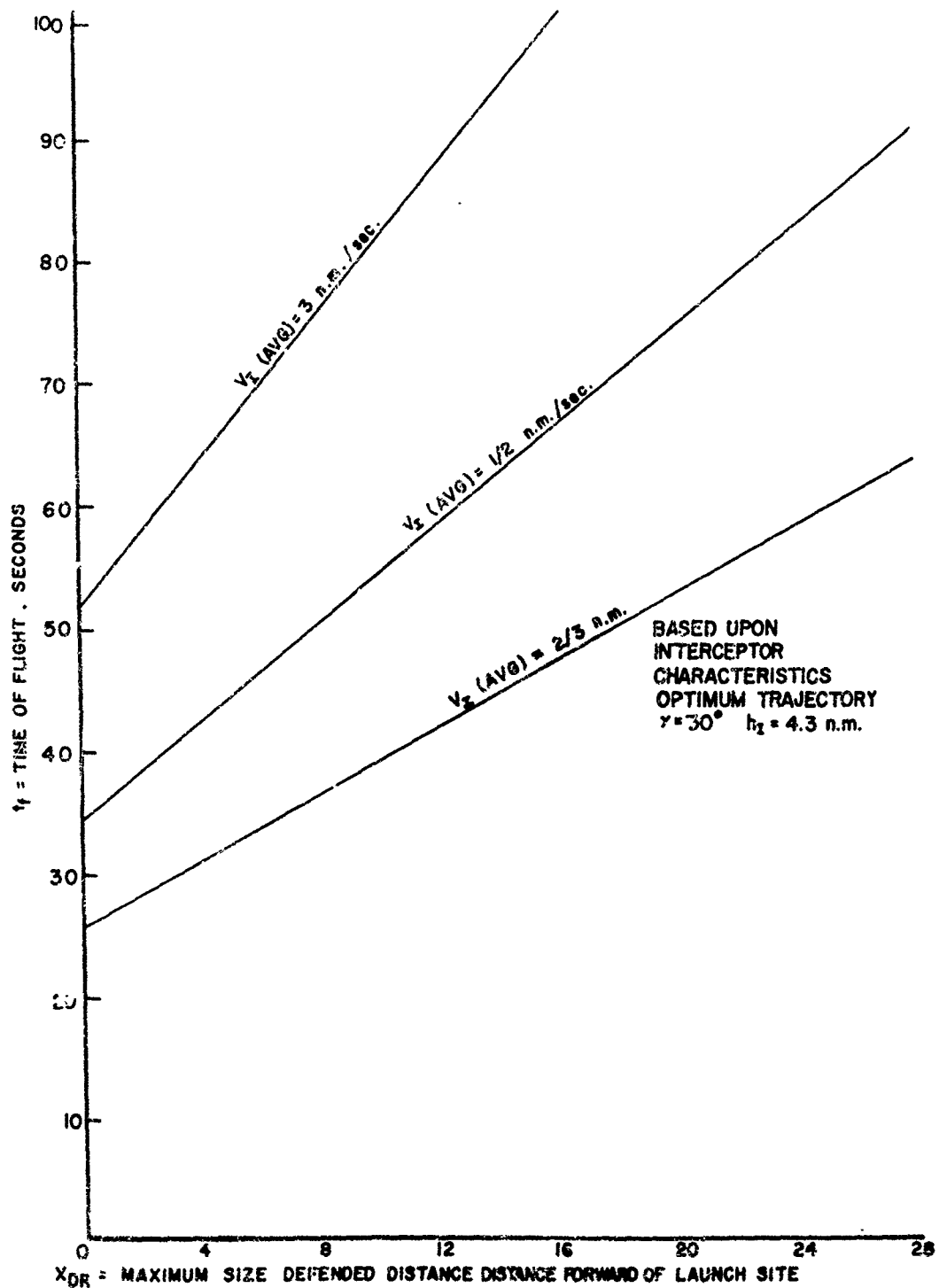


FIGURE 3-3. MAXIMUM DEFENDABLE DISTANCE FORWARD OF THE LAUNCH SITE

SECRET

trajectory. Based upon the optimum intercept trajectory, the target impact point is 37.5 n.m. and based upon the horizontal trajectory, the target impact point is 36.5. Thus the optimum interceptor trajectory exaggerates the spread of impact altitudes and only increases the range to the impact point by one n.m. As a result, major emphasis has been placed upon the horizontal interceptor trajectories for targets impacting the earth rearward of the launch site. Figure 3-4 shows the size of the defended distance for the rearward intercept point as a function of the interceptor time of flight on a horizontal trajectory using the average interceptor velocity as a parameter.

3.1.3 TOTAL TIME OF FLIGHT AVAILABLE

The simplified relationship for determining the total time available after detection to effect an intercept can be expressed as follows:

$$t_f = t_{TD} - t_{TI} - t_I - t_R$$

derived from Figure 3-5 where

- t_f = the available time of flight for the interceptor.
- t_{TD} = the target flight time between initial detection and impact with the ground.
- t_{TI} = the target flight time between interception and impact with the ground.
- t_I = the time required to initiate a target track.
- t_R = the time required to ready the interceptor for firing after a target track has been initiated.
- θ_A = the minimum elevation angle for the acquisition radar.

For a given range of initial radar detection, t_{TD} and t_{TI} are inversely proportional to the target average velocity, while t_I and t_R are independent of the target. The minimum time of flight can be seen to exist where the radar detection range is minimum and the target velocity is maximum. The target velocity increases for target launch angles above and below 45° for targets with a given ground range and also increases with increasing ground range. The minimum detection range occurs for short-range targets fired from within the maximum detection range of the radar. Thus, there is some minimum ground-range target against which the system can defend. In order to obtain an estimate of this limit, air trajectories for

SECRET

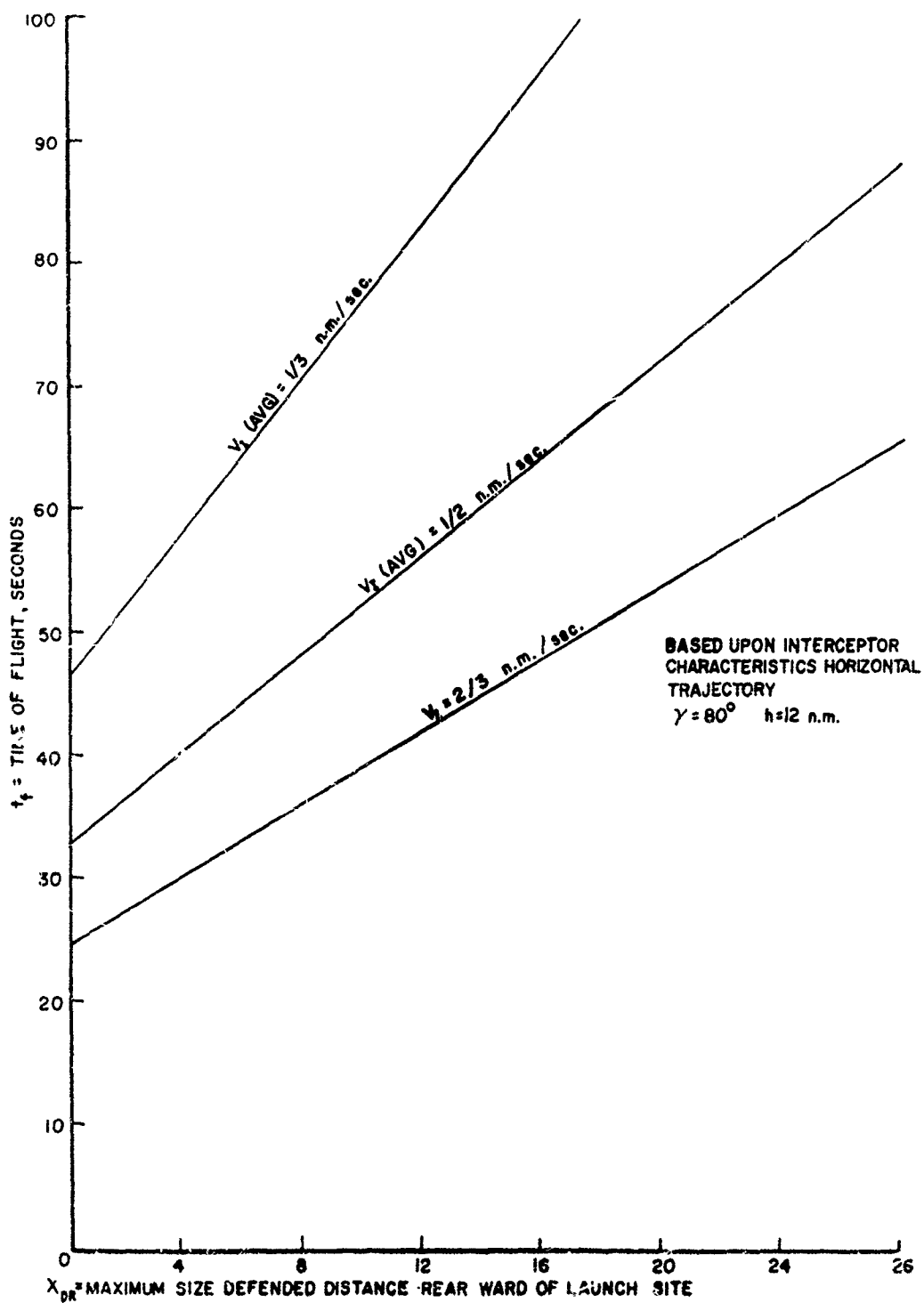


FIGURE 3-4. MAXIMUM DEFENDABLE DISTANCE REARWARD OF THE LAUNCH SITE

SECRET

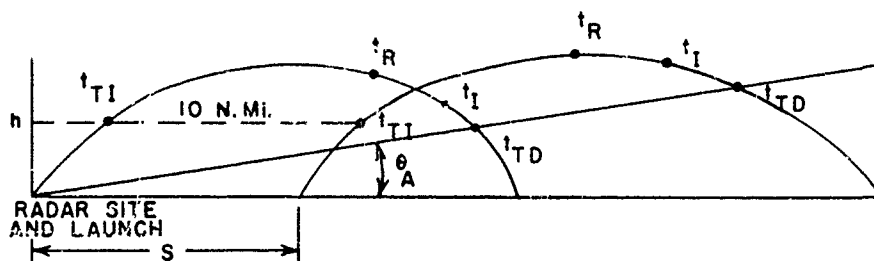


FIGURE 3-5. TARGET TRAJECTORY TIMING LIMITATION

various ground ranges of the Redstone missile were studied. The two assumptions made were:

$$t_I = 15 \text{ seconds}$$

$$t_R = 30 \text{ seconds}$$

Various values of the minimum acquisition radar elevation angles θ_A were chosen as a parameter. The value of t_f can be plotted as a function of the ground range of the Redstone missile, assuming an interception at 10 n.m. altitude.*

These data for the target impacting the ground at the radar site are shown in Figure 3-6. Based only upon time available, a 90-second interceptor flight time would limit the minimum target-ground-range against which the system could defend to 45 n.m. for $\theta_A = 2.5^\circ$ or 60 n.m. for $\theta_A = 10^\circ$.

The data for the target impacting the ground 40 n.m. forward of the radar site are shown in Figure 3-7. In this case a 90-second interceptor flight time limits the minimum target ground-range to 50 n.m. for $\theta_A = 2.5^\circ$ or 75 n.m. for $\theta_A = 10^\circ$.

From Figures 3-3 and 3-4, a 90-second flight time is observed to be equivalent to a defended distance of approximately 28 n.m. forward and rearward of the launch site where the interceptor maintains an average velocity of 1/2 n.m. per sec.

* Similar curves for targets of ground ranges greater than 200 miles were reported in PLATO Finzi Report Phase One, Section 7.1.

SECRET

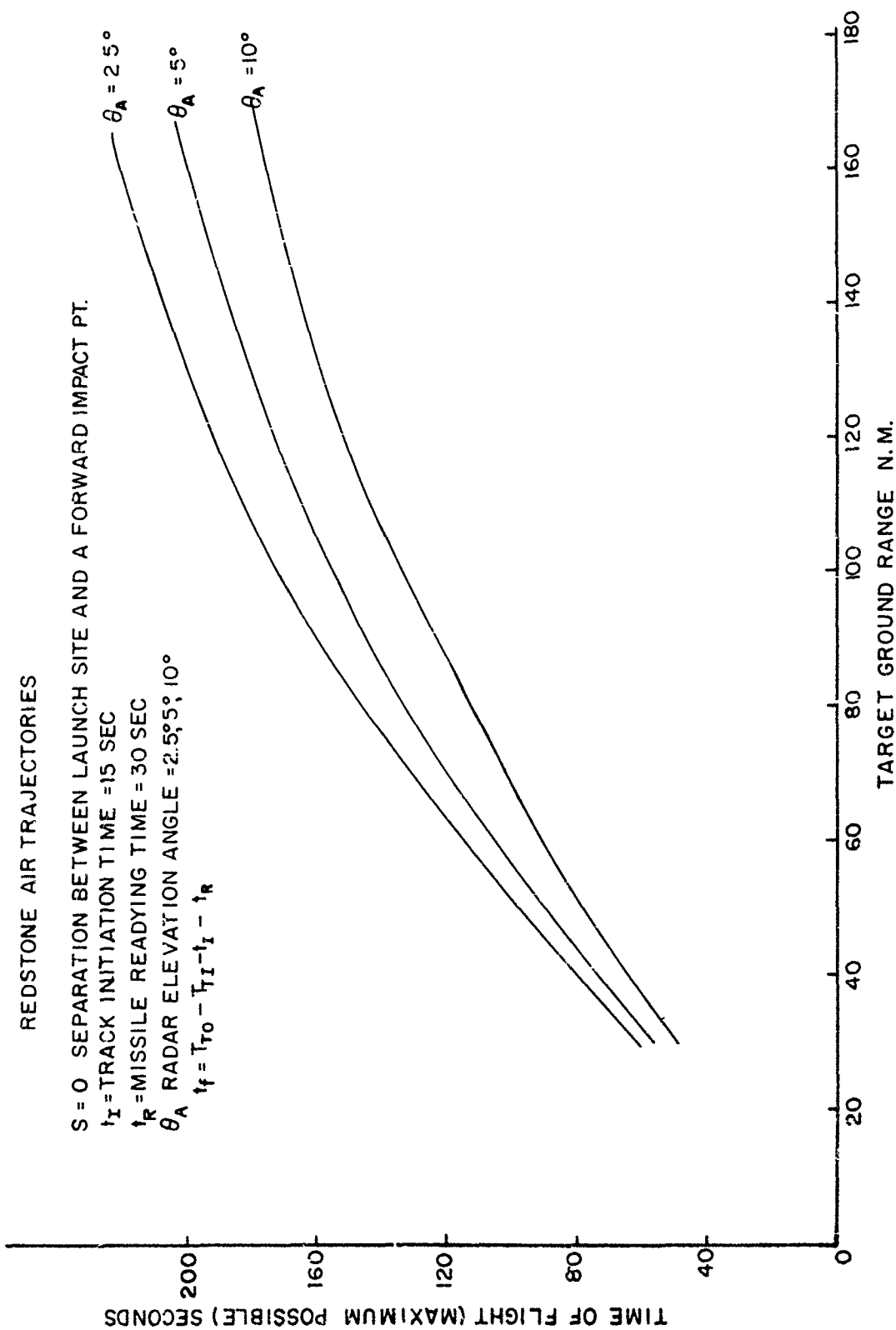
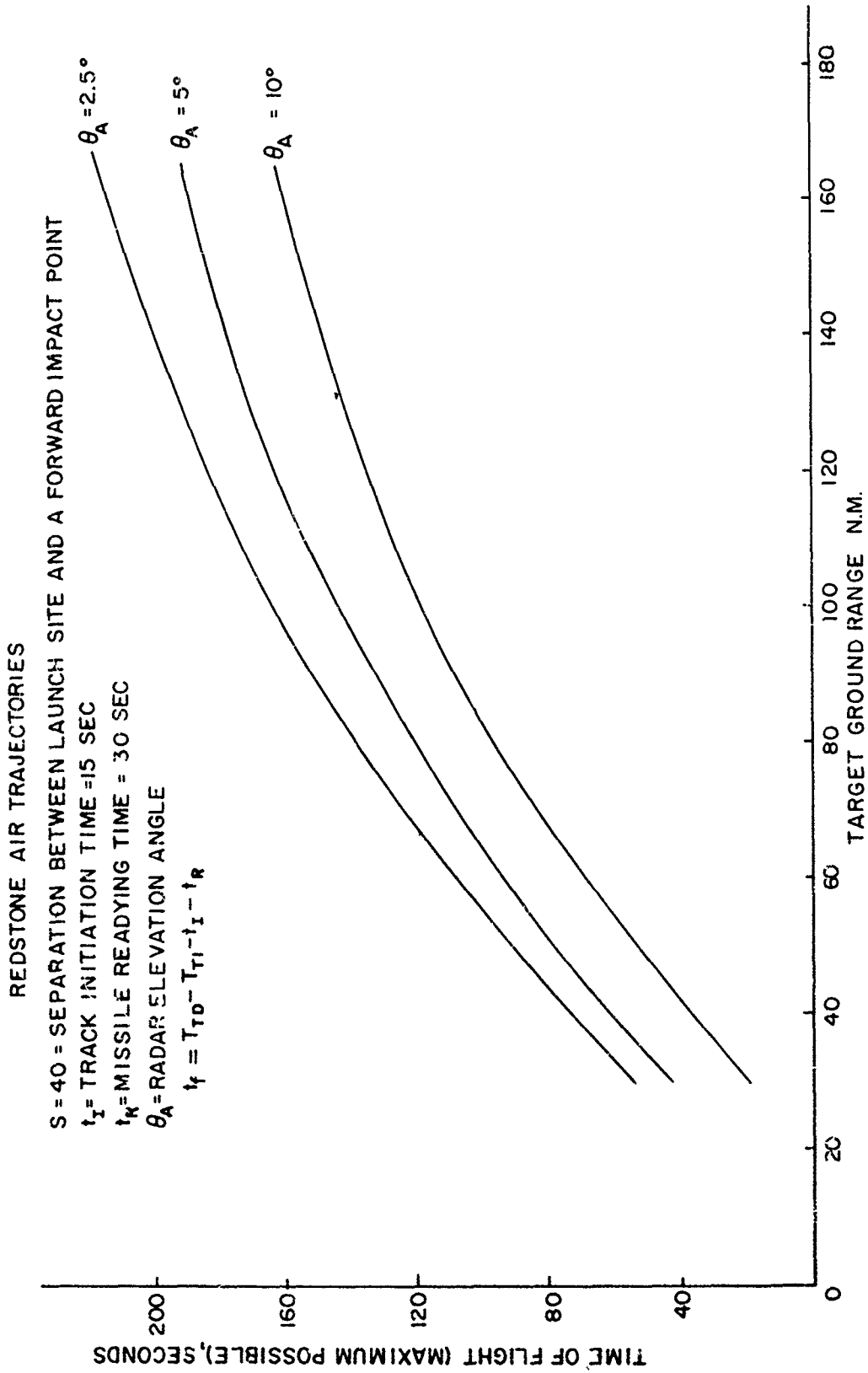


FIGURE 3-6. MAXIMUM TIME OF FLIGHT FOR THE INTERCEPTOR TARGET (45 N.M. LIMIT)

SECRET



SECRET

FIGURE 3-7. MAXIMUM TIME OF FLIGHT FOR THE INTERCEPTOR TARGET (50 H.M. LIMIT)

SECRET

3.1.4 VOLUMETRIC COVERAGE OF THE ACQUISITION RADAR

The volumetric coverage of the acquisition radar limits the defended area in two ways:

- (1) The limit in azimuth coverage, θ_s
- (2) The limit in vertical coverage, θ_R

The limit in azimuth coverage of the acquisition radar imposes a limit upon the direction from which the enemy must be assumed to launch target missiles against a given area to be defended. If the enemy is assumed to be capable of firing missiles from anywhere within the acquisition radar azimuth coverage, the ground area which can be defended (excluding the reduction of defended ground area due to the enemy warhead effective radius of damage) must lie totally within the coverage of the acquisition radar. When the radius of damage is subtracted, the acquisition radar becomes undefendable from enemy missiles fired from the edges of the radar coverage. Therefore, the acquisition radar azimuth coverage must exceed the sector, θ_E , from which enemy missiles may be fired as shown by the geometry of Figure 3-8. The minimum distance between the acquisition radar and a target impact point, Y_I , must be greater than the enemy warhead damage radius in order to defend the radar. The effect of displacement of the center of the acquisition radar coverage relative to that of the precision tracking radar was discussed in Section 8 of the PLATO Phase I Report. The net

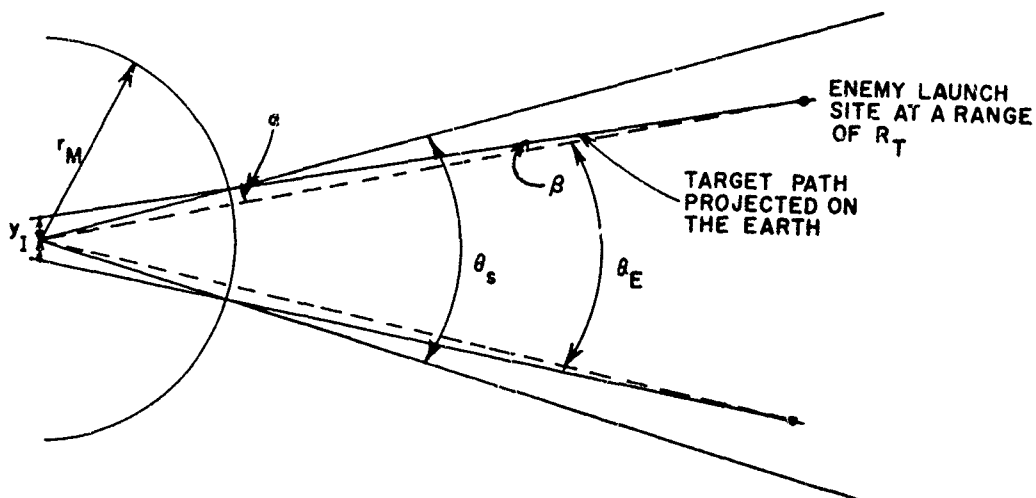


FIGURE 3-8. AZIMUTH COVERAGE LIMITATION GEOMETRY

SECRET

effect is to increase the size of the total defended area when the acquisition radar is displaced to the rear of the precision tracking radar; but the defended area behind the acquisition radar may be somewhat decreased.

The coverage limits in the vertical plane affects the maximum possible flight time because of the lower edge of the beam as seen in Section 3.1.3, and affects the maximum backward coverage because of the upper edge of the beam as will be shown now.

From Figure 3-8 the expression for θ_E can be shown to be

$$\theta_E = \theta_s - 2\alpha + 2\beta$$

or

$$\theta_E = \theta_s - 2 \sin^{-1} \left(\frac{y_I}{r_M} \right) + 2 \left(\frac{y_I}{R_T} \right) \quad (57.3)$$

Now if the distance defendable = y_D ,

$$y_D = y_I - r_{DG}$$

where

r_{DG} = the radius of blast damage if detonated on the ground.

r_M = the maximum range at which the target may leave the sector of acquisition radar coverage.

R_T = the ground range of the target.

$$\theta_E = \theta_s - 2 \sin^{-1} \left(\frac{y_D + r_{DG}}{r_M} \right) + 2 \left(\frac{y_D - r_{DG}}{R_T} \right) \quad (57.3)$$

The relationship between y_D and θ_E is plotted in Figure 3-9 where r_M is allowed to vary as a parameter. The following values of the other quantities were assumed:

$$R_T = 1000 \text{ n.m.}$$

$$r_{DG} = 7.67 \text{ n.m.}$$

$$\theta_s = 60^\circ$$

The values of r_M shown in Figure 3-9 may be obtained by varying the maximum range of the triangulation radar or by programming the triangulation prediction computer in such a way that the target may leave the view

SECRET

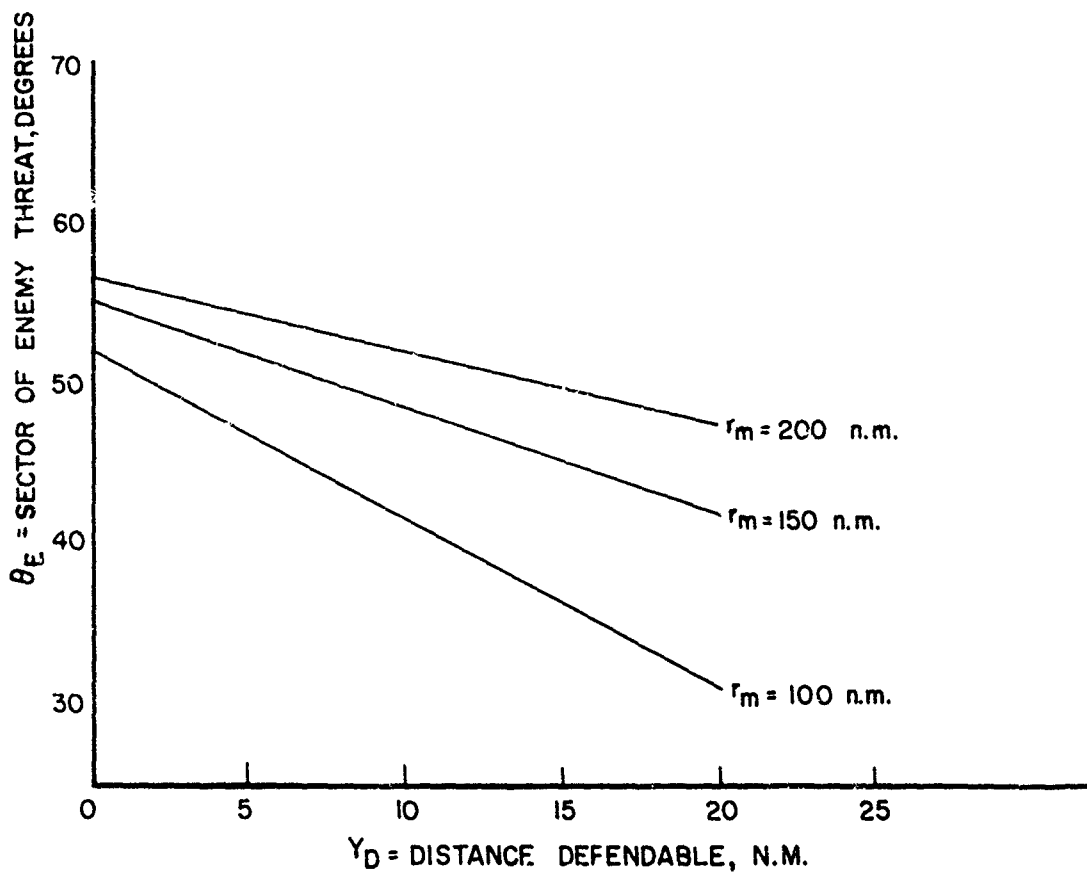


FIGURE 3-9. AZIMUTH COVERAGE LIMITATION OF THE DEFENDED AREA

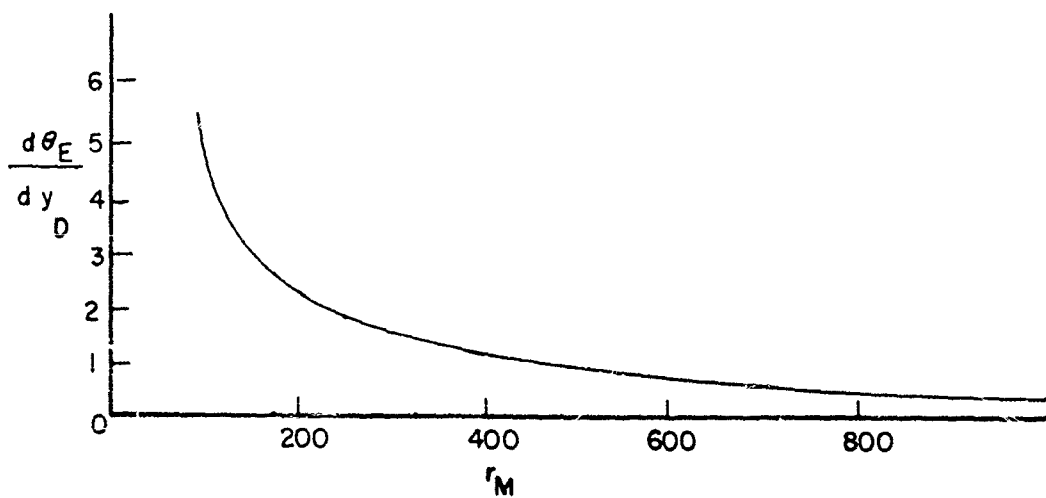


FIGURE 3-10

SECRET

of the acquisition radar before it enters the range of the triangulation radar. However, if $\frac{d\theta_E}{dy_D}$ is plotted versus r_M (Figure 3-10), the slope, $\frac{d}{dr_M} \left(\frac{d\theta_E}{dy_D} \right)$, can be seen to be getting small (disregarding the sign) for values of r_M greater than 200 n.m. On the other hand, if the azimuth angle of the acquisition radar θ_s were increased, θ_E increases directly by an equal amount.

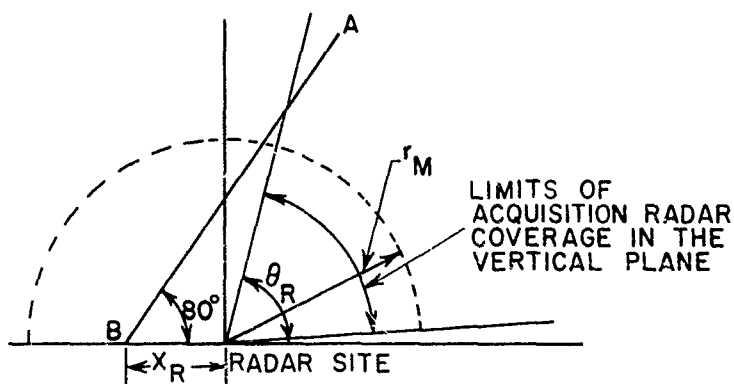


FIGURE 3-11. ACQUISITION RADAR COVERAGE

Figure 3-11 shows an 80° target trajectory AB* leaving the sector of the acquisition radar coverage at the maximum permissible range, r_M . The value of the rearward coverage, X_R , can be derived from the following equation:

$$X_R = r_M \left(\frac{\sin \theta_R}{\tan 80^\circ} - \cos \theta_R \right)$$

If θ_R is the angle between the horizontal and the upper edge of the beam and is assumed to be equal to 85°, then

$$X_R = r_M (.094)$$

When the radius of ground damage r_{DG} is subtracted, the distance defensible X_{DR} becomes

$$X_{DR} = (.094)r_M - 7.67$$

* 80° is assumed to be the highest trajectory angle which reasonably might be expected.

SECRET

In order to increase the ground coverage in the rear of the acquisition radar the following steps can be taken:

- (1) The detection range of the triangulation radar can be increased.
- (2) The triangulation prediction computer can be made capable of accepting a discontinuity in data from the time the target leaves the view of the acquisition radar until it is picked up by the triangulation radar.
- (3) Extend the vertical and horizontal angle of coverage.

The rate of change of defended distance, X_{DR} , with respect to r_M is small. Thus an increase in r_M nets little increase in the rearward defended distance and at the same time is very costly to obtain. However, the triangulation radar can be moved forward of the acquisition radar by an amount, d , without losing any rearward coverage but gaining defended distance forward by an amount d at no extra cost. The value of d is expressed as follows:

$$d = 2 r_M \sin (90 - \theta_R)$$

when

$$\theta_R = 85^\circ$$

and

$$r_M = 140 \text{ n.m.}$$

$$d = 24.4 \text{ n.m.}$$

In this example r_M is assumed equal to the maximum range of the triangulation radar.

3.1.5 THE INTERCEPT-POINT PREDICTION ACCURACY AT LAUNCH

The intercept-point prediction accuracy at launch imposes a limit on the usable interceptor time of flight and thus on the defended area. The reason for this limitation is the restricted altitude band within which an interception can be made. The upper limit on the altitude is imposed by the air density required to produce sufficient maneuver to effect an interception and the lower limit is imposed by the allowable ground damage from the enemy warhead. The basic model for this limitation was developed in the 7th PLATO Quarterly Progress Report, Section 3.1.2.2.. A more accurate expression for the most limiting value of intercept-point prediction error has since been derived:

SECRET

$$\sigma_{PL} = \frac{\Delta h}{\frac{6\lambda}{\sqrt{4 + \lambda^2}} \left[\frac{V_T}{V_T + V_I} (1 - \cos \Gamma) + \frac{V_I}{V_T + V_I} \left(\frac{2 \sin \Gamma}{\lambda} \right) + \cos \Gamma \right]}$$

where

Δh = the height of the interception altitude band.

Γ = the angle through which the interceptor must turn from the midcourse path to get onto the target's inverse trajectory.

and

$$\lambda = \frac{1}{\sin \Gamma} \left(\frac{V_T}{V_I} + \cos \Gamma \right)$$

In order to demonstrate the limitation imposed upon the defended area as a result of the restricted band of altitudes for performing interceptions, targets launched at various angles are being studied. The 45° case is chosen as an example. In Section 3.1.2 above, the time of flight was related to the size of the defended distance forward and rearward of the radar and launch site. The defended distance specifies the most distant intercept point for an attacking target from whence the slant range to the target at launch can be determined. From the slant range and the target characteristics, the intercept point prediction error at launch can be derived. These data are reduced to one curve by plotting prediction error at launch versus the distance defendable as shown in Figures 3-12 and 3-13 for forward and rearward intercept points respectively. Superimposed upon these curves are the maximum values of σ_p which are permissible at launch, in order to obtain a 99% probability of interception σ_{PL} based upon the restricted band of altitudes for performing interceptions. These data are based upon Phase I acquisition radar characteristics. Under these circumstances, the maximum distance defendable to the forward against a 1000 n.m. 45° target is 7.4 n.m. and a 14 n.m. distance is defendable rearward of the radar and launch site.

In order to increase this defendable distance, two steps might be taken:

- (1) Introduce "time control" into the interceptor. That is, make the interceptor absorb time after launch by using drag brakes, or by using a variable thrust engine.
- (2) Improve the acquisition radar accuracy and hence the intercept-point prediction accuracy.

PREDICTION ERROR LIMITATION ON DEFENDED DISTANCE
 INTERCEPT FORWARD OF THE LAUNCH SITE
 ALTITUDE OF INTERCEPT = 6 N M
 R_T = TARGET GROUND RANGE (N.M.)
 γ = ANGLE OF TARGET IMPACT = 45°
 RANGE OF RADAR ≈ 300 N.M.
 RADAR ANGULAR ACCURACY ± 1°
 σ_{PL} = THE EQUIVALENT ALTITUDE LIMIT ON THE VALUE
 OF σ_p AT LAUNCH
 T_A = TIME ABSORBED BY TIME CONTROL (SEC)

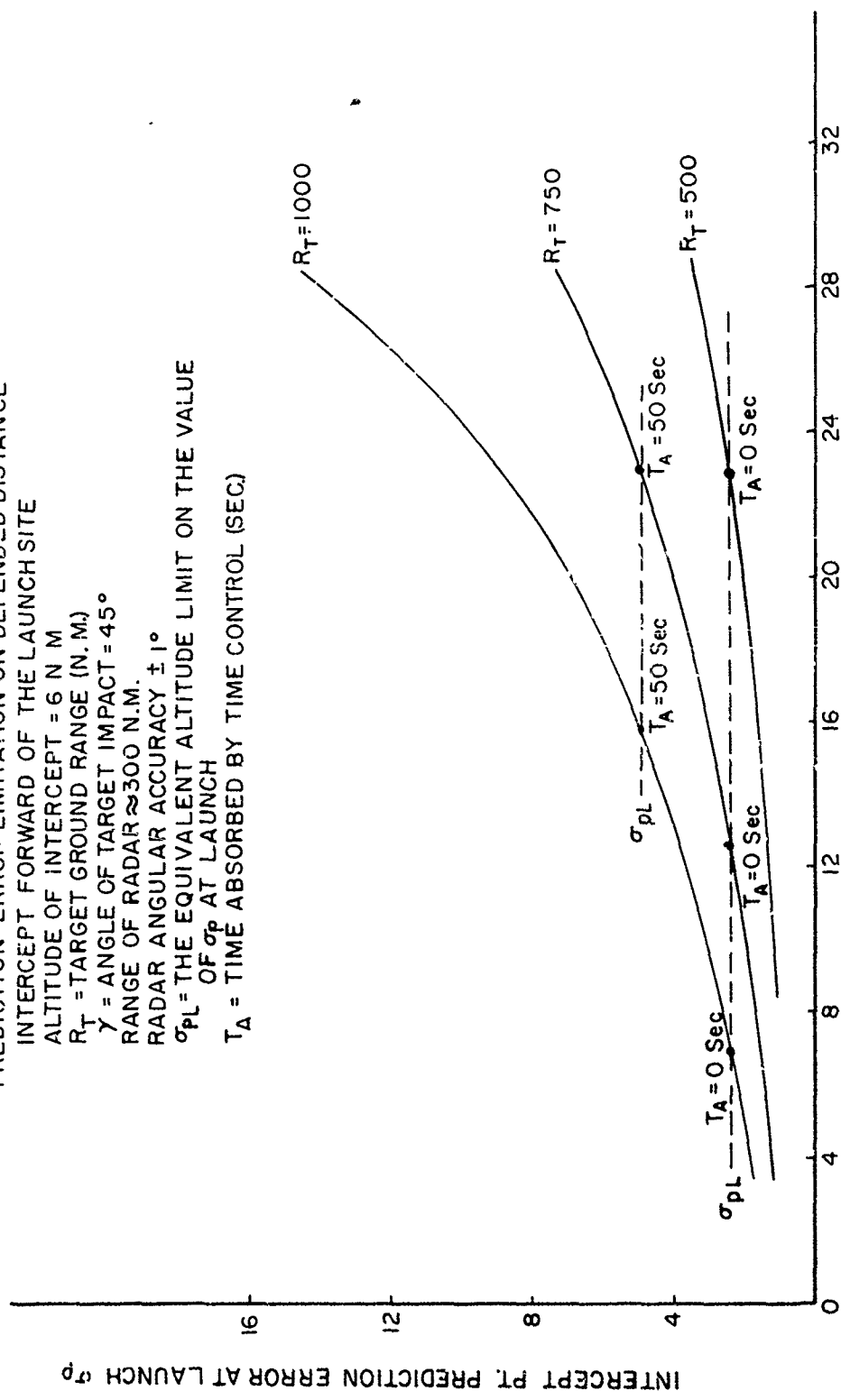


FIGURE 3-12. PREDICTION ERROR LIMITATION ON DEFENDED DISTANCE (1)

SECRET

INTERCEPT REARWARD OF THE LAUNCH SITE (HORIZONTAL TRAJ.)

ALTITUDE OF INTERCEPT = 12 N.M.

R_T = TARGET GROUND RANGE N.M.

γ = ANGLE OF IMPACT 45°

RANGE OF RADAR 300 N.M.

RADAR ANGULAR ACCURACY $\pm 1^\circ$

σ_{PL} = THE EQUIVALENT ALTITUDE LIMIT ON THE VALUE OF G_p AT LAUNCH

T_A = TIME ABSORBED BY TIME CONTROL (SEC)

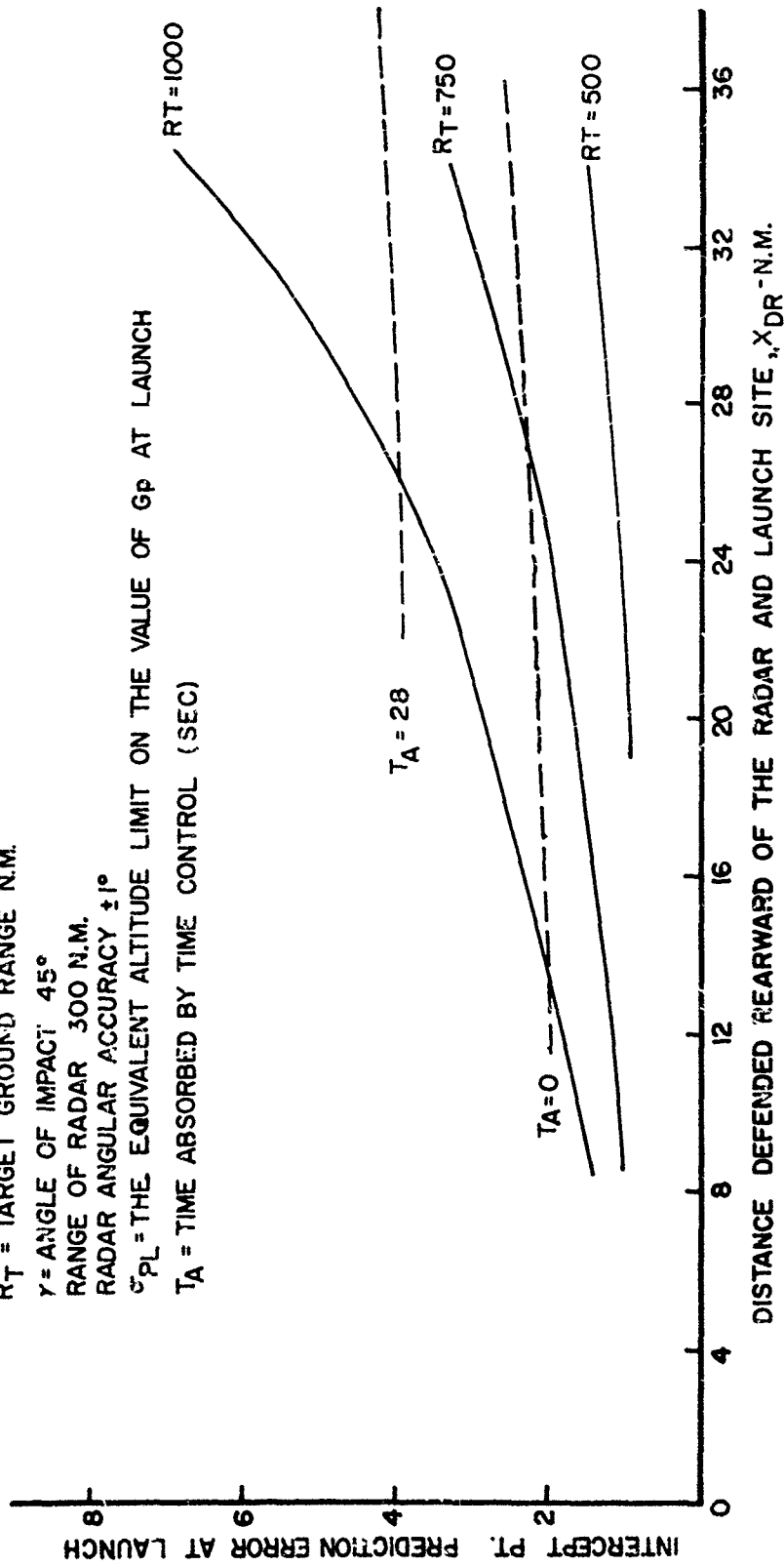


FIGURE 3-13. PREDICTION ERROR LIMITATION ON DEFENDED DISTANCE (11)

SECRET

SECRET

In Figures 3-12 and 3-13, the value of σ_{PL} is computed for time control, T_A , equal to zero, and an additional value. This other value was chosen at the appropriate magnitude to provide twice as high a limiting value of σ_{PL} . If T_A is defined as the amount of time absorbable, the expression for σ_{PL} has been derived.

$$\sigma_{PL} = \frac{\Delta h + T_A \frac{V_T V_I \sin \Gamma}{V_T + V_I}}{\frac{6\lambda}{\sqrt{4 + \lambda^2}} \left[\frac{V_T}{V_T + V_I} (1 - \cos \Gamma) + \frac{V_I}{V_T + V_I} \left(\frac{2 \sin \Gamma}{\lambda} \right) + \cos \Gamma \right]}$$

An increase in the radar accuracy and therefore the prediction accuracy, reduces the prediction error at launch. The σ_p curves for the various ground-range targets effectively are lowered in Figures 3-12 and 3-13, thereby causing them to intersect the σ_{PL} curves at larger values of defended distance. A decrease in prediction error by a factor of approximately 4 appears to be entirely feasible and these data are plotted in Figures 3-14 and 3-15. With this improvement in accuracy, the defendable distance is 24 n.m. forward and approximately 36 n.m. rearward for the 1000 n.m. 45° target. If, in addition, time control is built into the interceptor, the defendable distances can be further increased.

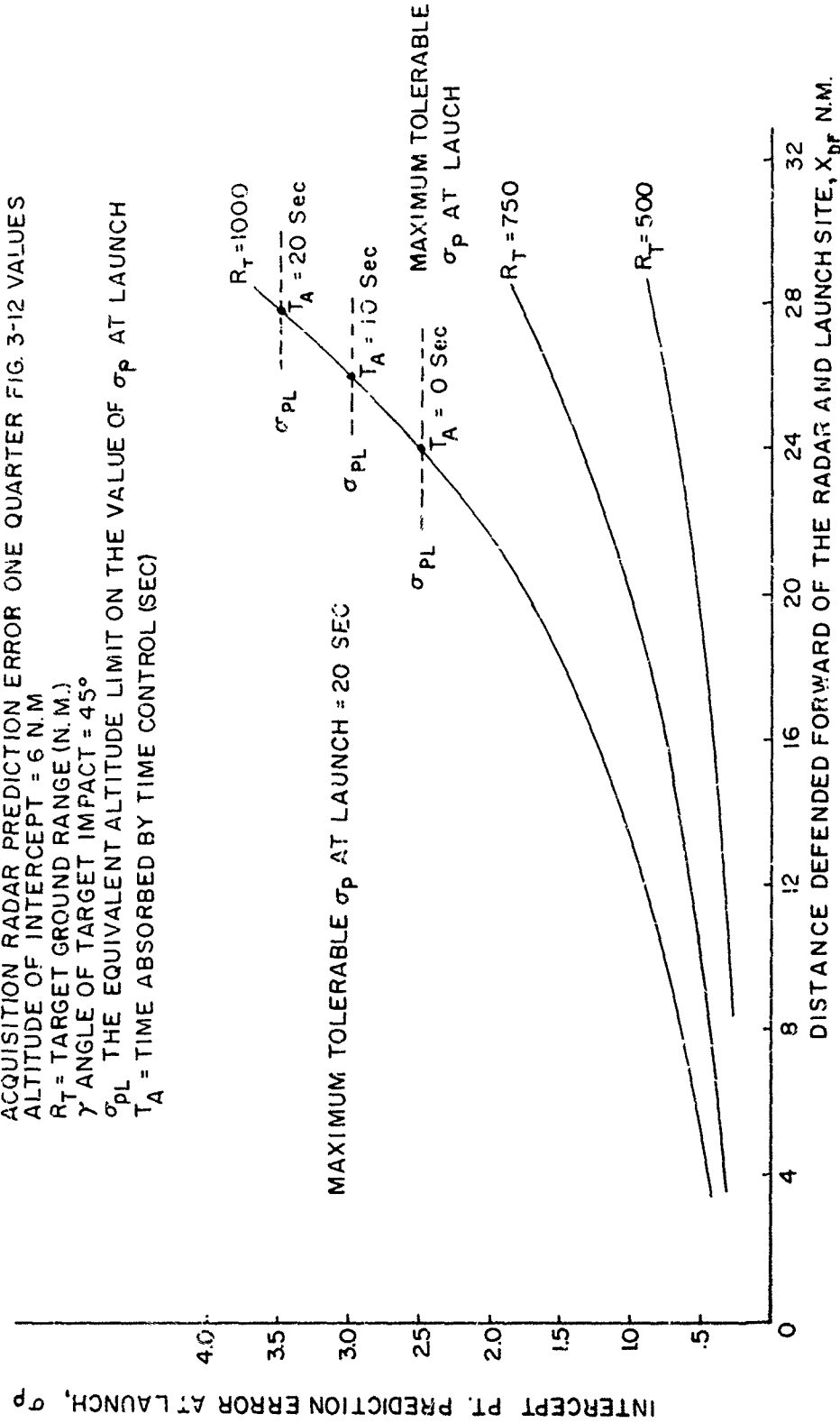
3.1.6 CONCLUSIONS

The actual defendable area is starting to take on clearer shape and size as a result of the limitations studied thus far. The extent of the limitations imposed by the intercept-point-prediction accuracy during the terminal phase and the interceptor terminal guidance characteristics are not yet known but are currently the subject of study.

In the case of each limitation, as it is studied, the steps which can be taken to extend the boundary of the defended area for a unit system have been evaluated. The rate of increase in the size of defended area with respect to each of these steps which might be taken can now be determined. The rate of increase in the system costs can also be evaluated for each of these steps. Two qualitative examples serve to demonstrate this approach. First in Section 3.1.4 discussing the volumetric coverage of the acquisition radar, the limits on the rearward coverage X_{DR} were derived. In that section, a comparison was made between an increase in the defended distance rearward of the acquisition radar as a result of an increase in the detection range of the triangulation and an increase in the over-all defended area as a result of shifting the triangulation radar forward. As a result of the analysis, a zero cost change was shown to result in a much greater

SECRET

INTERCEPT FORWARD OF THE LAUNCH SITE
 ACQUISITION RADAR PREDICTION ERROR ONE QUARTER FIG. 3-12 VALUES
 ALTITUDE OF INTERCEPT = 6 N.M.
 R_T = TARGET GROUND RANGE (N.M.)
 γ = ANGLE OF TARGET IMPACT = 45°
 σ_{PL} = THE EQUIVALENT ALTITUDE LIMIT ON THE VALUE OF σ_p AT LAUNCH
 T_A = TIME ABSORBED BY TIME CONTROL (SEC)



SECRET

FIGURE 3-14. PREDICTION ERROR LIMITATION ON DEFENDED DISTANCE (1111)

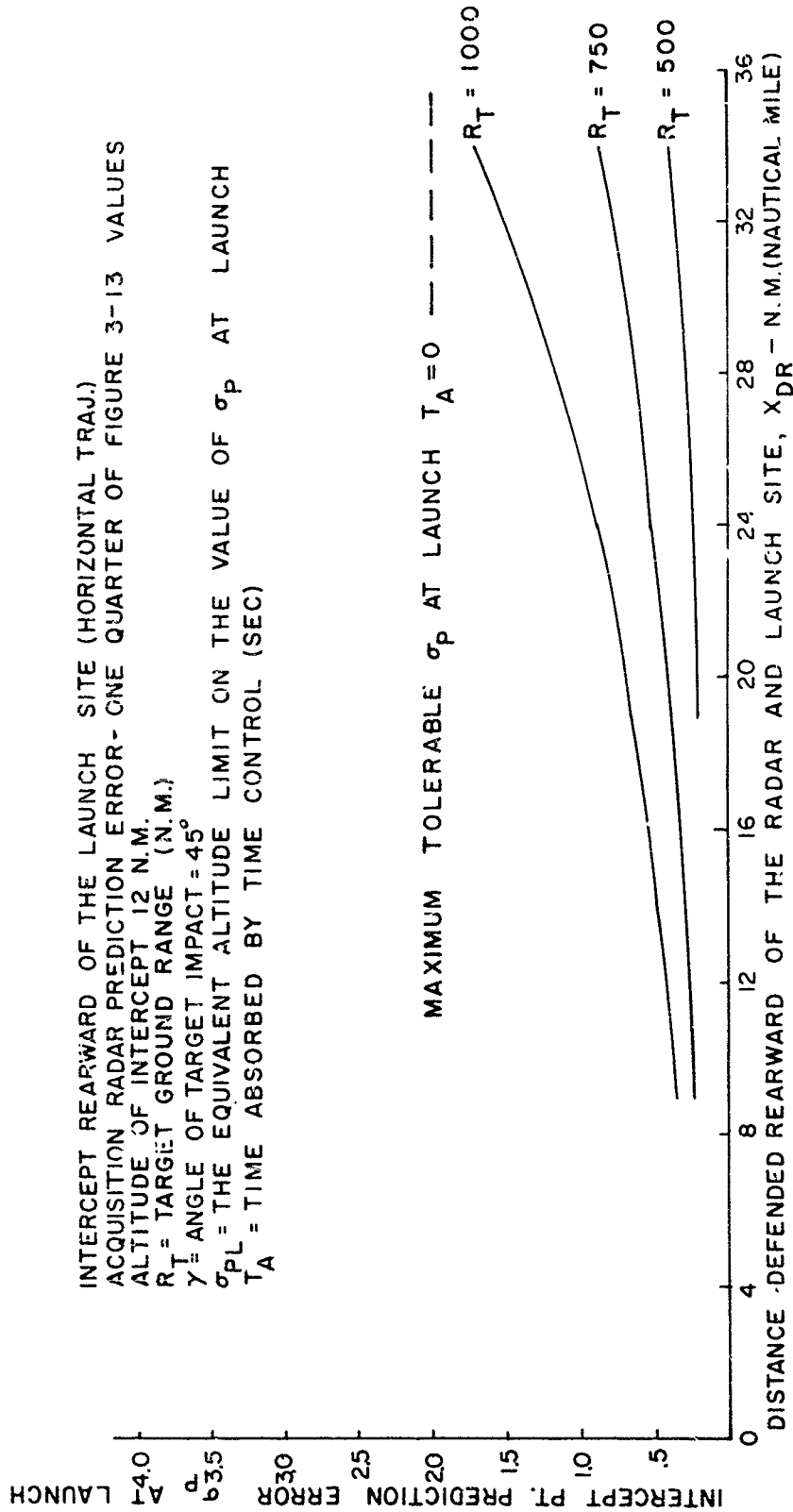


FIGURE 3-15. PREDICTION ERROR LIMITATION ON DEFENDED DISTANCE (IV)

SECRET

increase in defended area than the high cost change of increasing the detection range of the triangulation radar.

A second example is taken from Section 3.1.5 where the intercept-point prediction accuracy at launch is discussed. Referring to Figure 3-12, time control can be compared to increasing the acquisition radar accuracy as a possible means for increasing the distance defendable. Time control of $T_A = 50$ seconds constitutes a major reduction in flight time compared with a total flight time of 90 seconds. Also, 50 seconds only increases the defended distance from seven n.m. to 16 n.m. The ability to attain 50 seconds time control is also in question. On the other hand, increasing the accuracy of the acquisition radar by way of beam splitting appears to present no major problems and a factor of approximately 4 does not seem unreasonable. With such an improvement, the defended distance is extended from seven n.m. to approximately 24 n.m. As a result of the data gathered during this study of defended area, a plot of the costs of the PLATO System as a function of defended area size under various assumptions as to the complexity of the PLATO system will be possible.

3.2 SYSTEM EFFECTIVENESS

3.2.1 COUNTER-BATTERY FIRE

The information processing part of the PLATO System is used to yield a prediction of the intercept point by predicting the actual ballistic trajectory of the target. As will be shown in 3.2.1.1 below, this data may be used to estimate the past history of the target and, together with additional analysis, based on missile operational characteristics, may be used to estimate the location of the target launching site. This enables the PLATO System to engage in counter-battery fire (after suitable modification of the control system) or else to activate other counter-battery weapons systems such as aircraft. The worth of PLATO in direct counter-battery fire requires the study of the PLATO missile in a ground-to-ground role with suitable guidance. This aspect of the problem will not be considered here. The value of counter-battery fire itself is open to question as will be shown below in 3.2.1.2.

3.2.1.1 Estimation of Launch Site

It was shown in Technical Report 4-2, "Mathematical Analysis of Target Trajectory, Smoothing Formulas and Prediction Accuracy", that the purely ballistic portion of the target path may be represented (for the ranges under consideration) by fifth order polynomial trajectory equations. This means that given exact values of position and velocity at one point of the path, the approximate equations have not deviated from the true path by more than 0.1 n.m. at a position corresponding to 200 seconds of further

SECRET

missile flight. An extended form of these equations could be made to satisfy this criterion for 600 seconds of flight time, in which case the ballistic path of a thousand mile range missile could be represented as accurately over the whole of its ballistic flight path, while shorter range missiles would be representable to greater accuracy.

The radar acquired data which is used to construct the ballistic trajectory is noisy and introduces errors which cannot be eliminated by improving the approximating equations. These errors, however, if introduced into the present equations, and if used only in that portion of the flight which is above the sensible atmosphere, introduce a forward prediction error with a standard deviation under 0.1 n.m. Using the same equations to predict back from the point of initial acquisition, these same radar errors give a prediction error whose standard deviation is essentially proportional to the time of prediction, so that the standard deviation for 600 seconds backwards on the trajectory is about 0.3 n.m.

When a deviation from the ballistic path is detected, we make use of Section V of Technical Report 4-2 which permits an estimate of the lift and drag coefficients of the target by fitting the deviations to known equations of motion. The ballistic path (outside the atmosphere) is symmetric about the apogee, so that we may transfer the conditions of re-entry directly to those of exit from the atmosphere. Using the estimated target parameters, it is possible to solve backwards from the exit point to locate a limiting point on the ground beyond which the launch did not take place (assuming good missile design and doctrine).

All known ballistic missiles with ranges over 50 n.m. are launched vertically, so that the true launch point cannot be determined by the procedure above. Launching doctrines, however, may all be approximated by a vertical rise and a circular turn onto the desired trajectory. (See Figure 3-16.) This is subject to individual design variations, but for some reasonable figure for height and radius of this turn will be estimable in the near future; the lateral acceleration in the turn will not be more than one-fourth the initial thrust-produced acceleration, and will probably be about one-sixteenth of that. Initial thrust-produced acceleration for a given range is not widely variable for good design. In NACA Report Technical Note No. 1401, page 40, Figure 3, parametrized curves for this are presented and these may be used to establish a most probable launch site and reasonable bounds on the possible displacement of the launch site from this point.

An analysis of a calculated trajectory in air for a Redstone missile of 150 n.m. 45° shows that with the current PLATO trajectory equations, and using a crude version of the method described above (see Figure 3-17).

SECRET

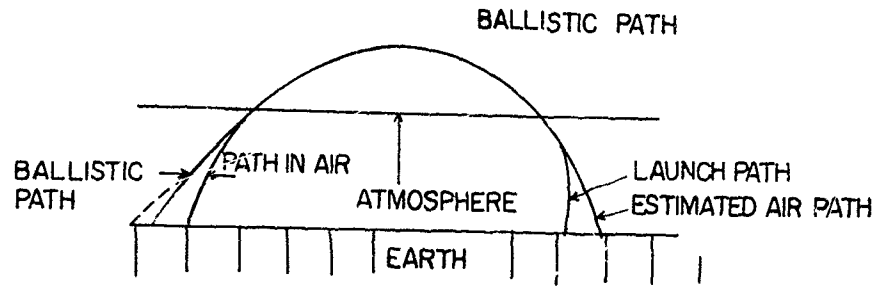
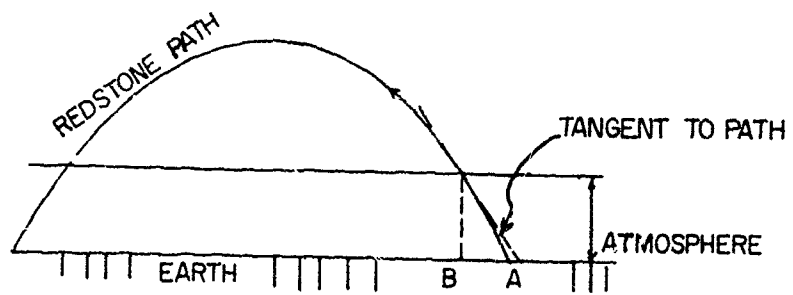


FIGURE 3-16



ESTIMATED LAUNCH SITE MIDWAY FROM A TO B

FIGURE 3-17

SECRET

SECRET

the location of the launch point will be accurate within 1 n.m. Using nuclear warheads, anything left at the launch site after launching can be destroyed.

3.2.1.2 Launch Site Countermeasures

The following paragraphs present a summary of what may be expected at a launch site at the time that the PLATO System is prepared to locate the launch site.

The Redstone missile may be launched from a launching mechanism similar to the meilerwagon, which was used to launch the V-2. Launchings from vehicles of this class may be effected in a small amount of time (say two hours from arrival at the site of the tactical battery to launch) and thereafter, all present are free to leave the area. In the case of V-2 this was done to preserve security on early launchings against London. Thus, unless the enemy is careless, there may be no launching site to attack within minutes after the target has attacked the PLATO System.

If, indeed, the enemy elects to stand still, the question arises as to the worth of the launching installation for these medium and short-range missiles. In the case of a V-2 type missile, this is negligible both in equipment and manpower.

For long-range missiles, the situation changes somewhat. The only American ballistic missile of this class is the Atlas. It will provide an adequate target, inasmuch as it is by its very nature a non-mobile vehicle, requiring large stockpiles of supplies for operation. A typical Atlas launch site is projected as covering an area of 20 square miles, which presents a large target worth locating, containing about 2,500 men and representing a cost of \$200,000,000.

3.2.2 SALVO VS. RIPPLE FIRE

Each PLATO interceptor will have associated with it a reliability which will certainly be less than one. In order to achieve a high (99%) over-all kill probability against each offensive target, the defense will undoubtedly have to launch several interceptors against each offensive missile. Consideration of effects on nearby interceptors by the detonation of one interceptor leads to an examination of two obvious choices for the order in which the interceptors may be placed on target.

On the one hand, if the interceptors make contact on target simultaneously, all may be detonated simultaneously (assuming fusing, etc., permit such simultaneity), and a larger and more effective "warhead" results.

SECRET

In order to accomplish any interception at all, the PLATO interceptor must be launched at a time when the prediction of the target's future position is accurate enough to ensure interception within the limitations which may be placed on permissible intercept altitude. For example, the upper altitude-limit might be that above which the maneuver capability of the interceptor is insufficient for final close-cut of errors. The lower limit might be that below which unacceptably high values of ground damage would ensue. In general, the longer one delays launching his interceptors, the more accurate will be his prediction of the intercept-point, and the smaller will be the corresponding circle of prediction error. The longer one delays launching his interceptors, however, the shorter will be their time of flight, and the more restricted will be the defended area. In the case of simultaneous contact with the target, replicate missiles may all be launched just as soon as one is sure enough that a single interception can take place within the maximum permissible altitude band. A useful criterion of the existence of sufficient prediction accuracy for this purpose is that a circle of radius $3\sigma_p$ be inscribable within the altitude band, as in Figure 3-18. Here, σ_p is the standard deviation of the predicted intercept point. The corresponding slant ranges at launch in the worst case (1000 n.m. range) may be expected to vary from about 85 to 98 n.m. for conditions as given in Figure 3-18. The spread in slant range arises from the spread in target-trajectory angles and intercept-point ranges which may occur. The computations are based on the material of TR4-2 and PLA 310/77.

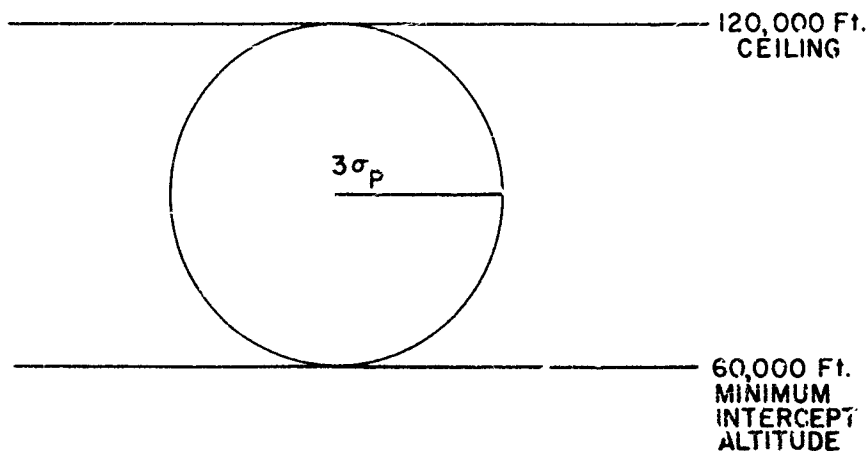


FIGURE 3-18

One expects to meet problems of extreme difficulty in attempting to bring about actual performance of a simultaneous interception on the part of several interceptors. Consider the requirement that all replicate interceptors must find themselves within lethal radius of the target at the instant of their warheads' detonation. Therefore, assuming a closing

SECRET

velocity of 12,000 ft./sec. and a lethal diameter of 1200 feet, a time control of 0.1 second or better is required in order to achieve simultaneity of target contact by two or more interceptors. Such extremely close control of on-target-time for several interceptors would demand a considerable enlargement of missile capabilities.

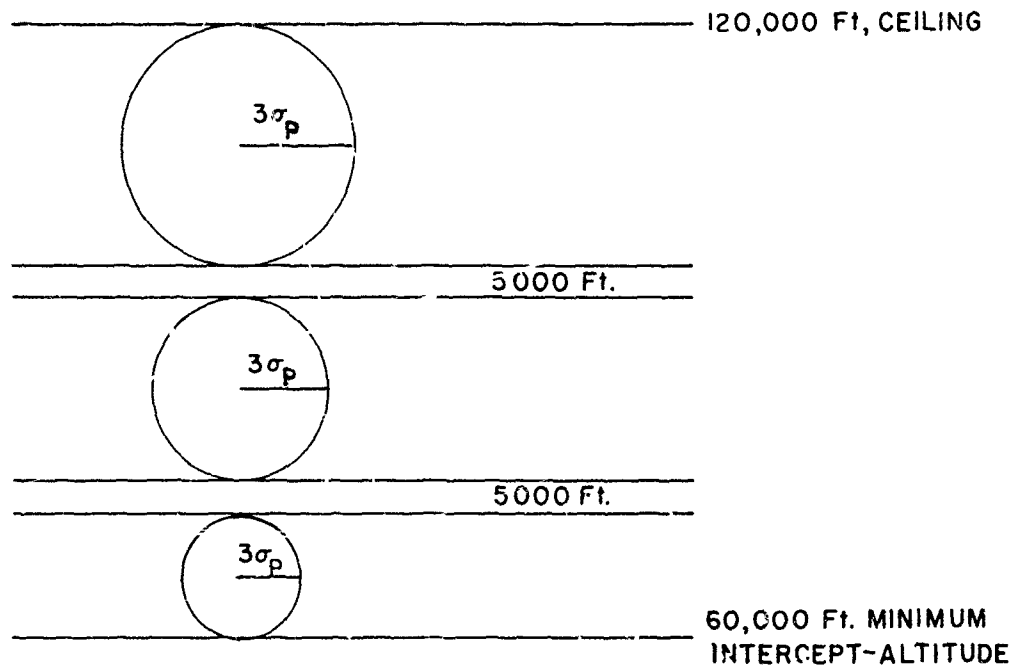
On the other hand, if sequential interception is essayed, later interceptors can function independently only if they are not crippled by the effects of earlier interceptor bursts. Earlier PLATO studies have estimated that the minimum separation thereby required to exist between interceptors, at detonation, is of the order of 5000 feet.

In the case of sequential interception, the serious missile-control requirements mentioned immediately above are relaxed. But let us consider the situation regarding the limitation on slant-range-to-target at launch time, as introduced in the preceding paragraph.

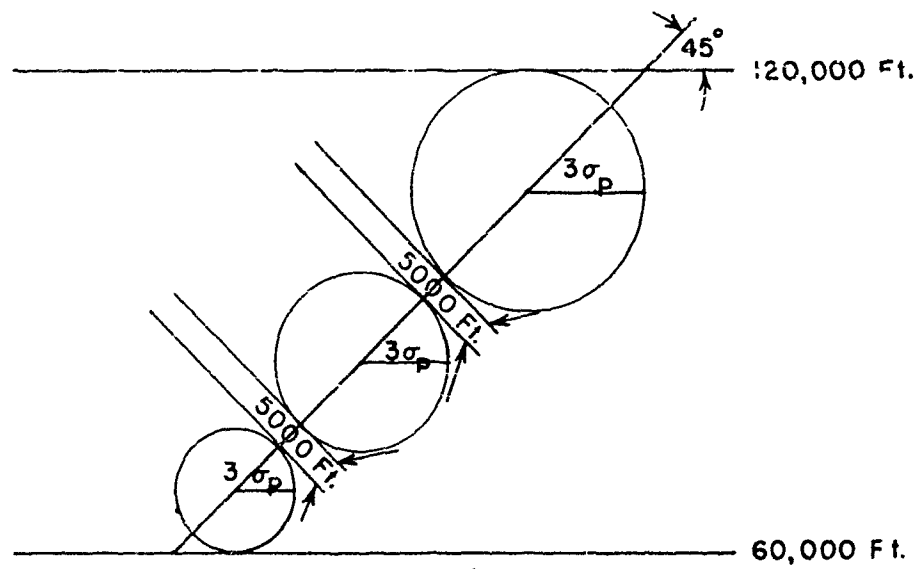
Let us postulate three interceptors in the sequence. Then each interceptor must have its launching delayed until its prediction-error circle is a good deal smaller than that of Figure 3-18, assuming no "range variability" in the missile. If one adopts an extremely conservative viewpoint, one may require that all of the error-circles be not only inscribable (centers in line) within the overall altitude-band of interception, but also that they be separated by 5000 feet as shown in Figure 3-19. Figure 3-19 (a) shows the limiting case for a 90° target trajectory. Figure 3-19 (b) for a 45° target trajectory. Actually it is probable that a less conservative requirement, i.e., slightly larger error-circles may prove to be acceptable. In any event, sequential interception may be seen to require a reduction in permissible prediction-error at launch to something like one-half to one-third the corresponding value for simultaneous interception. Numerical estimates of the resulting reduction in slant-range-at-launch are now being made. Considerations mentioned elsewhere (Section 3.1) in the present report emphasize that we can ill afford to reduce defended area by introducing further limitations on the maximum range-at-launch.

We have seen that close time-control of actual interception may impose an intolerable burden upon the missile capabilities in the case of simultaneous interception. Similarly, we find the shorter slant-ranges at launch which are demanded by the smaller error-circles of sequential interception are quite unacceptable. Clearly, neither alternative is acceptable. Other factors which bear upon the choice between these two modes of interception have been considered and indicate no clear-cut superiority of one over the other.

SECRET



(a)



(b)

FIGURE 3-19

SECRET

SECRET

However, a way out has been suggested. Recall that the reason for launching replicate interceptors is to overcome the limitations placed on single-shot kill probability by the lack of perfect reliability of the individual interceptor. Since we expect an overall kill-probability of 99%, we anticipate that more than one interceptor will successfully contact each target. But only one interceptor is required to come within the lethal radius of the interceptor to assure a kill. To bring about one such encounter with each target is the objective of the entire PLATO system. Now, suppose we launch the set of replicate defending missiles at the range permitted by an error-circle such as Figure 3-18, so as to achieve as nearly simultaneous contact with the target as may be. No reduction in range-at-launch is brought about, and no burdensome time-control requirements are imposed. One or more of the interceptors will approach the target on the final attack phase with some variable distance between interceptors. The distances separating them may be greater or less than the mutual interference distance. The computing facility is now asked to compare predicted miss distances for the several interceptors individually and to detonate the warhead of that interceptor which has the smallest miss distance. Other interceptors which are in the range of mutual interference would be lost, but this is unimportant since the overall objective is achieved.

3.2.3 INTERCEPT ALTITUDE

PLATO Technical Report 3.3-1* gave estimated ground damage and "expected" ground damage for nuclear bursts of various sizes and altitudes. These results were computed by making a first-order approximation to effects of atmospheric attenuation, and by projecting the thermal flux on a horizontal plane. The horizontal projection resulted in a picture in which thermal ground-damage rapidly approached zero as the burst altitude neared ground level. The worst case of all, and the more realistic, would be that for which thermal intensity is considered incident on a surface normal to the radius from the burst point. The minimum intercept-altitude is that burst altitude which gives maximum acceptable damage at the ground level.

The equation* used to obtain thermal intensity on a unit horizontal area was:

$$Q = \frac{E \exp \left[\frac{kt}{h} \sqrt{R_g^2 + h^2} \right]}{4\pi(R_g^2 + h^2)} \cdot \frac{h}{(R_g^2 + h^2)^{1/2}} \quad (1)$$

* PLATO Technical Report 3.3-1, "Selection of Intercept Altitude", by M. Stutzman, J. Eng, and H. Greenberg, 10 January 1955. (Secret)

SECRET

where

Q = thermal intensity on horizontal area, $\frac{\text{cal}}{\text{cm}^2}$

E = thermal energy of the weapon, calories

h = altitude of burst, feet

R_g^2 = ground range of burst, feet

k = absorption coefficient of atmosphere, feet^{-1} (or kilometers^{-1})

t = equivalent thickness of uniformly absorbing atmosphere, feet (or kilometers)

The fraction $\frac{t}{h}$ was taken to be unity when $t > h$.

The fraction $\frac{h}{(R_g^2 + h^2)^{1/2}}$ served to project the thermal flux on a horizontal surface.

We have reviewed the values* for k and t and find them reasonable for the degree of approximation which seems warranted. Omitting the horizontal projection factor in equation 1 gives:

$$Q = \frac{E \exp\left[-\frac{kt}{h} \sqrt{R_g^2 + h^2}\right]}{4\pi(R_g^2 + h^2)} \quad (1a)$$

Equation 1a has been used to give a revised estimate of thermal intensity at ground points. The results for a clear day ($k = 0.1 \text{ km}^{-1}$ and $t = 10 \text{ km}$)[#] and 3 MT yield are illustrated in Figure 3-20. (A thermal yield of 6.7×10^{12} calories per 20 KT was assumed.)[†] Inasmuch as acceptable thermal intensities vary widely for elements in a tactical area, we have not interpreted the results in terms of damage levels. One observes in Figure 3-20 that for a clear day the thermal intensity at ground zero is estimated at $10 \frac{\text{cal}}{\text{cm}^2}$ for a burst of 3 MT yield at about 56,000 feet.

* PLATO Technical Report 3.3-1, "Selection of Intercept Altitude", by M. Stateman, J. Eng, and H. Greenberg, 10 January 1955 (Secret).

[#] This corresponds to a visibility of about 24 land miles in the region below 10 km and to infinite visibility above 10 km.

[†] "The Effects of Atomic Weapons", Los Alamos Scientific Laboratory, September 1950 (Unclassified).

SECRET

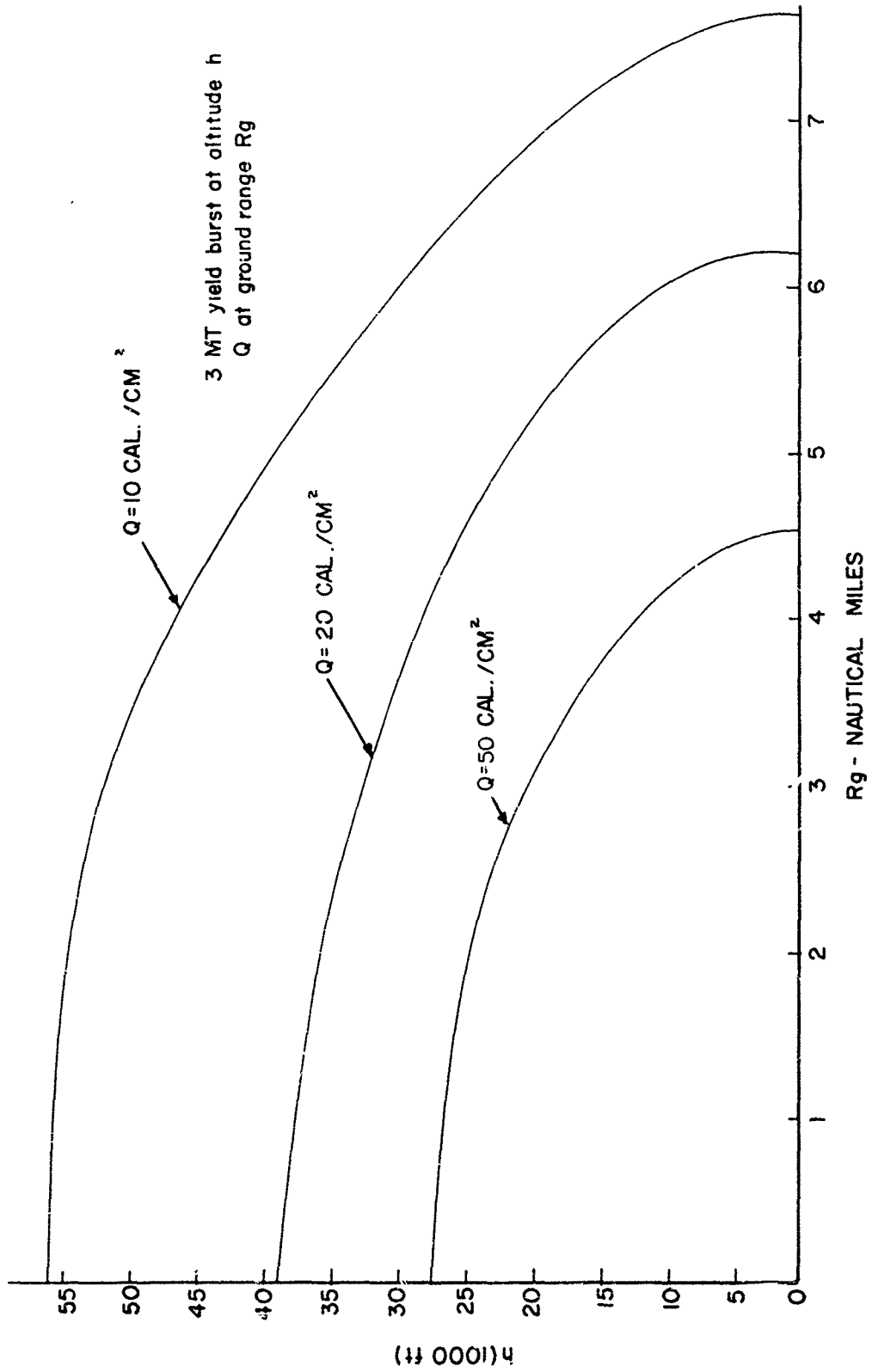


FIGURE 3-20. TOTAL THERMAL INTENSITY AT GROUND LEVEL, CLEAR DAY

SECRET

SECRET

Computations now in progress will treat similarly the case of a cloudy day with $k = 0.5 \text{ km}^{-1}$, $t = 5 \text{ km}$. This corresponds to a visibility of slightly less than 5 miles below an altitude of 5 km and infinite visibility above that level.

It is desirable to include estimates equivalent to those outlined above for yields ranging from 50 KT to 3 MT. In order to concentrate this information in a modest number of characteristic curves, it appears desirable to consider the advantages of employing dimensionless products as variables. Relationships among various dimensionless products are now under study. If the results of such a study follow the pattern of earlier dimensional analyses, one may also look for useful conceptual aids to emerge.

3.2.4 SYSTEM VULNERABILITY

3.2.4.1 Possibility Of Enemy Attack On PLATO

The attainment by the PLATO system of a high level defensive capability against ballistic missiles may cause the enemy to use other means of attacking the installations in the defended area (such as airplanes), or alternatively, may cause the enemy to attack the defensive system itself in order to permit effective attack on installations in the defended area. Thus, if the survival probability of the defended area against ballistic attack were 0.99, say, while the survival probability against an air attack of comparable magnitude were significantly lower, say 0.75, it would be quite likely that the enemy would resort to attack by air rather than by missile. As a consequence, if a high level defense against ballistic missiles is attained, the requirements as to the supply of interceptors and defensive warheads during a war may be greatly diminished since the enemy would be forced to use weapons other than ballistic missiles to achieve success.

To defend against the alternate enemy approach of attacking the defensive system itself, the vulnerability of the PLATO system to all forms of enemy action that can be directed against it, must be minimized. Consideration of the various ways of attacking the PLATO system (neglecting electronic countermeasures) leads to the conclusion that aircraft and short range missiles represent the major threats.

3.2.4.2 Attack By Short Range Missiles

The exact minimum range ballistic missile against which PLATO will be effective has not been determined. For missiles of longer than minimum range, the system will provide its own defense if all of its components lie within the defended area. The most effective defense against the shorter range missiles is to site the system so that it is beyond their range.

SECRET

It may be presumed that any area in which the PLATO system will be installed will be of sufficient military value to warrant some level of defense by friendly aircraft. The effectiveness of this defense is unknown but it is unlikely to reach the 0.99 level proposed for the PLATO system. It will probably be more effective against high level attacks than against low level due to lack of radar coverage, ineffectiveness of airborne intercept radar, and the restricted maneuverability of interceptors at low altitude.

3.2.4.3 Atomic Weapons Attack

Enemy aerial attacks directed specifically against the PLATO system, utilizing high level aircraft carrying atomic weapons, are not considered likely. This is based on the premise that if the enemy has the capability of attacking the PLATO system in this manner, he can similarly attack any installation in the defended area and will probably choose to attack directly the installations being defended. On the other hand, low level attacks by enemy aircraft utilizing conventional bombs and rockets are likely to be directed against the PLATO system.

The overall vulnerability of the Plato system is dependent upon the individual vulnerabilities of the various components or installations and the redundancy of these components in the system. The most vulnerable part in the system, as now envisaged, is undoubtedly the acquisition radar which is continuously radiating and is physically large and difficult to disguise. In addition, it is a part of the system which is not functionally required to be redundant. Other parts of the system are vulnerable to a varying but lesser degree.

Although the likelihood of atomic attack directed against the PLATO system itself is considered to be small, the system should be dispersed so that damage will be minimized if such attack takes place in the area where the system is installed. Pertinent data indicates that large radar antennas will suffer moderate damage (sufficient to prevent use until extensive repairs are effected) from atomic blast overpressures of the order of 3 psi and that radios, radar, and other electronic equipment are moderately damaged by 5 psi. The blast effect is considered to be the major cause of damage to equipment of this type, and this factor can be used for developing a pattern for the dispersing of the system to minimize damage. Based on the 3 psi criterion, parts of the system must be separated from one another by distances of the order of 12.5 miles to prevent any two from being damaged by one weapon of 1000 KT yield. For the 5 psi criterion and for weapons of 160 KT, the required separation is approximately 5 miles. While a defensive philosophy of "minimum damage" requires all parts of the system to be separated by some minimum distance, a modification of the

SECRET

philosophy to "maintenance of operating capability" would require only the redundant parts to be separated.

3.2.4.4 Attack By Low-Flying Aircraft

The establishment of an effective defense against low-flying aircraft using anti-aircraft guns and rockets is very costly. Some anti-aircraft gun or rocket defenses may exist in the areas in which PLATO systems are installed but the wide dispersion of the PLATO system will minimize the protection they can provide for the system. Some attached or organic defensive weapons will therefore be required with the maximum use of protective cover, and redundancy of the most vulnerable components. The entire question of how much redundancy should be built into the system, in addition to that required for proper system functioning, is one which will be studied as more system details and cost information become available. In arriving at a decision, consideration will also be given to the individual equipment reliabilities and the redundancy which must be provided to meet the system reliability requirements.

3.2.5 NATURE OF GROUND INSTALLATIONS

3.2.5.1 Introduction

As part of the continuing study of the requirements on the system, further study was made of the tactical installations PLATO may be required to defend. An idealized model of the tactical area was developed and on the basis of this model some tentative requirements for the size of the defended area have been derived. Operational models for the PLATO field unit with various sub-system capabilities were applied to this idealized tactical area to show the effects on the defended area of some of the alternative sub-system performances. The performance of the system in the defense of cities was also investigated briefly. For this role we have attempted to evaluate the performance when the size of the defended area has already been set by the tactical role. Study of the requirements is continuing and will be presented in subsequent reports.

3.2.5.2 Tactical Unit Size

The tactical doctrines of the U. S. Army are currently undergoing study and revision to take into account the effects of nuclear weapons. Most thinking seems directed toward smaller and more mobile units. On the basis of Operations Research Office, Glen L. Martin, and Continental Army Command reports, it appears that the sizes of the installations will differ at the front and the rear of a tactical area. The largest size ground units in the rear will be airfields which will occupy approximately four

SECRET

square miles, while the battalion size troop units in the forward area will occupy approximately one square mile.

3.2.5.3 Tactical Unit Proximity

Two factors are basic to the mutual proximity of tactical units.

(a) It will be very difficult to develop a high survival probability against nuclear attack by aircraft.

(b) Even if high level defense against aircraft can be developed, the ground units will not be concentrated because it would then be advantageous for the enemy to expend considerable effort to saturate the defensive systems. These attacks could be by missile or aircraft.

In view of the above factors, ground targets in a tactical area will be dispersed. If we assume that the tactical area commander will choose to disperse his installations so that only one will be damaged by one nuclear weapon, then the units must be separated by a distance equal to the diameter of the lethal effects of the largest size nuclear weapon the enemy would reasonably use. This distance is estimated as between 10 and 20 miles for installations in the rear, and between three and seven miles for troop units in the forward area.

3.2.5.4 Model Tactical Area

Knowing that the tactical area of the future will consist of many small dispersed units, it is possible to set up an idealized tactical area based only on the unit size and the dispersion between units. Such an area is shown in Figure 3-21.

The idealized tactical area shown in this figure would be modified in an actual situation to allow for tactics and terrain. Any terrain allowances would cause the units to be separated further. If the tactical situation requires the risk of losing more than one unit per attacking weapon, this would decrease the separation.

The number of installations defended increases in steps as the defense radius is increased. This step function is shown in Figure 3-22 for the rear area case. Taking the unit size as two miles in diameter and the dispersion between the closest points of adjacent installations as ten miles, the placement of the center of the defense for maximum coverage and the ideal radii can be worked out simply from the geometry. A forward area case is shown in Figure 3-23. For this case a unit size of one mile diameter, dispersions of three miles between battalions seven miles between divisions, and 15 miles between corps were assumed. Part or all of the 19 unit sites within the division area might be occupied at one time.

SECRET

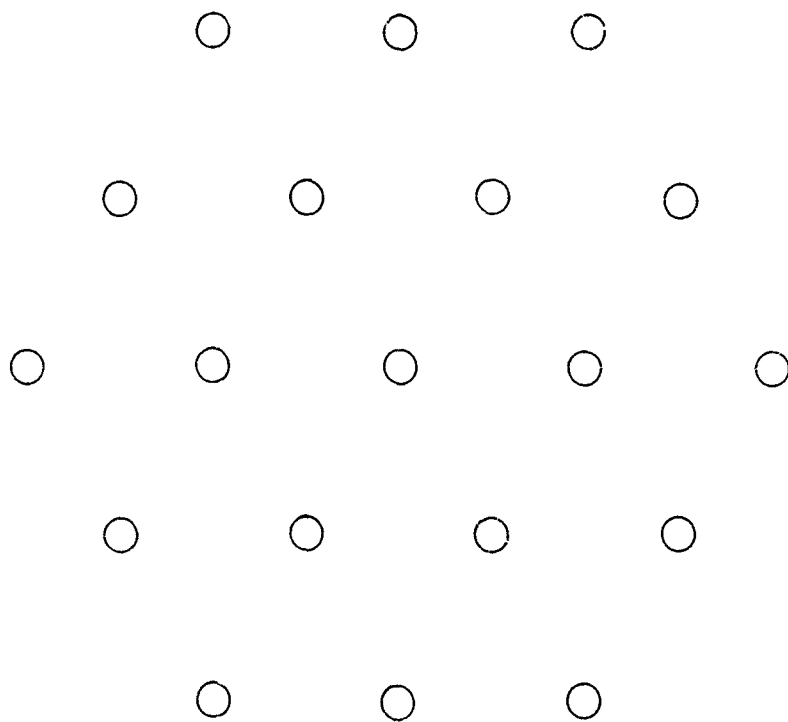


FIGURE 3-21. AN IDEALIZED TACTICAL AREA

SECRET

SECRET

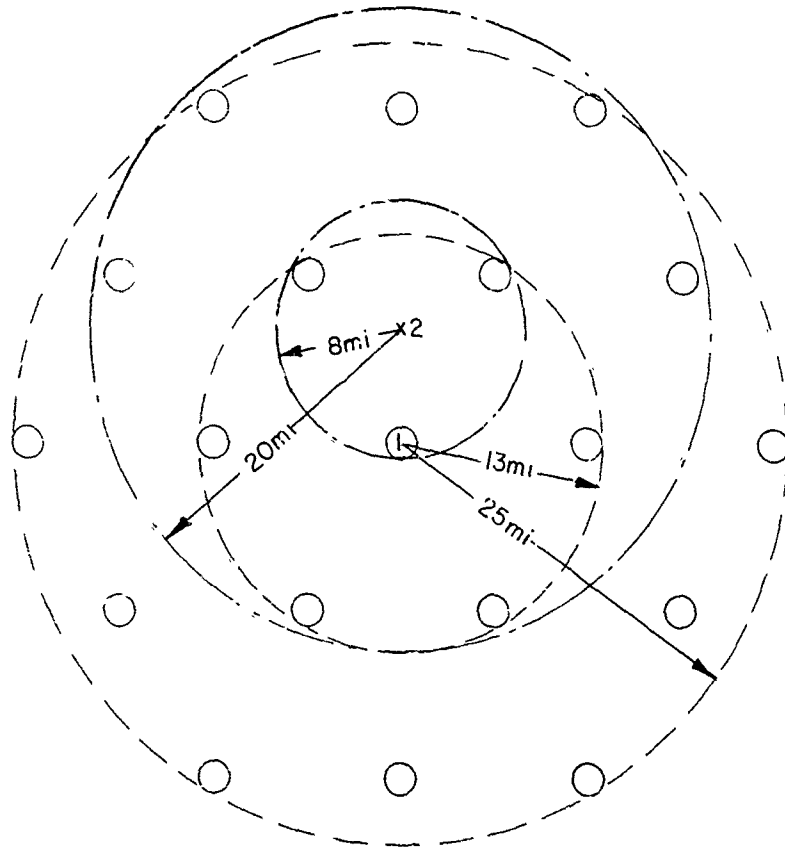


FIGURE 3-22. AN IDEALIZED REAR SECTION OF A TACTICAL AREA WITH DEFENSE SYSTEMS OF VARYING RANGE OF CAPACITY

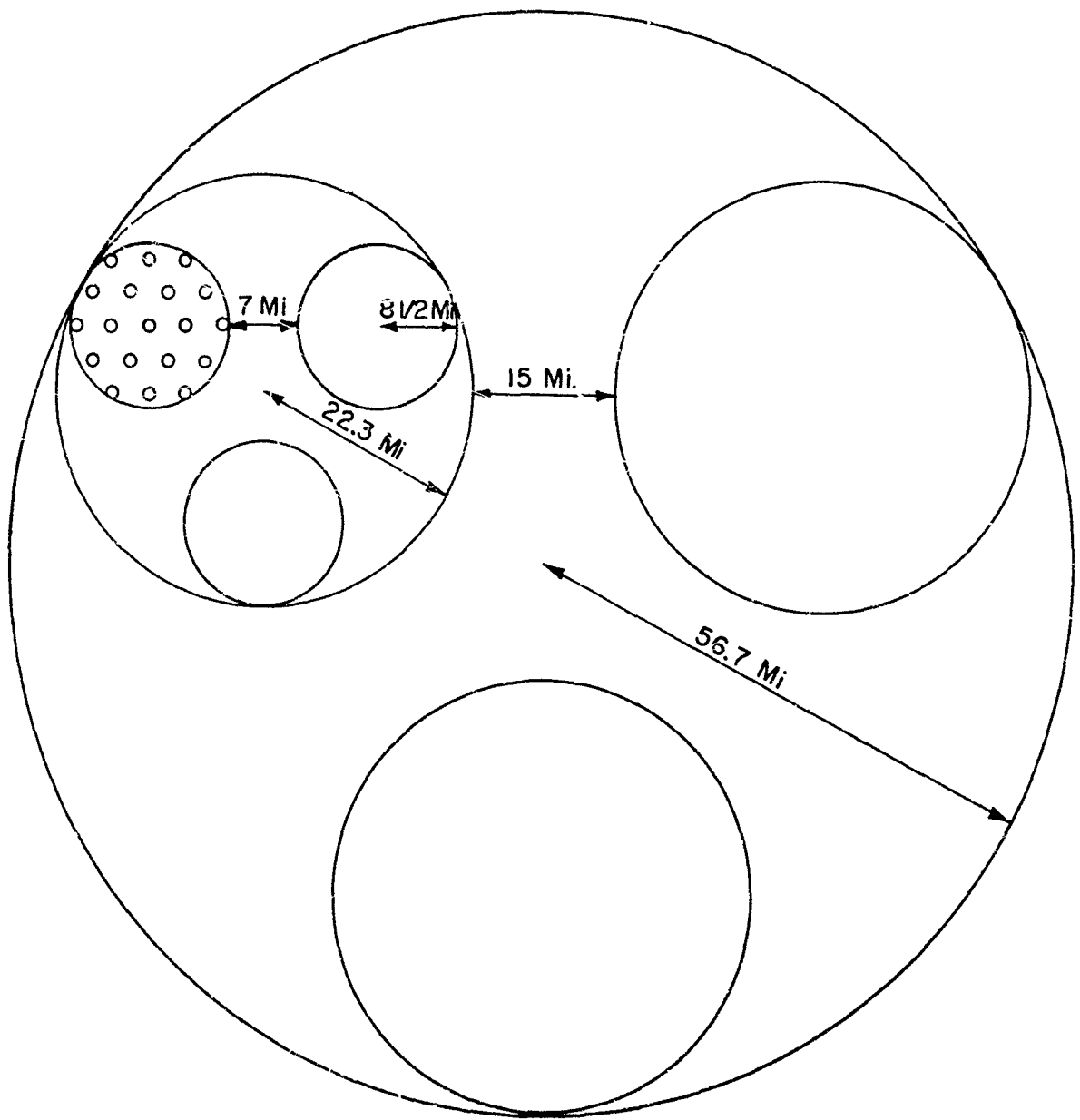


FIGURE 3-23. AN IDEALIZED FORWARD SECTION OF A TACTICAL AREA

SECRET

The number of sites for different size defended areas based on the assumed unit area sizes and dispersions is shown in Figure 5-24 for the rear case. The specific numbers shown may vary as the study continues; however, the step nature of the graph is characteristic.

In addition, the final choice of the desired size of the defended area will be governed by many factors not covered here, such as technical feasibility considerations, costs, the problems associated with combining several systems, and other operational factors.

OPERATIONAL MODELS

Since the PLATO system probably will not be used in the forward part of the tactical area, only the rear case will be considered further. Three models for the PLATO field unit operation in the rear are considered:

- Model I. The PLATO radar and missiles have equal area capability.
- Model II. The PLATO radars have less area capability than the missiles.
- Model III. The PLATO radars have more area capability than the missiles.

Before evaluating these models, additional considerations can be noted.

- (1) The criterion for location of launch sites is still open. However, in order to reduce the vulnerability of the PLATO system to other forms of attack, redundancy of the launch sites, with the same dispersion (ten miles) as among other installations, is required. The number of launch sites is assumed to be at least three.
- (2) As the number of launch sites is increased, the number of warheads required in the supply chain will increase. The number of warheads expended, however, is not affected by the number of launch sites.
- (3) In order to prevent saturation of the system, several launchers are required at each launch site. The number of launchers required will be small if the missiles at all three sites have sufficient range capability to cover the entire defended area. If the missile coverage from the three sites does not overlap, more missiles and warheads will be required at each site.

SECRET

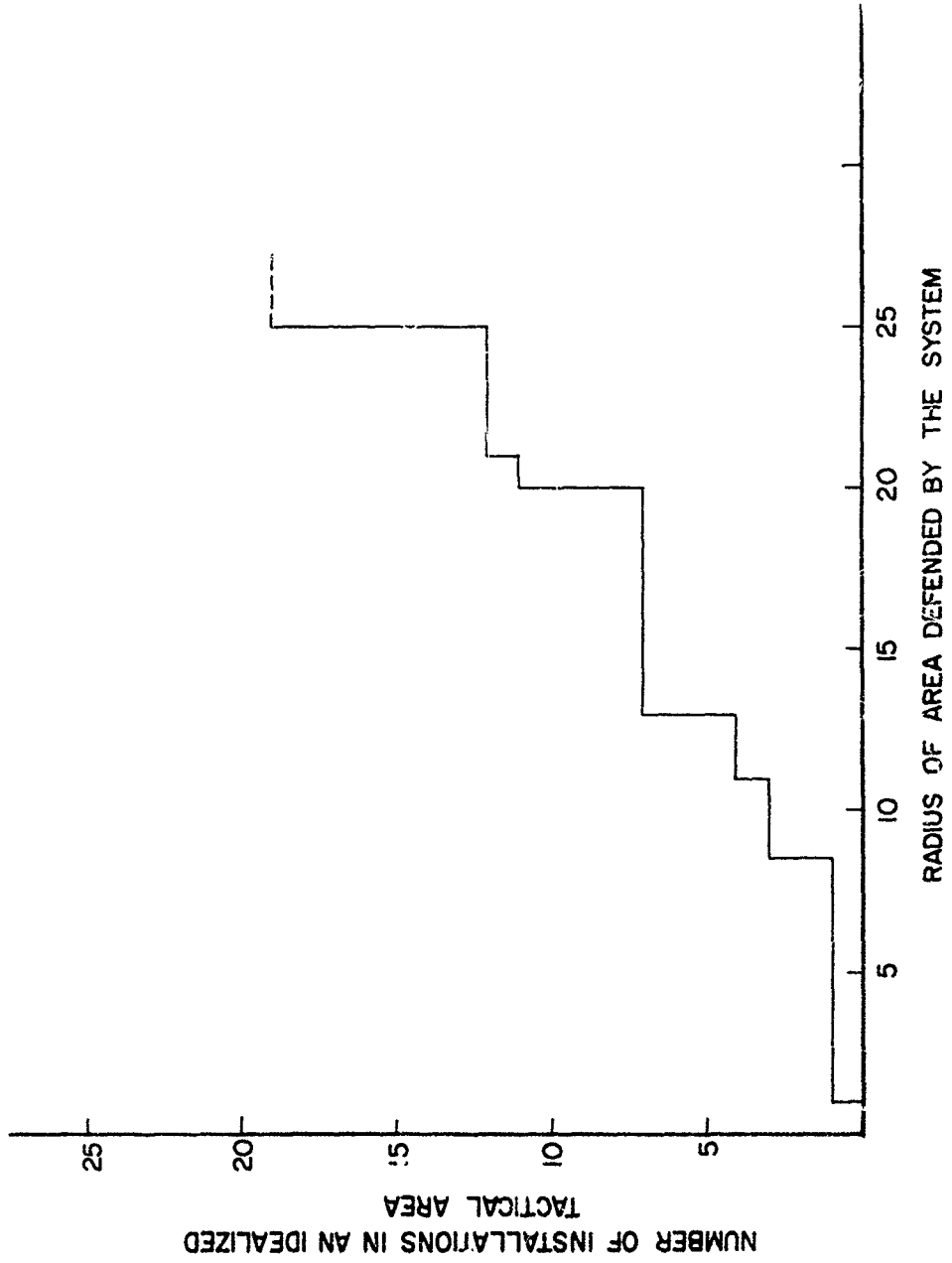


FIGURE 3-24. NUMBER OF INSTALLATIONS DEFENDED IN THE REAR OF THE TACTICAL AREA VS. THE RADIUS OF THE DEFENSE SYSTEM

SECRET

SECRET

Model I is shown in Figure 3-25. In this model only the center installations are covered from all three launch sites. Model II is shown in Figure 3-26. In this model all the installations are covered from all three launch sites. Model III is shown in Figure 3-27. In this model none of the installations are covered from three sites. Model II requires the smallest stockpile of missiles and warheads, but the most performance from the missile. Model III requires the least missile performance, but the largest stockpile.

The choice between these models will result from further study of technical feasibility, costs, defense against simultaneous attacks, etc. These problems are under study and the integration of the results of these studies with the models will be presented in succeeding reports.

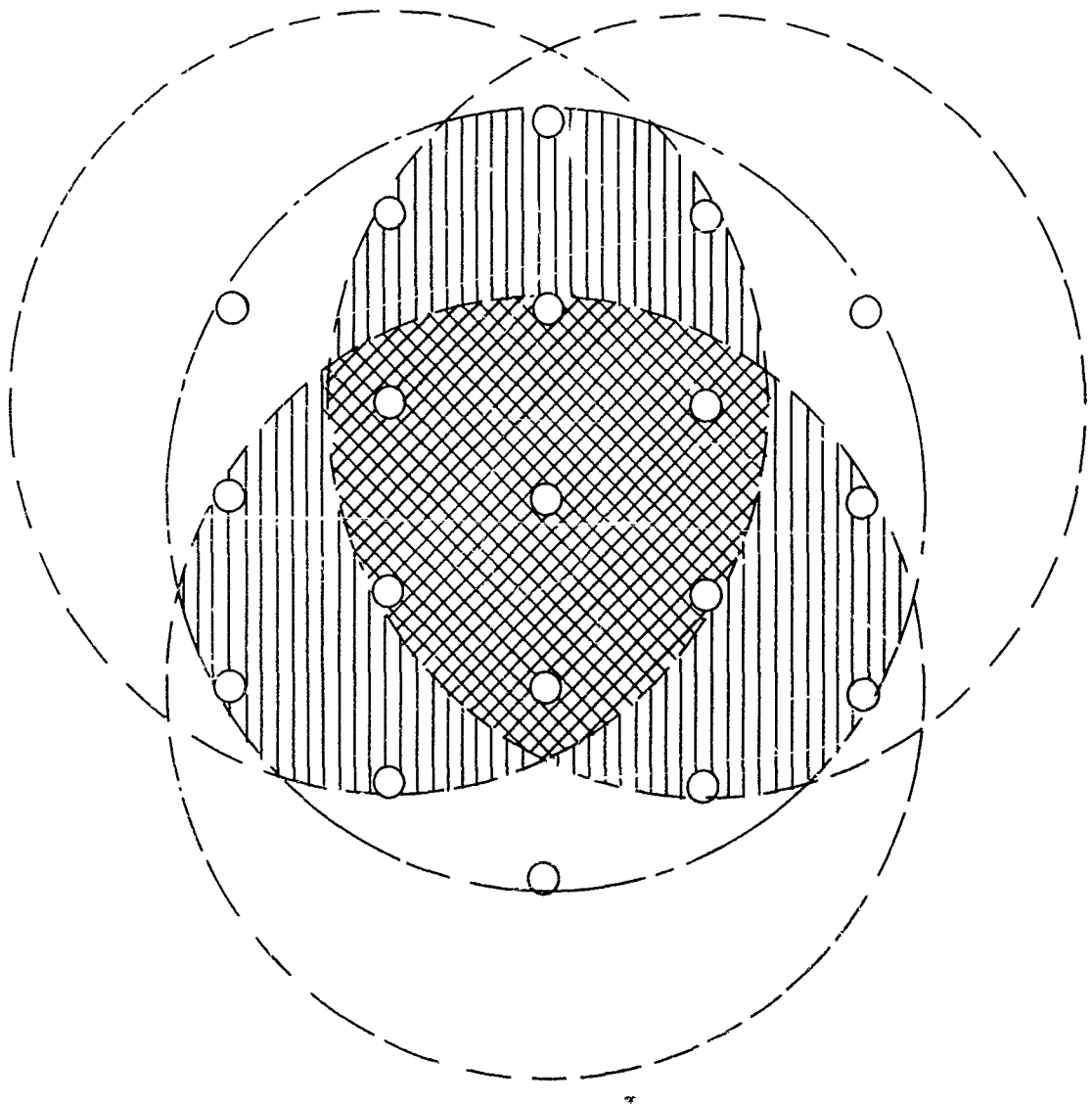
3.2.5.5 Defense Of Cities

In order to obtain some idea of the performance of a PLATO system used in the defense of cities, we have examined the large cities in England and the proximity of these cities to each other. Data on England was used because this information was readily available and England is among the more densely populated areas in Western Europe. This brief study showed that all except two cities have areas of less than 60 square miles.

Although the size of the defended area to meet the tactical requirements for the PLATO system has not been set, it will most likely be much larger than 60 square miles. Therefore, the proximity of cities was examined to determine the number of cities protected by a likely PLATO system. In order to obtain a measure of performance, circles of 12.5, 25, and 50 mile radii were placed around the 57 cities with populations of over 100,000 so as to contain the largest number of these cities. This data is presented in Figure 3-28, which shows that if a defense radius of 50 miles is used, nine such defenses will protect all the large cities in England. If a defense radius of 25 miles is used, 13 such defenses are required to protect all the large cities. If the defense radius is 12.5 miles, 28 such defenses are required (This is a calculated value although not shown on the figure.) This figure also shows that as the defenses are allocated to locations where the large cities are not fortuitiously close together, the percentage of the area with high population density decreases.

For example, Figure 3-28 shows that if five PLATO systems are assigned to defend England and the system defense radius is 50 miles, then about 90 percent of the large cities will be protected. If the defense radius is 25 miles, then about 70 percent of the large cities will be protected. If the defense radius is only 12.5 miles, only 45 percent of the cities are protected.

SECRET



- RADAR COVERAGE LIMIT (25 MILE RADIUS)
- MISSILE COVERAGE LIMIT (25 MILE RADIUS)
- XXXXXXXXXX COVERAGE FROM 3 LAUNCH SITES
- ===== COVERAGE FROM 2 LAUNCH SITES

FIGURE 3-25. MODEL 1, EQUAL RADAR AND MISSILE RANGE CAPABILITIES

SECRET

SECRET

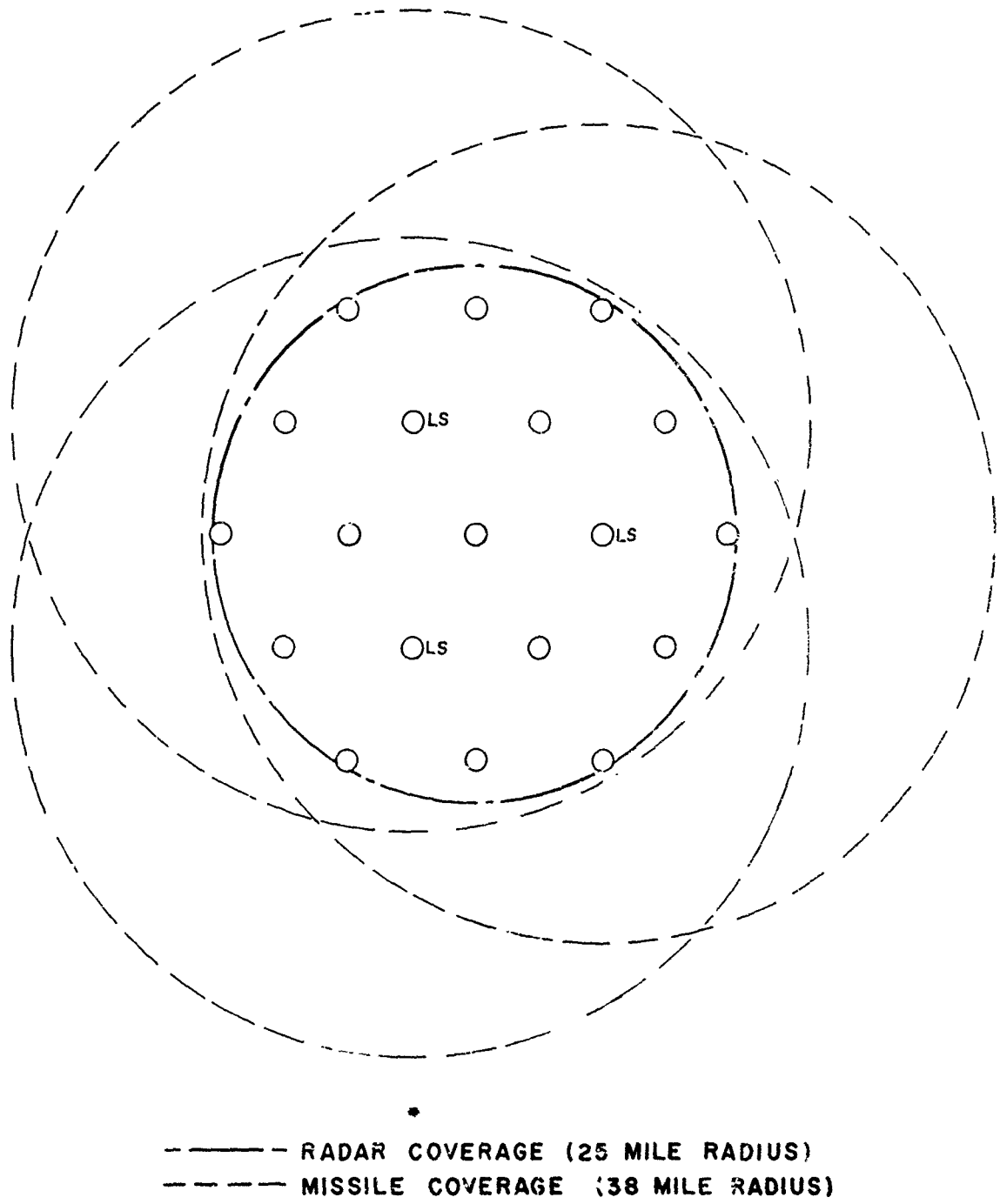
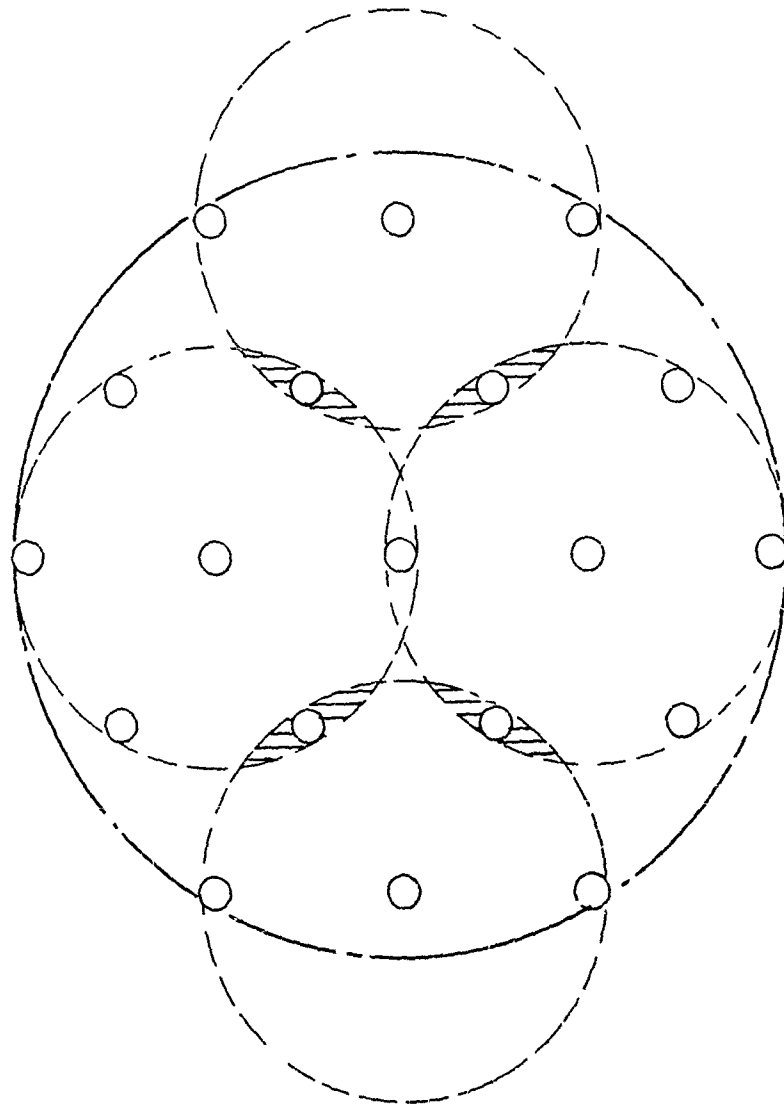


FIGURE 3-26. MODEL II, RADAR RANGE CAPABILITY LESS THAN MISSILE RANGE CAPABILITY

SECRET



——— RADAR COVERAGE (25 MI. RADIUS)
- - - - MISSILE COVERAGE (13 MI. RADIUS)
==== COVERAGE FROM 2 LAUNCH SITES

FIGURE 3-27. MODEL III, RADAR RANGE CAPABILITY GREATER THAN MISSILE RANGE CAPABILITY

SECRET

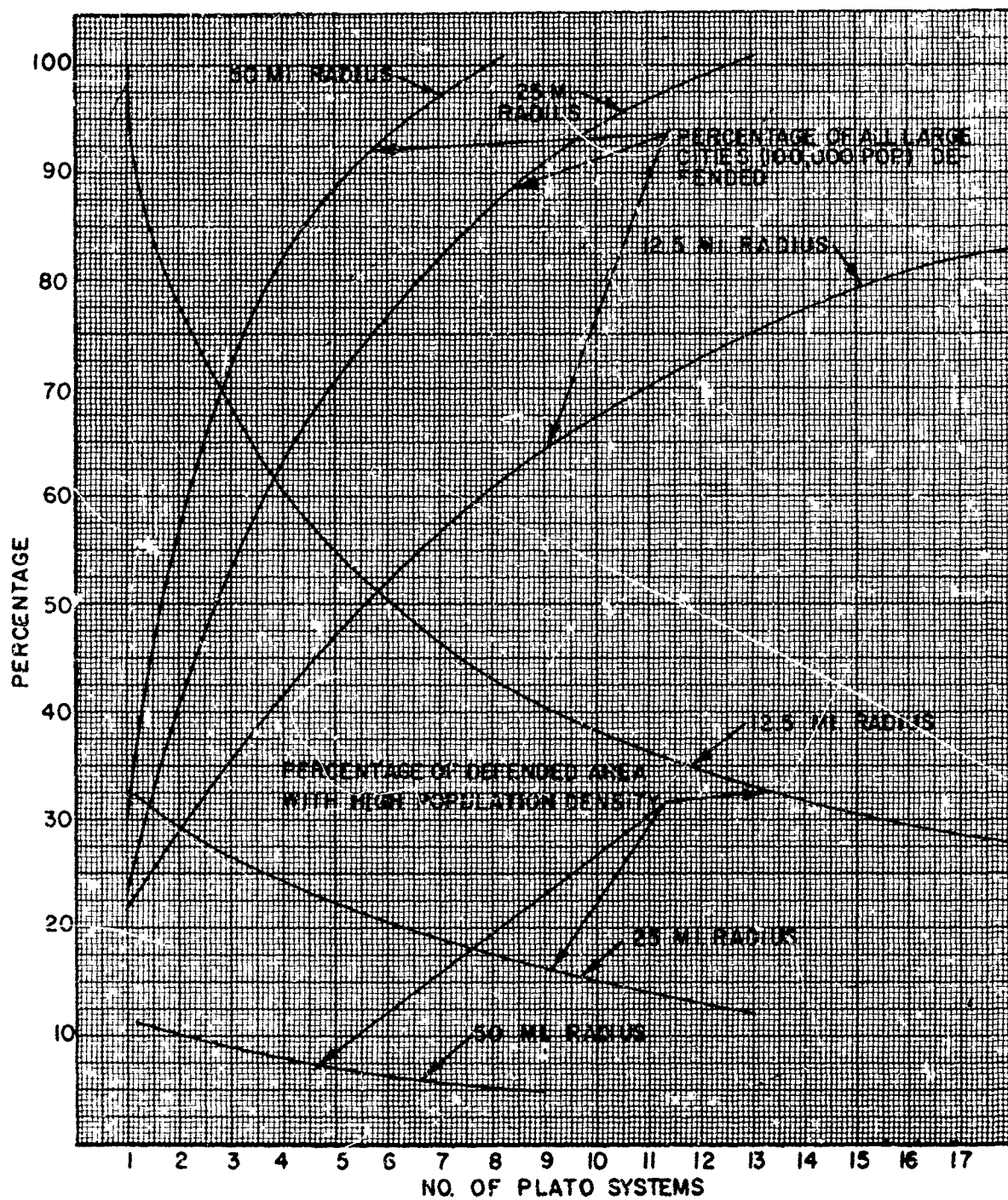


FIGURE 3-28. NUMBER OF PLATO SYSTEMS TO DEFEND THE LARGE CITIES OF ENGLAND

SECRET

Not all of the area within the defense has a high population density, so that, for example, for the 50, 25, and 12.5 mile radii of defense, the portions of the areas with the high density are 5 percent, 20 percent, and 55 percent, respectively.

This study of cities shows that a PLATO defense designed for tactical areas would provide good performance in the defense of cities.

REFERENCES

1. Operations Research Office, *Report ORO-R-14*
Chevy Chase, Md. 27 August 1953.
2. Glen L. Martin Co., *Ballistic Missile System-Ground Support*, ER7067B, March, 1955.
3. PLATO Report 210/36, *Trip Report, Continental Army Command*, August 1955.
4. Rand-McNally and Co., *World Atlas*, N.Y., 1950.

3.2.6 TECHNIQUE OF ENEMY ATTACK

Preliminary work has been done to investigate the best tactics which the enemy can use to attack ground installations defended by a PLATO system. The analysis consists of two phases: a study of enemy tactics to penetrate the defense system and a study of enemy tactics which will optimize damage to the defended ground installations. Aspects of the first phase are presented at this time.

Because no defense can be absolutely perfect, each attacking target missile will have a certain probability of penetration. How this probability can be increased by tactics which exceed the capacity to defend is the main thesis of the first analysis. Results of the investigations will be applied to a future more rigorous analysis of effectiveness versus costs.

3.2.6.1 Enemy Tactics

The obvious enemy tactic to penetrate the defense is to exceed the defense capacity of any of the individual components in the PLATO system. This can be accomplished by having more attacking target missiles than can be handled simultaneously by the prediction system, by exceeding the rate of fire of the interceptor launchers, or by continuous fire which exhausts the supply of interceptors. Note that there still exists a certain probability of penetration if none of the above is accomplished; however, this

SECRET

is considerably smaller than if there are target missiles which cannot be defended against.

To facilitate analysis, the PLATO defense system is considered to consist of a fire control system and an interceptor missile system. In addition, it is believed that the components can achieve the below listed capabilities before cost and complexity of additional capacity become prohibitive.

- (1) Acquisition Radar and Prediction System: capable of handling approximately 6 target missiles simultaneously.
- (2) Triangulation and Illuminating System: capable of handling approximately 24 target missiles and airborne interceptors simultaneously.
- (3) Guidance System: capable of handling 18 airborne interceptors.

Exact capabilities and requirements for the fire control system and interceptor missile system are to be determined by the results of present and future analysis.

The most critical component in the fire control system is the prediction computer which has a fixed simultaneous tracking capacity. Because a prediction computer track is occupied for a specific length of time, the computer is said to be saturated when

$$(e_{i+T} - e_i) = S$$

where

T = simultaneous tracking capacity of the prediction computer.

i = the reference number of the target missile in a sequence of at least T attacking target missiles.

e_i = time at which a computer track engages the i^{th} target missile.

S = the duration of engagement for a single track.

If the left hand term is less than (S), there will be more target missiles than can be defended against, and these extra target missiles will have a probability of nearly one in destroying the defended ground installations. Assuming that the dispersion of arrival times about the intended arrival time approximates a Gaussian distribution, the equation which indicates how well the enemy succeeds in saturating the defense systems:

SECRET

$$q = \frac{\bar{n}}{T \sigma \sqrt{2\pi}} \int_S \exp\left\{\frac{-x^2}{2\sigma^2}\right\} dx$$

where

q = index of saturation

T = maximum target missile capacity of the prediction computer

\bar{n} = number of arriving target missiles

σ = standard deviation of arrival times about intended arrival time

S = duration of engagement for a single track

When q is less than one, the prediction computer will not be saturated. When q is equal to one the computer is saturated with the number of target missiles during (S) equal to the tracking capacity. When q is greater than one, there will be an excess of target missiles, and the defense fails to intercept all attackers.

Because the duration of engagement for a single track is of the order of 90 seconds, it appears that the enemy could well have the capability of mounting a simultaneous attack. Data from the Redstone Arsenal indicated the following ranges of variations for arrival time as a result of various factors:

- | | |
|---|----------------|
| (1) Variation in actual flight time | 5 secs. |
| (2) Variation in take-off time after ignition (depending on type of ignition) | 1.5 - 10 secs. |
| (3) Variation in synchronizing launch times | 2 secs. |
| (4) Variation in missile preparation time | 10 mins. |

Note that the latter can be easily overcome by preparing extra missiles and firing those which are ready. Furthermore, if the enemy desires simultaneity of arrival, he will design a system necessary to achieve this objective. Also, since the PLATO system is being planned to achieve simultaneity with several interceptor missiles, it would be folly not to give the enemy credit for achieving a similar capability. Conversations with CONARC indicate that simultaneity is possible, especially since PLATO is planned for five to ten years in the future. It should also be noted that

SECRET

simultaneity need not be accomplished with a large number of target missiles considering the lethal radius of an atomic warhead and the size of the defended area.

Another method by which the enemy can hope to attack the defended area without being intercepted is to fire more missiles than the defense is capable of intercepting with its available supply of interceptors. This is actually a very costly procedure and would not be resorted to unless all other methods fail. However, it could occur during a sustained attack during which the catastrophic "super saturation" fails to materialize.

Therefore, the basic load and resupply rates must be predicated on the expected number of target missiles and the probable strategic allocation of the critical material to this type of defense.

If N is the number of target missiles expected to arrive successfully during a given interval of time, I the number of interceptors to be launched per target missile, the supply of interceptors must be at least

$$M = \frac{N I}{u}$$

where u is the reliability of interceptors considering checkout or launching failure. Should the actual number of attacking missiles be greater than was expected, the system will still be able to defend provided the situation is recognized before the interceptor supply is exhausted. This requires that the number of interceptors must be decreased to some new value I_i (no longer a fixed value) such that

$$\sum_{i=1}^{\bar{n}} \frac{I_i}{u} = \frac{N I}{u}$$

where \bar{n} = number of target missiles actually arriving.

The defense will fail if the launchers cannot maintain a certain required minimum rate of fire, regardless of the number of target missiles which can be handled by the prediction computer and the availability of interceptors. Two types of launchers are contemplated to maintain the required rate of fire: individual launchers for each of the interceptors and automatic launchers. The case of individual launchers is quite simple in that the required number of launchers must equal the number of interceptors expected to be launched during an attack.

The case of automatic launchers is somewhat more complex. A minimum of $\frac{T I}{J}$ launchers must always be available in order to defend against T

SECRET

simultaneously arriving target missiles. Additional launchers must be available if the reload cycle is greater than the duration of track engagement, hence

$$L_A = \frac{T I t_L}{u S}$$

where L_A is the required number of automatic launchers and t_L the time to ready a launcher and interceptor.

3.2.6.2 Probability Of Defense

A mathematical model for the probability of defending the ground installations successfully has been developed in terms of the number of enemy missiles launched, their reliability, and the PLATO defense capability.

The probability D_n that none of the target missiles penetrate is of the form

$$D_n = \sum_{i=0}^Q B(n, i, r) P_i$$

where

$B(n, i, r)$ = the binomial probability of i target missiles arriving successfully out of n launched missiles, each having a reliability of r .

P_i = the probability of intercepting the i target missiles successfully

Q = maximum number which the system can intercept due to limitations in computer capacity or number of available interceptors.

The equation is valid under the condition that the number of attacking missiles is less than the number of expected target missiles. Hence, D_n is the best the system could expect to attain.

It will be observed that the equation is essentially the same as the one which appeared in Section 3.2.1 of the 7th Quarterly Report. The earlier equation did not take cognizance of the fact that tracking of target missiles and interceptors were two distinct and separate functions. The new equation takes into account that the two functions are separate and distinct and that computer tracks for target missiles and interceptors are not interchangeable.

SECRET

Evaluation of the equation for various values of the parameters is still in progress. However, analysis so far indicates a point of diminishing returns occurs for a prediction computer capacity of about six simultaneous target missiles and a defense with 18 successfully launched interceptors.

It further appears that the enemy must increase his efforts in large increments rather than by small increments if his chances of success are to be materially increased. Consequently, the defense should be prepared to increase its capability by large increments if a high level defense is to be maintained.

3.2.6.3 Future Work

It is planned to extend the present work to encompass additional attack techniques on an effectiveness versus cost basis. Such considerations will include likely distribution of enemy effort within a defended zone so as to minimize his chances of over-kill, and the effect of widely dispersed launch sites on survival probability.

Adaptability of the PLATO defense system against other weapons is also under consideration.

3.2.7 AVAILABLE WARNING TIME FOR PASSIVE DEFENSE

In normal operation the PLATO system must predict a point of impact for each potentially dangerous target detected by the radar. This prediction is made regardless of the location of this impact point with respect to the defended area. This prediction can serve as a warning to the defended area and to the areas adjacent to it. At a recent conference with the Continental Army Command, they stated that even 30 seconds warning could materially reduce the troop casualties due to an atomic blast.

The flight time remaining after the first impact prediction is plotted in Figures 3-29 and 3-30 against ground ranges and launch angles of enemy missiles. From these figures it can be seen that the maximum warning times against short-range Redstone-type missiles launched at a 45° angle of elevation vary from 126 seconds for 30 n.m. range to 244 seconds for 150 n.m. range. As the target missile range increases, the warning time increases up to a maximum of 289 seconds at 300 n.m. and then decreases to a minimum of 129 seconds at 1000 n.m. when the target missile is launched at a 45° angle of elevation. If the radar is forward of the impact, the amount of warning time is increased; and if the radar is behind the impact, the amount of warning time is decreased.

SECRET

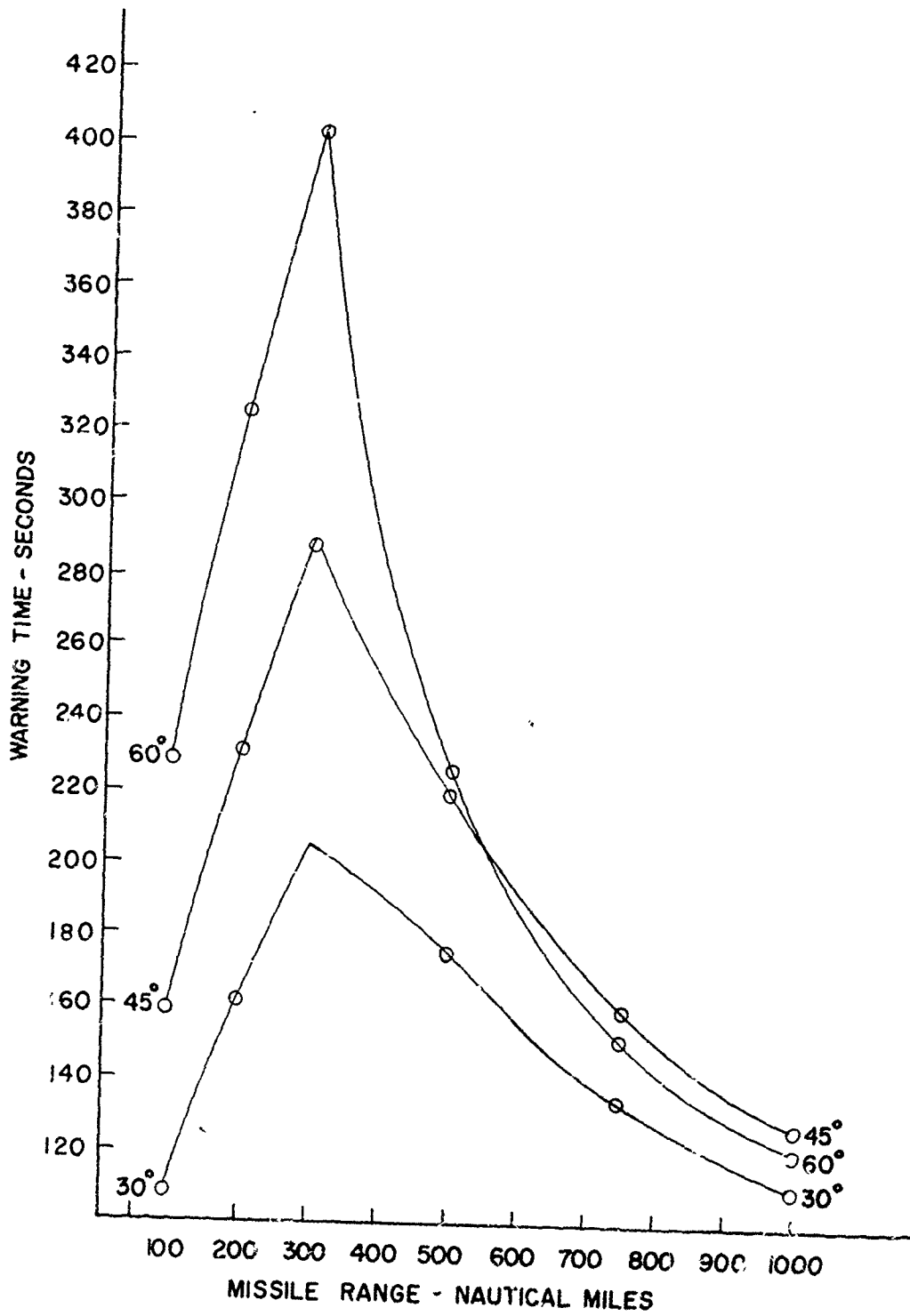


FIGURE 3-29. MAXIMUM WARNING TIME AGAINST MISSILE RANGE WITH 30°, 45°, 60° LAUNCH ANGLE OF ELEVATION

SECRET

SECRET

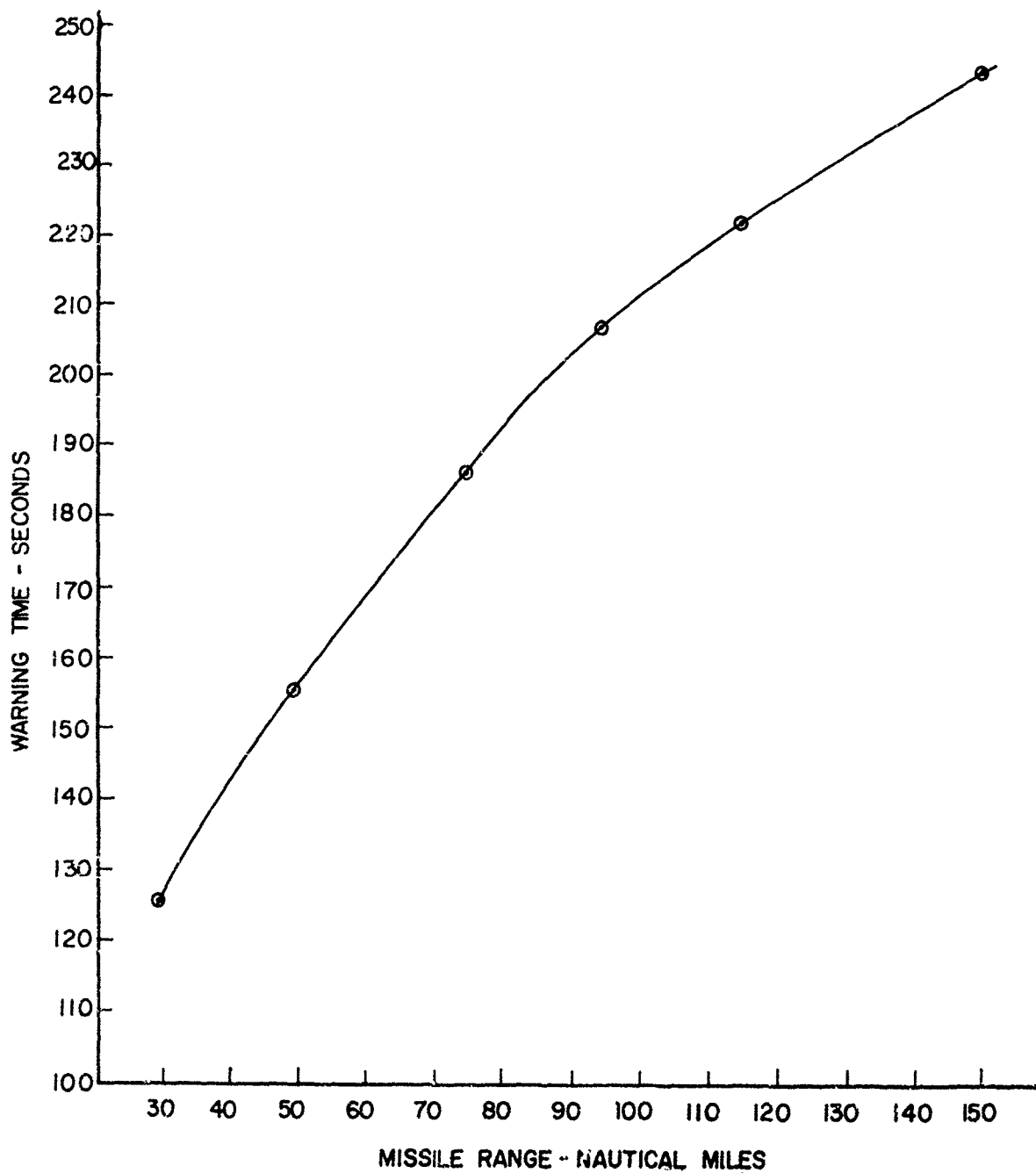


FIGURE 3-30. MAXIMUM WARNING TIME AGAINST REDSTONE MISSILE RANGE, WITH LAUNCH ANGLE OF 45°

SECRET

SECRET

As the launch angle of elevation increases from 30° through 45° to 60°, the warning time is correspondingly larger for short and medium range target missiles. However, in the case of the longer range missiles (750 n.m. and 1000 n.m.) the 45° launch angle of elevation yields an amount of warning time greater than the warning time provided by the 60° launch angle of elevation.

Predicting where the missile will impact on the ground involves an error. This error is dependent upon the range of the missile and its launch angle. This error must be considered here because it affects the size of the area to be alerted. The size of the area to be alerted becomes smaller as the length of tracking time is increased (and therefore the impact point prediction error is decreased). On the other hand, an increase in tracking time reduces the amount of warning time and, consequently, the time which the defended area has to take defensive measures. Due to the initially large size of the possible impact area, the problems of disseminating the warning will be severe, and the number of false alarms will be high.

The following is an example of the decrease in the size of the area to be alerted by increasing the tracking time. If an impact prediction is made on a target missile of 1000 n.m. range, launched at 45°, when it is 225 n.m. from the radar, 106 seconds of warning is available, but the area that must be alerted is of 45 n.m. radius. By waiting until the target missile is 150 n.m. away, the warning time is reduced to 68 seconds for a possible impact area of 12 n.m. radius. The decision as to when the warning should be issued, may be reserved for the field commander to make on the basis of this kind of information, calculated in advance.

In general, the PLATO system can furnish sufficient warning to troop units to allow them to take cover and, thereby, minimize casualties from atomic attack.

Further study is required in order to determine optimum warning time and size of the area that must be alerted.

SECRET

61

SECRET

SECTION IV
ENGINEERING STUDIES

4.1 ACQUISITION RADAR

4.1.1 GENERAL

During the last quarter the acquisition radar studies have included:

- (1) Further consideration of the effects of radar parameters on overall system performance, and how these parameters may be varied to increase defended area.
- (2) Engineering studies, to more completely specify the radar form and performance.

The following sections present the progress in each of the above categories.

4.1.2 RADAR PARAMETERS AND SYSTEM OPTIMIZATION

The relationship of radar performance and system optimization has two aspects; the variation of measures of system performance, such as defended area, with variations in radar performance; and the costs of making such variations compared to the costs of variations in other system parameters. The radar parameter which most directly affects system performance is σ_{p1} , the standard deviation of target prediction error at the time of launch of the interceptor. The prediction accuracy is in turn controlled mainly by the following:

- (1) Single point or present position measurement accuracy of the radar (σ_{p1})
- (2) The radar scan interval (T_s)
- (3) The maximum range of detection (r_0)
- (4) The location of the radar with respect to the impact point (D) and volumetric coverage of the radar.
- (5) The possibility of the use of triangulation radar data blended with acquisition radar data.

These topics will be discussed in turn.

SECRET

SECRET

4.1.2.1 Present Position Measurement Accuracy

In Quarterly Progress Report No. 7, the possibilities of beam interpolation and beam-splitting as means of improving acquisition radar angle measurement were discussed. It was pointed out that these methods are limited in accuracy by random noise errors at long range and by non-random or bias errors at short range. Three cases, corresponding to three different levels of sophistication in radar design, have been postulated. These are:

Case I: Essentially the Phase I radar with angle measurement accuracy limited at long range by beam selection errors and at medium and short range by angle quantization in one-beamwidth steps.

Case II: A radar limited in angle measurement accuracy at long range by beam selection, beam-interpolation, and beam-splitting errors varying approximately as R^{-2} , and at short range by bias or non-random errors of magnitude $\beta/4$, where β is the beamwidth.

Case III: Similar to Case II except that improved range measurement is postulated, and a short range bias error of magnitude $\beta/6$ is assumed.

These cases were chosen to encompass the possibilities in radar design which affect present position measurement accuracy. The detailed range and angle dependence of σ_m for these cases is being studied. In the 7th PLATO Quarterly Report, the beam interpolation accuracy results were presented for one method of beam interpolation. The effect of the beam selection process on radar accuracy has been derived and is presented below:

4.1.2.2 Errors in Radar Angle Measurement Due to Errors in Beam Selection

The accuracy of the angle indication in the Case I radar is determined by the probabilities of selecting each of the individual beams. This selection is accomplished on the basis of relative signal strength in the presence of noise. Since the signal strength in each of the beams is a function of the angular coordinate of the targets (ξ^*), the probability distribution will similarly depend on ξ^* . Consider Figure 4-1. In this figure the target is located at ξ^* near the center of beam ξ_0 , resulting in a high probability of selecting beam ξ_0 and small but finite probability of selecting the adjacent beams. For a target near the cross-over point of adjacent beams, the probability distribution is as shown in Figure 4-2. In this case, since the signal strengths in adjacent beams are approximately equal, the probabilities of selecting either of the two adjacent beams are approximately equal. As the range of the target increases, the signal to noise ratio decreases, and the distributions are spread out and reduced

SECRET

in amplitude until at infinite range the probability of selecting a given beam is uniform over all beams.

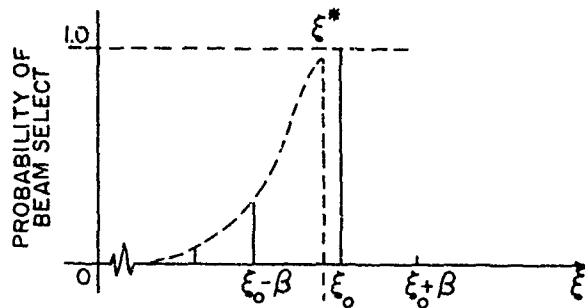


FIGURE 4-1. TARGET NEAR CENTER OF BEAM ξ_0 .

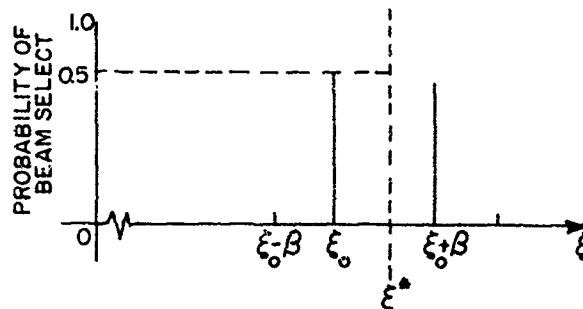


FIGURE 4-2

In the Case I acquisition radar design, (where no beam interpolation is done) with a target at $\xi^* = \xi_0$, the probability of selecting the ξ_0 beam is approximately

$$P(\xi_0) = 0.98$$

$$P(\xi_0 + \beta) = 0.01$$

and

$$P(\xi_0 - \beta) = 0.01$$

At maximum range ($\frac{S}{N} = 13\text{db}$).

SECRET

SECRET

The variance of this distribution is

$$\sigma_{\xi_0}^2 = 0.02\beta^2$$

and the standard deviation is

$$\sigma_{\xi_0} \cong 0.14\beta$$

For a target at $\xi^* = \xi_0 + \frac{\beta}{2}$ the probability distribution is

$$P(\xi_0) \cong 0.5$$

$$P(\xi_0 + \beta) \cong 0.5$$

The variance of this distribution is

$$\sigma_{\xi + \frac{\beta}{2}}^2 \cong \left(\frac{\beta}{2}\right)^2$$

and

$$\sigma_{\xi + \frac{\beta}{2}} \cong 0.5\beta$$

The accuracy of the Case I radar at maximum range is, therefore, a function of the angle being measured. Furthermore as the range decreases, only that variance calculated for targets in the vicinity of beam center can be improved. The variance calculated for targets at beam cross-over can never be better than $\left(\frac{\beta}{2}\right)^2$ since the selection is ambiguous at that point.

In the Case II and III radars a pair of beams, corresponding to the two strongest signal levels, must be selected for interpolating. Probability functions, similar to those above, can be derived for all the possible pairs. When the target appears at an angle ξ^* , close to the crossover point between two adjacent beams, the probability of a correct pair selection is a maximum. When the target appears close to beam center the probability of a correct beam select approaches 0.5, since the selection of the correct pair is ambiguous.

Consider the effect of selecting an incorrect pair, i.e., selecting ξ_0 and $\xi_0 - \beta$ when the target lies between ξ_0 and $\xi_0 + \beta$. The amplitude comparison system described in the 7th PLATO Quarterly Report measures angle by subtracting the logarithms of voltages derived from Gaussian-

SECRET

shaped beams. Because of this instrumentation the relative signal strengths at the output of each beam channel can be described by the functions of Figure 4-3. When a correct pair is selected, e.g. ξ_0 and $\xi_0 + \beta$, the algebraic signal difference is linearly proportional to the departure from

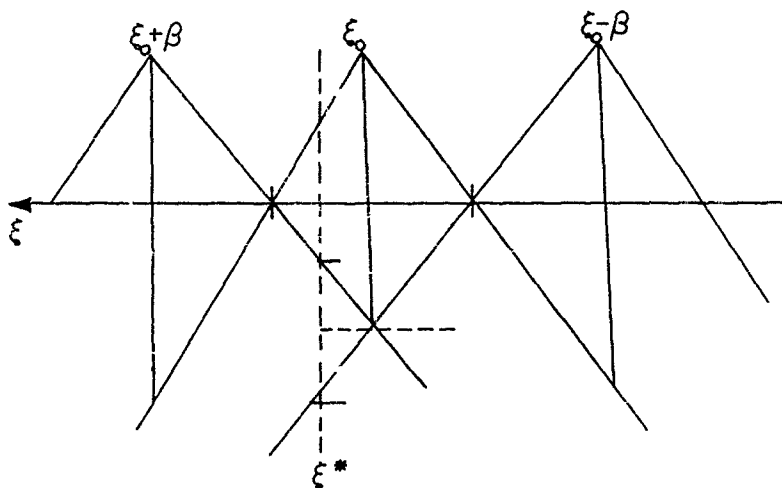


FIGURE 4-3

beam cross-over. When an incorrect pair is selected, the signal difference will only be proportional to the departure from cross-over of the pair selected if the transfer characteristic of each channel is logarithmic. Since all so-called "logarithmic" amplifiers must depart from a logarithmic transfer characteristic in the small signal region, a bias in the angle indication may be expected to develop for those cases in which incorrect pair selection produces low signal-to-noise ratios in one channel or the other.

To reduce the bias error introduced by incorrect pair selection, several alternatives are available. The pair selection process can, at the expense of power and/or system complexity, be made to have a small region of ambiguity near beam center (ξ_0). In that event, the bias error most frequently introduced, will be small.

Another possibility is to alter the low gain region of the beams, such that linearity of interpolation is maintained over a wider region than that described above. The cost in this case is a more stringent set of tolerances on both the electrical and mechanical antenna design.

A third alternative uses more than two beams for interpolation. By this means the first moment of the signal strength vs. angle distribution is employed in the estimation of a mean target angle. The necessity of selecting a correct pair is thus avoided with its attendant possibility of bias error, but at the expense of achieving adequate signal level in all beams employed.

SECRET

4.1.2.3 Coordinate Transformation Errors

The radar accuracy is adversely affected by the necessary coordinate transformation from the radar coordinates R , η , and ξ , to orthogonal earth coordinates (X_e , Y_e , and Z_e). An analysis has been made of the effects of the coordinate transformations in the acquisition radar, which shows that it is possible to neglect the second order effects in the non-linear transformation of noise in the coordinate transformation, and thus it is possible to simulate the target data at the input to the prediction computer without simulation of the acquisition radar. The analysis also shows that the radar window cannot be enlarged in one direction without paying by loss of coverage in the other direction. That is, surfaces of constant η and ξ need not intersect if either constant is more than 45° greater or less than 90° . Furthermore, the errors due to noise forbid approaching too closely to the corners of the radar window. The analysis, which makes it possible to express the noise component of radar measurement accuracy in earth's coordinates, is suitable for evaluating the effect of present position measurement accuracy on prediction accuracy.

4.1.2.4 The Radar Scan Interval (T_s)

The standard deviation of prediction error σ_p is proportional to $(V_T T_s)^{1/2}$ where V_T is the target velocity. This dependence arises from the usual inverse $N^{1/2}$ relation in least squares smoothing, where N is the total number of observations used in the smoothing. Since transmitted power is inversely proportional to T_s , this dependence indicates that a two-fold increase in predicted accuracy can be obtained at any range by a four-fold reduction in T_s , which requires in turn a four-fold increase in transmitted average power.

4.1.2.5 The Maximum Range of Detection (r_o)

For the accuracy model of Case I, σ_p can be expressed as a function of the ranges of initial detection (r_o) and the target range (r_n) at the time of launch of the interceptor. The exact expression is given as equation 39 of Technical Report 4-2, *Mathematical Analysis, etc.* An approximate form of this relation which is more convenient for the system optimization studies has been derived:

$$\sigma_p \doteq 5.1A (r_o V_T \Delta t)^{1/2} \exp. 5.2 \left(\frac{r_n}{r_o} - 1/2 \right) (1 - 1.4a) \quad (1)$$

where A is a constant, V_T is target speed, Δt is radar scan interval, r_n is the range at the N th data point, and $a = \frac{r_i}{r_o}$ where r_i is the range at intercept.

SECRET

This relation is valid within 10% when

$$1/4 < \frac{r_n}{r_o} < 3/4$$

for targets impacting at the radar. Figure 4-4 presents σ_p versus r_n for a 875 mile trajectory, with $A = 7/300$, $V_T = 2$ mi/sec., $\Delta t = 3$ seconds and $a = 0.05$ and 0.1383 . We can find the effect on prediction accuracy at launch of using a different value of initial detection range. It is convenient to express the change in σ_p in terms of a change in P_o , the radar power corresponding to a maximum detection range r_o . Differentiating equation 1 with respect to r_o , we get

$$-\frac{\Delta \sigma_p / \sigma_p}{\Delta P / P_o} = 1.3 \frac{r_n}{r_o} - 1/8 \quad (2)$$

For example, for $r_o = 300$ miles and $r_n = 100$ miles, the relative decrease in σ_p is 0.31 times the relative increase in radiated power. Equation 2 is plotted as a function of r_n with r_o as a parameter in Figure 4-5. The dotted extensions of the curves show approximate behavior beyond the regions of validity of equation 2. For comparison, the relative decrease in σ_p per relative increase in radiated power which is obtained at all ranges by increasing scan rate proportionally is shown as a straight line of magnitude 1/2. It can be seen by inspection of Figure 4-5 that if σ_{p1} must be decreased for a launch range r_n , then if r_n is less than the range at intersection of the two curves, that it is more economical in power to increase the scan rate; while if r_n is greater than the range at the intersection point, it is preferable to increase maximum range r_o . The maximum range at which this crossover occurs for any value of launch range is given by equating the right hand term of equation 2 to 1/2, yielding $r_o = 3.5 r_n$.

A similar analysis has been accomplished for the radar of Case II and Case III (assuming, no bias error limits on angle measurement accuracy) and $\sigma(Z_1) = A_r^2$. The prediction accuracy is given by

$$\sigma_p = \sqrt{12} A \sqrt{V_T \Delta t} r_n^{3/2} \left(\frac{r_o}{r_o - r_n} \right)^{3/2} \quad (3)$$

for targets impacting at the radar. Figure 4-6 presents σ_p vs. r_n for $A = 7/300$, $V_T = 2$ m/sec. and $\Delta t = 3$ sec. By differentiating this equation, we get:

$$-\frac{\frac{\Delta \sigma_p}{\sigma_p}}{\frac{\Delta P}{P_o}} = \frac{3}{8} \frac{r_n}{r_o - r_n} \quad (4)$$

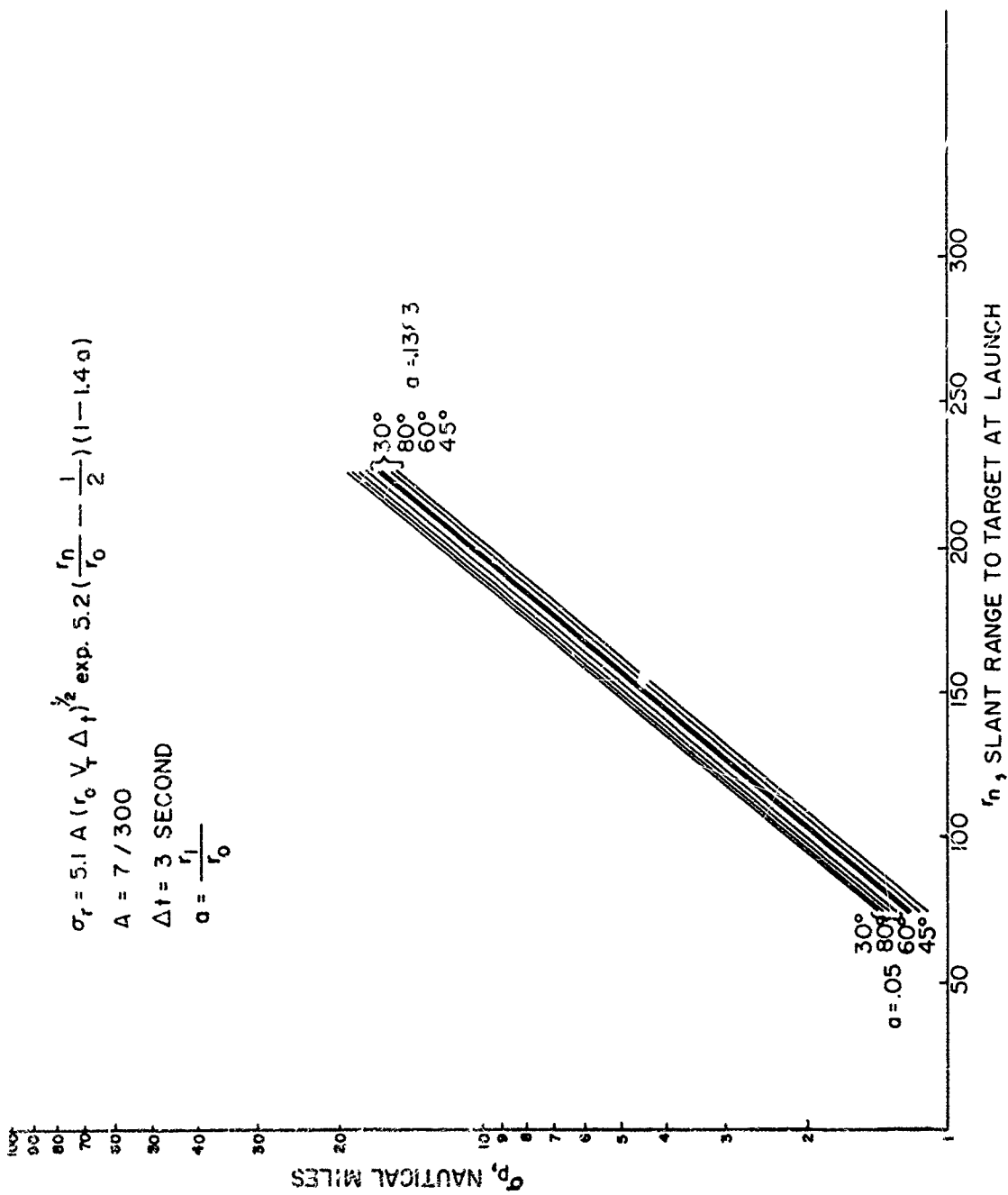


FIGURE 4-4. PREDICTION ACCURACY VS RANGE AT LAUNCH, CASE I RADAR

SECRET

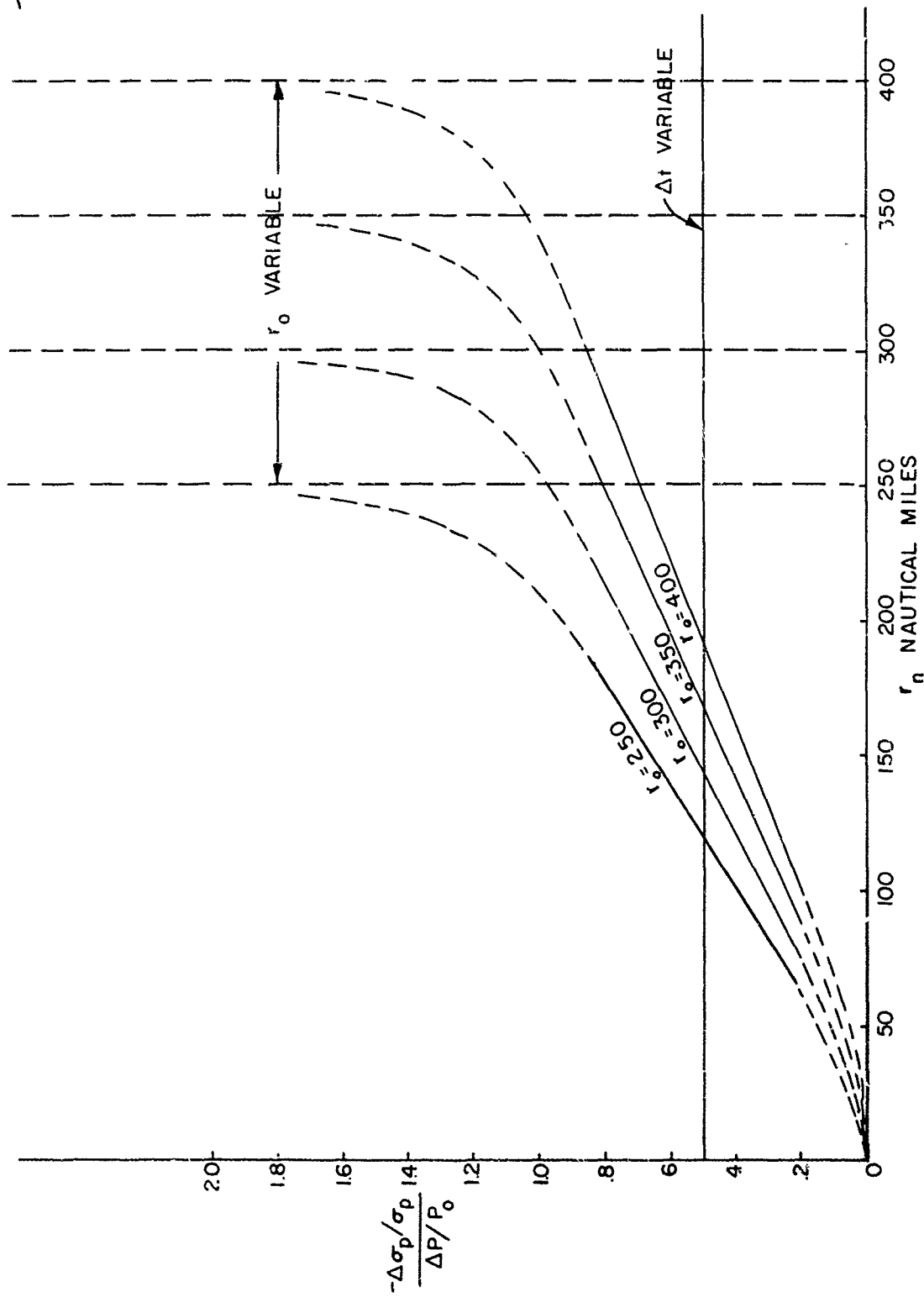


FIGURE 4-5. RELATIVE INCREASE IN PREDICTION ACCURACY AT LAUNCH PER RELATIVE INCREASE IN POWER VS TARGET RANGE AT LAUNCH, CASE I RADAR

SECRET

SECRET

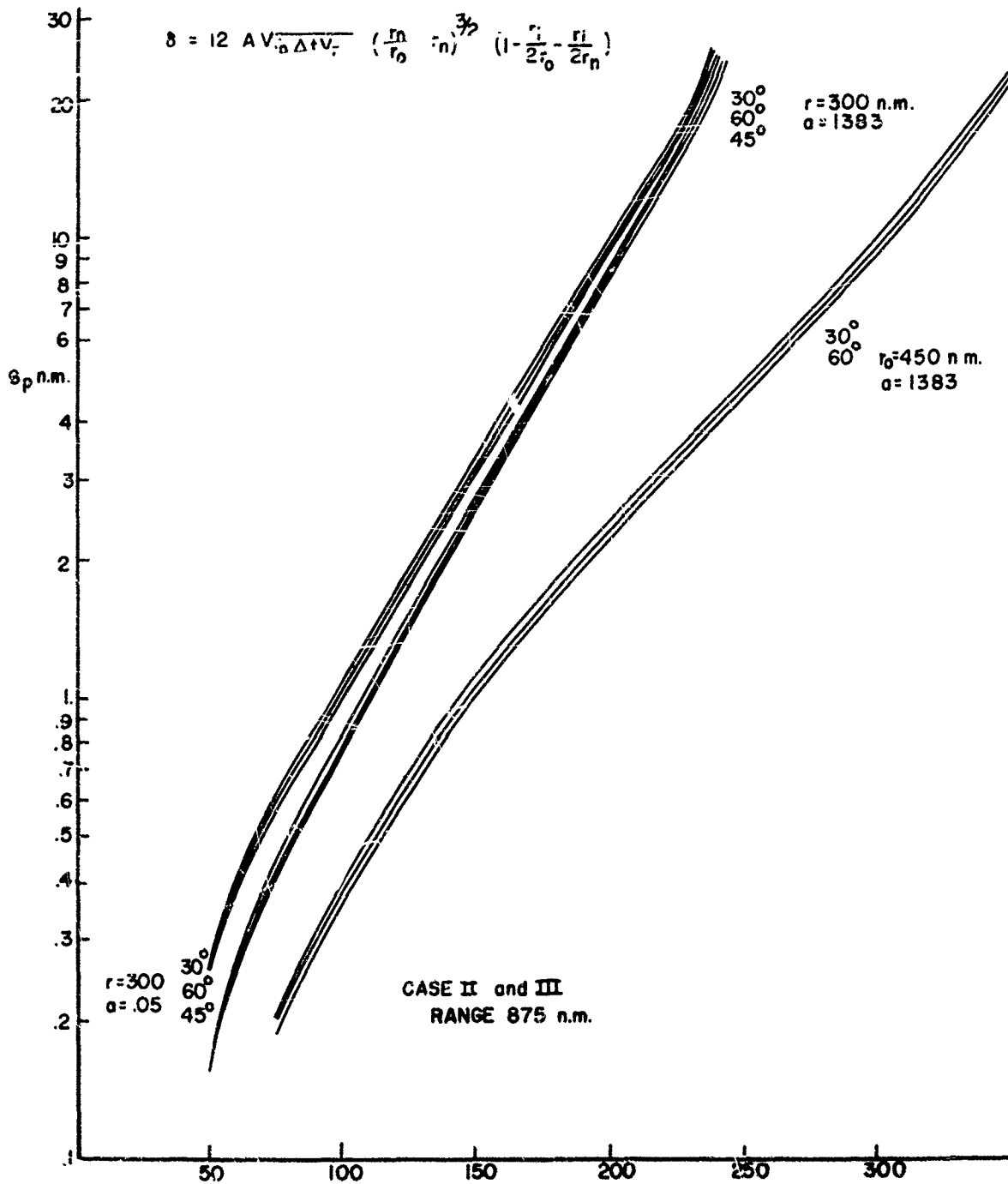


FIGURE 4-6. PREDICTION ACCURACY VS RANGE AT LAUNCH, CASE II AND III RADAR

SECRET

This equation is plotted as a function of r_n with r_o as a parameter in Figure 4-7. As in Case I, if σ_{p1} must be decreased for a launch range r_n , then if r_n is less than the range at the intersection of the curves for variable r_o and variable Δt , it is more economical in power to increase the scan rate; whereas if r_n is greater than the range at the intersection point it is preferable to increase r_o . The r_o for which this crossover occurs for any value of r_n is obtained in the same way as before, yielding $r_o = 1.75 r_n$.

From the above relationships, it is possible to find the costs in terms of radar power of increasing the time of flight of the interceptor and hence the target range at launch. It can be seen that increases in r_o through increases in P_o are much more effective in reducing σ_p for Cases II and III than for Case I. This result can be understood when it is noted that for Cases II and III increases in r_o also bring about reductions in σ_m at all ranges through increased signal-to-noise ratios, while in Case I increasing r_o only increases track length. It should be emphasized that in addition to the restrictions on the validity of these results listed above, the results are limited to some extent by the approximations used for σ_m in the three cases. Although the results are believed to be adequate for system optimization, a refined analysis of this problem is under way.

4.1.2.6 Radar Location and Volumetric Coverage

The effects of radar location and volumetric coverage are discussed in the Phase I Report and in Section 3.1 of this report.

4.1.2.7 Blending of Radar Data

The possibility of improving prediction accuracy at launch by blending triangulation radar data with acquisition radar data has been considered. The difficulty with this approach is that the triangulation radar system must be located in such a way as to meet terminal accuracy requirements, and when this is done, the resulting accuracy of blended target data at the time of launch may not be materially better than the accuracy of acquisition radar data alone. There will be a region for any track, however, in which blended data will improve the prediction accuracy, but there is little design freedom in choosing the location of this region.

The relationships summarized in the preceding paragraphs indicate how factors in radar performance which significantly affect overall system performance (such as σ_p) can be related to more fundamental radar parameters such as power, type of data processing, scan rate, etc. In system optimization, increased performance in one component can be exchanged for reduced performance in another. The criterion for deciding what performance

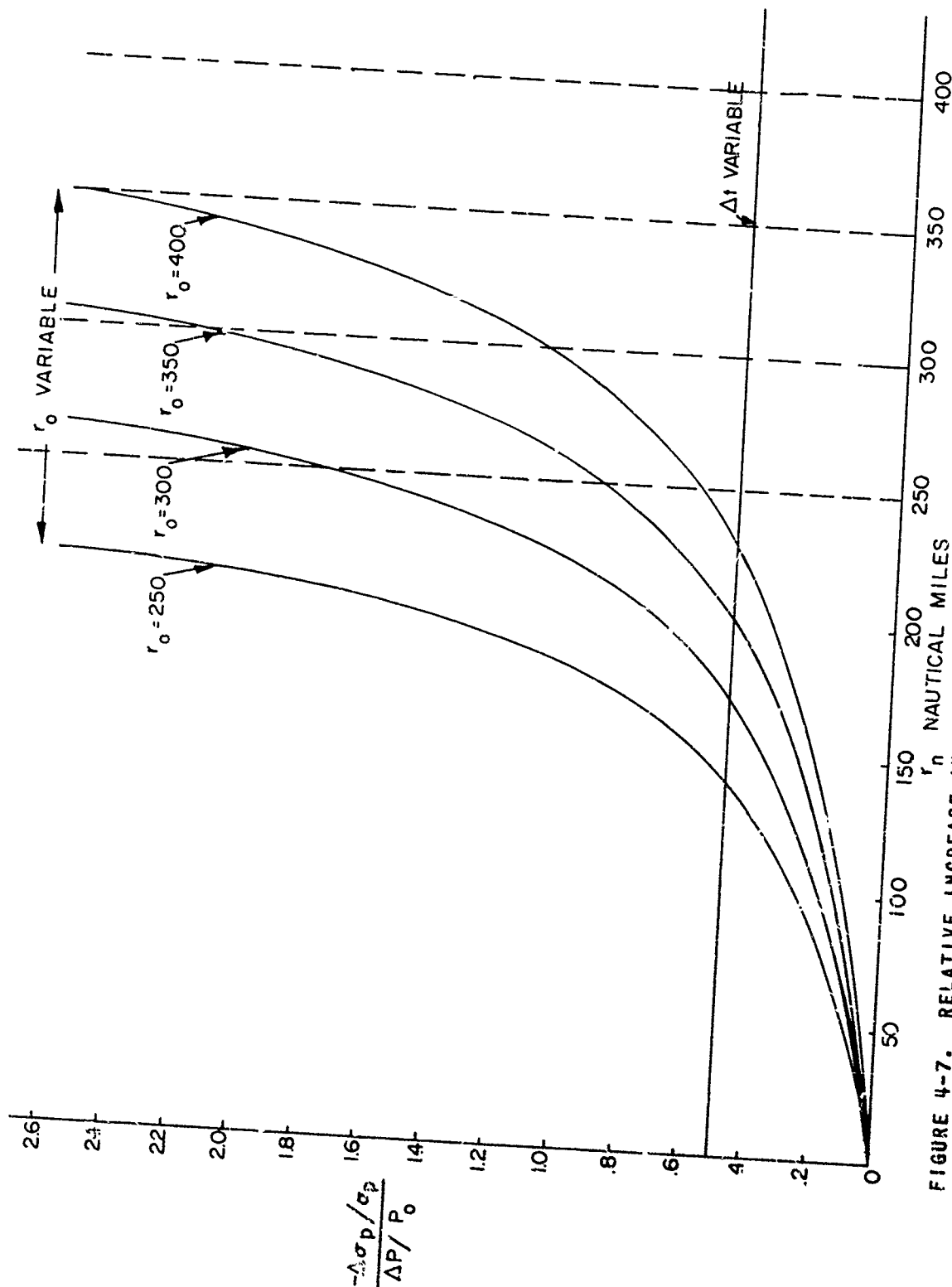


FIGURE 4-7. RELATIVE INCREASE IN PREDICTION ACCURACY PER RELATIVE INCREASE IN POWER VS TARGET RANGE AT LAUNCH, CASE II AND III RADAR

SECRET

exchanges to make involves knowledge of the generalized costs (purposely undefined here) of achieving overall performance with various components. To this end, crude cost estimates for the three cases of the acquisition radar (for a 300 mile maximum range version) have been made. No cost estimates have yet been made for longer range versions of the acquisition radar. These cost estimates and the conclusions drawn from them will be reported elsewhere. This much can be said however: the realization of the Case II radar characteristics is only moderately difficult compared with the Case I radar, while Case III will probably be comparatively quite difficult to achieve and the costs will be high. Since the Case II radar represents a substantial performance improvement over Case I, at moderate cost, the final radar design will probably be based on Case II or Case III rather than Case I. A decision to build the Case III radar could only be justified by greatly reduced cost in other components of the system, so that the final design will probably be based on Case II.

4.1.3 ENGINEERING STUDIES

In this section will be summarized some phases of progress in specifying the acquisition radar characteristics.

4.1.3.1 Target Fluctuation

The PLATO target echo is subject to fluctuations in amplitude which are produced by several independent mechanisms. These sources include the target cross-section, the atmosphere and ionosphere and the radar itself. If the receiver output passes through a threshold device whose level is a fixed multiple of the rms receiver noise level, then echo fluctuations about the expected amplitude can result in target fades. Target fades can reduce the range of track initiation, can cause loss of established tracks, and can reduce prediction accuracy. The radar track initiation computer and prediction computer must be designed to achieve satisfactory performance for all possible fade conditions. A considerable effort is being made to specify a fluctuation model which is as realistic as possible in order to facilitate this design. In this section will be discussed some preliminary results of a study of the fluctuations in target cross-section.

The target characteristics which affect its instantaneous cross-section are:

- (1) The target flight path relative to the location of the radar.
- (2) The programmed attitude of the missile referred to the flight path tangent.
- (3) Perturbations in attitude due to stabilization (or lack of it), aerodynamic loading, etc.

SECRET

- (4) The angular cross-section variation which is a function of the details of target geometry such as fins, tankage, etc., and of the frequency and polarization of the incident radiation.

The above factors have been combined for several target trajectories with three different stabilization programs (assumed perfectly executed) and for the angular cross-section plots given in Figure 4-8, in curves A and B. This study indicated that for these cases the target cross-section is correlated over the radar time-on-target and also over many scan intervals, so that it is quite possible to have cross-sections well above or well below the expected values for five to ten scans. The effect on the radar blip-scan ratio and on the tracking system of such fluctuations is being studied.

An inspection of curves A and B of Figure 4-8 reveals that the cross-sections for horizontal and vertical polarization are either uncorrelated or inversely correlated as a function of angle. It was suggested that the use of circular polarization on transmission and reception (which is required on reception because of the Faraday effect, cf. the 7th PLATO Quarterly Report) might insure that the instantaneous cross-section would always be fairly close to its maximum value on either polarization. An analysis of this possibility has been made which suggests that the circular polarization cross-section lies within the limits

$$1/2[\Sigma_1^{1/2} - \Sigma_2^{1/2}]^2 \leq \Sigma_3 \leq 1/2 [(\Sigma_1^{1/2} + \Sigma_2^{1/2})]^2,$$

where

Σ_1 = vertical polarization cross-section

Σ_2 = horizontal polarization cross-section

Σ_3 = circular polarization cross-section.

These limits have been plotted as curves B and C of Figure 4-8. The analysis does not reveal what the probability distribution of Σ_3 is, nor is a valid method of analysis known which will make it possible to deduce Σ_3 from angle plots of Σ_2 and Σ_1 . Further study of fluctuation problems is planned.

4.1.3.2 Survey of RF Power Sources

Because of the imminence of initiation of detailed design work on an experimental version of the PLATO acquisition radar, it was desirable to determine the availability of high power sources of radio frequency energy. During this reporting period, therefore, a survey has been made to determine

SECRET

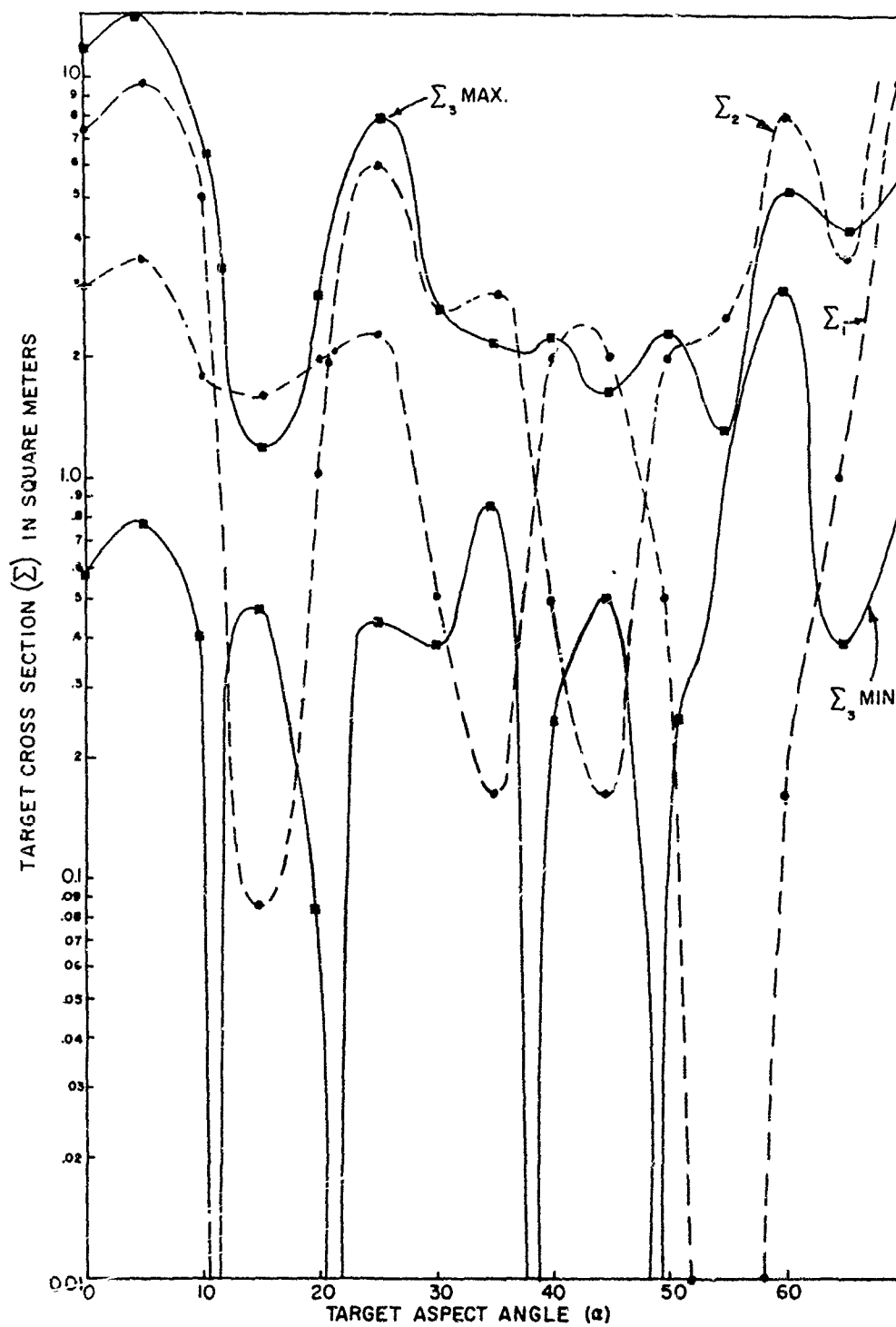


FIGURE 4-8. CROSS SECTION OF A V-2 TYPE MISSILE AT 300 Mc. (O.S.U.)

SECRET

SECRET

the current capability of the tube manufacturing industry to supply vacuum tube generators of high power in the ultra-high frequency region and to learn the development plans of leaders in this field and what they see as feasible development objectives in the next few years.

The "state of the art" is essentially this: there is no tube available as a standard item which will meet the requirements of the PLATO acquisition radar transmitter. There is, however, a great deal of development activity at all of the manufacturers contacted, namely Eitel-McCullough, Inc., General Electric Co., RCA, and Sperry-Rand, Inc. The tube types under investigation include triodes, tetrodes, klystrons, and traveling wave tubes, with power output goals of up to 10 megawatts peak. Some of these tubes are in the latter stages of development and not only are samples suitable for the acquisition radar available for initial experimentation, but they are planned to be listed as standard commercial items within the near future.

It has been known for some time that no tubes were on the market which would meet the acquisition radar total power requirements. Hence consideration has been given to the possibility of a low-level phasing system which would drive power amplifiers associated with antenna elements or groups of elements. In addition to the fact that this method makes possible early realization of an experimental system, it is of more than immediate interest because it potentially provides a number of operational advantages, including the following:

- (1) It eases the problem of handling power at very high peak levels in transmission lines, rotating joints, power dividers and phasing elements.
- (2) It is a "modular" solution of the problem, with its attendant transport, logistical and maintenance advantages.

It has been decided to place initial emphasis on this method of power generation and control. Figure 4-9 is a block diagram of a possible low level phasing system.

The tube type desired for use in early experiments with the acquisition radar transmitter would be capable of peak power outputs of about 0.5 megawatts up to about 250 megacycles with a duty factor up to 0.005 and with pulse lengths as great as 100 microseconds.

In the commercially available category the closest approach to this is the GL 6251, a tetrode manufactured by the General Electric Company. This tube, designed for TV service, is capable of only about 50 kilowatts peak power output.

SECRET

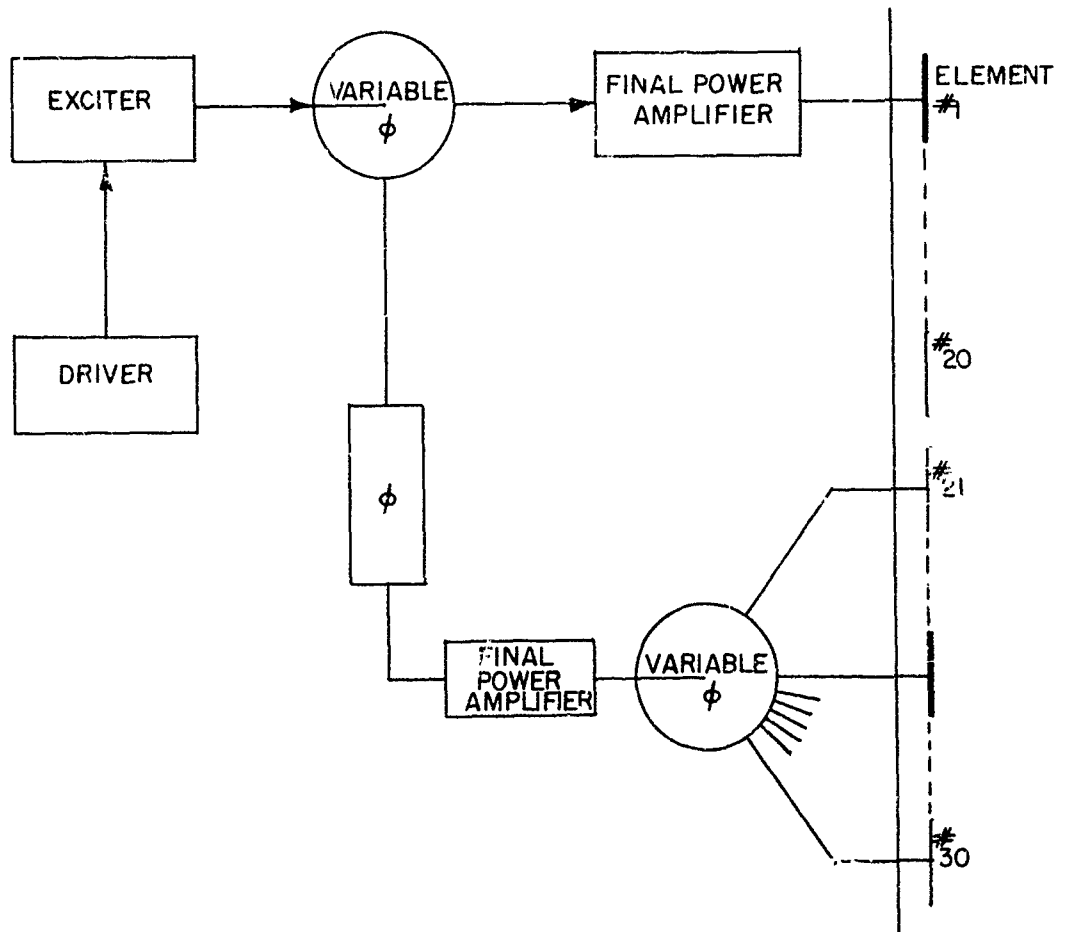


FIGURE 4-9. POSSIBLE LOW-LEVEL PHASING SYSTEM

SECRET

SECRET

In advanced development is the RCA type A 2515, a UHF beam power tetrode which is a pulse version of the RCA 6448, used extensively in UHF TV service. The performance expected from this tube by RCA engineers would satisfy the requirements stated above. Sample tubes will be available for experimentation in the fall of 1955.

Although there are a number of tubes available which from plate dissipation and maximum frequency considerations are otherwise suitable for this application, limitations on permissible plate voltage and on available cathode emission preclude obtaining peak powers much in excess of their continuous power generation capabilities. In other existing types employed for pulsed operation use of an oxide cathode limits pulse duration to a 6 to 10 microseconds maximum.

Due to increased interest in the generation of high peak powers in the UHF band, a great deal of development work is going on with both the negative grid and klystron types. In about two years there probably will be working models of both types capable of producing peak powers of as high as 5 to 10 megawatts in the UHF band at high duty factors and with long pulses. Negative grid types will probably offer the advantages of smaller size than a klystron of the same power, greater frequency mobility and higher efficiencies. Their gains will be lower, however, probably in the region of 20 db.

In the klystron case primary advantages will be gain (over 30 db) and circuit simplicity. An additional advantage might be a reduction in pulse modulator size through the employment of a "floating anode" capable of beam switching with essentially zero power. This technique, developed by Eitel-McCullough, may possibly be unsuitable because of incomplete tube cut-off during normal radar dead time with resultant noise production and loss in effective receiver sensitivity. Disadvantages would be greater size, (although this is only true at the low end of the UHF band,) lower efficiency and a requirement for anode voltages in the 100 to 120 kilovolts range. One prominent klystron designer has estimated, for example, that a three-cavity 250-megacycle klystron could be developed in about 18 months which would have a peak power output capability of at least three megawatts gain greater than 30 db and efficiency of 40 to 50 percent. It would be about 15 feet long and two feet in diameter and would require over 100 kilovolts anode voltage.

4.1.3.3 Antenna Mechanical Design Study

The American Machine and Foundry Co. has conducted under sub-contract with Sylvania a preliminary mechanical design study for the acquisition radar antenna. This study was designed to (a) examine alternative proposed

SECRET

antenna configurations and determine the mechanical arguments in favor of each proposed form, and (b) for a particular selected form, furnish preliminary information concerning size, weight, transportability, erection methods, and approximate costs of the structure necessary to support the radiating elements to within the desired tolerances.

Two forms of the acquisition radar fan beam antenna system have been examined, as shown in Figures 4-10(a) and 4-10(b).

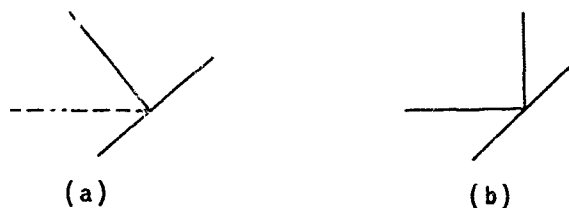


FIGURE 4-10. ALTERNATE FORMS OF THE ACQUISITION RADAR ANTENNA SYSTEM

The inclined inverted T structure of Figure 4-10(a) has been chosen tentatively for the reasons outlined in Quarterly Progress Report No. 7.

For this inclined inverted T structure of Figure 4-10(a), a preliminary mechanical design has been obtained. The plan presented, while representing any one of a number of possible combinations of structural shapes and erecting methods, does show that the requirements of the radar antenna structure for erection and transportation can be met without great difficulty. A pictorial view of the proposed antenna is shown in Figure 4-11.

The horizontal transmitting antenna presents little mechanical difficulty; the array is divided into five 30' sections for trailer transportation. The inclined member consists also of five sections 2 1/2' x 5 1/2' x 30'. Both members are of aluminum tubing.

To aid in assembly and erection, a small crane is provided similar to a telephone pole-erecting truck. The sections are bolted together on the ground, and attached to the 45° column support member. The crane will be able to lift the assemblage to about 15°. From there on the rear trailer on which the column support member rests is winched forward until the desired angle is achieved, and fine angle adjustment accomplished by means of the jack pads. Equipment weights are approximately as follows: inclined member 1000#/section, 5000# total; horizontal member 3000# total; support columns 1500# total. The antenna may be loaded for transportation on one full trailer and four semi-trailers conforming to standard roadability and clearance requirements, pulled by five 5-ton cabs (tractors). One V-17A/MTR derrick and maintenance truck (standard military vehicle) will suffice for the handling crane. It is estimated that the antenna may be physically

SECRET

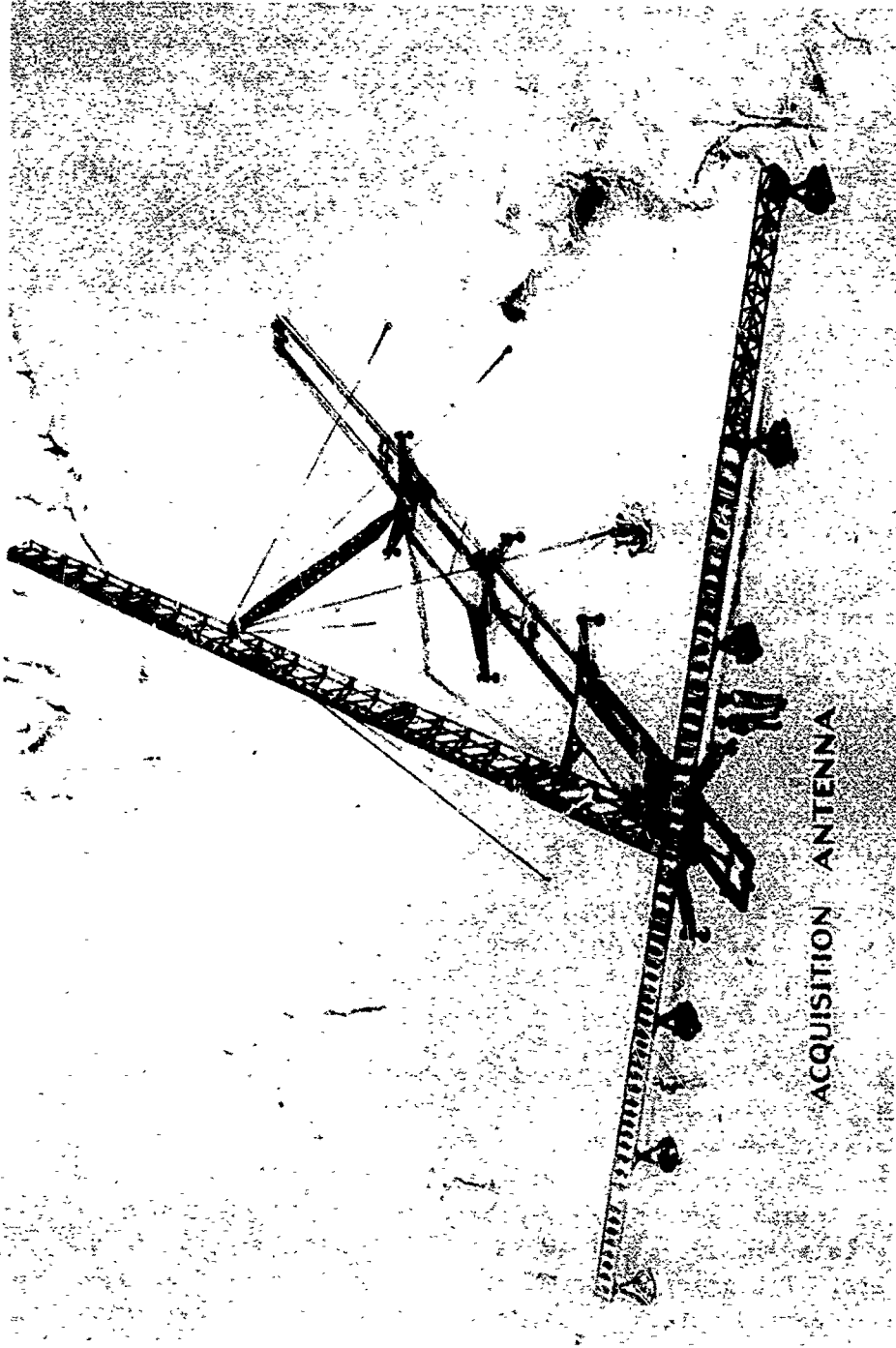


FIGURE 4-11. PICTORIAL VIEW OF PROPOSED ANTENNA

SECRET

erected in eight hours, and disassembled ready for transportation in about four hours. In formulating the tolerance requirements for the above study, they were set so that beam wander due to the 45° member deflection from all loads (dead weight, electrical equipment, ice, snow, wind, etc.) would be only a very small contribution to the over all system error (in particular beam wander was held to 1/50 beamwidth or less). These requirements have been met for all factors except possibly temperature expansions, which might conceivably cause a wander as great as 1/10 beamwidth. It is possible to overcome this difficulty also if the effort is shown to be warranted.

4.2 PRECISION TRACKING RADAR

4.2.1 GENERAL

In this reporting period the precision tracking radar studies have included:

- (1) Further consideration of the effects of tracking radar parameters on overall system performance.
- (2) Engineering studies, to more completely specify the tracking radar characteristics.
- (3) Preliminary consideration of tracking radar behavior in the face of countermeasures.

All of the activity has centered around the range triangulation system, with the exception of pencil beam tracker mechanical studies (which are reported in Section 4.2.3), and a survey of developmental and operational baseline systems. The latter were undertaken because of the possibility of developing improved anti-jamming systems, and because of the applicability to the range triangulation system, of already developed special techniques such as synchronization and transponder systems.

4.2.2 TRACKING RADAR PERFORMANCE AND SYSTEM OPTIMIZATION

As in the case of the acquisition radar, the relationship of precision tracking radar characteristics and system optimization has two aspects:

- (1) The variation of measures of system performance, such as defended area, with variation in tracking radar performance.
- (2) The costs of making such variations, to the costs of variations in other parameters which would produce the same system performance.

The precision tracking radar parameter which most directly affects system performance is σ_p , the standard deviation of target prediction error,

SECRET

during the late mid-course and terminal phases of the interception. The target prediction errors are controlled by such factors as:

- (1) Present position measurement accuracy of the precision tracking radar (σ_m).
- (2) The sampling interval.
- (3) The smoothing time.
- (4) The location of the precision tracking radar centroid with respect to the target trajectory.

The terminal prediction accuracy in the precision tracking radar (PTR) cannot be specified in as straightforward a manner as σ_{p1} for the acquisition radar, because

- (1) The PTR prediction accuracy is a stronger function of the target path through the field of the PTR.
- (2) The sampling intervals, smoothing times and range tracking servo bandwidths are dynamically related to the target and interceptor accelerations under aerodynamic forces.

Consequently, the approach which has been adopted in determining the effects of PTR performance on system performance, is a system simulation program. The emphasis of the PTR studies in the quarter has been on obtaining a more accurate description of the PTR performance. In PLATO Quarterly Report No. 7, a summary of the measurement errors in the PTR was given. Technical Report 4-6, *The PLATO Range Triangulation System*, contains a fuller description of the PTR performance as known at the beginning of the quarter. A computational program has been prepared whose objectives are:

- (1) A refined and more detailed survey of the accuracy field of the PTR, particularly for the 30-mile baseline, five station configuration, which is considered optimum. (See the 7th PLATO Quarterly Report.)
- (2) A detailed study of low-altitude weapon tracking accuracy.
- (3) A study of the accuracy of the PTR when degraded by a 15-mile translation of the target illuminator, or by the loss of one of the receiving stations, leaving an asymmetrical geometry.

Rough estimates have been made of the costs of the PTR for use in the system optimization program. These estimates are reported elsewhere. It

SECRET

appears, however, that the triangulation radar costs will not be greatly affected by any expected variations in size of defended area or in data accuracy requirements.

4.2.3 ENGINEERING STUDIES

4.2.3.1 Pencil Beam Tracker Mechanical Studies

The pencil beam tracker has been considered a secondary alternative to the large triangulation system because of the difficulties of maintaining the required tolerances and calibration. The project activity on the pencil beam tracker has largely been limited to mechanical feasibility studies which are being done by Steel Products Engineering Co., of Springfield, Ohio, under subcontract.

The pencil beam tracker being considered operates at S band with a 20-foot diameter dish. This large dish size is necessary in order to obtain satisfactory range with realizable powers. An overall skin-tracking absolute accuracy of 0.5 mil has been the objective and has been shown to be approximately attainable. The problem, therefore, is one of designing a tracker about three times the Nike size while maintaining or improving its accuracy, eliminating as much as possible the many sources of absolute accuracy drift and at the same time considerably increasing the dynamic operating rates.

Of the gimbaling systems considered to date, only two configurations seem to be capable of being balanced, namely the scaled-up Nike mount, shown in Figure 4-12 and the mount represented in Figure 4-13. The mechanical studies have made it clear that the difficulties associated with unbalanced systems are so great that it is desirable to consider balanced systems only. Hence the mechanical studies are now confined to these two gimbaling systems.

In the mount as shown in Figure 4-13 the base remains stationary. The first motion is turning of the large yoke on its rollers in the lower base. This corresponds roughly to the elevation motion in normal mount use. The second motion is a tilting of the dish about the axis which spans the yoke arms. This corresponds to an azimuth (traverse) motion. This amounts to a conventional gimbaling system laid on its side so that the limiting cylinders, as discussed below, do not intersect the field of fire.

The gimbaling systems of Figures 4-12 and 4-13 have different tracking rate requirements, which arise from the non-orthogonality of the plane containing the PBT and two successive track points, and the rotational axes. The actual rotational capabilities of the mount, together with the maximum target velocity in a plane perpendicular to each axis, define a

SECRET

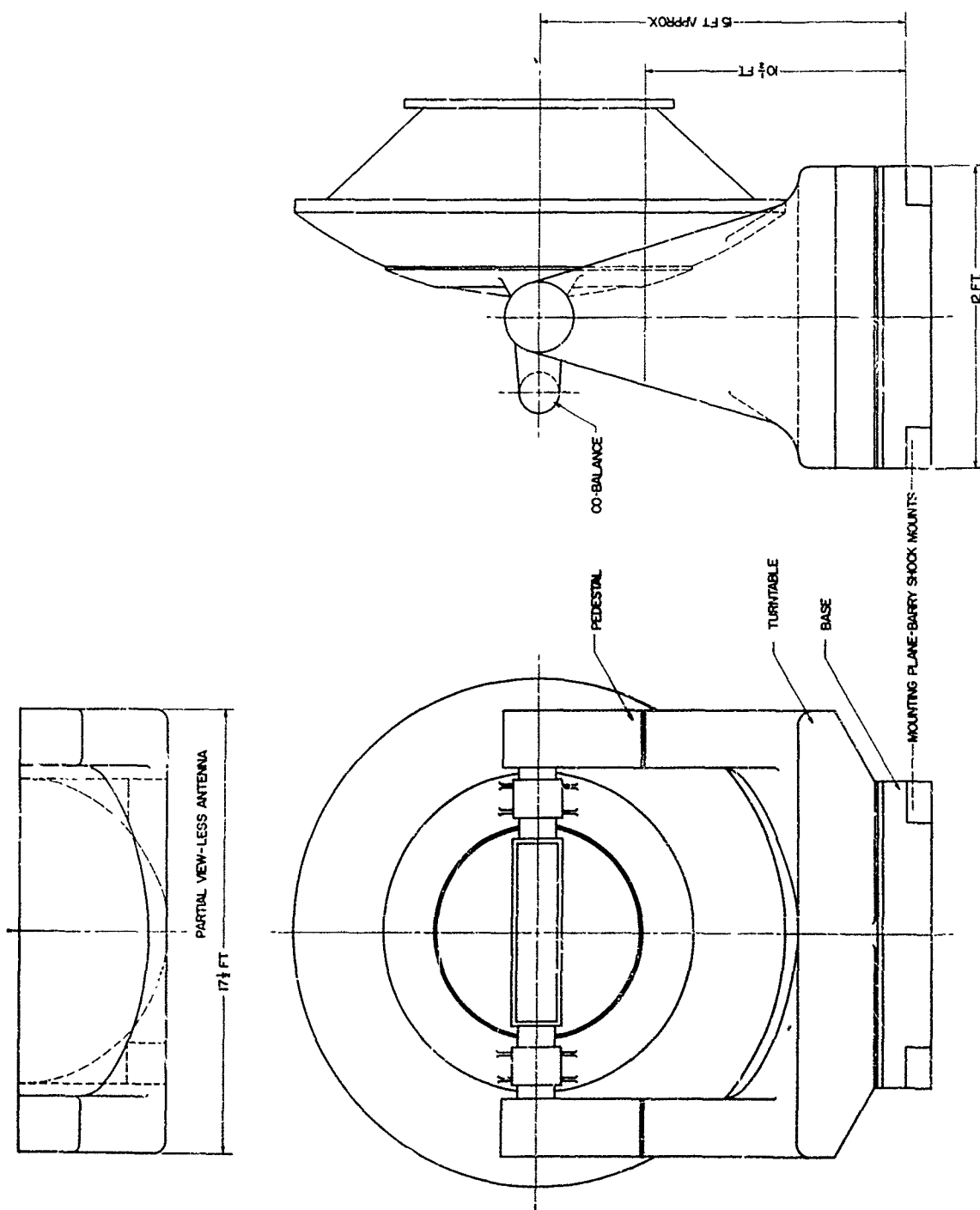
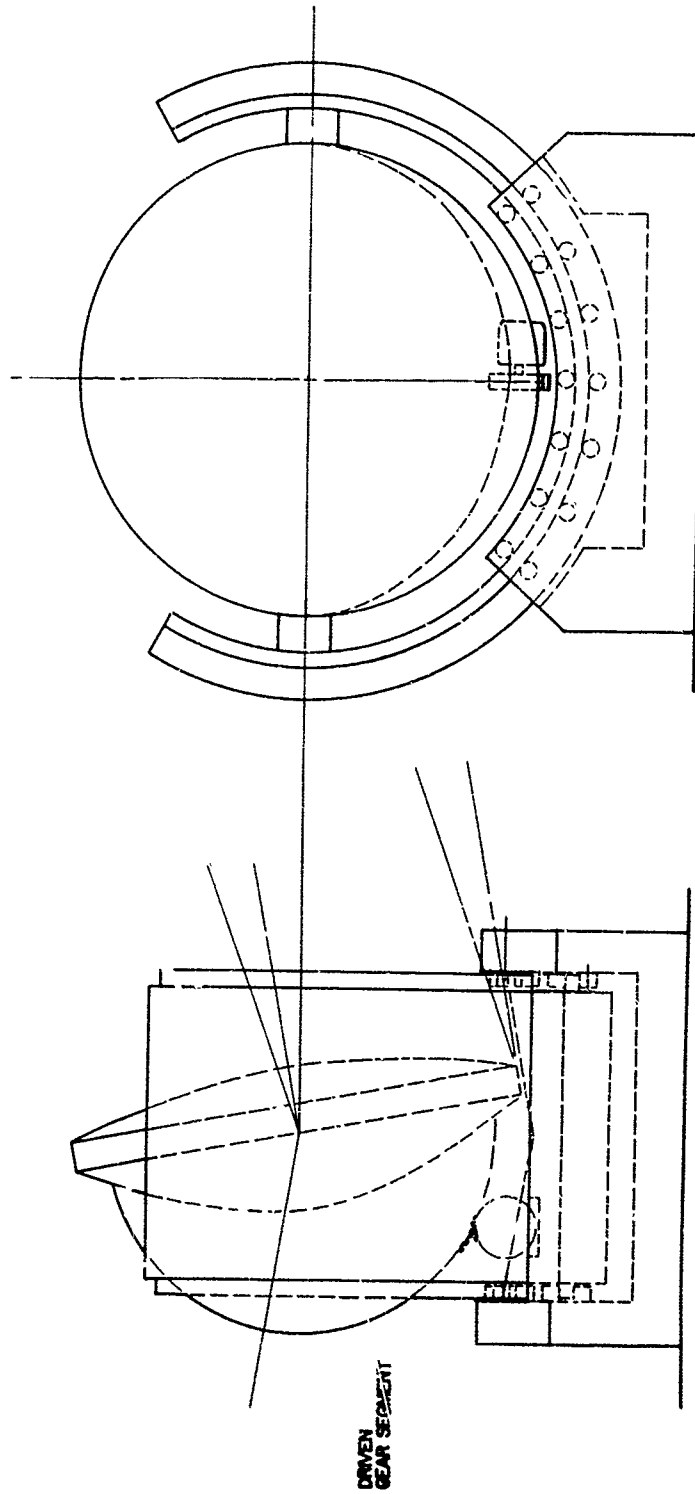


FIGURE 4-12. NIKE-TYPE ANTENNA MOUNT

SECRET



SECRET

FIGURE 4-13. YOKE-TYPE ANTENNA MOUNT

SECRET

cylinder of closest allowable approach to that axis, within which the rotational characteristics of the mount will be exceeded by high speed targets. For the Nike-type gimbaling system (Figure 4-12) one limiting cylinder is vertical, and if its radius is limited to 1.2 miles in order to make the ineffective zone acceptably small, then maximum rotation rates of $100^\circ/\text{sec}$ and maximum accelerations of $220^\circ/\text{sec}^2$ are required. For the mount of Figure 4-13, a larger radius can be tolerated for the limiting cylinder because its firing axis is horizontal and can be oriented normal to the expected directions of target approach. Thus, maximum rates of $30^\circ/\text{sec}$ and $20^\circ/\text{sec}^2$ should be adequate.

The principal mechanical problem for the mount of Figure 4-13 is that of producing a balanced design of a yoke approximately 30 feet in diameter such that the yoke can be disassembled for transport, and yet maintain satisfactory tolerances. The Nike-type gimbaling systems do not appear to have such severe mechanical problems. However, they do present the difficulty that the prohibited regions lie in the field of fire of the system, and consequently require higher turning and acceleration rates. They also require that provision be made to transfer track between radars in the event the intercept is predicted to occur within a prohibited region of the tracking radar first assigned. Both mounts can accept a radome.

The weight of the Nike-type mount is presently estimated at 52,000 pounds. The weight of the yoke-type about 1.50 times as great. Effort is being made toward reducing these weights.

The mechanical studies are continuing with emphasis on realization of a satisfactory design in terms of transportability and mechanical error.

4.2.3.2 Analysis of Various Triangulation Systems

An error analysis has been made of triangulation systems of configuration similar to the range sum system, in which each receiver measures either an elevation angle or an angle between the line-of sight and a fixed horizontal direction. This analysis was undertaken because such systems are less susceptible than the range sum system to active jamming by the target missile. By making use of a predicted point, it has been shown that the analysis of these angle systems is similar in form to that of the range sum system. Normalized standard deviations of error, σ/k , have been computed where σ is the standard deviation and k is a number related to the ability of a receiver to measure either range sum or angle. If the assumption is made that angle can be measured as accurately as range, then an angle system is probably as good as a range sum system. However, at long range, each of these systems has good accuracy in one direction and poor accuracy in the two normal directions. The range sum system has good

SECRET

accuracy in the radial direction, whereas the angle measuring systems have poor accuracy in this direction. Likewise, the range sum system has poor accuracy in the direction that either angle system has good accuracy. All systems deteriorate at long ranges.

The assumption that angle can be measured as accurately as range is a critical one. The angle measurements which depend on physical orientation of a structure are subject to mechanical and calibration difficulties as in the pencil beam tracker. The angle measuring systems which seem to have promise are the short base line systems which use phase information such as direction finders or interferometers. Long base line systems measuring phase difference or range difference by correlation methods are also promising. All of these systems should be resistant to jamming originating in the target, but would be susceptible to other countermeasures. These systems are still under study.

4.2.4 COUNTERMEASURES

To date only one form of possible enemy countermeasure against the precision tracking radar has been considered in any detail. In the next quarter other countermeasures will also be considered.

A potent countermeasure against the precision tracking radar would be decoy targets released by the target missile near the terminal phase of the interception. It is assumed that these decoy targets would be released in the form of cylindrical rods resonant at the radar wavelength. In the upper atmosphere such rods would presumably travel with the target and not be resolved by the radar. As the air density increases, however, the rods would fall behind the target due to drag differences, and would have the effect of pulling automatic range tracking gates off the true target. Thus the effectiveness of these decoy rods depends on their behaving like the target at high altitude and then separating from the target just before interception. It has been shown that the maximum deceleration of a high speed target impinging on the atmosphere is given by

$$\left(\frac{dV}{dt}\right)_{\max} = \frac{aV_0^2}{2e} \quad (1)$$

where a depends only on the angle of incidence and the atmosphere properties, V_0 is the initial velocity, and e is the Napierian base. It has also been shown that the height at which this maximum deceleration occurs is

$$h|_{\dot{V}_{\max}} = \frac{1}{\gamma} \log_e \frac{2K_D}{a} \quad (2)$$

SECRET

where γ is an atmospheric constant,

$$K_D = \frac{\rho_o C_D A}{2m},$$

where

ρ_o = air density at surface,

C_D = drag coefficient,

A = drag area,

m = mass.

Thus the maximum deceleration depends on entry velocity and is independent of the physical characteristics of the body, while the height at which this maximum deceleration occurs is independent of entry velocity but is a function of the physical characteristics of the body.

Calculations of drag distance have been made for likely targets and 1/4-inch diameter resonant cylindrical rods. The drag distance is the defect in distance covered by the body due to drag. At 176,000 feet, near the beginning of the homing phase, the drag distance for the assumed target is eight feet and that of the rod is 3500 feet. The target is thus hardly affected by the atmosphere while the rod lags behind by roughly one-half nautical mile, and is resolved by the precision tracking radar. Furthermore the separation between target and rod is increasing at an exponential rate. The altitude of maximum deceleration for the assumed target is about 8000 feet; for the rod it is 140,000 feet. The rod characteristics can be adjusted to stay relatively close to the target through midcourse, and then to separate rapidly at the most critical time, near the end of the interception.

A simple calculation shows that about 30 resonant iron rods weighing a total of ten pounds would be required to give an echo equivalent to a target missile in the 200-megacycle region. If $\lambda/10$ dipoles were used, 45 dipoles weighing a total of three pounds would be needed. If aluminum rods were used, the weight could be further reduced by a factor of 0.25.

Decoys could also be used as a means of saturating the system during the acquisition phase, if many packets of rods were released just within maximum range and separated from the target by at least five miles in range. This could easily be done for a long range missile but would be harder to do for the lower-flying short range missiles. Such a tactic might saturate the prediction computer or require large numbers of interceptors to be committed to insure killing the targets.

CONFIDENTIAL

In the precision tracking radar it is possible to prevent track-breaking through the use of leading edge tracking rather than early-late gate tracking, or by use of circuits which discriminate against the decoys on the basis of observed accelerations. The details of these circuits have not been worked out, but are believed not to present serious difficulties. Other forms of ECM will be considered together with means of countering them in the next quarter.

4.3 THE TRACK INITIATION COMPUTER AND THE PREDICTION COMPUTER

Several changes have been proposed for the track initiation computer since the last quarterly report. Some of these are relatively minor in nature while others may involve radical changes in the scheme listed in the 7th PLATO Quarterly Report. For that reason this report will contain a description of the track initiation plans now under consideration. A discussion of the sources of extraneous alarms in the acquisition radar will also be included; it will be these alarms which will necessitate many of the future alterations in the computer design. (Here a rather broad definition of extraneous alarms or noise is used to designate any alarm which is not caused by the target missile.)

For contrast, the prediction computer scheme presented previously (see TR 4-2 and the 7th PLATO Quarterly Report) has survived almost intact. As a result of simulation studies now under way and partially completed, the various numerical techniques used seem to converge rapidly and to the correct result. The one addition to the plans for the computer is a timing or traffic control plan for the prediction computer. This is described in Section 4.3.3.

4.3.1 TRACK INITIATION

The track initiation computer is designed to take information from the acquisition radar, to examine this information to see whether a target missile is present and to pass the sorted information on to the prediction computer. (See Figure 4-14.)



FIGURE 4-14. BLOCK DIAGRAM OF COMPUTERS

CONFIDENTIAL

Actually, the track initiation computer receives its information not from the acquisition radar but rather through an intermediary, Buffer I. A buffer, it will be recalled, is a device which can receive and store information at any rate and which passes on this information when the computer calls for it. The timing scheme which the track initiation computer uses is as follows. There is a clock in the computer which emits pulses at fixed intervals of time (actually the length of the interval will correspond to the length of a radar scan; at the moment, this is thought to be three seconds.) The computer operations are divided into two modes: an outer mode and an inner mode (See Figure 4-15). When the computer enters the outer mode it is ready to start processing the radar information as it is received. During the inner mode the computer accepts data only from its internal memory and is not connected to input or output. The outer mode usually begins after the scan begins therefore alarms may already be present in the buffer.

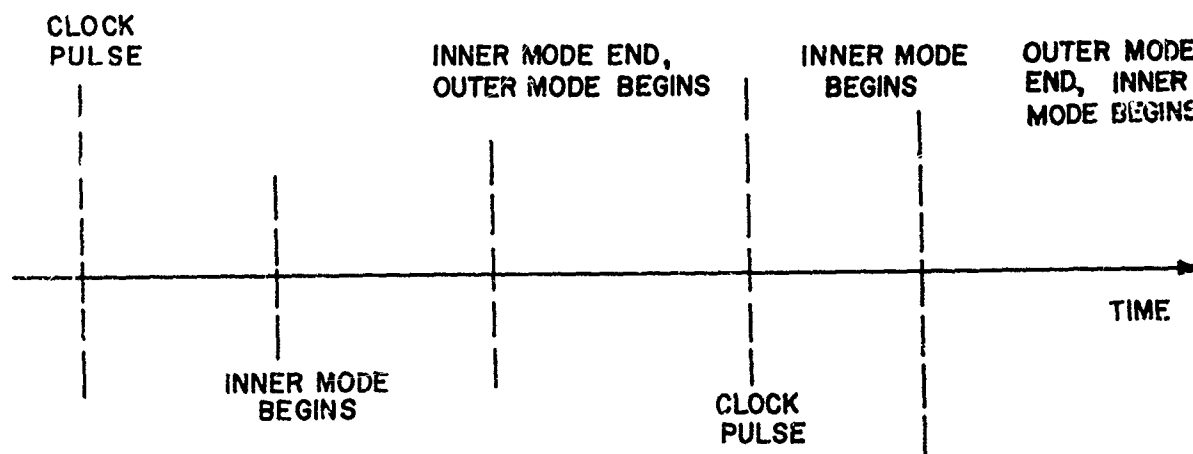


FIGURE 4-15. TIMING SCHEME

These will be processed first. The length of time after the clock pulse before the outer mode begins will be discussed later. As long as the computer is in its outer mode the computer

- (1) Searches to see whether a clock pulse has occurred since the beginning of the outer mode.
 - a. If a clock pulse has occurred the computer goes into its inner mode.
 - b. If a clock pulse has not occurred the computer
- (2) Searches to see whether any information is present in the buffer.

CONFIDENTIAL

- a. If alarms are present in the buffer, it processes the oldest such alarm and then returns to 1.
- b. If no alarm is present in the buffer it returns to 1.
(See Figure 4-16).

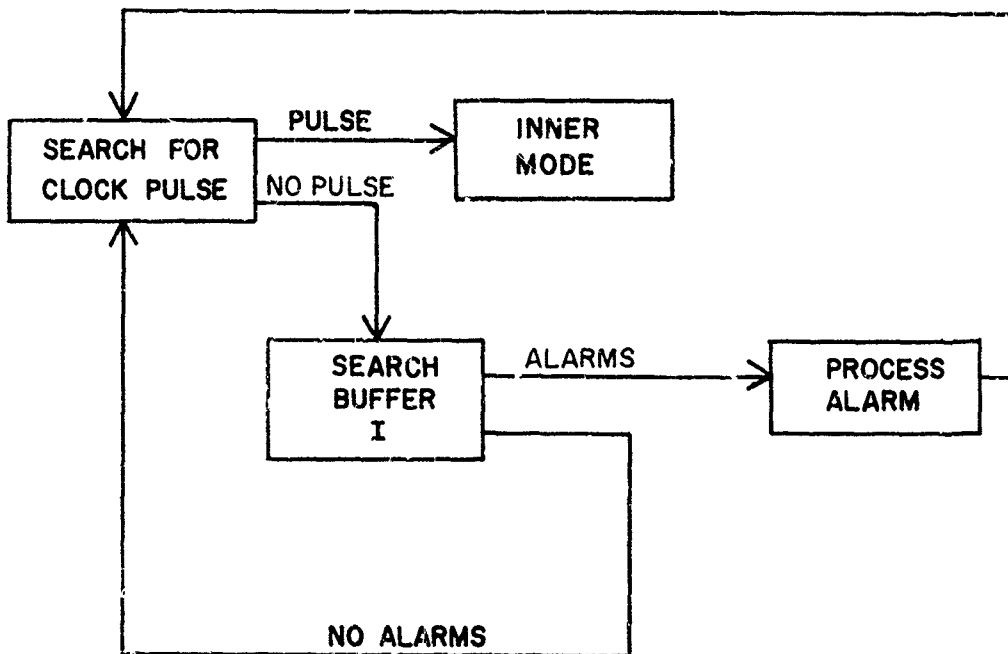


FIGURE 4-16

The only way the computer can leave its outer mode is by the occurrence of a clock pulse. When a clock pulse occurs, the computer enters its inner mode. Here the computer takes all the information in the buffer, stores it in an internal memory, and then clears the buffer. This information is then processed in rapid succession while the buffer begins to receive information from the next scan. After completing this processing operation the computer performs some housekeeping which is necessary to prepare it for the next outer mode. This operation will be described later. As soon as the housekeeping is completed, the computer returns to its outer mode. The length of time spent in the inner mode will depend on the number of alarms remaining to be processed when the inner mode begins. The actual processing of information is performed in a manner similar to that described in the 7th PLATO Quarterly Report. However, there are a sufficient number of changes in the method described there to warrant a description. As before alarms are compared to form pairs, then triples,

CONFIDENTIAL

and finally tracks. A track is defined as a set of four alarms whose coordinates form a possible target missile path. In addition, it is necessary for the computer to continue tracks, i.e., once having established a track it will be necessary to continue plotting the track and therefore to send into the prediction computer fresh alarms which lie along the path of the supposed target. Alarms, pairs, etc., are saved for three scans even though they have not been continued. At the end of three scans if they have not been continued they are dropped from the computer memory. The alarms coming in are always assumed to be in scan 0; the previous scan is scan 1; the scan before that is scan 2, and the next preceding scan is scan 3. When the processing operation is begun, an alarm in scan 0 is compared first with each of the tracks in scan 1 then with the tracks of scan 2 and next with the tracks of scan 3. The alarm is then compared with the triples, next with the pairs, and finally with the alarms. In each case the comparison is made first with the objects in scan 1, then with those of scan 2, and then with those of scan 3.

Two alarms, $P_4: (\eta_4, \xi_4, R_4, t_4)$ and $P_3: (\eta_3, \xi_3, R_3, t_3)$ form a pair when

$$\left| \frac{\eta_3 - \eta_4}{t_3 - t_4} \right| = |u| \leq a$$

$$\left| \frac{\xi_3 - \xi_4}{t_3 - t_4} \right| = |v| \leq b$$

$$\left| \frac{R_3 - R_4}{t_3 - t_4} \right| = |w| \leq c$$

where a , b , and c are constants dependent only on the geometry of the radar and on the expected speed of the target missiles and have been determined in the 7th PLATO Quarterly Report. Given the established pair P_3 , P_4 and its associated straight-line velocity components u , v , w , an alarm $P_2: (\eta_2, \xi_2, R_2, t_2)$ combines with the pair to form a triple if

$$|\eta_2 - \eta_4 - u(t_2 - t_4)| \leq d$$

$$|\xi_2 - \xi_4 - v(t_2 - t_4)| \leq e$$

$$|R_2 - R_4 - w(t_2 - t_4)| \leq f$$

where d , e , and f are constants dependent on the geometry of the radar and on the expected missile speed. If $P_2 P_3 P_4$ forms a triple, an improved

CONFIDENTIAL

set of "straight-line" velocity components u, v, w can be generated by an averaging process. Then the alarm $P_1: (\eta_1, \xi_1, R_1, t_1)$ combines with the triple to form a quadruple if

$$|\eta_1 - \eta_4 - u(t_1 - t_4)| \leq g$$

$$|\xi_1 - \xi_4 - v(t_1 - t_4)| \leq h$$

$$|R_1 - R_4 - w(t_1 - t_4)| \leq i$$

where again $g, h,$ and i are constants. If $P_1P_2P_3P_4$ form a quadruple, then they will form a track if

$$(\eta_1 - \eta_4)^2 + (\xi_1 - \xi_4)^2 + (R_1 - R_4)^2 \geq j(t_1 - t_4)^2$$

where j is a constant. This last test is used to eliminate slowly moving as well as stationary targets. If $P_1P_2P_3P_4$ form a track, then $P_0: (\eta_0, \xi_0, R_0, t_0)$ continues the track if the track continuation criterion discussed in the 7th Quarterly report is passed.

When an alarm P_1 is compared with say a triple P_{234} , then even if $P_1P_2P_3P_4$ does not form a track, some positive information may be extracted, for example $P_1P_3P_4$ may form a triple. In this case, as in all others, all subtests should be made, unless, of course, $P_1P_2P_3P_4$ forms a track.

Each positive test result is listed in the temporary memory. This memory is divided into four parts.

- (1) The continued tracks
- (2) The new tracks
- (3) The triples
- (4) The pairs

After all the tests have been made using all the alarms of the scan, the computer is ready to perform its housekeeping. The first track in 1 is listed in row 0 of the continued tracks and the latest alarm is sent on to the prediction computer. The second track in 1 is examined to ensure that it is different from the first track. If it is, then it is listed in row 0 of the continued tracks and the latest alarm is sent on to the prediction computer. If it is the same as the first track, then it is dropped from the track initiation computer memory. Similarly, the third alarm is compared to see whether it is different from the first two alarms, etc. Having examined all the continued tracks, the computer performs the same sort of operation with the new tracks. It takes, for example, the third track

CONFIDENTIAL

in 2 and examines this track to see whether it is different from the tracks in 1 and the first two tracks in 2. If it is, then it is listed in row 0 of the tracks memory and the four alarms are assigned a track number and sent on to the prediction computer. The process for the triples is somewhat different. Not only must the computer determine that a triple hasn't already been listed as a triple, but it must ensure that a triple doesn't occur as a subset of a track. That is, if $P_1P_2P_3P_4$ is a track and $P_1P_3P_4$ is a triple, then $P_1P_3P_4$ should not be listed in row 0 of the triples register. As an illustration of this operation, suppose the computer has processed the first triple in 3 and wishes to process the second triple; the computer first sees that the second triple is not identical with the first triple. If they are the same, the computer drops the second triple from its memory and goes onto the third triple. If they are not the same, the computer checks to see if the second triple has occurred as a subset of a track. If it has, then again the triple is dropped. If it has not, then the triple is listed in row 0 of the triples register. A similar operation is performed with the pairs in the temporary memory, where not only are the pairs checked to ensure distinctness but also to ensure that they have not occurred as subsets of either the tracks or the triples.

The computer next goes through rows 1 and 2 of the (regular) memory, removes those tracks, triples, pairs and alarms which have been continued and lists in row 0 of the alarms register those alarms of scan 0 which have not continued any track, triple, pair, or alarm. Finally, the rows are relabeled with row 0 becoming row 1, row 1 becoming row 2, and row 2 becoming row 3. Row 3 is discarded (and will be used for the next row 0). The computer is returned to its outer mode and the processing of alarms from the next scan begins.

4.3.2 EXTRANEIOUS ALARMS

The alarms coming into the acquisition radar may have originated from many sources. All those alarms which do not arise from a target missile will be classified as extraneous alarms or noise. It is the aim of the acquisition radar and of the track initiation computer to eliminate as many of these extraneous alarms as possible while at the same time maintaining as high a degree of sensitivity as possible. These two aims may be incompatible; in that case a closer look at the entire noise problem is indicated. Some sources of noise are listed under two headings below. The first group are typical of those that will be handled in the radar while the second group is characteristic of those to be handled by the computer.

4.3.2.1 Alarms Typical Of Those Handled By The Acquisition Radar

When there is pulse interference from other radars a filtering may be introduced into the acquisition radar if the radars are using essentially

CONFIDENTIAL

different frequencies. If the signals from the other radars are similar then more subtle methods such as modulation envelope coding or carrier coding must be used. CW interference may be attacked by frequency shifting or by filtering. For clutter, area discrimination (in both azimuth and range) as well as MTI (carrier coding) may be used. Noise jamming may occur from natural sources such as the sun, stars, etc., or from enemy action.

4.3.2.2 Alarms Typical Of Those Handled By The Track Initiation Computer

Interference from extraneous objects may be divided into essentially two classes: planes and meteors. The meteors will be eliminated for the most part by their short duration. That is, they would fail to pass the pairs test set up in 4.3.1. At least during a meteor shower they might provide the danger of computer saturation if their number became excessive. Slow-moving planes are eliminated by the test performed in Section 4.3.1 which tests the velocity of a quadruple. Again, these planes are capable of causing saturation if sufficiently many of them were capable of flying in a range which the acquisition radar covers. For example, in the low angle coverage of the radar (5°) and at a range of 150 miles from the radar, planes flying at an altitude of 70,000 ft. or greater would be picked up by the radar. Another problem presents itself in that in a few years the speed of fast planes may approach that of slow missiles in which case these planes would pass the track initiation test and be sent on to the prediction computer. Presumably here further discriminatory tests could be made.

Internal noise is assumed to come from tube noise and the like and is assumed to have a mean of three per scan (one per second) and a Poisson distribution. This source has been discussed in some detail in the 7th PLATO Quarterly Report. It will suffice here to mention the results of computations performed in order to determine the number of pairs from internal noise sources alone. It has been shown* that the probability of exceeding seven pairs is 0.0026 so that it would seem that this source does not place an excessively severe strain on the computer.

4.3.3 THE PREDICTION COMPUTER

The prediction computer was discussed in some generality in the 7th PLATO Quarterly Report. What will be added here is a detailed description of the timing cycle of the information flow, and of the adjust computation.

* PLA 251/16

CONFIDENTIAL

4.3.3.1 The Timing Cycle

The scheme for the timing cycle (or traffic control) is similar in many ways to that proposed for the track initiation computer. Information is sent to the prediction computer from two different sources: the track initiation computer and the triangulation radar. The prediction computer sends its processed information to the guidance computer and to the triangulation radar. For both inputs and outputs it is assumed that buffers are available. In addition, there is a master clock which sends in pulses at intervals of length T seconds. The computer operates in two modes.

Outer Mode

- (1) The computer tests to see if a clock pulse has occurred since the last time such a test has been made.
 - a. A pulse has occurred and the computer enters the inner mode.
 - b. A pulse has not occurred and the computer goes on to 2.
- (2) The acquisition buffer is tested for information.
 - a. There is information present. The computer processes this information and then goes on to 3.
 - b. There is no information present. The computer goes on to 3.
- (3) The triangulation buffer is tested for information. The results here are the same as in 2 above except that the computer goes on to 1.

Inner Mode

- (1) The information contained in the input buffers is emptied into certain cells of the prediction computer.
- (2) Critical decisions are made.
- (3) The information is processed to produce new values of ξ_1 , ξ_2 , ξ_3 , ξ_4 , ξ_5 , ξ_6 , the six parameters of the target trajectory which are used in the long range prediction.
- (4) The required outputs are produced and sent to the output buffers.
- (5) Non-critical housekeeping is performed and the computer returns to the outer mode.

CONFIDENTIAL

Item 5 can actually overlap the time allotted to the outer mode and, in fact, 5 could be considered as being part of the outer mode. The timing cycle can be represented therefore as:

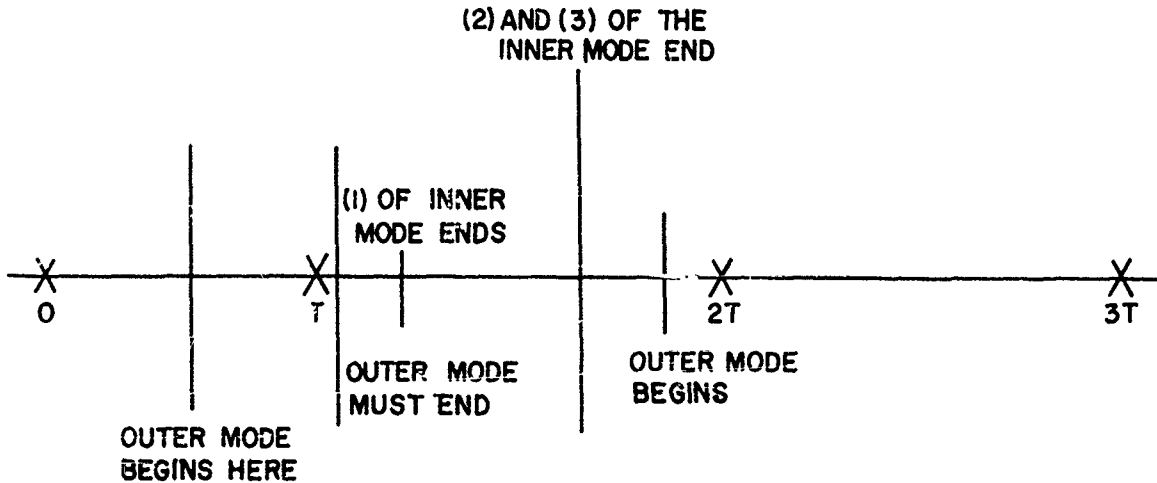


FIGURE 4-17

Item 2 of the inner mode refers to those decisions which the computer must make before beginning its processing operations; for example, which tracks should be processed first, which data should be ignored, etc.

Item 3 of the inner mode is, of course, the basic function of the prediction computer and will be described in the next sections.

Item 5 contains such operations as the dropping of non-continued tracks.

For the outer mode, the order between 2 and 3 is not rigid. It may be changed or 1 could follow both 2 and 3 and then 1 could lead into 2 or 3 alternately.

4.3.3.2 Information Flow

In the above timing cycle description, information processing was mentioned several times. This processing operation depends somewhat on the source of the received information: the acquisition radar or the triangulation radar.

CONFIDENTIAL

Acquisition Radar Information

Information from the acquisition radar is first sent to the track initiation computer where it is processed and then sent on to the buffer of the prediction computer. When the alarm arrives at the buffer it consists of three (rectangular) coordinate numbers (x, y, z), the time of reception (t) and a track number (#) so that the information is given by five coordinates (x, y, z, t, #). There are several schemes for storage of this information in the buffer: chronologically, according to track number, or both chronologically and according to track number. For the purposes of this paper the third scheme will be adopted so that the alarms are assumed to be stored according to track number and according to age. Note that information is assumed to arrive at the buffer at the same time the rest of the computer is engaged elsewhere and independently of which mode the computer is in.

When the computer decides to go to the input buffer, it must decide which track it should look at first. One scheme for making this decision is to search the length of the buffer in a periodic manner. Suppose the computer has decided on a track number; it then takes out the *most recent* alarm with that track number and sends it to the established track discriminator. This discriminator compares the track number of the alarm with a list of the track numbers of well established tracks.

When the discriminator does not have the alarm track number on its list, the alarm is sent on to the new track register discriminator where it is listed (or stored) with previous alarms (if any) with the same track number. Now the discriminator counts the total number of points (including this latest one) having this track number.

(1) The total number is less than four. Then the processing is ended. (It should be remarked that another scheme which is receiving consideration is that instead of ending the processing at this point, the computer should go back to the track initiation buffer and take the remaining points (at least three in number) from the buffer, send them to the new track register discriminator and proceed as in 2 below).

(2) The total number is four. The four points are then taken from the new track discriminator and fitted to a fifth order polynomial. The distance between each of the four points and the curve is next determined and each of these distances compared with a specified quantity.

If each of the distances is less than the specified quantity, then all points are assumed to be good, polynomial coefficients are sent to the partial sums register, the coefficients are sent to the coefficient register,

CONFIDENTIAL

the established track discriminator has added to its list of well-established track numbers the number of the present track, and the processing is ended.

If one of the distances is more than the specified quantity, then the point associated with this distance is assumed to be false, the remaining points are returned to the new track discriminator and the processing is ended.

If at least two of the distances are more than the specified quantity, then the oldest point is dropped, the remaining three points are returned to the new track discriminator, and the processing is at an end.

When the discriminator has the alarm track number on its list, the new or nth point is sent first to be checked against the predicted nth point. The predicted nth point is gotten by taking the time t_n associated with the measured nth point and evaluating the equation associated with the track at t_n . (The equation will, of course, be determined by use of the (n-1)st and preceding points.) This is one of the uses of the polynomial evaluation box.

- (1) The new point fails the check test. Then the split track routine is activated. Just what this consists of requires more study but at any rate the processing is ended.
- (2) The new point passes the check test. It is then sent on to the box which generates terms for the adjust computation and from there to the adjust computation itself. The adjust computation makes use of the previously stored coefficients and partial sums which are pulled into the adjust computation box. After the adjust computation is ended, the adjusted coefficients and partial sums are sent to the appropriate registers and the processing is ended. This completes the discussion of the processing operation using acquisition radar information.

Triangulation Radar Information

For triangulation radar information essentially only that described above in (2) for the acquisition radar is used. However, the triangulation radar receivers send multiple information which must first be transformed. Again, the exact timing, etc., of this information may be treated in a variety of ways but the following scheme seems reasonable. The information from a triangulation receiver consists of the time of arrival of the alarm together with the measured range sum and the track number. The buffer obtains this information from each of the receivers and stores it again

CONFIDENTIAL

according to track number and chronology. When the processing begins, the computer senses that the information being sent in is from the triangulation radar and sends it to the triangulation transformation box which converts the range sum to position errors (δ_x , δ_y , δ_z) by making use of the predicted range sum. (It may be necessary to subject these to nth point checks; however, it will be assumed that this is not needed.) Some of the information concerning range sums must also be used to generate the weights to be associated with the alarm in the adjust computations. The position error together with the weight is then sent on to the generation of terms for adjust computation. The processing operation is completed in the same manner described for the acquisition radar.

Assume now that the machine has decided to enter its output producing phase. As was the case for the processing operation, the form of the output operations will depend on whether the triangulation radar stage has been reached or not. Here the situation is further complicated by the existence of multiple tracks. However, as before, only one track will be pursued from the beginning to the end of the output phase.

There is a definite switch-over point in the output phase when the slant range of the target is, say, at 150 miles. At this point it becomes necessary to begin sending information to the triangulation radar. Hence, the first action of the computer upon entering the output phase would be to check the slant range. (Since the target may be assumed not to fly backward, the check need only be made as long as the range is more than 150 miles.) This check is to be made in the range discriminator as follows:

When the range is greater than 150 miles, the coefficients (ξ_1, \dots, ξ_6) are taken from the coefficient storage register and combined appropriately to form the equations.

$$x = x(t)$$

$$y = y(t)$$

$$z = z(t)$$

which are then stored in the polynomial evaluation box. The equations $60,000 = z(t)$ and $45,000 = z(t)$ are solved for t to get t_I , the intercept time and t_g , time to go. The pierce point $x = x(t_I)$, $y = y(t_I)$ and the pierce angle direction numbers $x(t_I)$, $y(t_I)$ are gotten. This ends the output phase.

If the range is for the first time not greater than 150 miles, all the above computations are made and, in addition, the following must be done. The equation $0 = z(t)$ is solved for t to get t_B , the time of impact. The

CONFIDENTIAL

impact point may then be gotten by $x = x(t_B)$, $y = y(t_B)$ and the impact point must be examined to determine whether it lies in the defended area.

- A. The point does not lie in the defended area. Then the output phase ends.
- B. The point lies in the defended area. Then μ_i , $\dot{\mu}_i$, (the expected range sum values) and possibly higher derivatives of μ must be computed for the triangulation radar receivers (i refers to the number of the receiver), and θ and ψ must be computed for the triangulation transmitter. In addition, the range discriminator is notified that the range for a particular track # is now less than 150 miles. The output phase ends.
- C. It may be necessary to regard this decision as a function with three values, the third being reached when the point lies on or near the border of the defended area. Just what decision must be reached in this case requires additional study.

If the range is less than 150 miles, the computation described above for this case must again be made and θ and ψ must be computed for the transmitter. This ends the output phase.

4.3.3.3 Mathematical Procedure for the Trajectory Fitting Process

The basic scheme used for prediction for the PLATO system does the following. The radar data points which yield position-time information concerning the target, are processed in such a manner that a trajectory along which the target missile is flying is determined. Prediction is then equivalent to extrapolation along the trajectory.

In what follows it will be shown what form of data processing is, how this determines the trajectory, and how a program for the Prediction Computer is obtained from the particular form of data processing described.

The PLATO Defense System is to defend against target missiles which will fly along a ballistic trajectory for a considerable portion of its flight time. Some means must therefore be available of determining ballistic trajectories. Now since the differential equation which must be satisfied by a particle following a ballistic path is of second order, it necessarily follows that if at any time t_0 , both the position and velocity of the particle are known then the particular ballistic path is completely determined. This means that if an earth coordinate system is used to denote position, then if for any given time t_0 one knows the six quantities

CONFIDENTIAL

$$\begin{aligned}x(t_0) & \quad \dot{x}(t_0) \\y(t_0) & \quad \dot{y}(t_0) \\z(t_0) & \quad \dot{z}(t_0)\end{aligned} \tag{1}$$

for a target missile, then the ballistic path is determined.

The question now to be answered is the following. Knowing the six quantities in equation 1 how can the ballistic path be characterized in terms of them so that extrapolation (prediction) can be performed? This question has been answered in Technical Report 4-2 as follows: Fifth order polynomials were derived to characterize the path in such a manner that extrapolation (prediction) within the limits required by the PLATO system would yield position information accurate to within 1/10 nautical mile.

To summarize:

The six quantities:

$$\begin{aligned}x(t_0) & \quad \dot{x}(t_0) \\y(t_0) & \quad \dot{y}(t_0) \\z(t_0) & \quad \dot{z}(t_0)\end{aligned} \tag{1}$$

completely determine a ballistic trajectory and the 3 fifth order polynomials

$$\begin{aligned}x(t) &= x(t_0) + \dot{x}(t_0)(t-t_0) + a_2(t-t_0)^2 + a_3(t-t_0)^3 + a_4(t-t_0)^4 + a_5(t-t_0)^5 \\y(t) &= y(t_0) + \dot{y}(t_0)(t-t_0) + b_2(t-t_0)^2 + b_3(t-t_0)^3 + b_4(t-t_0)^4 + b_5(t-t_0)^5 \\z(t) &= z(t_0) + \dot{z}(t_0)(t-t_0) + c_2(t-t_0)^2 + c_3(t-t_0)^3 + c_4(t-t_0)^4 + c_5(t-t_0)^5\end{aligned} \tag{2}$$

where $a_2, \dots, a_5, b_2, \dots, b_5, c_2, \dots, c_5$, are given functions of the six quantities in (1), will completely characterize a ballistic trajectory for purposes of extrapolation (prediction) necessary to the PLATO system.

The question to be answered next is: How is the radar data to be used to determine the six quantities of (1)?

The answer is as follows:

The fifth order polynomials of (2) are fitted to the data points in the least square sense using the six quantities of (1) as parameters to optimize the fit. Technical Report 4-2 discusses several alternative methods in detail for obtaining this fit. We shall discuss the method which leads to a fairly simple computer program.

CONFIDENTIAL

The procedure of taking cognizance of the probability of the magnitude of errors in the measurement of the points, when fitting a curve to a set of measured points is called weighting.

During the computational routine of making the fit, a number called a weight is associated with each of the measured points for the purpose of weighting.

Now since the data points, which we will be fitting curves to, are the result of radar measurements which in general have a varying accuracy dependent on range, our computational procedure of fitting must necessarily generate the proper weights if we are to make the best use of the information at hand.

The manner in which we make the fit is to make three separate fits, one for each coordinate.

For example, assume we have a set of data

$$\begin{array}{cccc} X_0, & Y_0, & Z_0, & t_0 \\ X_1, & Y_1, & Z_1, & t_1 \\ \vdots & \vdots & \vdots & \vdots \\ X_m, & Y_m, & Z_m, & t_m \end{array}$$

We will fit the fifth order polynomial for x to the X data, using $x(t_0)$, $\dot{x}(t_0)$ as parameters, the polynomial for y to the Y data, using $y(t_0)$, $\dot{y}(t_0)$ as parameters, and the polynomial for z to the Z data, using $z(t_0)$, $\dot{z}(t_0)$ as parameters to optimize the fit. Each fit will use the proper weights (as nearly as can be derived). After the three fits are made, an iterative fitting procedure is used to account for crossed parameters.

Summary:

Re-writing equation 2,

$$\begin{aligned} x(t) &= x(t_0) + \dot{x}(t_0)(t-t_0) + A[x(t_0), \dot{x}(t_0), y(t_0), \dot{y}(t_0), z(t_0), \dot{z}(t_0), t] \\ x(t) &= y(t_0) + \dot{y}(t_0)(t-t_0) + B[x(t_0), \dot{x}(t_0), y(t_0), \dot{y}(t_0), z(t_0), \dot{z}(t_0), t] \\ z(t) &= z(t_0) + \dot{z}(t_0)(t-t_0) + C[x(t_0), \dot{x}(t_0), y(t_0), \dot{y}(t_0), z(t_0), \dot{z}(t_0), t] \end{aligned}$$

Step I

Minimize

$$\sum_{i=0}^m a_{i,x}^2 [X_i - x_1(t_0) - \dot{x}_1(t_0)(t-t_0) - A(0,0,0,0,0,0,t)]^2 \quad (3a)$$

CONFIDENTIAL

using $x_1(t_0)$, $\dot{x}_1(t_0)$ as parameters,

$$\sum_{i=0}^n a_{1,y}^2 [Y_i - y_1(t_0) - \dot{y}_1(t_0)(t-t_0) - B(0,0,0,0,0,0,t)]^2$$

using $y_1(t_0)$, $\dot{y}_1(t_0)$ as parameters,

$$\sum_{i=0}^n a_{1,z}^2 [Z_i - z_1(t_0) - \dot{z}_1(t_0)(t-t_0) - C(0,0,0,0,0,0,t)]^2$$

using $z_1(t_0)$, $\dot{z}_1(t_0)$, where the $a_{1,x}$, $a_{1,y}$, $a_{1,z}$ are the proper weights for the X_1 , Y_1 , and Z_1 data respectively.

Step II

Minimize:

$$\sum_{i=0}^n a_{1,x} \left\{ X_i - x_2(t_0) - \dot{x}_2(t_0)(t-t_0) - A[x_1(t_0), \dot{x}_1(t_0), y_1(t_0), \dot{y}_1(t_0), z_1(t_0), \dot{z}_1(t_0), t] \right\}^2 \quad (3b)$$

using $x_2(t_0)$, $\dot{x}_2(t_0)$ as parameters, and minimizing the analogous quantities for the Y and Z data.

This step by step procedure is continued until

$$\begin{array}{ll} x_n(t_0) \longrightarrow x(t_0) & \dot{x}_n(t_0) \longrightarrow \dot{x}(t_0) \\ y_n(t_0) \longrightarrow y(t_0) & \dot{y}_n(t_0) \longrightarrow \dot{y}(t_0) \\ z_n(t_0) \longrightarrow z(t_0) & \dot{z}_n(t_0) \longrightarrow \dot{z}(t_0) \end{array}$$

According to the above procedure we accomplish a least square fit to the $n+1$ data points

$$\begin{array}{l} X_0, Y_0, Z_0, t_0 \\ X_1, Y_1, Z_1, t_1 \\ \vdots \\ X_n, Y_n, Z_n, t_n \end{array}$$

Query: What is done when the next data point X_{n+1} , Y_{n+1} , Z_{n+1} , t_{n+1} arrives at the computer?

Answer: It can be shown that we need only solve the three following systems.

CONFIDENTIAL

$$A^x \begin{pmatrix} \Delta x(t_o) \\ \Delta \dot{x}(t_o) \end{pmatrix} = \begin{pmatrix} a_{n+1}^2 (X_{n+1} - x(t_{n+1})) \\ a_{n+1}^2 (X_{n+1} - x(t_{n+1}))(t_{n+1} - t_o) \end{pmatrix} - B^x \vec{\Delta a}$$

$$A^y \begin{pmatrix} \Delta y(t_o) \\ \Delta \dot{y}(t_o) \end{pmatrix} = \begin{pmatrix} a_{n+1}^2 (Y_{n+1} - y(t_{n+1})) \\ a_{n+1}^2 (Y_{n+1} - y(t_{n+1}))(t_{n+1} - t_o) \end{pmatrix} - B^y \vec{\Delta b}$$

$$A^z \begin{pmatrix} \Delta z(t_o) \\ \Delta \dot{z}(t_o) \end{pmatrix} = \begin{pmatrix} a_{n+1}^2 (Z_{n+1} - z(t_{n+1})) \\ a_{n+1}^2 (Z_{n+1} - z(t_{n+1}))(t_{n+1} - t_o) \end{pmatrix} - B^z \vec{\Delta c}$$

These equations are derived from equation 3b by the usual method of differentiation with respect to the parameters to obtain necessary conditions for minimization. The Δ 's are the adjustments to be made in the six basic quantities in absorbing the information contained in the new data point.

An important fact can now be brought out, and that is that the Prediction Computer will never need to retain all the past data points.

The computer needs only to operate on the current data point, and use the previous information by means of the computation involved in obtaining $x(t_{n+1})$, $y(t_{n+1})$, $z(t_{n+1})$, but these three quantities can be computed from the six basic quantities

$$\begin{array}{ll} x(t_o) & \dot{x}(t_o) \\ y(t_o) & \dot{y}(t_o) \\ z(t_o) & \dot{z}(t_o) \end{array}$$

The computation for the solution of equation 3 is called the adjust computation, and derives its name from the fact that an adjustment is made of the six basic quantities by use of the current data point.

The Use of Triangulation Radar Data in the Adjust Computation

The Triangulation Radar system yields positional information by means of multiple measurements of range sums. This radar is a precision radar and is assumed to be relieved of the searching function; this means that the radar is told where to look. It is, therefore, convenient for the

CONFIDENTIAL

radar to measure error of predicted range sum, i.e., the radar measures the difference between the range sum it was told to look at and the range sum at which the target is actually seen. The data output of the Triangulation Radar to the Prediction Computer can be considered as a set of measured errors of predicted range sum, one measurement for each receiver.

Analyses have been carried out to obtain the following:

- A. The means by which a set of errors of predicted range sum are converted to a single error of predicted position.
- B. The means by which a variance is to be associated with the error of predicted position so that weights (consistent with acquisition weighting) can be formulated for the triangulation radar data.

The analysis for A is carried out making use of the individual receiver accuracies and geometry to obtain the most probable magnitude and direction of the position error.

The analysis for B essentially accounts for receiver accuracies and geometric distortion to obtain the best weight to be used with the position error found.

It can be shown that

$$\begin{pmatrix} \delta X_n \\ \delta Y_n \\ \delta Z_n \end{pmatrix} = W^{-1} \begin{pmatrix} \eta_n^1 \\ \eta_n^2 \\ \eta_n^3 \end{pmatrix}$$

where the vector

$$\begin{pmatrix} \eta_n^1 \\ \eta_n^2 \\ \eta_n^3 \end{pmatrix}$$

accounts for

- a. measured errors of range sum,
- b. weighting for accuracies of the various receivers
- c. some geometry.

The matrix W^{-1} accounts for

- a. weighting for accuracies of the various receivers
- b. effects due to geometric distortion.

CONFIDENTIAL

If at time t_n the target should have been at $x(t_n)$, $y(t_n)$, $z(t_n)$ (according to the prediction equations), then a non-zero vector

$$\begin{pmatrix} \delta X_n \\ \delta Y_n \\ \delta Z_n \end{pmatrix}$$

means that the Triangulation Radar system has actually seen the target at $X(t_n) + \delta X_n$, $y(t_n) + \delta Y_n$, $z(t_n) + \delta Z_n$.

It has been proved that

$$\sigma^2(\delta X_n) \sim W_{11}^{-1}$$

$$\sigma^2(\delta Y_n) \sim W_{22}^{-1}$$

$$\sigma^2(\delta Z_n) \sim W_{33}^{-1}$$

where W^{-1} is the element of the i th and j th column of the W^{-1} matrix.

This means that this is the accuracy with which the Triangulation Radar system determines the position error. The weight to be used for each coordinate error should, therefore, be some quantity proportional to the reciprocal of the respective variance.

So we see that we have the following

$$X_n - x_n(t_n) = \delta X_n \quad a_{n,x}^2 \sim \frac{1}{W_{11}^{-1}}$$

$$Y_n - y_n(t_n) = \delta Y_n \quad a_{n,y}^2 \sim \frac{1}{W_{22}^{-1}}$$

$$Z_n - z_n(t_n) = \delta Z_n \quad a_{n,z}^2 \sim \frac{1}{W_{33}^{-1}}$$

and this is all that is necessary to perform the adjust computation for a correction of our six basic quantities.

4.4 GUIDANCE STUDIES: EXTENSION TO THREE DIMENSIONS

The two phases of guided flight- Midcourse and Terminal guidance - have been studied and models developed in two dimensions.^{1,2} The two

¹ PLATO Final Engineering Report, Phase I; April 1955

² PLATO Seventh Quarterly Report

CONFIDENTIAL

dimensional simulation² of mid-flight is currently in progress. The following sections develop the mathematical flow diagrams for the three dimensional guidance computer design. The midcourse and terminal guidance systems will be developed separately with a discussion of the transition phase from the midcourse form of the guidance computer to the terminal form.

The present guidance computer design describes the flight trajectory by specifying its x, y, z, position coordinates in a cartesian coordinate system with origin located at the launch site. Interceptor and target missile position and heading data is first transformed into this coordinate system before entering the guidance computer proper. Based on this data, the guidance computer computes commands for the interceptor missile which will originate in this coordinate system. The command computations and input and output quantities are described in vector form, since the notation is simpler and more generally descriptive than the trigonometric form of notation. The vector quantities will usually be defined in terms of their components along the x, y, and z axes.

When the vector commands for missile guidance have been computed in the x, y, z ground coordinate system, they must be transformed into the coordinate system defining the missile airframe axes. Therefore it is necessary ultimately to determine the direction cosines which relate the ground - fixed coordinate system to the unit vectors fixed to the airframe along the roll, pitch, and yaw axes, respectively. Specification of the airframe axes as pitch or yaw is arbitrary for a cruciform missile launched vertically. For purposes of this report the pitch axis may be arbitrarily defined at time of launch as the one aligned with the ground coordinate x-axis direction.

During flight, changes in missile orientation must be continuously computed, without ambiguity or loss of directional sense. This may be done either on the ground or in the air, or a combination of both. The form and location of this computation depends on the method of roll control system used and the source of data concerning missile rates of rotation.

The analysis to be presented here was developed on the basis of a missile roll control system with gyro instrumentation which maintains the yaw wingplane perpendicular to the ground-plane (i.e., pitch axis horizontal or parallel to the ground at all times). However, the model has sufficient generality so that any other coordinate plane can be taken as a gyro reference, instead of the ground plane. Extension of the system to the alternative case of a zero-roll missile, in which rotational freedom about the

- - - - -
² PLATO Seventh Quarterly Report.

CONFIDENTIAL

missile roll axis is reduced to a minimum, is possible simply by computing the third Euler angle (bank angle). Commands derived for the vertical wing assumption could then be transformed through this angle of rotation to properly proportion them to the true pitch and yaw axes.

4.4.1 THE MIDCOURSE GUIDANCE SYSTEM

The objective of midcourse guidance is to deliver the interceptor missile into the predicted ballistic trajectory of the target missile. Although the PLATO missile is designed for maneuver capabilities normal to its heading, which are greater than expected target maneuvers, the interceptor in the present design is assumed to have no thrust control; while the target missile may have large and controllable deceleration capabilities.

Therefore, it is desirable to minimize the effect of this longitudinal control disparity on miss distance by delivering the interceptor missile into a head-on collision course with the target. Tangential acceleration differences then only effectively delay the time of collision.

Radar noise resolution and target prediction error at high altitudes, and probable ground damage at low altitudes, necessitate intercept of the target missile, and hence termination of the midcourse flight, within a prescribed range of altitude. The factors affecting the spread of intercept altitudes are the uncertainties of prediction of target time-of-arrival and of midcourse flight time. These factors force us to launch the missile early. It is, therefore, desirable to maintain the missile on a trajectory during midcourse whose flight time is known from prior simulation, and which is known to be efficient from the standpoint of required time and energy expenditure. The desired trajectory must be capable of functional description so that the guidance computer can make error estimates and control the missile path in some systematic way.

Because of its generality a polynomial form of path specification is employed, in which ground range coordinates x and y are specified as polynomial functions of altitude, z . The polynomials are fitted to endpoint boundary conditions of position, slope, and curvature at the launch site and on the target inverse trajectory at an altitude (Z_0) chosen for end-of-midcourse. Additional conditions may be required as for example, restraints on the path curvature to prevent commands in excess of the available missile maneuver capability; these restraints are functions of range and heading at end of midcourse in both x and y directions. Flight time and curvature restraints for the midcourse path would be stored in computer memory as a function of the endpoint conditions of target range and heading.

CONFIDENTIAL

Midcourse path describing functions will therefore be defined in the form

$$x = f(z) = \sum_{i=0}^n a_i z^i \quad (1)$$

$$y = g(z) = \sum_{i=0}^n b_i z^i \quad (2)$$

where the a_i 's and b_i 's are determined by substituting functions of end-point boundary conditions and other restraints into nth order matrix solutions for the coefficients. Some of them may be zero.

Because of the simpler instrumentation required for the missile and autopilot, normal acceleration was selected as the controlled variable and the commanded quantity transmitted to the missile. The normal acceleration vector command is derived from both the directed curvature of the path describing function and from the vector position deviations of the target and interceptor missiles from the desired path.

The commanded maneuver is derived from two sources: (1) The directed curvature of the desired flight path is multiplied by the missile velocity squared, to produce a vector acceleration command which, if perfectly executed, would maintain the missile on the desired path (or a parallel course). (2) To this is added a corrective command proportional to the vector position deviation of the missile from the desired path. This error-correction component is multiplied by a gain factor designed to distribute corrections evenly along a large portion of the remaining flight time, regardless of the actual missile heading.

The method of compensation for motion or wander of the path endpoint caused by target prediction uncertainty can be one of two alternatives: (1) Add a vector position correction in the error loop which horizontally translates the desired flight path as the endpoint wanders, and thereby generates additional error-correcting commands, (2) Recompute the desired path by substitution of the new endpoint conditions in the matrix solution for the polynomial coefficients. The choice between these methods will be possible after study of the results of the two dimensional simulation currently in progress.

The three dimensional guidance system model for the midcourse phase will be introduced separately from the model for terminal phase flight, to simplify the description. However, it is important to consider the method of transition from midcourse to terminal phase flight, and this will be considered later.

CONFIDENTIAL

Figure 4-18 shows the closed-loop midcourse guidance system model. Figure 4-19 shows the guidance computer block diagram for the proposed midcourse model. The computer is fed information on target missile predicted position (\underline{R}_T) and heading vector $[d/ds(\underline{R}_T)]$ at the chosen end-of-midcourse altitude (Z_o) from the target prediction computer, and actual interceptor missile position (\underline{R}_I) from the missile tracking radar. (s) denotes the implicit parameter, path length.) The computer processes this data in the ground-fixed coordinate system defined in paragraph 4.4. A description of the computer functions follows:

4.4.1.1 Programmed Path Coefficient Computer

When an enemy threat from a PLATO target has been detected, a launch site is selected based on launch site coverage capabilities. The target missile's predicted position and heading are then transformed into launch site coordinates and become upper end-point boundary conditions to which the midcourse path describing functions must be fitted. The describing functions define the x and y ground range coordinates of the midcourse trajectory as nth order polynomial functions of altitude, (Z) (see equations 1 and 2). The fitting process (determination of the polynomial coefficients) is accomplished by solution of a square matrix whose order corresponds to the number of boundary conditions and curvature restraints imposed on the polynomial functions. The path-describing functions then define the desired position vector \underline{R}_c as a function of the altitude coordinate, (z).

4.4.1.2 Error Command Computer

Figure 4-20 shows the error command computation in symbolic form. \underline{E}_T represents the amount by which the target missile predicted position $\underline{R}_T(t_g, Z_o)$ at the altitude Z_o (computed at present time-to-go, t_g) differs from the stored prediction value $\underline{R}_T(t_{g_o}, Z_o)$. $\underline{R}_T(t_{g_o}, Z_o)$ was the endpoint boundary condition $\underline{R}_c(Z_o)$ for the original computation of the nominal path functions at time of launch (t_{g_o}). The function of the error-correction loop is to produce a missile deviation \underline{E}_I from the nominal path which accumulates over the midcourse flight in the proper direction to cancel the target prediction deviation from the nominal path. \underline{E}_I is computed by differencing the interceptor missile's actual measured position $\underline{R}_I(t_g)$ at time t_g with the nominal path position vector $\underline{R}_c(Z_I)$ associated with the measured missile altitude, Z_I . The relative error, $\underline{E}_H = (\underline{E}_T - \underline{E}_I)$ is then the basis for corrective commands to the missile. (See Figure 4-21.)

The relative error vector, \underline{E}_R , which has no vertical component, can be viewed as the horizontal translation which would bring the interceptor missile back on the nominal path if this path were itself translated

CONFIDENTIAL

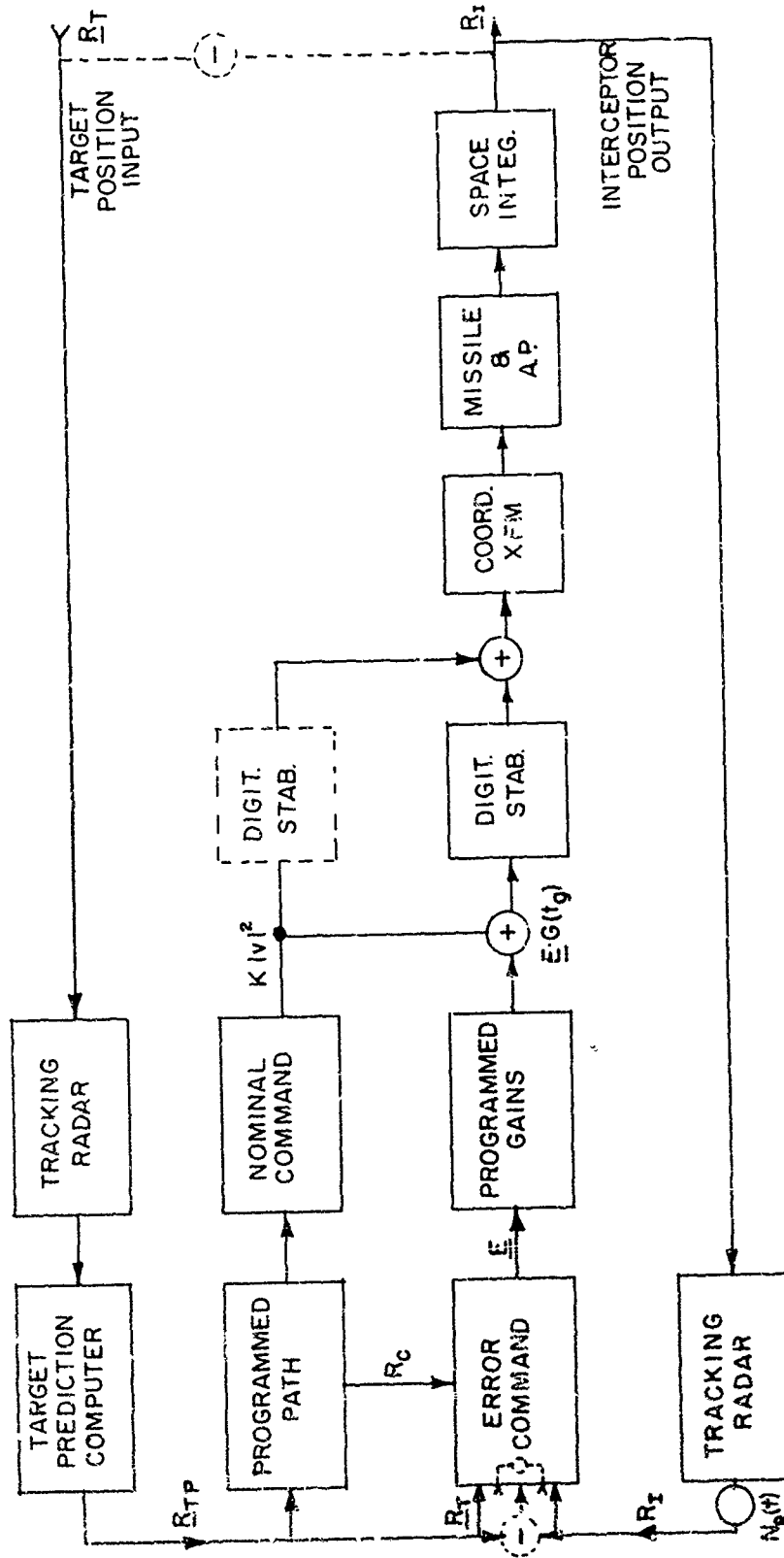
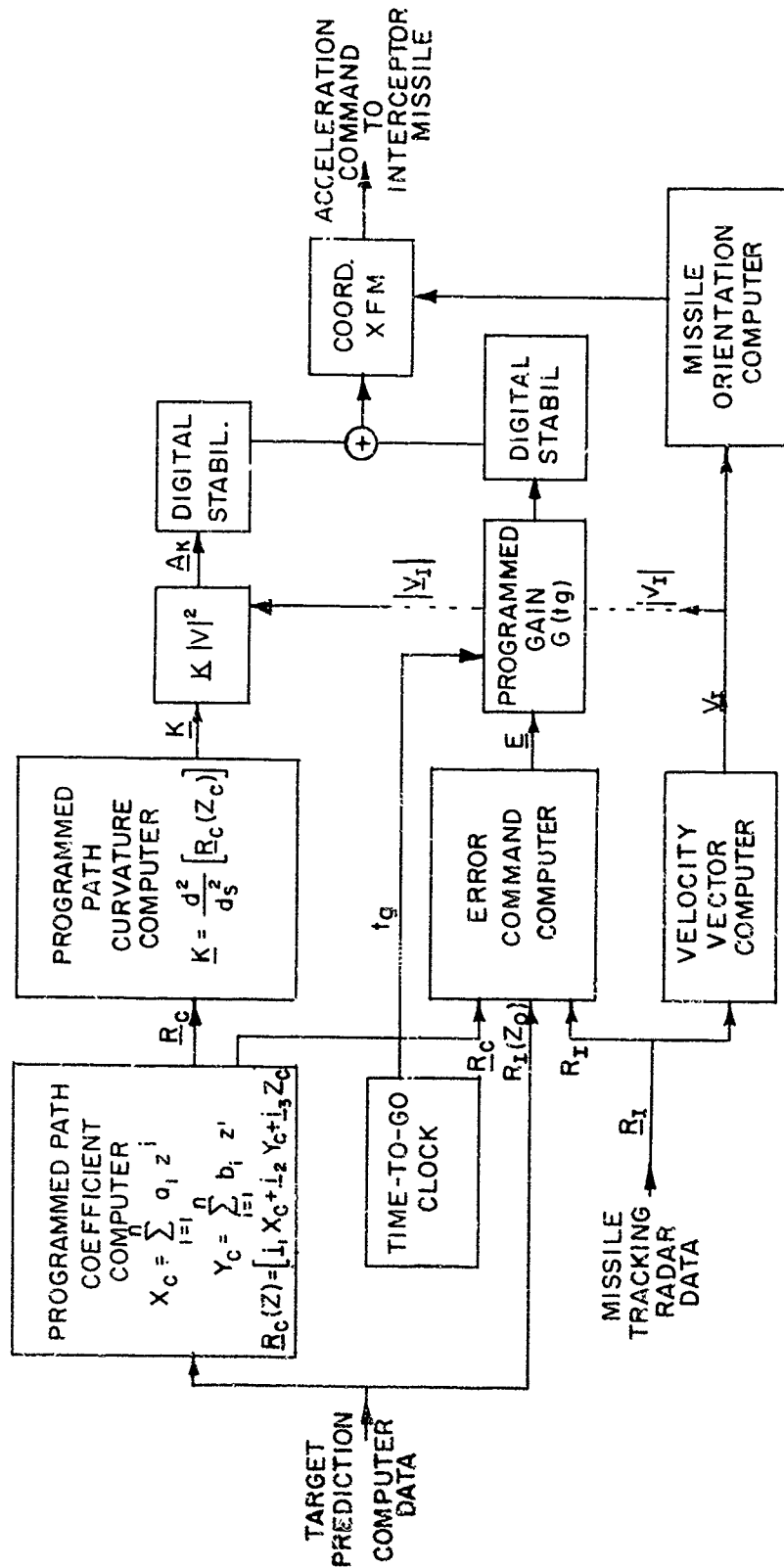


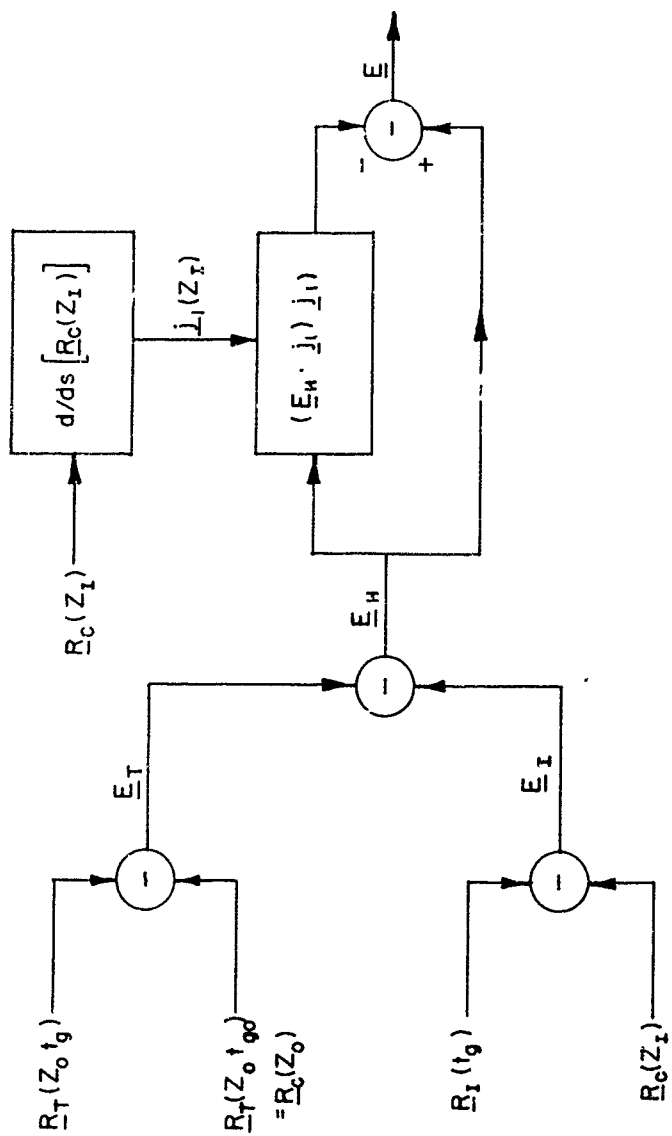
FIGURE 4-18. CLOSED LOOP MIDCOURSE GUIDANCE SYSTEM

CONFIDENTIAL



CONFIDENTIAL

FIGURE 4-19. MIDCOURSE GUIDANCE COMPUTER BLOCK DIAGRAM



$R_T(Z_0, t_g)$ = PRESENT TARGET PREDICTION
 $R_T(Z_0, t_{g0})$ = ORIGINAL TARGET PREDICTION
 $R_C(Z_0)$ = ENDPOINT OF PROGRAMMED PATH
 NOTE: $R_T(Z_0, t_{g0}) = R_C(Z_0)$
 $R_I(t_g)$ = PRESENT INTERCEPTOR POSITION
 $R_C(Z_1)$ = PROGRAMMED PATH POSITION AT PRESENT INTERCEPTOR ALTITUDE
 s = (IMPLICIT) PATH LENGTH PARAMETER
 E_T = ENDPONT WANDER OR TARGET DEVIATION
 E_I = INTERCEPTOR DEVIATION FROM PROGRAMMED PATH
 E_H = RELATIVE ERROR DEVIATION IN A HORIZONTAL PLANE
 E = RELATIVE ERROR DEVIATION COMPONENT PERPENDICULAR TO PROGRAMMED PATH TANGENT
 j_1 = PROGRAMMED PATH TANGENT

FIGURE 4-20. ERROR COMMAND COMPUTATIONS

CONFIDENTIAL

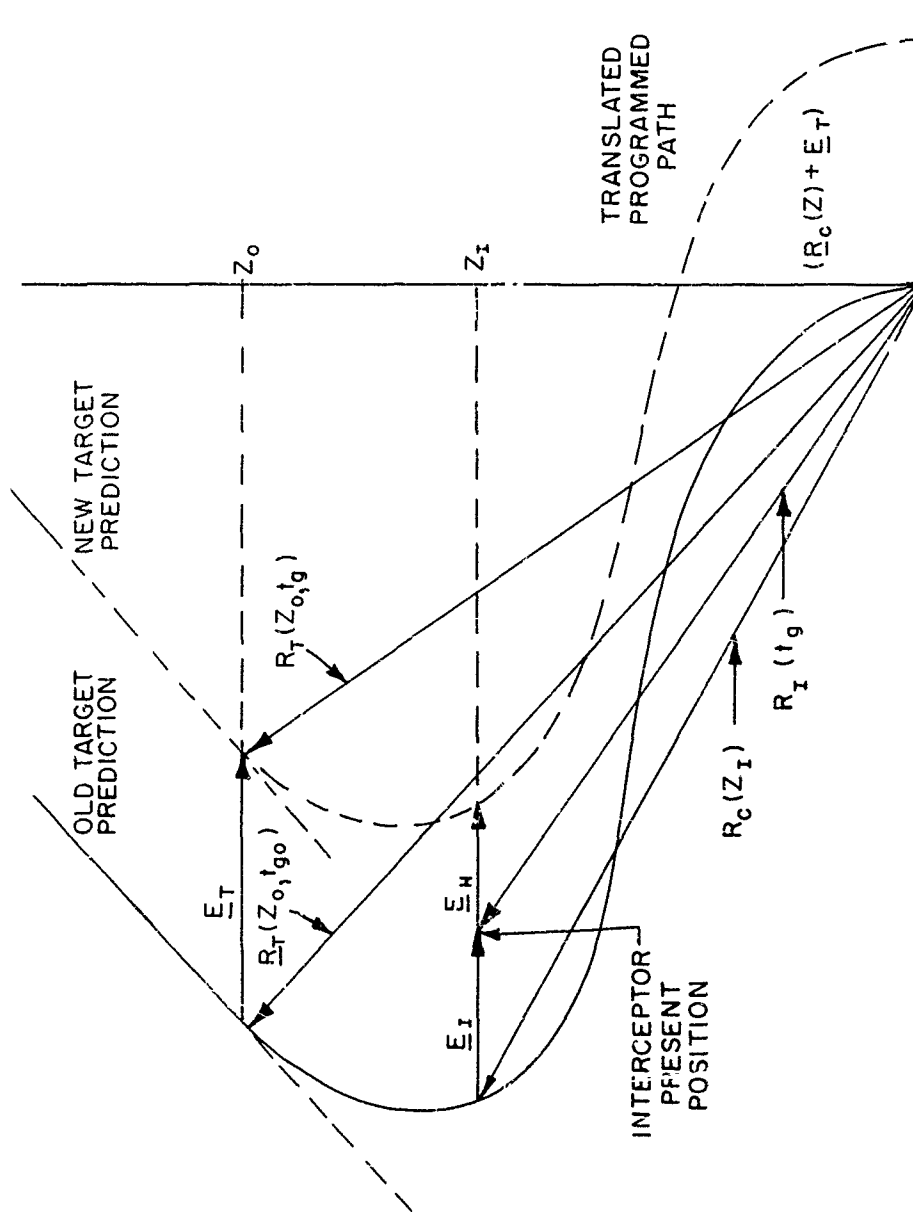


FIGURE 4-21. RELATIVE ERROR DEVIATION

CONFIDENTIAL

CONFIDENTIAL

horizontally by the amount of target deviation, \underline{E}_T . The translated nominal path could be represented by the vector sum $\underline{R}_C(Z_I) + \underline{E}_T$ (see Figure 4-21).

Consider the same picture redrawn to a larger scale as in Figure 4-22. The missile has an error from the translated nominal path \underline{E}_H in the horizontal direction. However, the point $\underline{R}_C(Z_I) + \underline{E}_T$ to which the vector \underline{E}_H directs the missile on this path may not be the easiest or most desirable point toward which the missile would try to fly if given error-correcting commands. In particular, \underline{E}_H becomes disproportionately large if the path slope approached the horizontal, which is possible for long-range intercepts. Therefore, it is desirable to compute an error \underline{E} from the interceptor missile to some closer point on the desired path.

To accomplish this, a simplified method was chosen which approximates the programmed path by the first term in its Taylor series expansion around the point $\underline{R}_C(Z_I)$. In other words, the programmed curve is replaced by its tangent, defined by the vector equation $\underline{j}_i = d/ds \{ \underline{R}_C(Z_I) \}$. The error, \underline{E} , is the perpendicular distance from the missile position to this line, and is found by subtracting from \underline{E}_H its component in the direction \underline{j}_i ; this component has the magnitude $(\underline{E}_H \cdot \underline{j}_i)$, since \underline{j}_i is a unit vector. Therefore, we have the resulting equation:

$$\underline{E} = (\underline{E}_H \cdot \underline{j}_i) \underline{j}_i$$

The linear approximation for the curve introduces errors in the computation \underline{E} , depending on the path curvature. Little advantage is gained by more accurate approximation for small errors, (≤ 100 ft.) since the radar noise in interceptor position measurement is comparable to the gain in geometric accuracy, for curve approximations of higher order than the straight line.

The largest source of error deviations is expected to be target prediction noise. When the error \underline{E}_H becomes too large for the linear approximation discussed above, it is proposed that the programmed path coefficients be recomputed, using the most recent target prediction data as a new upper endpoint. This has other advantages since large error components are reduced, and more realistic re-appraisals of remaining flight time may be available.

It might be argued that since the interceptor missile heading should be approximately parallel to programmed path tangent during flight, the horizontal error vector \underline{E}_H could be sent directly to the final coordinate transformation, where its components, normal to the roll axis, are extracted. If the missile roll axes were known to be truly parallel to the nominal path tangent, then the same vector command \underline{E}_H , would result. However, since radar measurement of heading vector is contemplated as one

CONFIDENTIAL

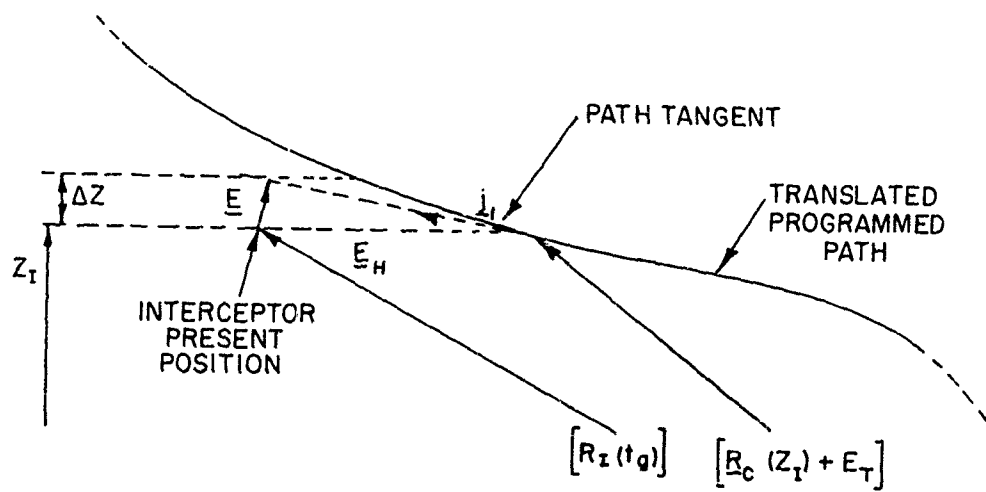


FIGURE 4-22. NORMAL COMPONENT OF ERROR

CONFIDENTIAL

CONFIDENTIAL

source of roll axis orientation knowledge, and since during near-horizontal flight the radar noise might cause an apparent positive or negative shift in elevation angle of the roll axis, the directional sense of the error correcting command components normal to the roll axis would be lost. Replacing \underline{E}_H by its component normal to the path tangent, \underline{E} , avoids this difficulty.

4.4.1.3 Programmed Path Curvature Computer

During flight, the directed curvature \underline{K} of the programmed path is computed and multiplied by the square of the magnitude of the interceptor missile velocity to obtain a nominal acceleration command vector $(\underline{K}) |V_I|^2$. Since the reciprocal of curvature is radius of curvature, R , and we know that a body of mass M moving in an arc of that radius with velocity V^2 develops centrifugal force equal to (MV^2/R) , the lift acceleration needed to oppose this force is $a_L = (V^2/R) = (V^2)(\underline{K})$.

The importance of this command component will be appreciated if the system performance is considered first with only a command based on the relative missile deviation from the programmed path, \underline{E} . Then there must always be a finite error \underline{E} before a command for missile maneuver is originated in the guidance system. With the nominal acceleration command added, if the interceptor missile is on the desired path ($\underline{E} = 0$), it will still follow the programmed course. In effect, the nominal command overcomes the delays incurred in awaiting the buildup of a deviation from the path to compute new commands.

Computation of K is simply defined by the equation $\underline{K} = d^2/ds^2 (R_c(Z_I))$ (Reference Eisenhart, *Introduction to Differential Geometry*, 1947, Page 18). This can be expressed as a function of the derivatives of $f(z)$ and $g(z)$, the path describing functions.

The question arises as to where on the nominal path should we compute the curvature, \underline{K} , or in other words, at what altitude coordinate value (Z) should we define it? Referring to Figure 4-22 and Section 4.4.1.2, we could pick the measured intercept altitude, Z_I , for the computation; or, we could take the closest point on the nominal path, again approximated by the linear path tangent. In this case the z component, (ΔZ) of the error vector, \underline{E} , is added to the measured altitude, (Z_I) to define a new altitude at which the nominal path curvature is computed.

The second choice has the advantage of reducing the effective delay or lead induced by \underline{E}_H at near-horizontal flight, (e.g., if the altitude

CONFIDENTIAL

Z_I is used, a large E_H means the curvature is computed at a curve point either far behind, or far ahead of, the actual nearest point to the deviated missile); endpoint wander noise which changes E_T may be transmitted more easily through the curvature computer. Therefore, the simulation program in two dimensions will investigate both methods.

4.4.1.4 Velocity Vector Computer

The function of the remaining blocks is to modify the derived command components and transfer them to the airframe coordinate system. Velocity magnitude is needed to derive normal acceleration commands from the computed path curvature. Velocity direction, or heading, may be needed for computation of missile orientation by some methods. This can be found as a unit vector by computing the vector position difference between two successive position measurements and dividing by its magnitude.

4.4.1.5 Programmed Gains

Commands based on the relative error, E , due to missile deviation and target endpoint wander, are scaled so that the error is reduced over a portion of the remaining flight time of midcourse. The basis for this is the desire to not commit the interceptor fully to correcting an observed error that may be due to the measurement noise or prediction noise at that instant. Thus the effects of noise are smoothed over a larger portion of flight time than a faster response would permit. The linear decrease of flight time implies an inversely increasing gain. The time varying gain effectively may be viewed as a time varying guidance system bandwidth which increases with the approach to the inverse trajectory: hence, earlier in flight, longer smoothing times are traded for dynamic response. Since the non-stationary prediction noise results in an endpoint accuracy increasing with the approach to the end of midcourse, the time varying guidance system bandwidth is appropriate.

4.4.1.6 Digital Stabilizers

The weapon guidance loop (Figure 4-18) is inherently unstable: The commanded quantity is acceleration and the measured quantity is position - the double integral of missile output acceleration. Since the system is a discrete data system (sampled data) and includes the digital computer, the stabilization under study is to be a digital program in the error loop. This type of stabilization operates on the sampled input data to produce weighted first (and possibly higher) order error difference terms. It is analogous to the addition of derivative terms for stabilization of continuous systems. A separate digital stabilizer is shown in the nominal command path in Figures 4-18 and 4-19 because it may be desirable to include higher order differences there also, but in a different program.

CONFIDENTIAL

It appears that the weapon guidance loop will have a bandwidth determined almost totally by gain and the double integration (i.e., smoothing delays and missile response times will be short relative to the closed loop response time). Consequently, the stabilization program may be adequate if designed simply for the double integration. These will be studied in the current simulation.

4.4.1.7 Coordinate Transform And Orientation Computer

After the nominal and error correcting components of commanded acceleration are combined, the resulting vector sum must be transformed from ground coordinates into the missile airframe coordinate system on the basis of knowledge concerning the actual present missile orientation. The transformed vector components in the pitch and yaw axis directions are then applied to the yaw and pitch autopilot control systems respectively, and produce maneuver accelerations in response to these commands. Any command components in the roll axis direction must be ignored since we presently assume no efficient means of controlling maneuver in this direction.

The function of the guidance computer is to perform this transformation or those parts of it which can most profitably be done on the ground. Discussion of the orientation computation is the subject of Section 4.5.1 of this Quarterly Report.

4.4.1.8 Time-to-go Clock

The missile is launched when the predicted earliest time of arrival of the target at the intercept altitude equals the stored value of maximum expected time-of-flight for the programmed midcourse trajectory plus the time factor required for the terminal phase of flight between end-of-midcourse and intercept altitudes. After launch, the time-to-go information is made available to the guidance computer by the target prediction computer or by a central clock for the purpose of adjusting the programmed error loop gains.

4.4.2 THE TERMINAL GUIDANCE SYSTEM

The terminal guidance system is characterized by error commands to the interceptor proportional to the predicted miss distance between interceptor and target. The determination of the estimated displacement vector, $E(t_g)$, at a future time, t_g , constitutes the major function of the guidance computer in this phase of guided flight. In discussing the design of the terminal guidance computer, it will be developed for prediction of target and interceptor paths by straight line extrapolation, i.e., an assumption of constant velocity over the command interval. Linear prediction has proven satisfactory in the two dimensional simulations against

CONFIDENTIAL

maneuvering targets (of the Redstone Class) and "air-brake" decelerating targets^{1,2}.

The vector geometry for this system is shown in Figure 4-23. The present position vectors for target (\underline{R}_t) and

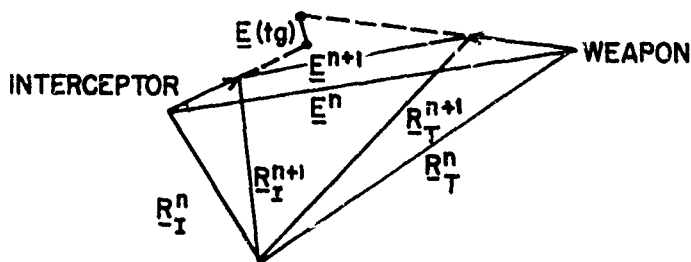


FIGURE 4-23

interceptor (\underline{R}_I) are shown for the (n)th and the (n+1) data intervals. The smoothing programs for target and interceptor position are not considered here and the velocities are specified from the first difference position:

$$\underline{V}_I = \frac{R_I^{n+1} - R_I^n}{T} \quad (1)$$

$$\underline{V}_T = \frac{R_T^{n+1} - R_T^n}{T} \quad (2)$$

$$\begin{aligned} \underline{V}_I - \underline{V}_T &= \frac{E^{n+1} - E^n}{T} \\ &= \frac{\Delta E}{T} \end{aligned} \quad (3)$$

where T is the data period

1. PLATO Final Eng. Report, Phase I.
2. PLATO Seventh Quarterly Report.

CONFIDENTIAL

The construction of the predicted displacement vector becomes

$$\underline{E}(t_g) = \underline{E}^{n+1} + \frac{\Delta \underline{E}}{T} T_g \quad (4)$$

based on the time-to-go to collision, T_g . The determination of T_g is made by finding the conditions in equation 4 to make its magnitude a minimum. Writing the magnitude of equation 4 in terms of its components in the ground coordinate system (x, y, z)

$$|E(t_g)|^2 = \left[E_x^{n+1} + \frac{\Delta E_x}{T} T_g \right]^2 + \left[E_y^{n+1} + \frac{\Delta E_y}{T} T_g \right]^2 + \left[E_z^{n+1} + \frac{\Delta E_z}{T} T_g \right]^2$$

$$\frac{d|E(t_g)|^2}{dT_g} = 0 = 2 \left\{ \left[E_x^{n+1} + \frac{\Delta E_x}{T} T_g \right] \frac{\Delta E_x}{T} + \left[E_y^{n+1} + \frac{\Delta E_y}{T} T_g \right] \frac{\Delta E_y}{T} + \left[E_z^{n+1} + \frac{\Delta E_z}{T} T_g \right] \frac{\Delta E_z}{T} \right\}$$

as a result of the constant velocity assumption, $\frac{\Delta \underline{E}}{T} = \text{constant}$. Collecting terms

$$\left[\frac{(\Delta E_x)^2}{T} + \frac{(\Delta E_y)^2}{T} + \frac{(\Delta E_z)^2}{T} \right] T_g = (E_x^{n+1}) \frac{\Delta E_x}{T} + (E_y^{n+1}) \frac{\Delta E_y}{T} + (E_z^{n+1}) \frac{\Delta E_z}{T}$$

The term on the left is recognized to be the $\left| \frac{\Delta \underline{E}}{T} \right|^2$ and on the right, the right, the dot product, $\left[\underline{E}^{n+1} \right] \cdot \left[\frac{\Delta \underline{E}}{T} \right]$, then

$$T_g = \frac{\underline{E}^{n+1} \cdot \frac{\Delta \underline{E}}{T}}{\left| \frac{\Delta \underline{E}}{T} \right|^2} \quad (5)$$

The physical meaning of equation 5 is better set forth by re-writing it as

$$\left| \frac{\Delta \underline{E}}{T} \right| T_g = \underline{E}^{n+1} \cdot \frac{\frac{\Delta \underline{E}}{T}}{\left| \frac{\Delta \underline{E}}{T} \right|}$$

CONFIDENTIAL

The conditions for the minimization of equation 4 can then be stated: that the projection of the displacement vector (\underline{E}^{n+1}) on the relative velocity vector ($\frac{\Delta \underline{E}}{T}$) equal the distance obtained by the relative speed acting over the time T_g (see Figure 4-24).

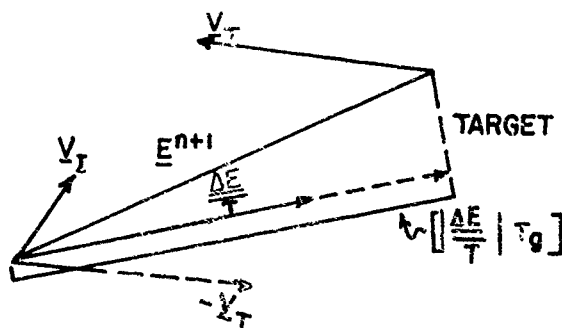


FIGURE 4-24

It remains to find the component of equation 4 in the plane normal to the velocity axis of the interceptor:

$$\underline{E}_{IV}(T_g) = [\underline{E}(T_g)] - [\underline{E}(T_g)] \cdot \left[\frac{V_I}{|V_I|} \right] \quad (6)$$

Knowledge of the missile roll orientation (or bank angle) is required to resolve equation 6 into the components for pitch and yaw commands. Again, the orientation computer may be partially ground based or wholly airborne depending on the system selected (refer to Section 4.5.1). The command component equation 6 may be corrected for angle of attack to find its projection along the normal to the missile axis. For the small angles of attack considered for the PLATO missile, even to the limiting angles, this may not be necessary.

The guidance computer flow diagram (Figure 4-25) is essentially the computations of equations 1 through 6: The heading computers (equations 1 and 2), the computation of time-to-go to collision (equation 5), the differencing of target and interceptor predictors to obtain the predicted displacement vector (equation 4), and the velocity axis normal component (equation 6). The inclusion of time varying prediction in the signal path of the interceptor has made necessary a time varying loop gain ($K(T_g)$) to maintain satisfactory dynamic performance throughout the final attack. For simplicity in this development the smoothing programs have been included

CONFIDENTIAL

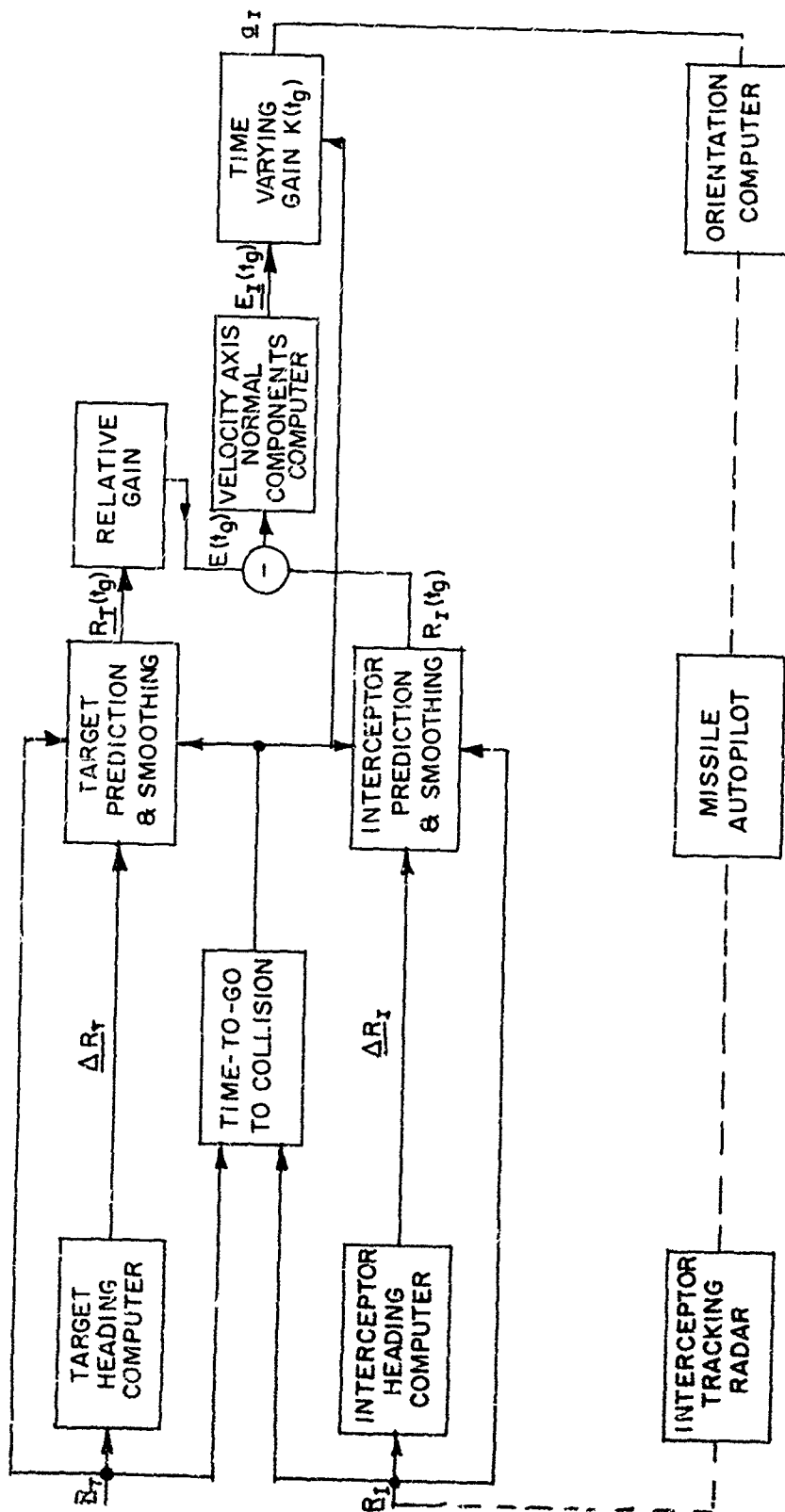


FIGURE 4-25. GUIDANCE COMPUTER FLOW DIAGRAM

CONFIDENTIAL

SECRET

CONFIDENTIAL

in the interceptor and target predictors. Another smoothing method more likely to be used is a least squares curve fitting to the weighted position data. The headings would be derived directly from the curve.

4.4.3 DISCUSSION ON TRANSITION FROM MIDCOURSE TO TERMINAL GUIDANCE

The transition to terminal guidance is considered to occur when the inverse trajectory has been attained. In general the missile will have been launched early by an amount of time determined by the sum of prediction time and flight time uncertainties. Consequently, the interceptor will more often arrive at the inverse trajectory with an excess of time over the nominal amount considered necessary for the final engagement (currently ten seconds is used although most encounters could be handled with less) and the interception altitude will increase.

The midcourse guidance concept of a programmed path could be continued by switching to flight along the inverse trajectory. However, this may be unnecessary and the terminal guidance concept described previously will be satisfactory throughout. It is necessary to examine the effective loss in interceptor capability if the target ballistic path is approximated by a straight line.

4.5 INTERCEPTOR

4.5.1 INTERCEPTOR PERFORMANCE OPTIMIZATION

Some general methods of determining the intercept envelope which have been developed previously indicate the strong interplay of the interceptor system characteristics and the radar system prediction characteristics. They also indicate that if the missile and radars are matched to obtain maximum forward area defense coverage, rearward area coverage is strongly dependent on air-frame capabilities.

It is necessary, therefore, to fix the remaining free parameters of the missile and trajectory configurations such that maximum rearward coverage is attainable within practical missile design limits.

Studies of the prediction characteristics of the PLATO system show that in general the prediction accuracy, associated with the planned intercept point, is considerably better for intercepts performed to the rear of the launch site. This is because more time is available for observation of the target in the radar fields of view which yields more data samples, and is also due to greater tracking accuracy.

It has also been shown that the minimum altitude point of the prediction error volume will occur close to the limits of the intercept envelope. The limiting condition is illustrated in Figure 4-26.

CONFIDENTIAL

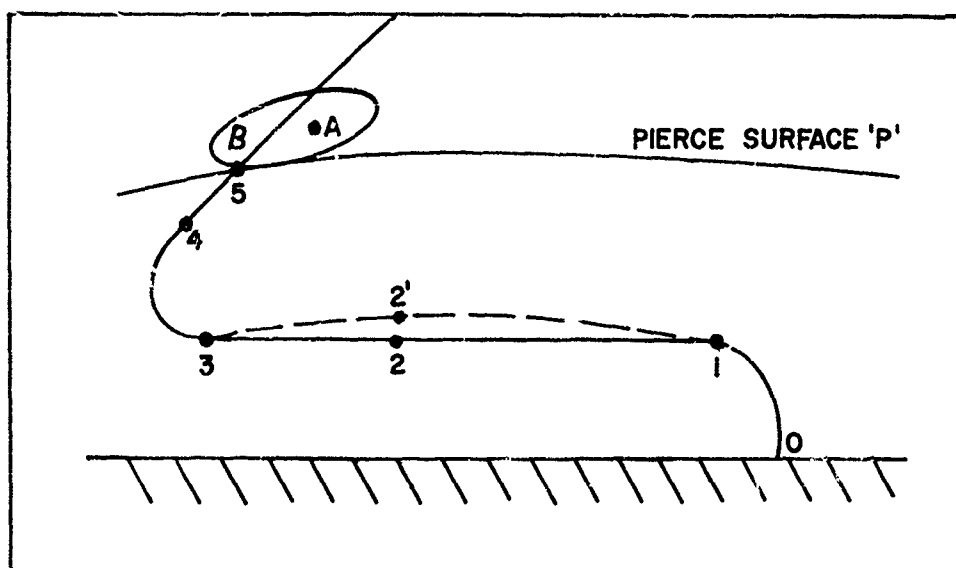


FIGURE 4-26. MINIMUM ALTITUDE POINT

The most rearward allowable intercept aiming point, A, is determined by point, B, (the lower extreme of the error volume, which is tangent to the "pierce surface", P) where B is defined as the most rearward trajectory that can be flown by the interceptor to a successful intercept. The nominal altitude for point B is 10 n.m.

It is necessary to determine the manner in which the maximum rearward intercept point, B, is dependent upon the interceptor, target and trajectory parameters.

In order to have the rearmost trajectory readily amenable to analysis, it is first approximated in the following manner: (See Figure 4-26).

0-1 is a powered push-over at constant life coefficient

1-2 is a powered level flight

2-3 is an unpowered level flight

3-4 is an unpowered pull-up at constant lift coefficient

4-5 is the terminal phase on the "inverse trajectory".

CONFIDENTIAL

It will be shown later that this is actually an efficient trajectory. The trajectory portions will be treated in inverse order, starting with the terminal phase (4-5. Figure 4-26).

The limiting effects of missile wing loading on the ability of the missile to fly the rearward trajectories and on rearward defensive coverage will be shown according to the doctrine stated above. For a definition of the symbols used in the analysis see Appendix V.

Terminal Phase (4-5)

The interceptor is assumed on a ballistic trajectory headed for the intercept point on an approximate "inverse" trajectory from that of the target. Prediction errors are small on the rearward trajectories so that the principal requirement is that the interceptor be able to counter possible target maneuvers.

For a descending target the maximum possible displacement normal to the original trajectory is:

$$Z_T = C_1 e^{-ah_5}$$

where

$$C_1 = \frac{\rho_o g C_L (S/W)}{2 a^2 \sin^2 \gamma} = \frac{1.85 \times 10^6 C_L (S/W)}{\sin^2 \gamma} \quad (1)$$

For the interceptor to secure an intercept, its displacement normal to the trajectory should be at least equal to Z_t . If the interceptor average velocity is \bar{V} and angular changes during the intercept run (4-5) are small:

$$Z_I = f(\bar{V}) e^{-ah_5}$$

where

$$f(\bar{V}) = \frac{\rho_o g C_L (S/W)}{2 a^2 \sin^2 \gamma} \left[e^{a \bar{V} t \sin \gamma} (a \bar{V} t \sin \gamma - 1) + 1 \right] \quad (2)$$

Under these assumptions, we can write:

$$\text{If } Z_I = Z_T, \quad f(\bar{V}) = C_1$$

it is seen that, in this case, the missile configuration required at intercept is independent of the intercept altitude. If it is further

CONFIDENTIAL

assumed that the maximum trimmable lift coefficient of the interceptor equals that of the target, then

$$\left(\frac{W}{S_I}\right) = \left(\frac{W}{S_T}\right) \left[e^{C_2 \bar{V}} (C_2 \bar{V} - 1) + 1 \right] \quad (3)$$

where

$$C_2 = a t \sin \gamma$$

Actually, there are numerous conditions which must modify this result, particularly for the rearmost intercept. For this case, the angular changes will not be negligible. There will be decreases in the interceptor velocity during the terminal phase due to large induced drag, as well as that due to the interchange of kinetic and potential energy.

When the angular changes become significant, the intercept criteria must be modified further. To minimize the system timing errors, it is desirable to correct the interceptor flight path so that the inverse trajectory is obtained at intercept. This condition will not permit the interceptor to maintain curvature in one direction.

The case of an interceptor turning with large normal accelerations is treated in Appendix VI. When this result is applied to the S-3 missile, in a terminal phase maximum lift coefficient turn, the normal displacement which is possible is actually considerably larger than that given by equation 2. Since a precise evaluation of the terminal phase must be closely tied in with the guidance problem, equation 2 will be used in this study as a conservative limit of the interceptor requirement.

Turns with High Normal Acceleration

This section deals with the portions 0-1 and 3-4 in Figure 4-26. The expression derived in Appendix VI, equation 2 for a vertical turn trajectory is:

$$\frac{B}{a} \frac{(\rho_i - \rho_{i+1})}{\rho_o} = \cos \gamma_i - \cos \gamma_{i+1} \quad (4)$$

The derivation utilizes the following assumptions:

- (1) Constant lift coefficient
- (2) Isothermal atmosphere ($\rho = \rho_o e^{-ah}$)
- (3) Constant mass

CONFIDENTIAL

(4) Normal acceleration large compared to gravity

(5) $\gamma_i < \gamma_{i+1}$

Equation 4 indicates that the trajectory geometry is independent of the missile velocities. The velocity variation is given by

$$V_{i+1}^2 = \left[V_i^2 + I_1(\gamma) - I_2(\gamma) \right] \left[e^{-2\left(\frac{D}{L}\right)(\gamma_{i+1} - \gamma_i)} \right] \quad (5a)$$

Where

$$I_1 = \frac{4 B T}{a \rho C_L S} \int_{\gamma_i}^{\gamma_{i+1}} \frac{e^{2\frac{D}{L}(\gamma - \gamma_i)} dy}{\frac{B}{a} e^{-ah_i} - \cos \gamma_i + \cos \gamma} \quad (5b)$$

$$I_2 = \frac{2g}{a} \int_{\gamma_i}^{\gamma_{i+1}} \frac{e^{2\frac{D}{L}(\gamma - \gamma_i)} \sin \gamma dy}{\frac{B}{a} e^{-ah_i} - \cos \gamma_i - \cos \gamma}$$

To obtain this form, the following additional approximations were made:

- (1) Constant lift to drag ratio
- (2) $V = r \frac{d\gamma}{dt}$ (i.e. $\dot{r}^2 \ll \dot{\gamma}^2 r^2$)

The first of these two approximations is ordinarily quite good for flight at high Mach numbers. When this is not true, the relation may be used stepwise. The second approximation can be checked against the trajectory for particular initial velocities.

From this expression, it can be seen that the velocity loss for a given angular change is monotonic in the drag-lift ratio. Since a certain minimum velocity is required after the turns, maximum rearward trajectories are obtained by utilizing the excess impulse available from the power plant to glide as far as possible during portion 2-3 (Figure 4-26) of the flight. Hence it is desirable to perform the maneuver at minimum drag per unit lift. For slender supersonic vehicles of moderate wing loading, this occurs in the vicinity of $C_L \approx 0.1$; at $L/D \approx 5$.

CONFIDENTIAL

Initial Turning Phase (0-1)

The push-over during the launching phase is considered in this study to occur at constant lift coefficient. Equations 4 and 5 give the results for this case when the acceleration normal to the trajectory due to gravity is small compared to the lifting acceleration and when the effect of the mass change is negligible. It can be shown that this is valid during the initial portion of the turn when the trajectory is near the vertical. If the axial acceleration due to thrust is substantially greater than gravity ($T/W \gg 1$) the velocity changes rapidly in time. When the drag and mass variation terms are negligible, the motion is given essentially by:

$$(T/W - 1) g t = V \quad (6)$$

For the initial portion of the turn, when the density variation can be neglected:

$$r = B_0^{-1}$$

and if

$$V = r \, dy/dt$$

$$\dot{\gamma} = \left(\frac{T}{W} - 1 \right) g B_0 \frac{t^2}{2}$$

The normal acceleration is given by

$$n g = \frac{V^2}{r} = B_0 (T/W - 1)^2 g^2 t^2$$

The ratio of lift normal acceleration to gravity contribution is given initially by

$$\frac{n}{\sin \gamma} = \frac{B_0 (T/W - 1)^2 g^2 t^2}{B_0 (T/W - 1) g^2 t^2 / 2} = 2(T/W - 1) \quad (7)$$

In the absence of drag forces, this value is a lower limit on the values during the turn. This is because the denominator becomes larger due to the higher order terms in γ while the normal force increases due to the decrease in $\cos \gamma$.

This initial portion of the trajectory is actually the most difficult to describe analytically, since it actually does contain the effects of gravity, drag, and mass variation.

CONFIDENTIAL

The drag term is particularly difficult to express, since the transonic transition usually occurs in this region. The lifting drag variation is not a simple function. Actually the rapid acceleration causes acoustical pressures which appreciably modify the steady state result. Analytical results indicate a reduction of the transonic drag coefficients to values well below those predicted by theory for steady flow. Virtually no experimental data has been obtained under conditions which simulate the problem well enough to be directly applicable.

The dynamic equation is given by

$$\frac{d(mV)}{dt} = T - D - mg \sin \gamma$$

Comparing the results of several digital computations of trajectories for the S-3 missile, (formerly the X-SAM-A-19-3 missile) an empirical expression which agrees well with the complete equation is given by

$$\frac{d(mV)}{dt} = \left(\frac{T}{W_0} - 1 \right) W_0 \quad (8)$$

It can be seen that this is correct for vertical flight in vacua. In using this for the push-over, it is assumed that the drag increases just enough to counteract the reduction in gravity deceleration. For turns in the altitude band from 10,000 feet to 30,000 feet, it is found that this gives results which predict the end velocity and time quite well. Since the drag characteristics are implicitly assumed when this expression is used, modifications of the drag characteristics of the final missile will not be evident in this portion of the trajectory.

Integrating equation 8 yields the following results:

$$V_1 = \left[\frac{T}{W_0} - 1 \right] g t \left(\frac{W_0}{W_1} \right) \quad (9)$$

The path length is given by

$$s_{0-1} = \left[\frac{T}{W_0} - 1 \right] g \left[\frac{W_0}{\dot{W}} \right]^2 \left[\frac{W_1}{W_0} - \ln \frac{W_1}{W_0} - 1 \right] \quad (10)$$

To obtain the end condition for W_1/W_0 , this is equated to the path length obtained from equation 4, Appendix VI.

CONFIDENTIAL

Choice of Wing Loading

Equation 4 describing the trajectory geometry provides information as to the wing loadings which can be considered for the PLATO Missile. This equation can be used as an approximation for the geometries of both the pull-up and the initial push-over. The most rearward trajectory requires the most turning. If an initial turn to the horizontal is followed by a pull-up to an inclination of the shallowest threat trajectory considered ($\gamma_T = 20^\circ$), an estimate of the order of the upper limit to the wing loading can be obtained.

Consider the initial turn to be performed at $W = W_0$. i.e., the change in wing loading is neglected. This assumes that the time spent in this turn is small.

$$C_L = (C_L)_{(L/D)_{\max}}$$

Then, as

$$B_0 = 1/2 \rho_0 g C_L \left(\frac{S}{W_0} \right)$$

$$\gamma_0 = 90^\circ$$

$$\gamma_1 = 180^\circ$$

$$\frac{B_0}{a} \left(\frac{\rho_0 - \rho_1}{\rho_0} \right) = 1$$

This expression actually overestimates the density difference required as compared to the case where the weight variation is included. Since $\rho_1 = \rho_3$ one can write

$$\frac{\rho_3}{\rho_0} = 1 - \frac{a}{B_0} \tag{11}$$

Consider the final turn to be performed at

$$W = W_e \quad C_L = (C_L)_{(L/D)_{\max}}$$

$$\gamma_4 = 20^\circ \quad B = B_e$$

$$\gamma_3 = 180^\circ$$

CONFIDENTIAL

Therefore

$$\frac{B_e (\rho_3 - \rho_4)}{a \rho_o} = 1 + \cos 20^\circ = 1.94 \quad (12)$$

Combining equations 11 and 12 yields:

$$\frac{W_e}{S} = \frac{841.5 (C_L)_{(L/D)_{max}} \left(1 - \frac{\rho_4}{\rho_o}\right)}{1.94 + \left(\frac{W_o}{W_e}\right)} \quad (13)$$

Using typical values for the S-3 missile (formerly designated as the X-SAM-A-19-3 missile)

$$(C_L)_{(L/D)_{max}} = 0.1 \quad \frac{W_o}{W_e} = 2.5$$

and if

$$\frac{\rho_o}{\rho_4} = 15$$

then equation 13 indicates a maximum wing loading $\left(\frac{W_e}{S}\right)$ of about 18#/ft². The assumption of constant weight in the push-over causes this to be lower than the actual maximum. (The S-3 configuration used 20#/ft².)

Since decreases in wing loading can only be obtained at the expense of the payload ratio, it is desirable to find the optimum based on structural weight. Beginning the pull-up at high altitudes requires very large wings, but lower initial velocities and therefore, less normal acceleration.

On this type of trajectory, the maximum normal force is associated with the beginning of the pull-up (point 3 in Figure 4-26). An empirical rule for structural weight of winged missiles which is commonly used is:

$$\frac{W_s}{W_e} = K \left(\frac{b n S}{\tau_r W_e} \right)^{1/2}$$

Where K is a constant.

CONFIDENTIAL

If a constant span/root thickness ratio, b/τ_r , is assumed, and if

$$\omega \cong \left(\frac{W_B}{K W_e} \right)^2 \left(\frac{\tau_r}{b} \right),$$

then

$$\omega \cong n \frac{S}{W_e} \quad (14)$$

Using equations 4 and 5 it is possible to minimize ω . If

$$S/W_e \cong \tau,$$

equation 4 gives

$$\rho_3 - \rho_4 = \Gamma/\tau$$

where

$$\Gamma \cong \left(\frac{\cos \gamma_3 - \cos \gamma_4}{\frac{1}{2} C_L} \right) 2 a$$

Since

$$n_3 = \frac{L}{W_e} = \frac{\rho_3}{2} V_3^2 C_L \tau$$

$$\rho_3 = N/V_3^2 \tau$$

where

$$N = \frac{2n_3}{C_L}$$

Rewriting equation 14,

$$\omega = \tau V_3^2 [\Gamma + \rho_4 \tau] \quad (15)$$

Equation 5 gives

$$V_3^2 = V_4^2 \exp \left[\left(\frac{2D}{L} \right) (\Delta\gamma) \right] + I_2$$

when

$$T = 0$$

CONFIDENTIAL

When ρ_4 , V_4 , and Δy are specified, the minimum value of ω can be found by setting $d\omega/d\tau = 0$.

The expression for $\partial I_2/\partial \tau$ must, at present, be evaluated numerically.

Level Flight (1-3)

This deals with sections 1-3 of the trajectory. Appendix VII derives the velocity relations for such flights. Appendix VIII treats inclined straight flight.

It is desirable to have the portion of the rearmost trajectory between turns in essentially level flight. Climbing during this portion will restrict the band of altitudes available for turning, while diving would cause more turning than necessary. This desire may be modified by considerations of the drag losses in this portion. Some additional gain in range can be obtained by following an essentially lofted ballistic path during this portion (1-2'-3 in Figure 4-26) since the time averaged density (and drag loss) will be lower. The additional turning in the pull-up that this brings about should not be significant. However, for convenience in analysis, the connecting portion, 1-3, will be treated as level flight.

The approximations used are the following:

- (1) $C_{Di} \ll C_{Do}$
- (2) $C_{Do} = K_o v^{-1}$
- (3) $\ddot{m} = T = 0$

The first approximation is consistent with the wing loadings indicated by the previous discussion. The second approximation is based on empirical drag measurements for slender supersonic vehicles. When the drag curve is matched at high Mach numbers, this approximation generally overestimates slightly the drag at lower velocities.

The general equations for the velocity variation developed in Appendix VII

$$V_{i+1} = \frac{T}{\dot{m} + K_1} \left[1 - \left(\frac{m_o - \dot{m}t}{m_o} \right)^{1 + \frac{K_1}{\dot{m}}} \right] + V_i \left[\frac{m_o - \dot{m}t}{m_o} \right]^{1 + \frac{K_1}{\dot{m}}} \quad (16)$$

When $\dot{m} = 0$ ($T = 0$) this reduces to

$$V_{i+1} = V_i e^{-k_2 t/m_2} \quad (17)$$

CONFIDENTIAL

The relations for the distance traveled are:

$$s_{i \rightarrow i+1} = \left[V_i - \frac{T}{\dot{m} + K_1} \right] \left[\frac{1 - \frac{\dot{m}}{m_0} t^2 + \frac{K_1}{\dot{m}} - 1}{2 + \frac{K_1}{m} - \frac{\dot{m}}{m_0}} \right] + \frac{Tt}{\dot{m} + K_1} \quad (18)$$

and

$$s_{2-3} = \frac{m_2}{K_1} [V_2 - V_3] \quad (19)$$

Conclusions

An analytic description of the missile trajectory performance has been obtained. This can be used to study the effects on the system performance of a variation of the missile parameters.

LIST OF REFERENCES

1. PLA 400/11 "The Matching of Radar and Missile Characteristics"
D.T. Barish - 24 May 1955
2. PLA 400/12 "Intercept Altitudes"
E. W. Schliehen - 6 June 1955
3. PLA 251/18 "Derivation of the Mathematical Formulas Which Govern the Relationship of the Prediction Error at Launch and Interceptor Excess Altitude Capability"
A. Wouk - 18 August 1955
4. PLA 320B/6 "Effect of Radar Location on Defended Range"
J. Wagner - 29 June 1955
5. PLA 320B/11 "'Blended' Accuracy"
M. Ritterman - 12 August 1955
6. PLA 320B/14 "Maximum Intercept Altitude"
D. Barish, H. Greenberg, J. Wagner - 7 September 1955

SECRET

4.5.2 AERODYNAMICS

4.5.2.1 Trajectory Studies

Coupled with the studies reported in Section 4.5.1, is a computational program of trajectory studies.

As in most performance studies it is desirable to know what flight path and thrust program will produce the maximum total energy at intercept with a minimum flight time. This usually resolves itself into a study of calculus of variations problems which must, even in the simplest case, be solved by graphical means.

The alternative method is to solve the problem on a trial and error basis in which several types of trajectories are calculated and the total energy at the common end point compared. This type of study is profitable in that the exact characteristics of the contemplated vehicle may be used and such variables as the weight, thrust, and, of course, lift and drag may be varied and the effect on performance noted for each type of trajectory.

Once the maximum terminal energy, minimum time type of trajectory has been determined, a suitably high order polynomial may be used to approximate the flight path. At present the following types of trajectories are being examined: (1) fifth, sixth, and seventh order vertical takeoff polynomials; (2) nearly horizontally launched with a rapid turn to gain altitude after Mach one has been exceeded; (3) straightline trajectories from launch point to intercept altitude; and (4) vertical launch with a turn to level flight at various altitudes to intercept range.

Past PLATO trajectory studies have made use of two dimensional equations in which the horizontal position of the missile is expressed as a function of the altitude.

$$x = \sum_0^n a_i h_i$$

Specifying certain characteristics of the two end conditions produces a fifth order polynomial. This fifth order polynomial appears acceptable for determining the forward trajectories. However, using this equation for intercepting to the rear of the launch site required normal accelerations which exceed the capabilities of conventional vehicles.

In order to reduce these high normal accelerations, additional equations are required. Therefore, sixth order equations were developed specifying the curvature at a certain altitude. The solution of this equation appeared to be one of trial and error in order to produce the desired

SECRET

reduction in rate of turning. Therefore a sixth order equation specifying a point in space through which the trajectory must pass was tried.

It was found that this sixth order equation did not sufficiently restrict the curvature, so two seventh order equations were set up specifying:

- (1) Two points through which the trajectory must pass.
- (2) A slope at a particular altitude and a point through which the trajectory must pass.

The present status of the study indicates that the former condition will allow the radius of curvature to be large enough to enable the normal acceleration to be within the capabilities of the interceptor. The study is continuing to determine the values of the coefficients and an empirical equation which will determine these for all intercepts.

With ranges required for intercept of the order of 180,000 feet, it is possible that a boost, or a thrust-time history, which is not constant, will be required. A number of varying thrust time histories are being studied, along with boost to ascertain the effect upon vehicle capabilities.

All PLATO trajectory analyses performed thus far are confined to the cases in which the target trajectory plane contains the interceptor launch site. These results may be used to establish lower limits to the lateral range.

Consider the trajectory for interception to the rear of the launch site (see Figure 4-27).

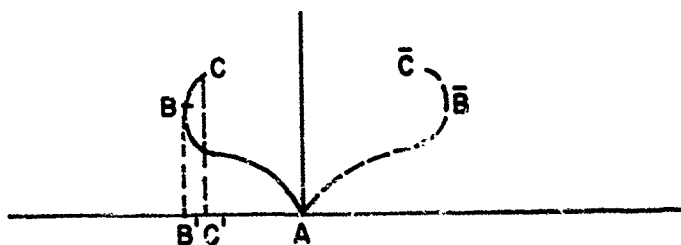


FIGURE 4-27

The interceptor is launched vertically from A, turns toward the rear and after covering a sufficient distance, returns to vertical flight at B.

SECRET

It continues the turn until terminal conditions are reached at C. This trajectory may be generalized into a group which includes lateral coverage.

Let the portion A-B of the trajectory be rotated about the vertical axis through A. The point B will then define a locus of points which the missile can reach in vertical flight. The segment B-C can be rotated by any desired amount about B-B' without any effect on its relationship to interceptor performance capability. If B-C lies in the target trajectory plane the resulting flight path is a feasible but not necessarily optimum interception course. For example, the forward trajectory would be A-B-C.

The point C would describe a circle with radius AB' centered forward of A by the distance B'C'. This is an inner bound to the maximum operating range. The attainable range would in general be greater than the amount given by this analysis; for example, the range along A-B-C is 55,000 feet as against 75,000 feet obtained with a fifth degree polynomial trajectory.

It has thus been demonstrated that the lateral range of the PLATO missile is at least as great as the rearward range.

4.5.2.2 Aerodynamic Heating

In the optimization of the PLATO vehicle, it was found that in some cases the vehicle would require a means of retaining its structural strength at high rates of heat input. This can be accomplished by several means but only with an increase in takeoff weight which is, of course, undesirable. An optimizing process was, therefore, undertaken with the view to reducing this additional weight to a minimum.

There is considerable information on the characteristics of boundary layers. Simplified means have been developed to determine with fair approximation the heat transfer on the surfaces of high-speed missiles. Using Fourier's steady-state heat flow equation, a theoretical study was made of the heating of an aluminum skin protected by a ceramic coating. The skin was considered a heat reservoir which was not allowed to exceed a certain peak temperature for structural reasons.

It was found that although sufficient information exists on the temperature recovery factors and heat transfer coefficients insufficient performance data were available to determine the worst conditions and typical values of skin weight. A large number of trajectories are being studied at present; it is anticipated that a more complete analysis of this problem will be completed in the near future.

In this study it will also be necessary to determine not only a theoretically best material or means of retaining structural strength at

SECRET

elevated temperatures, but also a method which will withstand handling, flexure, and shock. This will necessitate checking commercially available materials and evaluating them.

4.5.2.3 Control Surface Evaluation

A study of the relative merits of unbalanced and overhang-balanced flaps, rectangular and triangular horn balanced flaps and spoilers as control surface elements on the PLATO A-3 missile is now in progress. Sectional views of the unbalanced and plain balanced flaps are shown in Figure 4-28.

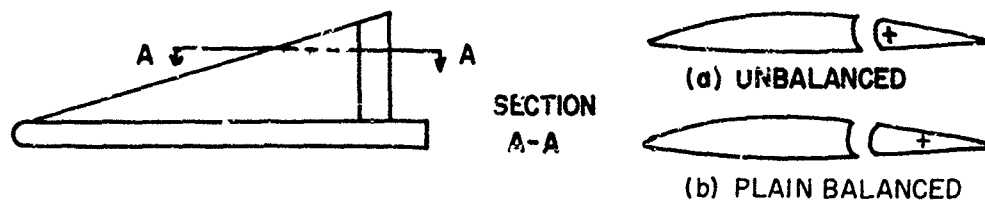


FIGURE 4-28

Horn balanced flaps are shown in Figure 4-29.

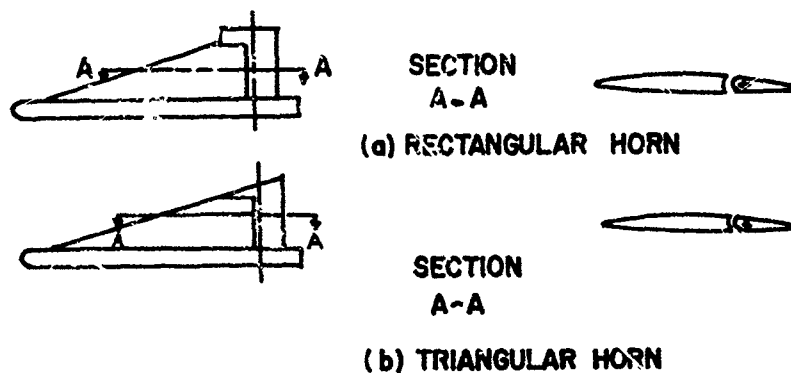


FIGURE 4-29

The function of the control surface acting as an elevon is to produce a lifting force and subsequent moment about the missile center of gravity. A pair of planar control surfaces operated differentially act as rolleron; i.e. they produce an aerodynamic moment about the missile body axis. The aerodynamic force acting on the control surface whether it is functioning as an elevon or rolleron is primarily dependent upon the inclination of the missile body axis relative to the missile velocity vector and the

SECRET

deflection of the control surface about its own hinge line. A spoiler control appears as in Figure 4-30.



FIGURE 4-30

A preliminary investigation made during the last quarterly period indicates spoilers have decreasing effectiveness with increasing angle of attack. The present design of the PLATO A-3 missile requires an angle of attack of approximately 15° to trim 25 g's at 60,000 feet altitude. The wing area or missile speed must be increased, or alternatively its maneuverability requirements decreased to make spoilers appear as an attractive choice for control surfaces. All flap types appear equally effective in producing control moments but differ appreciably in their hinge moment properties. Rectangular and triangular horn balances may be incorporated into the flap design so as to yield low hinge moments over a wide range of supersonic speeds but are ineffective in subsonic flow. This latter characteristic should present no problem to the PLATO missile design. Jet vane controls could be incorporated as primary means of control during the launch phase if the low speed characteristics of the aerodynamic surfaces should prove unsatisfactory.

Figure 4-31 shows the order of magnitude of the hinge moments experienced with the PLATO A-3 missile flying Phase I trajectories. The control surface analyzed in obtaining these results is a triangular horn balanced flap with a total single flap area equal to 10% of one exposed wing panel. The hinge moment coefficients from which the hinge moments were derived are zero roll angle data presented in Douglas Report SM-18629 for a model similar to the Nike B. Actually the hinge moments are critically influenced by the missile roll angle and the deflection of the opposite pair of planes control flap and to a lesser degree by pitching and roll motions.

The data of Figure 4-31 are now in the process of being coordinated with the design of the missile autopilot to redistribute, if necessary, the dynamic characteristics of the airframe and autopilot to achieve an optimum compromise of design meeting terminal speed of response requirements. The output of this coordinated study should determine the size of the PLATO missile control surface, its maximum rate of deflection, linearity of aerodynamic coefficients, and control surface power requirements.

SECRET

SECRET

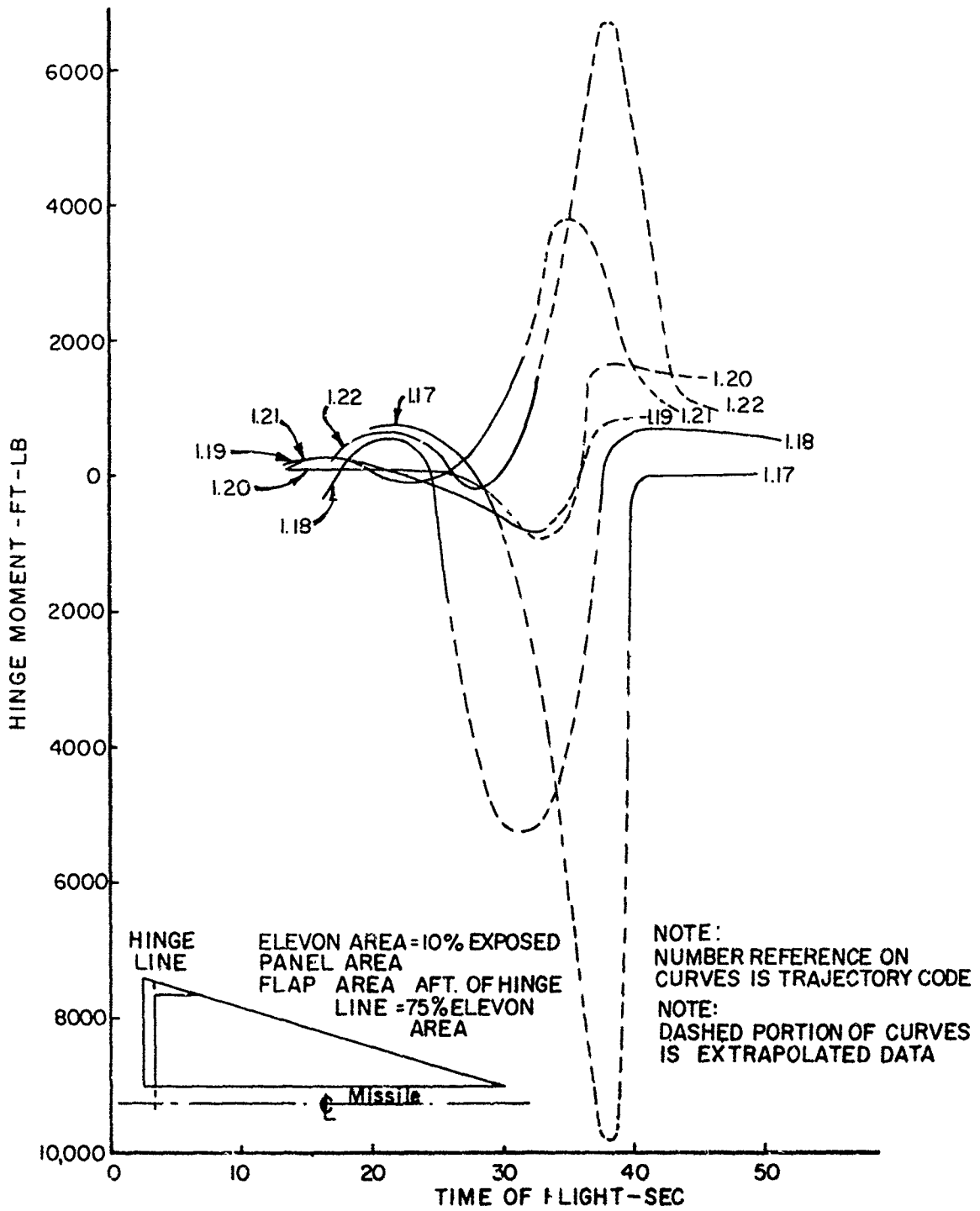


FIGURE 4-31. HINGE MOMENTS, S-3a MISSILE, TRIANGULAR HORN

SECRET

4.5.2.4 Launch Phase Aerodynamic Coefficients

A simulation study of the S-A-3's transient response to cross winds during ascent after launch is in progress. This program requires a knowledge of the missiles static and dynamic subsonic aerodynamic characteristics. The following list of aerodynamic coefficients represents values derived for this flow regime. All methods used in the analysis although of a theoretical or semi-empirical nature have been previously verified by experiment.

- | | |
|---|--|
| (1) (a) $C_{L\alpha} = 1.85/\text{rad.}$
using (b) | (1) (a) NACA RM A57G08 by
Nielsen, Kaattari,
and Anastasio |
| (b) $C_{L\alpha}$ (Wing alone) = 1.33/rad | (b) Institute of Aero-
nautical Sciences,
Preprint #313, Jan.
1951 by H. R. Lawrence. |
| (2) $C_{L\delta} = 0.20/\text{rad.}$ | (2) 1(b) |
| (3) $C_{M\alpha} = +0.0934/\text{rad.}$ | (3) 1(a) |
| (4) $C_{M\dot{\theta}} = \frac{-2.23}{V} / \text{rad/sec.}$ | (4) NACA RML50C02 by Goodman
and Jacquet. |

where

$$L_{\alpha} = C_{L\alpha} S q \alpha$$

$$M_{\alpha} = C_{M\alpha} q S l \alpha$$

$$M_{\dot{\theta}} = C_{M\dot{\theta}} q S l \dot{\theta}$$

$$M_{\delta} = C_{M\delta} q S l \delta$$

$$S = 192.5 \text{ ft}^2$$

$$l = 42 \text{ ft}$$

$$q = \text{dynamic pressure}$$

The drag coefficient was obtained from modified Nike I Flight test data.

$$C_{D0} = 0.01085$$

where:

$$D_0 = C_{D0} S q$$

SECRET

4.5.3 DYNAMICS

In the last quarterly progress report a simplified block diagram for an autopilot employing integral control was developed. This block diagram is shown in Figure 4-52. The characteristic equation for this system is:

$$\begin{aligned} & \left(1 + K_A K_c K^1 K_R \right) s^4 + \left\{ 2 \zeta_n \omega_n + K_c \left[1 + K^1 K_A \left(1 + K_R K_I + 2 \zeta_{\dot{\gamma}} \omega_{\dot{\gamma}} K_R \right) \right] \right\} s^3 \\ & + \left\{ \omega_n^2 + 2 \zeta_n \omega_n K_c + K^1 K_A K_c \left[\omega_{\dot{\gamma}}^2 K_R + K_I + 2 \zeta_{\dot{\gamma}} \omega_{\dot{\gamma}} \left(1 + K_R K_I \right) \right] \right\} s^2 \\ & + K_c \left[\omega_n^2 + K^1 K_A \omega_{\dot{\gamma}}^2 \left(1 + K_R K_I \right) + 2 K^1 K_A \zeta_{\dot{\gamma}} \omega_{\dot{\gamma}} K_I \right] s + K^1 K_A K_c K_I \omega_{\dot{\gamma}}^2 = 0 \end{aligned} \quad (1)$$

where

$$K^1 = K_{\dot{\gamma}} \frac{\omega_n^2}{\omega_{\dot{\gamma}}^2}$$

As stated in the last progress report, this system will be optimized for the instant of maximum dynamic pressure. During this instant, $\omega_{\dot{\gamma}}$ will be very much larger than any of the frequencies encountered so that the following approximation may be made:

$$s^2 + 2 \zeta_{\dot{\gamma}} \omega_{\dot{\gamma}} s + \omega_{\dot{\gamma}}^2 \approx \omega_{\dot{\gamma}}^2 \quad (2)$$

Using this approximation, equation 1 reduces to:

$$\begin{aligned} s^4 + \left(K_c + 2 \zeta_n \omega_n \right) s^3 + \left[\omega_n^2 + K_c \left(K_R K_A + 2 \zeta_n \omega_n \right) \right] s^2 + K_c \left[\omega_n^2 + K_A K \left(1 + K_R K_I \right) \right] s \\ + K^1 K_A K_I K_c = 0 \end{aligned} \quad (3)$$

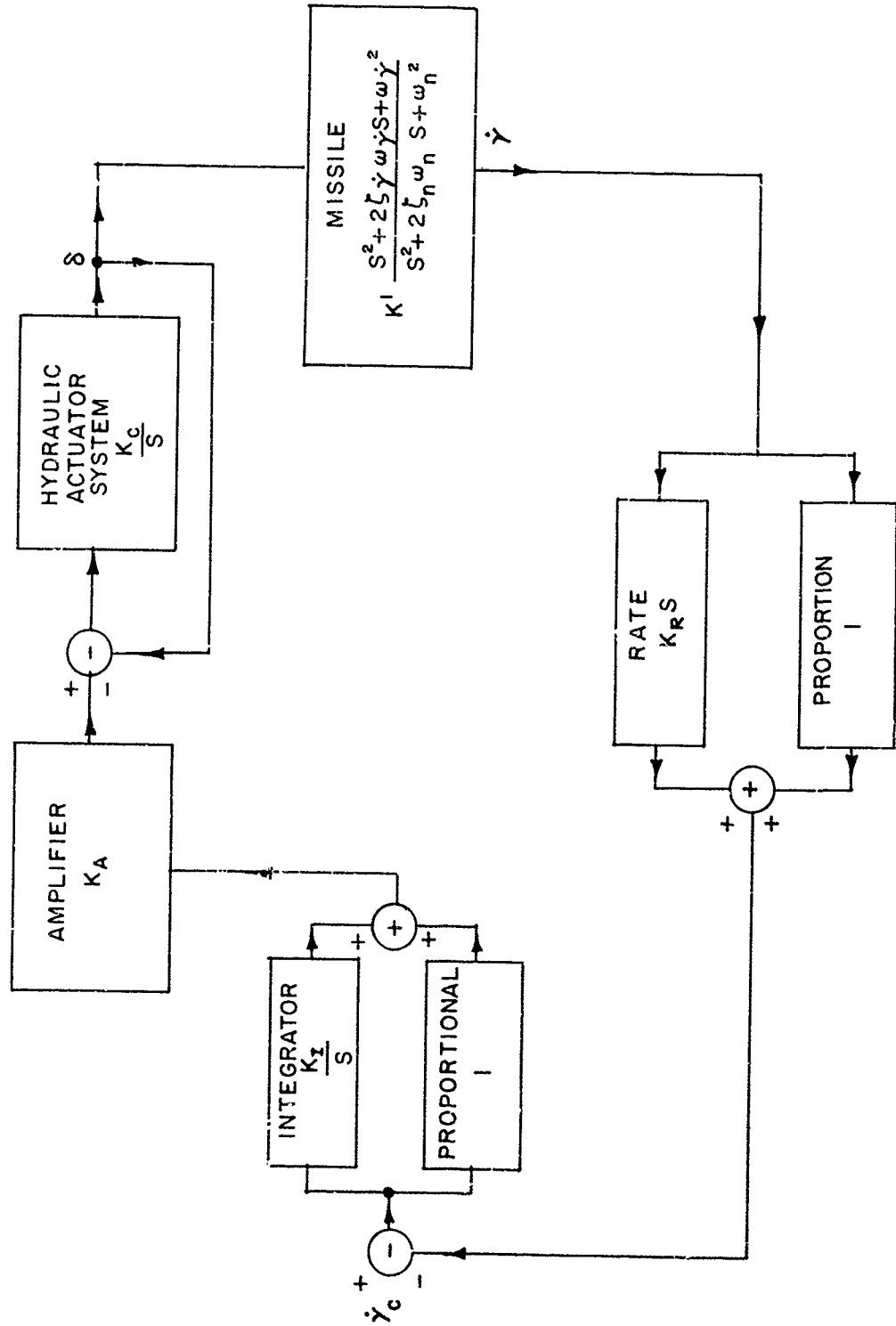
where

$$K = \omega_{\dot{\gamma}}^2 K^1 = \omega_n^2 K_{\dot{\gamma}}$$

Equation 3 may be used for the first approximation in the determination of the gains of the system.

It can be seen that the sum of the roots of equation 3 is almost entirely dependent on the hydraulic system gain, inasmuch as $K_c \gg 2 \zeta_n \omega_n$. This may also be noted from the fact that the hydraulic actuator system as

SECRET



SECRET

FIGURE 4-32. BLOCK DIAGRAM OF INTEGRAL TYPE CONTROL SYSTEM

SECRET

shown in Figure 4-32 acts as a low pass filter. Therefore, a more detailed analysis of the hydraulic actuator system was made in PLA 414/2.

Hydraulic Actuator System

The presently contemplated actuator system for the PLATO missile autopilot is shown in Figure 4-33. This system may be represented by the operational block diagram shown in Figure 4-34. By making use of the fact that the natural frequency of the valve, ω_v , will be very large compared to the frequencies of the rest of the system, and combining ω_G and ω_h in such a way as to give a fictitious hydraulic natural frequency, ω_a , and a fictitious hydraulic damping ratio, ζ_a , the block diagram of Figure 4-34 may be reduced to that of Figure 4-35. It is this block diagram that will be used for the determination of the hydraulic system response.

A great deal of information concerning the operation of the hydraulic system can be learned from a consideration of the transfer function of the system shown in Figure 4-35. For a large ω_a the system becomes that shown in the simplified block diagram of Figure 4-33. It may be pointed out that the system can not be improved, i.e. an increased ω_a , by just improving either the actuator or linkage since ω_a is less than the natural frequency of either one. Furthermore, an inspection of the characteristic equation of the system of Figure 4-35,

$$\frac{s^3}{\omega_a^2} + \left[2 \frac{\zeta_E \omega_E}{\omega_a^2} + \frac{2 \zeta_a \omega_a}{\omega_a^2} \right] s^2 + \left(1 + \frac{\omega_E^2}{\omega_a^2} + \frac{4 \zeta_E \omega_E \zeta_a \omega_a}{\omega_a^2} \right) s + K_c + \frac{2 \zeta_a}{\omega_a} \omega_E^2 = 0 \quad (4)$$

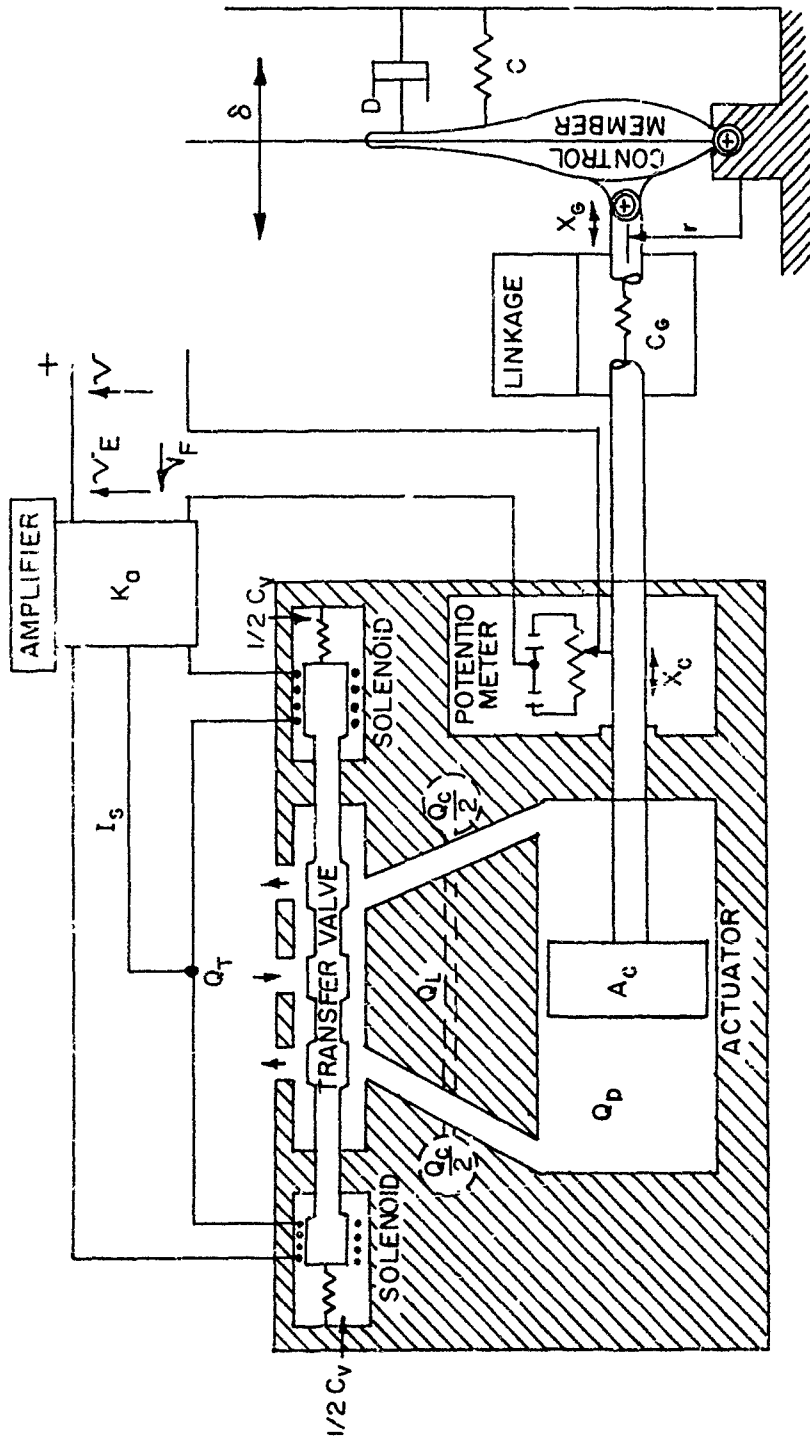
and the fact that $\omega_a \gg \omega_E$, a first approximation for stability is:

$$2 \zeta_a \omega_a > K_c \quad (5)$$

The desired response of the system of Figure 4-35 would determine the value of K_c since that is the most significant constant in the expression. In general K_c would have a value of about 25 sec^{-1} . The value of ω_a would most likely be in the order of 20 to 40 sec^{-1} . This in turn establishes minimum values of ζ_a . The natural frequency of hydraulic fluid compressibility resonance, ω_h , is defined by:-

$$\omega_h = \sqrt{\frac{B\Gamma^2 A_c^2}{V_c I_E}} \quad (6)$$

SECRET



SECRET

FIGURE 4-33. HYDRAULIC SYSTEM

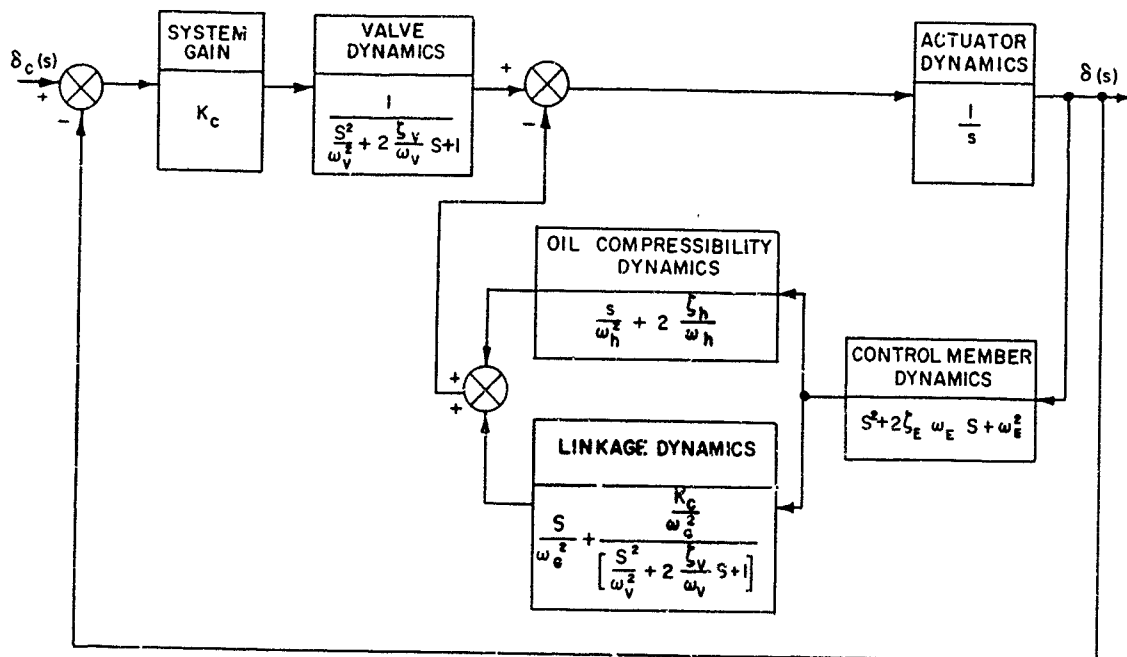


FIGURE 4-34. OPERATIONAL BLOCK DIAGRAM

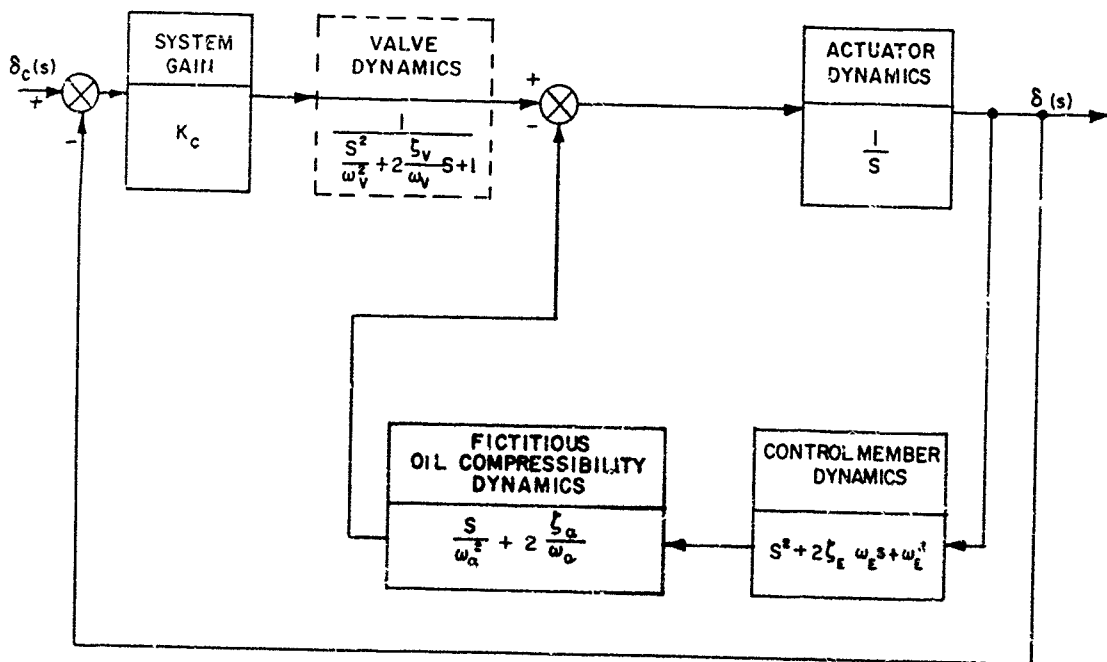


FIGURE 4-35. MODIFIED BLOCK DIAGRAM

SECRET

The volume under compression is:

$$\begin{aligned} V_c &= A_c x_c \\ &\approx A_c r \delta_{\max} \end{aligned} \quad (7)$$

It appears that the maximum torque required from the actuator for the PLATO missile will be approximately 1.5 times the maximum aerodynamic torque, giving-

$$T_{E_{\max}} \approx 1.5 C \delta_{\max} \quad (8)$$

Furthermore, neglecting the linkage damping,

$$T_{E_{\max}} \approx r A_c P_{\max} \quad (9)$$

Substitution of equations 7, 8, and 9 into equation 6 gives the following relation:

$$\omega_h \approx 1.23 \omega_E \sqrt{\frac{B}{P_{\max}}} \quad (10)$$

For example, if $B = 200,000$ psi and the maximum pressure used is 3000 psi, then

$$\omega_h \approx 10 \omega_E$$

This shows the dependence of the natural frequency of the hydraulic system on the aerodynamic loads on the control surface. At present, the aerodynamics group is working on the determination of the aerodynamic loads on the elevon surface. In addition, since the pivot arm, r , is designed into the system, and the maximum pressure is most likely 3000 psi, the piston area of the actuator is determined by the dynamic torque requirements of the elevon.

4.5.3.1 Autopilot

Since the determination of the gains of the autopilot depends upon the value of K_c , and this value is not available as yet, work on the autopilot was concentrated on methods of optimizing the system rather than on the system itself. One analytical method has been investigated.

In this method, equation 3 is used as the characteristic equation of the system. It is also written as the product of factors, two factors being real and the other two, complex conjugates. One of the

SECRET

real roots is set equal to the real part of the complex root, giving the following expression for the characteristic equation 3:

$$(s + \rho_c)(s + \rho_1)(s + \rho_c + j\omega_c)(s + \rho_c - j\omega_c) = 0 \quad (11)$$

where ω_c is the design frequency of the system.

The value of K_c is already determined from the actuator requirements. Therefore, by choosing the value of ω_c which is in general determined by external requirements, the value of ρ_c can be computed for a minimum gain system, i.e. minimum K_A , from the following sixth order equation:

$$a_0 \rho^6 + a_1 \rho^5 + a_2 \rho^4 + a_3 \rho^3 + a_4 \rho^2 + a_5 \rho + a_6 = 0 \quad (12)$$

where

$$a_0 = -8$$

$$a_1 = 12 (\rho_c + 2 \zeta_n \omega_n)$$

$$a_2 = -23 \omega_c^2 - 12 \zeta_n^2 \omega_n^2 - 36 \zeta_n \omega_n K_c - 3 K_c^2 - 12 \omega_n^2$$

$$a_3 = 56 \zeta_n \omega_n \omega_c^2 + 28 \omega_c^2 K_c + 20 \omega_n^2 K_c + 8 \zeta_n \omega_n K_c^2 + 16 \zeta_n^2 \omega_n^2 K_c + 8 \zeta_n \omega_n^3$$

$$a_4 = -12 \zeta_n \omega_n^3 K_c - 6 \omega_n^2 K_c^2 - 24 \zeta_n^2 \omega_n^2 \omega_c^2 - 48 \zeta_n \omega_n \omega_c^2 K_c - 6 \omega_c^2 K_c^2 + 16 \omega_c^4 - 12 \omega_c^2 \omega_n^2$$

$$a_5 = 8 \omega_c^2 \omega_n^2 K_c - 16 \zeta_n \omega_n \omega_c^4 - 8 \omega_c^4 K_c + 8 \zeta_n \omega_n \omega_c^2 K_c^2 + 16 \zeta_n^2 \omega_n^2 \omega_c^2 K_c + 8 \zeta_n \omega_n^3 \omega_c^2$$

$$a_6 = \omega_n^4 K_c^2 - 4 \zeta_n \omega_n^3 \omega_c^2 K_c - 2 \omega_c^2 \omega_n^2 K_c^2 + 4 \zeta_n^2 \omega_n^2 \omega_c^4 + 4 \zeta_n \omega_n \omega_c^4 K_c + \omega_c^4 K_c^2$$

Generally, there will be only one solution which is real, positive and less than $1/4 (K_c + 2 \zeta_n \omega_n)$. The last requirement is due to the fact that it is not desirable to have ρ_1 the dominant root.

Once ρ_c has been determined, the values of K_A , K_I and K_R are formed from the following expressions:

$$K_A = \frac{-\omega_c^2 K_c + 2 \zeta_n \omega_n \omega_c^2 + \omega_c^2 K_c - 2 \omega_c^2 \rho_c + 6 \zeta_n \omega_n \rho_c^2 + 3 K_c \rho_c^2 - 8 \rho_c^3}{2 K_c K} \quad (13)$$

$$K_I = \frac{-3 \rho_c^4 + (2 \zeta_n \omega_n + K_c) \rho_c^3 - 3 \omega_c^2 \rho_c^2 + (2 \zeta_n \omega_n \omega_c^2 + \omega_c^2 K_c) \rho_c}{K_c K K_A} \quad (14)$$

SECRET

$$K_D = \frac{-\delta \omega_c^2 + (6 \zeta_n \omega_n + 3 K_c) \rho_c - \omega_n^2 - 2 \zeta_n \omega_n K_c + \omega_c^2}{K_c K K_A} \quad (15)$$

Taking representative values for a numerical example:

$$\omega_n = 7 \text{ rad/sec}$$

$$\zeta_n = 0.3$$

$$K_c = 25 \text{ sec}^{-1}$$

$$\omega_c = 16 \text{ rad/sec}$$

the following gains were determined by this method for the system:

$$\rho_c = 3.9$$

$$KK_A = 102.2$$

$$K_I = 7.25$$

$$K_R = 0.14$$

The response, $\dot{\gamma}$, of the missile to a step input command of $\dot{\gamma}_c$ is shown in Figure 4-36. It might be pointed out that the damping ratio of this system is low. This is demonstrated by the response of δ which is shown in Figure 4-37. However, this method does give the area in which the gains should lie and by starting with these values and using a method such as the root locus, the damping ratio and hence the response can be improved, thereby decreasing the oscillatory nature of the δ response.

Programming

In order to have the same response during the flight, or at least a desirable response, it is necessary to program the gains of the system. Again, equation 3-34 will be used for the first investigation. In order to keep the shape of the response constant, the roots of the characteristic equation must be kept constant. The sum of the roots is equal to $K_c + 2 \zeta_n \omega_n$ with $K_c \gg 2 \zeta_n \omega_n$. Therefore, by keeping K_c constant, the sum of the roots will not change by much. It will be noted that the amplifier gain K_A always appears with the elevon gain K . Therefore, the product KK_A will be kept constant, or K_A programmed inversely proportional to K . The product of the roots is equal to $K_A KK_C K_I$. Since the product KK_A is programmed to remain constant, and K_c is constant, by leaving K_I constant the product of the roots will not change. By programming K_R in such a way as to keep the coefficients of the S^2 and s terms constant, the

SECRET

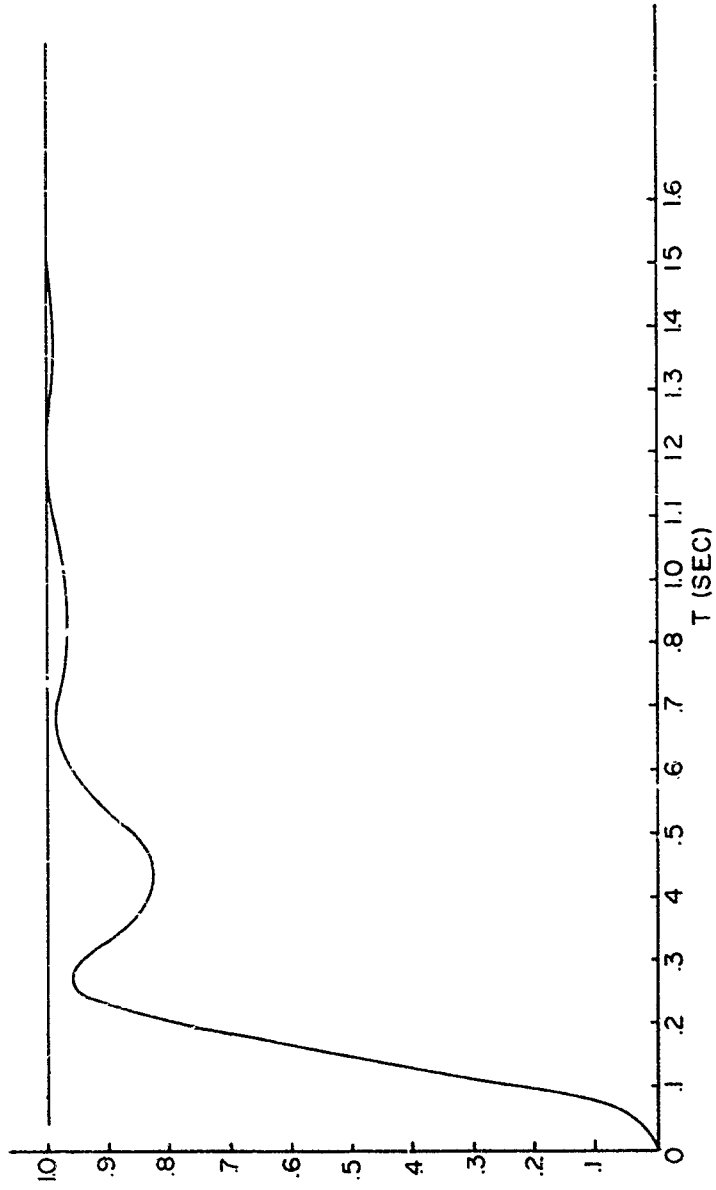


FIGURE 4-36. TRANSIENT RESPONSE OF MISSILE TO A UNIT STEP ACCELERATION INPUT OF ONE RADIAN/SEC

SECRET

SECRET

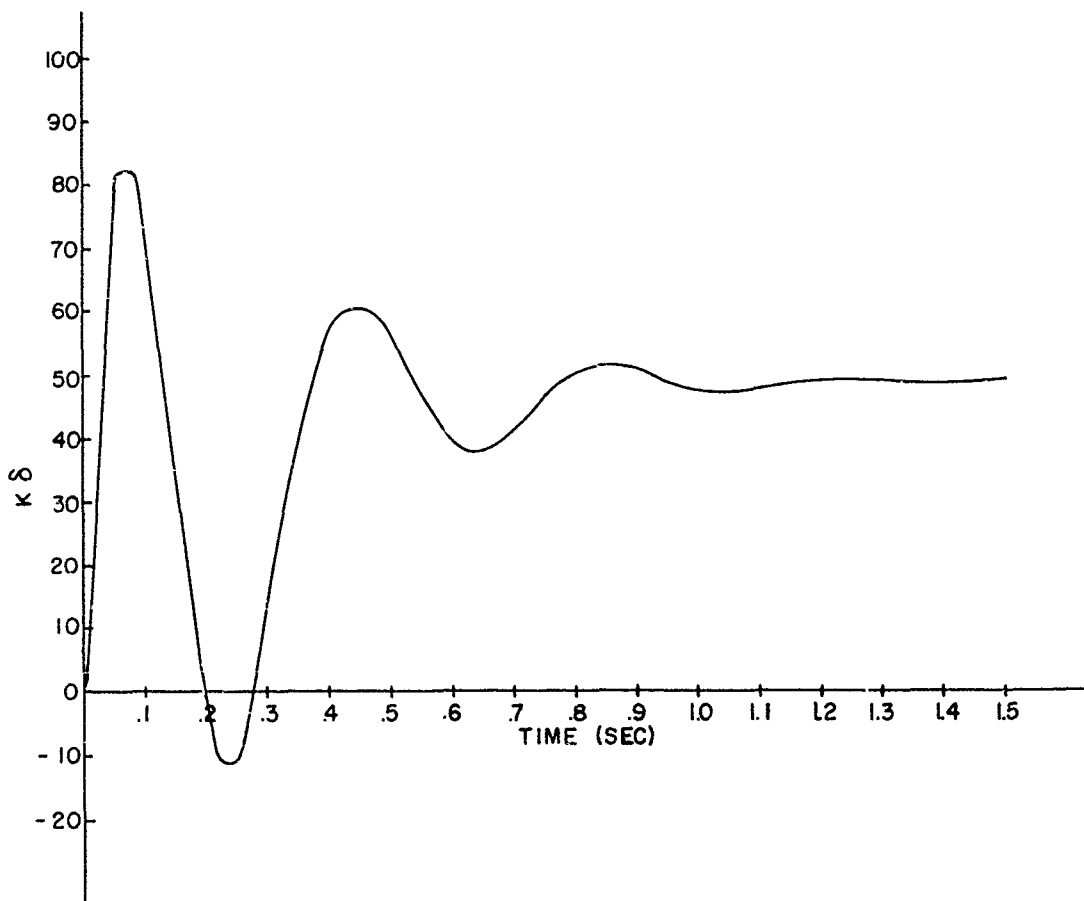


FIGURE 4-37. TRANSIENT RESPONSE OF CONTROL SURFACE TO A UNIT STEP ACCELERATION INPUT OF ONE RADIAN/SEC

SECRET

SECRET

characteristic equation will remain essentially the same throughout the flight. Therefore, only K_A and K_R need be programmed. This has been borne out by simulation studies made on a digital computer by the fire-control group. It should be pointed out that this analysis is a very rough first approximation. Equation 4-33 does not hold true throughout all flight and therefore, for low values of ω_γ , another scheme for programming must be employed.

4.5.3.2 Launch Phase

The missiles under consideration at present are aerodynamically unstable during the vertical launching phase. As such it is possible that a wind could cause a missile to turn over, with the missile being considered lost. Therefore, a separate investigation of the launch phase has been initiated. The problem is being done on the analog computer at Project Cyclone, Reeves Instrument Corporation.

GLOSSARY

A_c	hydraulic actuator cylinder area	ft^2
B	bulk modulus of hydraulic fluid	lb/ft^2
C	combined aerodynamic and structural spring constant of elevon	$lb\ ft/rad$
C_G	spring constant of linkage structure	lb/ft
C_v	spring constant of transfer valve	lb/ft
D	combined aerodynamic and structural damping coefficient of elevon	$lb\ ft\ sec$
D_G	damping coefficient of linkage structure	$lb\ sec/ft$
d_v	damping coefficient of transfer valve	$lb\ sec/ft$
I_E	mass moment of inertia of elevon about swivel point	$slug\ ft^2$
K_c	overall gain of hydraulic actuator system	sec^{-1}
K_γ	control coefficient	sec^{-1}
L_c	hydraulic leakage coefficient	$ft^5/lb\ sec$
m_v	mass of transfer valve spool	slugs
p	pressure across piston of actuator cylinder	lb/ft^2

SECRET

GLOSSARY

r	arm from actuator piston to swivel point of elevon	ft
S	laplace transform operator	sec^{-1}
T_E	net torque applied to the elevon from the hydraulic actuator through the linkage structure	lb/ft
V_c	total volume of hydraulic fluid under compression	ft^3
x_c	hydraulic piston displacement from initial equilibrium position	ft
x_G	linkage displacement from initial equilibrium position	ft
x_v	valve spool displacement from initial equilibrium position	ft
δ	control surface deflection	rad
δ_c	effective command signal to system	rad

$$\zeta_a = \frac{1 + \frac{K_c}{2 \zeta_n \omega_h} \left(\frac{\omega_h}{\omega_G}\right)^2}{\sqrt{1 + \left(\frac{\omega_h}{\omega_G}\right)^2}} \quad \zeta_c = \text{fictitious damping ratio of hydraulic fluid compressibility resonance}$$

$$\zeta_E = \frac{1}{2} \frac{D}{\sqrt{CI_E}} = \text{damping ratio of elevon system}$$

$$\zeta_h = \frac{1}{2} L_c \left\{ \sqrt{\frac{V_c r^2 A_c^2}{\delta^2 I_E}} \right\}^{-1} = \text{damping ratio of hydraulic fluid compressibility resonance}$$

$$\zeta_v = \frac{1}{2} \frac{d_v}{\sqrt{m_v C_v}} = \text{damping ratio of transfer valve system}$$

$$\omega_a = \frac{\omega_G \omega_h}{\sqrt{\omega_G^2 + \omega_h^2}} = \text{fictitious natural frequency of hydraulic fluid compressibility resonance} \quad \text{rad/sec}$$

SECRET

GLOSSARY

ω_E	=	$\sqrt{\frac{C}{I_E}}$	= natural frequency of elevon system	rad/sec
ω_G	=	$\sqrt{\frac{r^2 C_G}{I_E}}$	= natural frequency of linkage system	rad/sec
ω_h	=	$\sqrt{\frac{Br^2 A_c^2}{V_c I_E}}$	= natural frequency of hydraulic fluid compressibility resonance	rad/sec
ω_v	=	$\sqrt{\frac{C_v}{m_v}}$	= natural frequency of transfer valve system	rad/sec
$\zeta_{\dot{\gamma}}$			control coupling damping ratio	
ζ_n			missile frame damping ratio	
$\omega_{\dot{\gamma}}$			control coupling natural frequency	rad/sec
ω_n			missile frame natural frequency	rad/sec

4.5.4 DESIGN

Use of a solid propellant rocket engine results in some important advantages in the PLATO system. However, there are some disadvantages as compared with the use of liquid propellants. In general, liquid propellants offer higher performance, both in terms of propellant specific impulse and total impulse/weight ratio. In addition, liquid propellants are less sensitive in terms of variation of thrust with engine temperature.

On the other hand, the solid propellant is a simple device with an established reliability in the neighborhood of 99% as compared with the 90% to 95% of liquid propellants. The higher cost of a solid engine is somewhat offset by the need of auxiliary equipment for the liquid. This would include propellant handling equipment, provision for inspection of tank linings exposed to corrosive fluids, and check-out for the various moving parts, i.e. valves, pumps, etc.

Because the comparison shows advantages for both methods of propulsion, a single design has not been selected. The S-3a configuration utilizes liquid propellants; the S-7 is designed around a solid engine. The advantages may be summarized as follows:

SECRET

	Solid Propellant	Liquid Propellant
Cost	Higher overall	Lower total cost but more expensive metal parts.
Weight	Greater	Lower
Size	More compact	Longer
Storage Life	1-3 years (occasionally more)	1-4 months
Handling	Very rugged	Care required
Transportation:	Single unit	Generally propellants transported separately.
Availability of Propellants:	Some oxidizers, particularly $KClO_4$ could become critical.	Some fuels such as JP-4 could compete with aircraft requirements locally.
Hazards:	Cracked propellant grain can lead to engine explosion on ignition.	Corrosive oxidizer requires handling precautions. Can damage tank if stored too long. Exhaust can be corrosive in damp atmosphere.
Shut-off- in flight:	Can be done-difficult.	Simple.
Field Service:	Visual inspection of exterior should be sufficient.	Propellants drained and refilled at intervals.
Ignition Delay (Estimated):	20 millisecc.	200 to 500 millisecc.
Center of Gravity, motion:	Predictable.	Depends on missile motions.
	Not subject to control by simple design changes.	May be adjusted during design.

SECRET

	Solid Propellant	Liquid Propellant
Effect of Storage Temperature:	If storage limits are exceeded, grain may crack. Thrust depends on grain temperature. Specific impulse relatively unchanged.	Little effect.
Test:	Cannot be test fired in field.	Can be test fired and reloaded.

Another advantage of the solid propellant rocket engine is that its casing made of an alloy itself to withstand the high internal pressure can be used as the load carrying structure of the missile. Starting with this basic structure, the wings, nose, boattail may be attached to the casing by the use of fittings incorporated in the casing design.

The interceptor structural design was based on a load factor of 10, fully loaded, permitting much higher load factors in the light weight conditions found toward the end of the flight. Although not yet determined, it would appear that this missile has comparable performance to the S-3a missile.

A comparison of the two propulsion systems appears to resolve itself into two parts. The liquid propellant is easy to design around and has higher theoretical performance. The solid propellant is rugged, reliable and easier to handle in the field. It would appear that if the solid propellant can be used without overwhelming penalties in cost or performance, it is a superior choice for tactical missile employment. Further comparisons of flight trajectories were made and will form our basis for a selection of missile type.

4.5.5 STRUCTURES

The S-7 missile wing has a delta planform with a semi-apex angle (determined by aerodynamic considerations) of 19° and a span of 223 inches. The fin is defined as the exposed portion of the semi-wing. The area of a fin is 91.5 square feet. Elevon area is 10% of the fin area. Fuselage stations (designated by FS) indicate the distances in inches from the nose of the missile (FSO) parallel to the missile centerline. Wing Stations (WS) indicate inches from the missile centerline (WSO) taken perpendicular to the centerline.

SECRET

The fin is attached by means of a root rib to the fuselage on WS 17 at FS 118.5 and FS 266.5. A stressed skin construction is used for the fin. The rear spar is located on FS 310 and extends from WS 17 to WS 97. The elevon is a horn-balanced type and is supported by the rear spar. Spars within the net fin (fin minus elevon) are located along constant per cent net chord lines from WS 29 outboard. Between WS 17 and WS 29, the spars are perpendicular to the fuselage centerline. Intermediate skin stiffeners are placed midway between adjacent spars. Ribs are parallel to the fuselage centerline at WS 29, 46, 63, 80 and 97. The internal structural arrangement of the wing is shown in Figure 4-38.

Spars together with the stressed skin form a torque box. Vertical shear is transmitted through the spars to the root rib and then to the fuselage.

The casing of the solid propellant will form the center section of the fuselage extending from FS 110 to FS 275. The means of doing this will be the subject of a further study program. The warhead can be attached directly to the forward end of this casing. With this type of support for the warhead, the missile nose section can be made non-load-carrying and therefore of a lighter and simpler construction. Similarly, electronic equipment can be attached to the aft end of the propellant casing, thereby relieving the necessity of making the boattail a load-carrying member.

4.5.6 INTERCEPTOR REFERENCE SYSTEM

A preliminary investigation into the requirements of a space reference system using inertial instrumentation has been performed. Basically, these requirements are those of providing to the guidance equipment adequate interceptor angular orientation information with respect to an earth-fixed coordinate system such that guidance commands will be executed with "sufficient" rapidity and accuracy.

Since the criterion of sufficiency depends on factors associated with the overall interceptor system (e.g. allowable trajectory errors, guidance loop dynamic response, etc.) evaluation of any given reference system as an independent component would be pointless. The analysis approach used in this investigation was a broad one dealing with types of systems rather than specific configurations; however, the manner in which these types could be instrumented was considered. In addition, certain general relations concerning the interdependence of measurement errors and resultant orientation errors were derived. Finally, the effect of orientation errors on a typical guidance system was determined.

In order to provide a basis for comparison, it was assumed that commands to the interceptor are always computed by the fire control computer

SECRET

as vector components in an orthogonal earth-fixed coordinate system and that the desired function of the reference system is to provide knowledge, somewhere in the guidance link, of the Euler angles (elevation, azimuth and bank) of the interceptor-fixed coordinate system with respect to the above earth-fixed coordinate system for the purpose of computing coordinate transformations.

It is conceivable that Euler angles might not exist explicitly anywhere; however, all of the required orientation relations between pertinent vectors can be expressed in terms of them, and in many cases the instrumentation does measure Euler angles.

4.5.6.1 Types of Reference Systems

The types of reference systems possible were divided into two main groups: (1) those requiring an information link to ground, and (2) wholly interceptor contained, or those which do not require an information link. The above two groups were further sub-divided into generic categories characterized primarily by the type of control requirement imposed. Table I summarizes the systems considered.

**TABLE I
SYSTEMS CONSIDERED**

CATEGORY	WHOLLY INTERCEPTOR CONTAINED	REQUIRING INFORMATION LINK
<p>1. Roll angle stabilized (i.e. roll angle as measured by a rate integrating gyro, for example, is kept zero by roll control system)</p>	<p>a. Direction of roll axis approximated by direction of velocity vector (tangent to trajectory) with elevation & azimuth of velocity vector measured from ground by radar.</p> <p>b. Same as (a) above with correction for angle of attack computed by ground-based interceptor analog.</p>	<p>a. Pitch and yaw rates measured in interceptor and transmitted to ground for computation of Euler angles.</p> <p>b. Lateral acceleration along pitch and yaw axes measured in interceptor and transmitted to ground. Pitch and yaw rates calculated from</p> $\omega = \frac{a}{V}$

TABLE I (Cont)

CATEGORY	WHOLLY INTERCEPTOR CONTAINED	REQUIRING INFORMATION LINK
2. Bank angle stabilized (i.e. bank angle as measured, for example, by a free gyro, is kept zero by roll control system.)	a. Elevation & azimuth of velocity vector measured from ground by radar. b. Same as (a) with a correction for angle of attack computed by ground-based interceptor analog.	a. Elevation and azimuth measured in interceptor and transmitted to ground.
3. Unstabilized (roll rate limited) i.e. no orientation variable is controlled with sufficient accuracy to permit assumption as to its value in ground computations.	a. Partial stable platform* providing elevation (or azimuth) and bank for partial coordinate transformation, with azimuth (or elevation) measured from ground for remainder of transformation. b. Stable platform* in interceptor for measurement of all Euler angles. All coordinate transformation performed in interceptor.	a. Stable platform* in interceptor for measurement of all Euler angles, these being transmitted to ground for computation of coordinate transformation.

* Term for configuration which provides all Euler angle information - not necessarily "platform" per se.

4.5.6.2 System Performance Description

A brief review of the reference systems tabulated in Table I indicated that little would be gained by use of an information link insofar as reliability or reduction of airborne instrumentation are concerned. The advantage in accuracy which might be gained in some cases appears to be outweighed in those cases by increased complexity. Consequently, detailed analysis was limited to the wholly interceptor contained reference systems. Should these be found inadequate, emphasis will be shifted to information link systems.

Roll Angle Stabilized Interceptor (no information link)

Elevation and azimuth of the interceptor velocity vector are measured by radar from the ground, and by virtue of the fact that roll angle is maintained at zero it can be shown that:

$$\phi = \int \dot{\psi} \sin \theta dt$$

SECRET

where

ϕ = bank angle

ψ = azimuth angle measured in a vertical plane

θ = elevation angle measured from the vertical

This system is the simplest wholly interceptor contained one in terms of airborne instrumentation and computation equipment, the total requirement being satisfied by a single rate integrating gyro.

Errors in bank angle due to angle of attack and radar errors in measurement of elevation and azimuth of the velocity vector can be very large, being of the form:

$$\Delta\phi = K \alpha' \tan \theta$$

where

$\Delta\phi$ is the error in bank

K is a factor such that $0 < K < 1.4$

α' is apparent angle of attack, i.e. the angle between the roll axis and radar-measured velocity vector.

θ is elevation angle measured from vertical

However, because of an additional relation which holds in this case, $\Delta\phi = \Delta\psi \sin \theta$, the error due to bank error, $\Delta\phi$, in direction cosines of the missile-fixed coordinate system with respect to the earth-fixed coordinate system is limited. In fact, calculations show that for a combined pitch and yaw angle of attack of 10° each, at $\theta = 84^\circ$ ($\tan \theta \approx 10$), the largest direction cosine error is approximately 15%. These errors can probably be reduced, if necessary, by the addition of a considerable amount of ground-based computer equipment which simulates interceptor dynamic performance and provides angle of attack correction.

Noise in $\dot{\psi}$ is a more difficult proposition and has not been analyzed as yet.

Bank Angle Stabilized Interceptor (No information link)

In this case, as in the roll stabilized case, elevation and azimuth of the interceptor velocity vector are measured by radar from the ground. Thus, by assumption:

SECRET

$$\phi = 0$$

$$\psi_{\text{Roll axis}} \approx \psi_{\text{Velocity vector}}$$

$$\theta_{\text{Roll axis}} \approx \theta_{\text{Velocity vector}}$$

The total instrumentation requirement of this system can be satisfied by a single free gyro.

The nature of errors in the bank stabilized system is similar to that in the roll stabilized system in that

$$\Delta\psi = K \alpha' \sec \theta$$

However, $\Delta\phi$ is zero (by assumption) so that ϕ and ψ errors are independent of each other. The resultant direction cosine errors can be prohibitive at an elevation angle θ close to 90° . In addition, a free gyro is subject to gimbal lock under some interceptor maneuvers.

Unstabilized System - Roll Rate Limited (No Information Link)

All attitude angles are measured in the interceptor and computation of the coordinate transformations is performed in the interceptor. Except for a possibility of gimbal lock which can occur during certain interceptor maneuvers, this system is probably more accurate than the other systems considered by an order of magnitude. On the other hand, it is approximately an order of magnitude more complex and expensive.

Idealized Typical Guidance Loop Response in the Presence of Orientation Errors

The step input response of a servo loop consisting of a position error sensing sampling radar, an interceptor of negligible dynamic lag compared with the sampling rate, and a guidance controller which produces clamped acceleration commands proportional to position error was determined. It was shown that the number of sampling periods required to reduce an error to 10% of its initial value is given by the relation:

$$m_R = \frac{1}{\log_{10} \frac{1}{\sqrt{1 - K\tau^2 \cos \xi + 1/4(K\tau^2)^2}}}$$

where

m_R = the number of sampling periods

K = the loop gain

SECRET

τ = sampling period

ξ = the orientation error (e.g. Bank error)

The degradation of "rise time", m_R , due to ξ is shown in Table II. In Table II the optimum $K\tau^2$ product for minimizing m_p was used. It should be noted that the optimum $K\tau^2$ cannot always be achieved because of maneuverability limitations and other reasons; however, the trend of results is similar in all cases.

TABLE II
"RISE TIME" VERSUS ORIENTATION ERROR AT
OPTIMUM $K\tau^2$

<u>ξ (degrees)</u>	<u>m_R minimum (number of periods)</u>
0	1
10	2
20	3
40	6
80	151

4.5.6.3 Conclusions

It is felt that the roll stabilized system offers sufficient promise of adequate accuracy at lowest cost, with no maneuverability limitations, to warrant exclusive consideration of this system at the present time.

4.5.7 COMMAND SYSTEM

The radio link between weapon missiles and ground installations is taking form best suited to satisfy the sometimes conflicting demands for reliability, invulnerability to countermeasures, minimization of logistics problems, and optimum satisfaction of performance requirements. The concept of this link, indicated in past reports, is undergoing changes to accommodate PLATO system developments now becoming well-defined.

4.5.7.1 System Aspects

- (a) No telemetering requirement is anticipated during interceptor flight.
- (b) The single omni-directional transmitter formerly envisaged as a center of communications to all missiles launched by a PLATO battalion will be displaced by a number of such

SECRET

transmitters, one located at each launch site. Different carrier frequencies in a selected band may be allocated to each such transmitter. Limiting the space within which missile communications must be maintained to trajectory limits of one launch site (instead of an entire PLATO area of defense as formerly conceived) should increase communications reliability and invulnerability to countermeasures alone because of the shorter range of transmission established by this limitation to one site.

- (c) A pulse-time code similar to that outlined in PLATO Quarterly Report No. 7 will permit identification of missiles from specific launching equipments. Missile response to commands will be provided only upon proper response to such a coded interrogation. The system in mind may be required to command 18 weapons simultaneously. The identification-interrogation coding technique is being expanded to accommodate numbers of this order.
- (d) Circular polarization of command transmissions is planned. Missile-borne antennas cannot be expected to have omnidirectional propagation characteristics. The nature of the trajectories to a high degree of probability might orient the missile to receive a minimum command signal. Coupled with this possibility is the phenomenon of interference patterns between directly-received command radiation and earth-reflected waves producing alternate areas of strong and negligible signal strength within interceptor trajectory space limits. Circular polarization minimizes such effects.
- (e) Transmission frequencies for the command link may well be on the order of several hundred megacycles. The missile size being considered for PLATO will allow for incorporating the moderate-sized antennas which these frequencies of operation will demand for near-omni-directional properties and circular polarization. These lower transmission frequencies, as compared with microwaves, are attractive in their superior propagation reliability and power requirements. Higher reliability and design flexibility is achievable also in point of components available; for example co-axial cable instead of waveguides or a wider of possible tube types. The lower frequencies permit greater tolerances in constructional practice and adjustment of circuitry.

SECRET

(f) Consideration has been given to use of individual interceptor illuminators somewhat like those used in PLATO target tracking. This technique does improve the countermeasures problem. Disadvantages are evident, however, in the increased system complexity and the excessive demand on computers, especially when defense against a saturation-type missile attack is anticipated.

4.5.7.2 Performance Requirements

The main function of the missile communications link will be to transmit a series of acceleration commands in two coordinates for each interceptor missile throughout its trajectory, at a rate of 1/2 second for each set of commands. The guidance computer will furnish this data in digital form. A conversion to an analog form of signal must be effected either in the missile equipment or on the ground prior to transmission. The latter alternative is preferred since it reduces missile-borne equipment complexity. A tolerable error of data transmission on the order of 1% is expected.

A second function of the radio link is to transmit intermittent commands such as on-off switching of thrust, possibly fuel metering, and warhead fusing and firing. Because of the critical timing requirement the firing of the warhead may necessarily be initiated with missile electronics of the proximity-fuse category. Self-destruction of the warhead may be commanded after a miss is scored or a target is destroyed by another interceptor. Some thought has been given to possible salvage of such warheads.

To obtain optimum signal for purposes of tracking the weapon missiles it is required to illuminate these missiles and provide for a response signal intended for detection and analysis by the PLATO precision tracking radar. The functions of illumination and response (repeater or responder-beacon) are to be a part of the missile communications link. As an additional requirement, it may be necessary to provide for identification of response of each weapon missile, as an aid to precision tracking. Communications must be maintained throughout the possible space in which interceptor trajectories may lie. Present estimates run to an extreme of a more or less cylindrical region of space 30 miles in radius and 20 miles in height.

4.6 GROUND COMMUNICATIONS NETWORK

As in the missile communications link, the data transmission network between ground installations is formulated with design objectives of reliability, invulnerability to countermeasures, and minimization of the logistics, as well as optimum satisfaction of performance requirements.

SECRET

SECRET

Considerably more data is required to be transmitted than carried by the interceptor link. Necessary dispersion of the ground installations, on the order of 20 miles maximum distance, and the requirements of maximum mobility makes radio-type data links mandatory.

An auxiliary voice-communications network is required, as well, for control of personnel and system operations from battalion headquarters, and for other operations such as alerting of personnel for missile preparations prior to launch, for maintenance-supply service orders, etc. Standard military communications circuits will be provided for these requirements and may be considered a minor problem, one essentially of detailing known components.

4.6.1 SYSTEM ASPECTS

4.6.1.1 Grouping of Ground Equipments

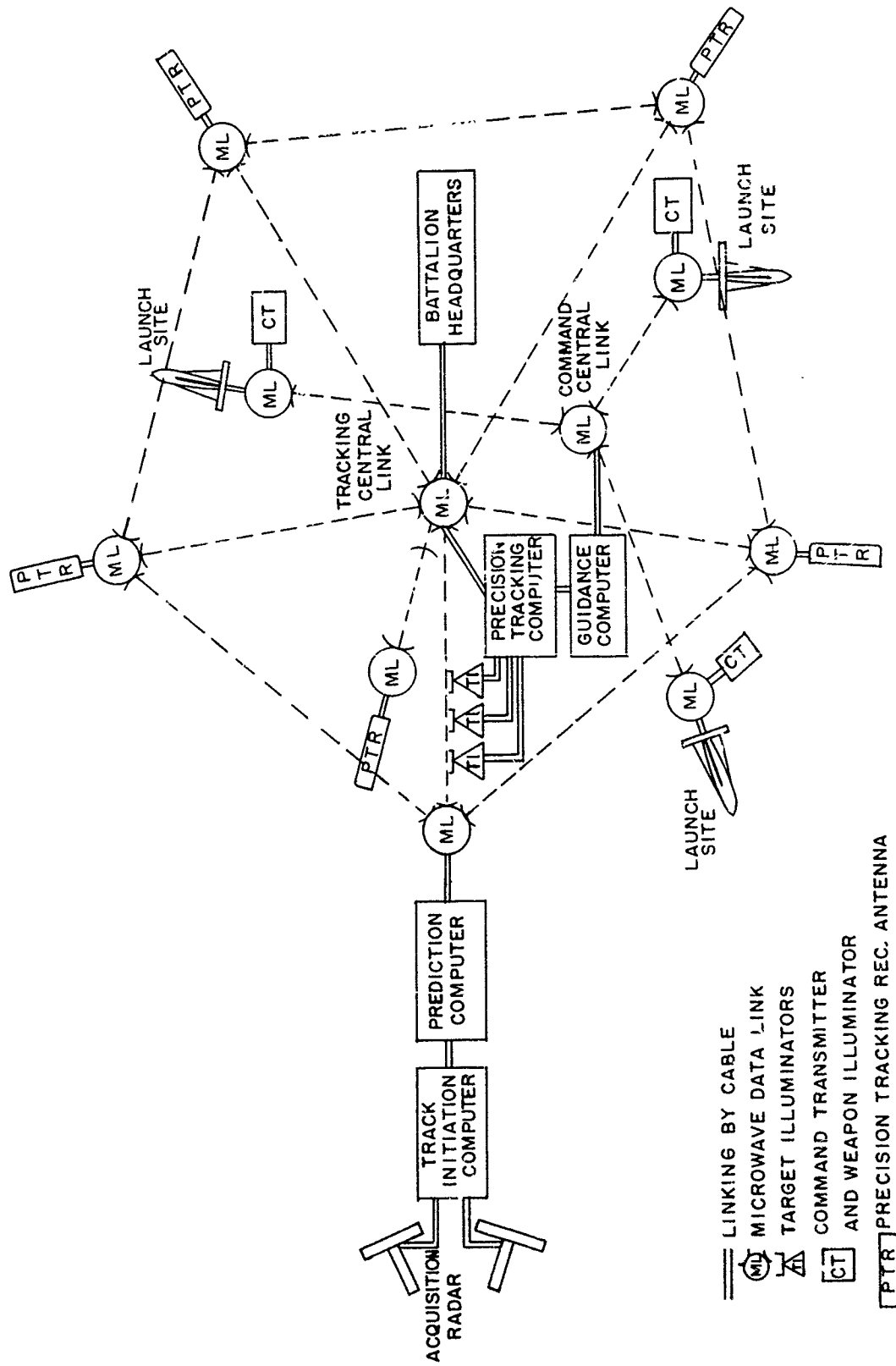
Obvious advantages in data transmission, reliability and system simplicity will be obtained if various ground equipments can be located within advantageous cable-connecting distance of each other. One or two miles of cable is visualized as a practical maximum. Longer field cable distances become increasingly susceptible to transmission difficulties. Of more compelling importance, longer cable lengths are open to sabotage and to conventional military assault.

Figure 4-39 outlines one possible concept of a PLATO data transmission network. It is to be noted that an area is selected close to the center of defense for grouping the track and guidance computers, the target illuminator site, and battalion headquarters. A center of communications for precision tracking information is located at this point. A separate communications link center for command transmission is also located at this point. One launch site may well be placed in this central area, cable-connected in this instance for relaying communications link. Other, more remote launch sites would require a microwave relay, as shown, for conveying missile commands via the missile command transmitter at those launch sites.

Following similar grouping procedures, it may be possible to locate in close proximity the acquisition radar, track initiation, and prediction computers and one station of the precision tracking radar sitings.

Each precision track antenna site is shown microwave-linked to its adjacent site as well as to the central data-gathering microwave station. It is possible that at a minor increase in network complexity, a major increase in reliability of tracking data transmission can be achieved by relaying data around one or more of the radial microwave paths in the event

SECRET



SECRET

FIGURE 4-39. GROUND-BASED DATA COMMUNICATIONS NETWORK

SECRET

of failure in one or more radial links due to component failure, enemy action, or other reasons.

4.6.1.2 Antennas

For economy of power, link isolations and security reasons, it is desirable to beam the transmissions from point to point. Minimization of antenna dimensions necessitates use of microwave carrier frequencies. Line-of-site transmission is implied. For appreciable range of transmission, the antennas must be elevated on towers, at least, as follows:

RANGE OF TRANSMISSION	THEORETICAL MINIMUM TOWER HEIGHT
d	$h = d^2/8R$
5. miles	4. + ft.
10.	17.
20.	67.
30.	150.
40.	267.

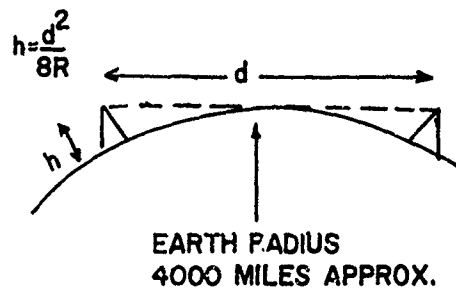


FIGURE 4-40

The height of tower required nominally for a 30. mile link distance makes the tower a highly vulnerable target. It is possible to transmit the data over one or more intermediate relay stations at an additional cost in complexity and a questionable gain in reliability. Further disadvantages are the necessity for supplying firm tower structures and the need for critical alignment in installation. Optimizing the beam angle will alleviate these difficulties.

SECRET

4.6.1.3 Propagation

Even with perfect line-of-sight geography, microwave relay experience reveals at times severe interruption to communications by variations in atmospheric conditions between relay stations. A choice of frequencies in the lower microwave bands or of frequencies below such bands may be in order to minimize such vagaries in communications. Reducing the range of transmission will, of course, help.

4.6.1.4 Data Encoding

Little is to be gained by quantizing data, such as is done in pulse-code modulation techniques. Transmission distances, the number of repeater transmitters, and the probability of interference (countermeasures, for example) are of a relatively low order. The circuit simplicity and inherent accuracy of direct modulation (amplitude or angular) of the microwave carrier recommends that this technique be followed in all links.

4.6.2 PERFORMANCE REQUIREMENTS

- (a) The purpose of the communications network is to interconnect the functions of the geographically separated ground installations. The following equipment groups are the significant ground-based units which are required to be linked:

- Acquisition radar antenna site
- Track initiation computer
- Prediction computer
- Precision tracking computer
- Guidance computer
- Precision tracking receiving antennas
- Launcher sites
- Missile command and illuminator equipment
- Headquarters of the PLATO battalion
- Service area of the battalion

The number of network terminals must be flexible to allow for the needs of any given defended area.

- (b) The data to be transmitted consists of signal output of receiving antennas, computer outputs, and missile command signals. The quantity of data per unit time to be transmitted over any given link is not yet an established figure. However, there is

SECRET

no evidence that this will constitute a problem in providing bandwidth or carrier frequencies necessary.

- (c) Geographical coverage is envisaged on the order of a circle of 30 miles radius. It may be necessary to provide communications over a larger area. The system should accommodate varying demands about this nominal figure.
- (d) A high degree of mobility is required.
- (e) Reliability of operation is of utmost importance.
- (f) Security against countermeasures including a reasonable immunity to sabotage is highly desirable.
- (g) The logistic problem should be kept in mind, in the interest of system optimization. This includes attention to reduction of the number and bulk of equipments, manufacturing ease, automaticity of operation, low cost in time and manpower for installation and disassembly for transport to new locations, inherent resistance to vibration, shock, temperature changes, etc.
- (h) Accuracy of data transmission. No limits have been suggested. It is considered desirable to minimize the problem by reducing the number of communication links required. Where links are necessary, a probable error will be evaluated.

CONFIDENTIAL

APPENDIX I
STATEMENT OF WORK

The Contractor shall furnish the work, labor, services and supplies necessary for, and shall institute and carry out, a program of studies and system analyses, not limited to but including appropriate calculations, scientific measurements, laboratory experiments and such other work within the scope of the program as may be indicated to be necessary as the program develops, of certain ballistic type missiles, which studies and analyses will be directed toward fulfillment of the following program:

(a) Objective

To determine the performance and design requirements of an anti-missile missile system, designated as GS-XS AM-A-19, under Project PLATO, that would be capable of being utilized as an effective countermeasure to the aforesaid certain ballistic type missiles, in order that a sound logical basis will be provided for evaluating the feasibility of such an anti-missile missile system.

(b) Scope of Program

The scope of the program shall be governed by the following factors:

1. Contractor's efforts shall be directed primarily toward the defense of tactical areas against present day missiles of the type herein-above referred to and toward missiles which may be expected in the near future. Defense of the zone of the interior will also be a consideration.
2. Primary consideration shall be given to the performance and design requirements of a guided anti-missile missile system that may be effectively utilized as a countermeasure to ballistic type missiles adapted to carry warheads of extremely high destructive properties.
3. The system study will include consideration of the critical nature of the time factor involved in and concerned with alerting by the use of a ground-based warning system, rapid identification, system readiness, rapid launching, and fire power and rate of fire.
4. Particular attention will be given to the nature and characteristics of the field operation of the anti-missile missile

CONFIDENTIAL

system including but not limited to mobility, ruggedness, simplicity, availability of manpower, security, safety and other related important factors.

5. The program provided for herein will include the investigation and study of a complete anti-missile missile system for an area defense network. Said system shall be a separate and distinct system, but insofar as practical, compatible with other defense systems.
6. Performance and design requirements of the anti-missile missile system shall provide for all-weather operation.
7. The program provided for herein shall be conducted and the results thereof shall reflect that the military requirement therefore is of an urgent nature.

(c) Phases of Work

Subject to the Time of Performance provisions of this contract, the program provided for herein shall be conducted in two (2) phases as hereinafter indicated and the Contractor agrees that its efforts shall be directed toward the accomplishment of the following items, but without limitation thereto.

1. Phase I

- a. To summarize the performance characteristics of surface-to-surface ballistic-type United States missiles, and also as far as is known the probable performance characteristics of foreign missiles to be expected in the near future.
- b. To review and evaluate previous counter-missile efforts in order to obtain the full benefit of such information as may be of value, and also to study previous work on surface-to-surface missile development.
- c. To estimate the essential features and numerical constants of a guided anti-missile missile system as related to target detection, target identification, target tracking and the area of interception with approximate minimum and ideal values of such characteristics as terminal ballistics, fusing, accuracy requirements guidance, control, stability, computation, maneuverability, time of flight, range speed, dimensions, weight, etc.

CONFIDENTIAL

- d. To outline a preliminary guided anti-missile missile system design with estimates of its approximate effectiveness and related costs.
- e. To study the effects of variations of the various specifications of the outlined guided anti-missile missile system on its overall effectiveness and the mutual relations between these variations.

2. Phase II

- a. To determine quantitatively the benefits to be obtained from improving certain performance characteristics and also to determine the costs which may be involved if these characteristics must be compromised due to the limitations of engineering techniques and technical progress with respect to the outlined guided anti-missile missile system.
- b. To prepare an adequate description of a preliminary design which can be put into construction over a period of the next several years to secure the expected optimum characteristics of the outlined guided anti-missile missile system. This description will have tabulated values and limits of the various characteristics involved. Sketches will be provided presenting the general constructional features of the overall system and the principal component sections. The important system concepts, estimates of production costs, and estimates of operating requirements for both men and material against typical enemy attacks will be provided.
- c. To prepare a program necessary to achieve an engineering design of a guided anti-missile missile prototype system. This will include the preparation of a table of estimated costs, manpower and time schedules, facilities required for a development program of laboratory studies, prototype development, field measurements, test flights, flight instrumentation, drawings and other estimates necessary to the plan of the program.

CONFIDENTIAL

APPENDIX II

BIOGRAPHICAL SKETCHES OF TECHNICAL PERSONNEL

WARD C. LOW - Engineering Specialist

Dr. Low received his bachelor's degree in physics from the University of Wyoming in 1943, and a Ph.D. in physics from Boston University in 1955. From June, 1943 to April, 1944, he was a physics instructor at the University of Wyoming. The years 1944-1945 were spent as a radio technician in the Navy. From 1946 to 1954 Dr. Low was at the Upper Atmosphere Research Laboratory at Boston University, where he was Assistant Director, Acting Director, and Project Supervisor. He worked on Air Force projects which deal with heat transfer in boundary layers, long-distance radio reception in high-altitude missiles, measurement of cross-modulation in the ionosphere, and high-altitude parachute dynamics. From 1954 to July, 1955, Dr. Low worked part time at the Massachusetts Institute of Technology as a research associate in the Heat Division of the Mechanical Engineering Department, and part time as a Research Director at the Cambridge Development and Engineering Corporation. He has several graduate-level physics courses at Boston University, and has authored numerous papers, technical notes, progress reports, and final reports connected with his work. Dr. Low is an Engineering Specialist in the Physical Analysis Section of the Analysis Department of the Missile Systems Laboratory.

KENNETH C. MATHEWS - Engineering Specialist

Mr. Mathews received a B.S. in electrical engineering at the Massachusetts Institute of Technology in 1946. From 1946 to 1948 he was employed by the Doelcam Corporation where his work consisted of electro-mechanical instrument development. From 1948 to 1950 he was employed by the University of Michigan where his work consisted of analog computer design and application to missile control problems. In 1950 he worked on system analysis for a bombing navigational computer for the A.C. Spark Plug Company. In 1950 he became supervisor in charge of the Instrumentation Section, Airborne Instrumentation for Cook Research Laboratories. From 1953 to 1955 he was Chief Electrical Engineer for the Doelcam Corporation, developing electronic and electro-mechanical instruments. In 1955 Mr. Mathews joined Sylvania's Missile Systems Laboratory where he is currently an Engineering Specialist in the Missile Department. His work consists of missile system analyses.

PETER M. HOSE' - Senior Engineer

Mr. Hose' received a B.A. and an M.A., both in aeronautical engineering, from the Brooklyn Polytechnic Institute in 1949 and 1950, respectively. In 1950 he worked as an operations analyst for the Operations Research

CONFIDENTIAL

179

CONFIDENTIAL

Office of the Johns Hopkins University. During this time he spent two years in Japan and Korea as an analyst and assistant field director, working on such problems as close support tactical air operation and weapons effectiveness. Another two years were spent at OCAFF, Fort Monroe, where problems pertaining to atomic warfare and field testing were studied, using standard mathematical methods and a newly developed system for war gaming. For a short period in 1950 he was with the American Power Jet Company as an aeronautical engineer and analyst, working on problems on sub-contract to ORO and the Air Force. In July, 1955, Mr. Hose¹ joined the Operations Research Section of the Missile Systems Laboratory

CYRIL J. BROWN - Senior Engineer

Mr. Brown received a B.S. degree in military science and engineering from the United States Military Academy in 1945 and an M.S. in electrical engineering from the Massachusetts Institute of Technology in 1951. In the years 1946 to 1949 he was in the Armed Forces Special Weapons Project, and from November, 1951, until May, 1954, he served as Radio Officer at Supreme Headquarters, Allied Powers Europe, in Paris, France. He has also completed the Advanced Signal Officers course at the Signal School. Mr. Brown joined Sylvania's Missile Systems Laboratory in July of 1955 as a Senior Engineer in the Operations Research Section of the Analysis Department.

JOSEPH FRANTANTUNO - Senior Engineer

Mr. Frantantuno received his B.S. degree in aeronautical engineering from the University of Rhode Island in 1941. From 1942 to 1944 he was stationed at the U.S. Naval Torpedo Station where he was a research and design engineer working on electro-mechanical control and gyro mechanisms. From 1944 to 1947 he was employed by General Electric Company where he worked on the design of power transformers, reactors, and circuitry for the betatron. From 1947 to 1950 he was employed by the Sargeant and Wilbur Manufacturing Company as a design engineer. Here he was engaged in the designing of a heat treating conveyor-type furnace. From 1950 to 1955 he served as a project engineer for the Gorman Manufacturing Company, working on the manufacturing of waveguide and electro-mechanical assemblies. In 1955 Mr. Frantantuno joined Sylvania where he is currently a Senior Engineer in the Missile Department of the Missile Systems Laboratory. His work consists of the analysis, evaluation, and survey of information regarding missile launching equipment and transportation equipment.

STANLEY RITTENBERG - Senior Engineer

Mr. Rittenberg received his B.A. degree in physics at Harvard University in 1947 and his M.S. degree in physics from Tufts College in 1949.

CONFIDENTIAL

He engaged in advanced doctorate study in physics at Brown University in 1950. From 1951 to 1955 he was employed by Goodyear Aircraft Company as a senior development engineer working on the physical analysis of electronic systems. He also has been engaged in the investigation of radar ground techniques. He recently joined Sylvania as a Senior Engineer in the Electronics Department.

CARL H. GUNDEL - Engineer

Mr. Gundel received his B.S. degree in physics from the Case Institute of Technology in 1955. Upon graduation he joined Sylvania as a Radar Engineer in the Electronic Section of the Missile Systems Laboratory.

ROBERT J. UHL - Senior Engineer

Mr. Uhl received his B.S. degree in mechanical engineering from the Massachusetts Institute of Technology in 1950. From 1950 to 1951 he was employed by the Watson Elevator Company, Research Division, designing mechanical components. He designed and tested remote control underwater optical equipment at the Massachusetts Institute of Technology's Visibility Laboratory from 1951 to 1952. For the next 3 years, he acted as mechanical consultant on acoustical devices in the Acoustics Laboratory of the Institute. From August, 1953, to August, 1955, he worked at the Air Force Armament Center, Eglin AFB, designing electro-mechanical instrumentation of aircraft and airborne equipment systems. In September, 1955, he joined Sylvania's Missile Systems Laboratory as a Senior Engineer in the Ground Equipment Section. His work consists of the analysis, services, checking, transporting and launching of missiles.

MARY A. FITZPATRICK - Engineer

Miss Fitzpatrick received her B.A. degree in mathematics from Manhattanville College of the Sacred Heart in 1947 and an M.A. degree in mathematics in 1952 from the Boston College Graduate School of Arts and Sciences. From 1949 to 1951 she was employed at Newton College of the Sacred Heart as an instructor of mathematics and physics. From September, 1950 to June, 1951, part-time, she also taught mathematics and physics at the Academy of the Sacred Heart. During the next two years, she worked at Jackson & Moreland, Engineers, Inc. as a mathematician. Another two years were spent at Chance Vought Aircraft, Inc. where she worked on airframe analysis and structure designing. For a short period in 1955 she was associated with Pratt & Whitney Aircraft as a structures design engineer working on such problems as jet engine analysis and vibration problems. Currently employed as an engineer in the Missiles Department of the Missile Systems Laboratory, her work consists of structural design analysis.

CONFIDENTIAL

JOSEPH M. VAN HORN - Engineer

Mr. Van Horn attended the University of Pennsylvania and Boston University studying mathematics and Massachusetts Institute of Technology studying chemical engineering. From 1949 to 1950 he worked at the Scott Paper Company's General Research Department. From 1951 to 1953 he was associated with the U.S. Army Ordnance Corps at Frankford Arsenal in the Pitman-Dunn Laboratory where his work consisted of research for ordnance use. For the next two years he worked under the U.S. Army for the Research and Development Command. He recently joined Sylvania as an engineer in the Mathematical Analysis Section of the Missile Systems Laboratory working on computer programming.

RICHARD E. RAPHAEL - Engineer

Mr. Raphael received his B.A. degree from Dartmouth College in 1954 where he majored in Government. He attended the Amos. Tuck School of Business Administration where he received his M.B.A. degree in Business Administration in 1955. For a short period he was employed by Raphael & Raphael, Public Accountants, as an accountant. He joined Sylvania in October, 1955, as an engineer in the Operations Research Section of the Missile Systems Laboratory where his work consists of business procedures and economic consulting.

HAROLD GLAZER - Senior Engineer

Mr. Glazer received his A.B. and M.A. degrees in mathematics from Boston University in 1949 and 1950, respectively. He is currently working on his Ph.D. in mathematical statistics at Boston University part-time. During September, 1949, to June, 1950, he assisted students at the University with mathematical and statistical problems. At Quartermaster Board, Fort Lee, Virginia, he worked as a research assistant from 1951 to 1953. For the next two years at the Harvard Observatory he was employed as an applied mathematician and is, at present, a part-time consultant for them. He is currently a Senior Engineer in Sylvania's Missile Systems laboratory working on problems of the program, "Adjust Computation" of the PLATO System, and also gives statistical assistance to the Operations Research and Physical Analysis Sections.

MURRAY FALKOWITZ - Senior Engineer

Mr. Falkowitz received his B.S. degree in electrical engineering from Syracuse University in 1952 and his M.S. degree from the University of Pennsylvania in 1955. From June, 1952, to September, 1953, he worked on the research of color TV systems for the Philco Corporation. 1953 to 1955 found him at the Radio Condenser Company working on the research and development of UHF and VHF TV tuners. He was responsible also for spurious

CONFIDENTIAL

oscillator radiation measurements. He joined Sylvania in August, 1955, and has since been working as a Senior Engineer in the Electronics Department of the Missile Systems Laboratory.

JOHN F. CALLAHAN - Engineer

Mr. Callahan received his B.S. degree in electrical engineering from Villanova in 1951. From graduation until his employment at Sylvania, he has worked for the Westinghouse Electric Corporation where he worked on electronic design engineering of nuclear instrumentation and control equipment. Currently, he is employed as an engineer in the Electronics Section of the Missile Systems Laboratory.

JAMES R. SIMS - Senior Engineer

Mr. Sims received his B.S. degree in electrical engineering from the University of Rhode Island in 1950. From graduation to 1954, his work consisted of design and development in the Fire Control Radar Section of Westinghouse Electric Corporation. For the next year he was employed by Lincoln Laboratories, Massachusetts Institute of Technology, as a staff member. He joined Sylvania in August, 1955, as a Senior Engineer in the Electronics Department of the Missile Systems Laboratory. His work consists of long-range radar development.

JOSEPH W. PAGE - Senior Engineer

Mr. Page received his B.A. degree from Harvard University in 1950 in engineering science and applied physics. Prior to his employment here, he worked for the Air Force Cambridge Research Center as an Electronic Scientist. Special projects there consisted of radar development, propagation studies and aircraft and control systems development. He joined Sylvania's Radar Section as a Senior Engineer in the Missile Systems Laboratory in October, 1955.

CONFIDENTIAL

APPENDIX III

CONFERENCES

VISITS BY PERSONNEL OF THE MISSILE SYSTEMS LABORATORY

TO: Bell Telephone Laboratories, Whippany, New Jersey
DATE: August 12, 1955
VISITED: C.A. Warren and J.R. Logie, Jr.
BY: E.W. Schlieben and E. Sieminski
SUMMARY: The current status of the Nike B communications was determined. Particular inquiry was made into the reasons for selecting the techniques used. Results of test runs were also discussed and a concept of the "hardware" problem was acquired

TO: Navy Department, Washington, D.C.
DATE: August 29 to August 31, 1955
VISITED: Pentagon Building at Arlington, Va., and at Constitution Ave., Washington, D.C.
BY: E.W. Schlieben
SUMMARY: (1) Discussed with top management the use of Dynamic Representation of Operations (DYRO) in operations studies of complex weapons systems and other systems.
(2) Explored the possibilities for hardware development.

TO: U.S. Air Force, Cambridge Research Center, Bedford, Massachusetts
DATE: July 26, 1955
VISITED: Seigfried Reiger
BY: E. Sieminski and D.J. Crowley, Jr.
SUMMARY: Conferred on data transmission techniques with a view to their applicability in the PLATO System; and inquired into several (classified) data processing systems under development.

TO: Headquarters of the Continental Army Command, Fort Monroe, Virginia
DATE: August 26, 1955
VISITED: Lt. Col. Difusco, and others
BY: F. Proschan and A. Wouk
SUMMARY: Captain Fuller, Office Chief of Ordnance arranged this meeting of Sylvania and Cornell representatives with the Combat Development Division of CONARC to discuss operational aspects of the PLATO missile system.

CONFIDENTIAL

185

CONFIDENTIAL

TO: Redstone Arsenal
DATE: September 8-9, 1955
VISITED: Redstone Guided Missile Development Division
BY: C. Jacobs and D. Price
SUMMARY: The purpose of the visit was to obtain information on the methods employed by Redstone in tracking their flight test vehicles; and to compare the free flight aerodynamic data of the Redstone missile with that of wind tunnel and theory.

VISITORS TO MISSILE SYSTEMS LABORATORY

REPRESENTED: U.S.A.F., Brussels
DATE: 18 July 1955
VISITOR: Major S. Schwiller
SUMMARY: Discussed some of the recent developments and research results obtained from the Air Research and Development Center, Brussels Contracting Office. None of these developments were immediately applicable to PLATO Project.

REPRESENTED: Penn. State University
DATE: 18 August 1955
VISITOR: P. Ebaugh and H.M. Hipsch
SUMMARY: A briefing on PLATO Project was made at the request of the Office of Chief of Ordnance.

REPRESENTED: AFRCRC, Bedford, Mass.
DATE: 28 July 1955
VISITOR: N. Stone
SUMMARY: Exchanged information on meteoric echoes and tropospheric angle-of-arrival variations.

REPRESENTED: RCA, Newark, N.J.
DATE: 23 September 1955
VISITOR: M. Klein
SUMMARY: Discussed application of RCA high power tubes.

REPRESENTED: AFRCRC, Bedford, Mass.
DATE: 28 September 1955
VISITOR: H. Whitney
SUMMARY: Discussed design of crystal controlled transmitters.

CONFIDENTIAL

APPENDIX IV
LIST OF PLATO INTERIM TECHNICAL P PORTS

The following internal working papers are available on request. Although conclusions reached in these documents are of a tentative nature and may be changed as a result of further study, it is felt that the material may be of sufficient interest to warrant dissemination. As this material is finalized it will be included in the quarterly report or will be published in technical reports.

- CONFID. - PLA 210/32 - MID-COURSE TRAJECTORY STUDY
H. Jacobs, Jr. - 24 August 1955
- CONFID. - PLA 210/34 - VULNERABILITY OF THE PLATO SYSTEM TO ENEMY ACTION
C. J. Brown - 31 August 1955
- CONFID. - PLA 210/35 - PLATO INTERCEPTOR READINESS TIME
M. Padin - 31 August 1955
- CONFID. - PLA 210/37 - INTERCEPTOR TRAJECTORY FLIGHT TIME INVESTIGATION
H. Jacobs, Jr. - 13 September 1955
- CONFID. - PLA 232/2 - REQUIRED RELIABILITY OF MAJOR ELEMENTS OF THE
PLATO SYSTEM
C. Brown - 12 August 1955
- CONFID. - PLA 251/18 - DERIVATION OF THE MATHEMATICAL FORMULAS WHICH
GOVERN THE RELATIONSHIP OF PREDICTION ERROR AT
LAUNCH AND INTERCEPTOR EXCESS ALTITUDE CAPABILITY
A. Wouk - 18 August 1955
- CONFID. - PLA 251/19 - ANALYTIC METHOD FOR PLATO MIDCOURSE PROBLEM AND
THE EFFECT OF PREDICTION ERRORS
G. Dewey - 9 September 1955
- CONFID. - PLA 251/20 - ERRORS OF PREDICTION OF TARGET POSITION DUE TO
NEGLECT OF AERODYNAMIC EFFECTS
E. Tandy - 12 September 1955
- CONFID. - PLA 251/21 - EXTENSION OF ANALYTIC METHOD TO ALONG-COURSE
ERROR DISTRIBUTION
G. Dewey - 16 September 1955
- CONFID. - PLA 252/1 - PROBABILITY OF DATA TRANSMISSION ERROR UNDER
STANDARD NOISE CONDITION
H. Greenberg - 7 July 1955

CONFIDENTIAL

- CONFID. - PLA 263/1 - SEQUENTIAL VS. SIMULTANEOUS INTERCEPTION
W. Low - 18 August 1955
- CONFID. - PLA 270/6 - MINIMUM SEPARATION BETWEEN INTERCEPTOR WITH
NUCLEAR WARHEADS, PER 60,000 FEET
G. Dewey - 15 July 1955
- SECRET - PLA 270/7 - LETHAL RADIUS OF PLATO WARHEAD VS. YIELD
G. Dewey - 3 August 1955
- CONFID. - PLA 270/8 - MULTIPLE-SHAPED CHARGE WARHEAD
B. Weinstein - 3 August 1955
- CONFID. - PLA 310B/1 - HEIGHT FINDER ACCURACY STUDY
L. Stevenson - 11 July 1955
- CONFID. - PLA 310/71 - MEASUREMENT ERRORS IN THE TRIANGULATION SYSTEM
C. Jacobs - 1 July 1955
- CONFID. - PLA 310/72 - ACQUISITION RADAR ANTENNA CONFIGURATION
S. Falconer - 7 July 1955
- CONFID. - PLA 310/73 - ACQUISITION RADAR ACCURACY
S. Falconer - 14 July 1955
- CONFID. - PLA 310/74 - PENCIL BEAM TRACKER PROGRAM
S. Falconer - 11 August 1955
- CONFID. - PLA 310/75 - ACQUISITION RADAR ANTENNA-OVER PRESSURE LIMITS
S. Falconer - 25 August 1955
- CONFID. - PLA 310/76 - PREDICTION ACCURACY AS A FUNCTION OF THE RANGES
AT BEGINNING OF TRACKING AND AT TIME OF LAUNCH
H. Jacobs - 1 September 1955
- CONFID. - PLA 310/77 - PREDICTION ACCURACY AS A FUNCTION OF THE RANGES
AT BEGINNING OF TRACKING AND AT TIME OF LAUNCH
S. Welles - 1 September 1955
- CONFID. - PLA 310/78 - M TRIANGULATION RADAR ACCURACY STUDY
C. Jacobs - 29 September 1955
- UNCLAS. - PLA 320B/8 - THE "ADJUST" COMPUTER PROBLEM
M. Ritterman - 5 July 1955
- CONFID. - PLA 320B/9 - SOLUTION FOR TIME-TO-GO TO INTERCEPT ALTITUDE
M. Ritterman - 18 July 1955
- CONFID. - PLA 320B/10 - RE-ENTRY HEATING OF ROD-TYPE RADAR DECOYS
M. Ritterman - 10 August 1955

CONFIDENTIAL

CONFID. - PLA 320B/11 - "BLENDED" ACCURACY
M. Ritterman - 12 August 1955

UNCLAS. - PLA 310B/12 - MATHEMATICAL ANALYSIS OF VARIOUS TRIANGULATION
SYSTEMS
M. Ritterman - 29 August 1955

SECRET - PLA 310B/13 - NUCLEAR REACTORS FOR PROPULSION OF THE PLATO
MISSILE
M. Ritterman - 2 September 1955

CONFID. - PLA 310B/14 - MAXIMUM INTERCEPT ALTITUDE
M. Ritterman 7 September 1955

UNCLAS. - PLA 310B/15 - TRIANGULATION RADAR ANALYSIS (CONT'D)
M. Ritterman - 12 September 1955

CONFID. - PLA 320/58 - A STUDY OF AN ACCELERATION COMMAND
R. Lechner - 11 July 1955

UNCLAS. - PLA 320/59 - LINEAR SMOOTHING PART I
N. Wolfsohn - 27 July 1955

CONFID. - PLA 320/60 - THE PREDICTION COMPUTER
L. Sokoloff and N. Wolfsohn - 29 July 1955

CONFID. - PLA 320/61 - TRAFFIC CONTROL IN THE PREDICTION COMPUTER
N. Wolfsohn - 22 July 1955

CONFID. - PLA 413/1 - TRAJECTORY TIME HISTORY VARIATION OF PLATO
MISSILE PITCH RATE AND NORMAL ACCELERATION
TRANSFER FUNCTION PARAMETERS
R. Vachss - 1 July 1955

CONFID. - PLA 413/2 - PLATO AIRFRAME TRANSFER FUNCTION
R. Vachss - 20 July 1955

CONFID. - PLA 414/1 - INTEGRAL TYPE CONTROL SYSTEM FOR PITCH CONTROL
H. Wexler - 20 July 1955

CONFID. - PLA 414/2 - DYNAMIC ANALYSIS OF HYDRAULIC ACTUATOR AND ELEVON
SYSTEM
H. Wexler - 8 September 1955

CONFIDENTIAL

CONFIDENTIAL

APPENDIX V
LIST OF SYMBOLS

- $B = \left(1/2\right) \rho_o \frac{S}{W} C_L$
- $B_o = B(W = W_o)$
- $B_e = B(W = W_e)$
- $b = \text{Wing span}$
- $C_D = \text{Drag coefficient } C_D = C_{D_o} + C_{D_i}$
- $C_{D_i} = \text{Induced drag coefficient (due to lift)}$
- $C_{D_o} = \text{Zero lift drag coefficient}$
- $D = \text{Drag force}$
- $G = \frac{B}{a} e^{-ah_i} - \cos \gamma_i$
- $g = \text{Gravitational acceleration}$
- $h = \text{Altitude}$
- $K_o = \text{Coefficient in expression for } C_{D_o}$
- $K_i = \left(1/2\right) \rho K_o S$
- $L = \text{Lift force}$
- $m = \text{Mass of the missile} \quad m = m_o - \dot{m}t$
- $m_o = \text{Take-off mass}$
- $\dot{m} = \text{Fuel consumption rate}$
- $m_e = \text{Empty mass}$
- $n = \text{Number of "g" 's}$
- $r = \text{Radius of curvature}$
- $s = \text{Distance along the trajectory}$
- $S = \text{Reference area of the missile}$
- $t = \text{Time}$

CONFIDENTIAL

CONFIDENTIAL

T = Thrust

V = Velocity

W = Weight

W_s = Weight of structure (airframe)

W_o = Take off weight

W_e = Weight after burnout

\dot{W} = Fuel consumption rate $\dot{W} = \dot{m}g$

Z = Missile displacement normal to initial trajectory

$\alpha = (22,000 \text{ ft})^{-1}$

γ = Trajectory angle

$\Delta\gamma$ = Angular change in heading

ρ = Air density

ρ_o = Sea level density $\rho_o g = 0.0765 \text{ #/ft}^3$

τ_r = Wing root thickness

ξ = Wing loading $= W/S$

Subscripts

T = Target

I = Interceptor

i = Index referring to numbers along the trajectory

CONFIDENTIAL

APPENDIX VI
INTERCEPTOR TURNS

I. TURN GEOMETRY

Assume that the "g"'s pulled in the turn are considerably greater than one. Then

$$n g = \frac{v^2}{r} = \frac{L}{m} = \frac{1/2 \rho C_L S v^2}{m}$$

or

$$\frac{1}{r} = \frac{1}{2} \rho C_L \frac{S}{m}$$

Assume that

$$\rho = \rho_0 e^{-\alpha h}$$

where

$$\rho_0 g = 0.0765 \text{ \#/cu. ft. and } \alpha = (22,000 \text{ ft})^{-1}$$

$$\frac{1}{r} = \frac{1}{2} \rho_0 g C_L \frac{S}{W} \cdot e^{-\alpha h}$$

and if

$$B = \frac{1}{2} \rho_0 g C_L \frac{S}{W}$$

$$\frac{1}{r} = B e^{-\alpha h} \tag{1}$$

if the turn is flown at constant lift coefficient, C_L , and it is assumed that W is constant.

The radius of curvature, r , is also described by

$$\frac{1}{r} = \frac{\frac{d^2x}{dh^2}}{\left[1 + \left(\frac{dx}{dh} \right)^2 \right]^{3/2}}$$

also

$$\frac{ds}{dh} = \sqrt{1 + \left(\frac{dx}{dh}\right)^2}$$

$$\frac{dx}{dh} = \sqrt{\left(\frac{ds}{dh}\right)^2 - 1}$$

$$\frac{d^2x}{dh^2} = \frac{\frac{ds}{dh} \cdot \frac{d^2s}{dh^2}}{\sqrt{\left(\frac{ds}{dh}\right)^2 - 1}}$$

Therefore

$$\frac{1}{r} = \frac{\frac{d^2s}{dh^2}}{\sqrt{\left(\frac{ds}{dh}\right)^2 \left(\frac{ds}{dh}\right)^2 - 1}}$$

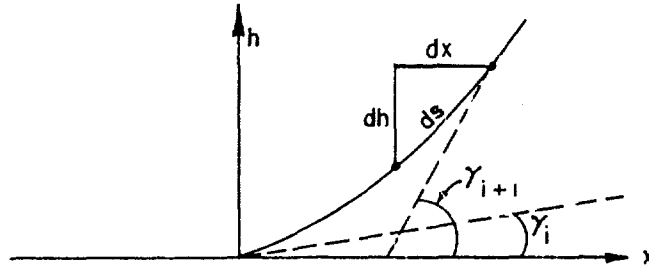


FIGURE VI-1

$$\frac{ds}{dh} = \frac{1}{\sin \gamma}$$

$$\frac{d^2s}{dh^2} = \frac{-\cos \gamma}{\sin^2 \gamma} \frac{d\gamma}{dh}$$

CONFIDENTIAL

The radius of curvature must be taken as negative because of the way γ was defined

$$\frac{1}{r} = \frac{-\frac{\cos \gamma}{\sin^2 \gamma} \frac{d\gamma}{dh}}{\frac{1}{\sin^2 \gamma} \sqrt{\frac{1}{\sin^2 \gamma} - 1}} = -\sin \gamma \frac{d\gamma}{dh}$$

$$\int_{\gamma_i}^{\gamma_{i+1}} \sin \gamma \, d\gamma = B \int_{h_i}^{h_{i+1}} e^{-ah} \, dh$$

$$\cos \gamma_i - \cos \gamma_{i+1} = \frac{B}{a} \left(e^{-ah_i} - e^{-ah_{i+1}} \right) \quad (2)$$

where

$$\gamma_i < \gamma_{i+1}$$

Care must be taken in defining γ because the integral on the right hand side is positive.

Let us now evaluate x

$$\cos \gamma = \frac{dx}{ds} ; dx = \cos \gamma \, ds = \cos \gamma \frac{ds}{dh} \, dh$$

Since

$$\frac{ds}{dh} = \frac{1}{\sin \gamma} ,$$

$$dx = \frac{\cos \gamma}{\sin \gamma} \, dh$$

$$\cos \gamma = \frac{B}{\gamma} \left(e^{-ah} - e^{-ah_i} \right) + \cos \gamma_i$$

$$\begin{aligned} -\sin \gamma \, d\gamma &= -B e^{-ah} \, dh \\ &= -a \left(\cos \gamma - \cos \gamma_i + \frac{B}{a} e^{-ah_i} \right) dh \end{aligned}$$

$$dh = \frac{\sin \gamma \, d\gamma}{a \left(\frac{B}{a} e^{-ah_i} - \cos \gamma_i + \cos \gamma \right)}$$

CONFIDENTIAL

Therefore

$$dx = \frac{1}{a} \frac{\cos \gamma \, d\gamma}{\frac{B}{a} e^{-ah_i} - \cos \gamma_i + \cos \gamma}$$

Integrate with the help of Peirce's "Table of Integrals" (integrals 304 and 300),

$$x = \frac{1}{a} \gamma_{i+1} - \gamma_i - \frac{2G}{a \sqrt{G^2 - 1}} \tan^{-1} \frac{\sqrt{G^2 - 1} \tan \frac{1}{2} \gamma}{G + 1} \Big|_{\gamma_i}^{\gamma_{i+1}} \quad (3)$$

where

$$G = \frac{B}{a} e^{-ah_i} - \cos \gamma_i \quad (4)$$

Let the path length, s, be evaluated.

$$\frac{ds}{dh} = \frac{1}{\sin \gamma}$$

$$ds = \frac{dh}{\sqrt{1 - \cos^2 \gamma}}$$

With the use of equation 2, dh can be written as a function of dy as before and the equation for ds can be integrated to give (using integral 300 in Peirce's "Table of Integrals"):

$$s_{i+1} = \frac{2}{a \sqrt{G^2 - 1}} \left[\tan^{-1} \frac{\sqrt{G^2 - 1} \tan \frac{1}{2} \gamma}{G + 1} \right]_{\gamma_i}^{\gamma_{i+1}} \quad (5)$$

Where G is defined in equation 4.

II. TURN DYNAMICS

There are three turns of interest: The initial turn, the turn onto the inverse trajectory, and the turn in the terminal phase. The latter two are unpowered in the case of maximum coverage trajectories; hence the

CONFIDENTIAL

thrust, T, is zero, and the mass is constant. In the initial turn there is thrust and a mass decrease. The acceleration is

$$\frac{d}{dt} (mV) = V \frac{dm}{dt} + m \frac{dV}{dt}$$

The differential equation obtained using this expression has not been solved. To circumvent this difficulty, the mass has been taken as a constant. This underestimates the final velocity for the following reason: A body with a decreasing mass will achieve a higher velocity than a body with a constant mass if the weights are the same at takeoff and they are accelerated by the same force. Thus one underestimates the final velocity in the initial turn by taking the mass of the missile to be constant and equal to the initial mass.

$$- m \dot{V} = (\text{Drag} - \text{Thrust}) + \text{gravity}$$

As the drag due to lift is large, $C_{D0} \ll C_{Di}$

$$- m \dot{V} = \frac{1}{2} \rho V^2 C_{Di} S - T + mg \sin \gamma$$

If

$$V = r \gamma$$

and

$$r = \frac{2m}{\rho C_L S}$$

then

$$\dot{V} = \frac{2m}{\rho C_L S} \dot{\gamma}$$

Hence

$$- m \dot{V} = m \frac{D}{L} V \dot{\gamma} - T + m g \sin \gamma$$

$$- \dot{V} = \frac{D}{L} V \dot{\gamma} - \frac{T}{m} + g \sin \gamma$$

$$- V \dot{\gamma} = \frac{D}{L} V^2 \dot{\gamma} - \frac{TV}{m} + g \cdot V \sin \gamma = - \frac{1}{2} \frac{d}{dt} (V^2)$$

$$h = V \sin \gamma \quad \text{Multiply through by } \frac{dt}{d\gamma}$$

CONFIDENTIAL

$$-\frac{1}{2} \frac{d}{d\gamma} (v^2) = \frac{D}{L} v^2 - \frac{TV}{m} \frac{dt}{d\gamma} + g \frac{dh}{d\gamma}$$

$$\frac{d}{d\gamma} (v^2) + \frac{2D}{L} v^2 + 2g \frac{dh}{d\gamma} - 2 \frac{TV}{m} \frac{r}{v} = 0$$

$$\frac{d}{d\gamma} (v^2) + \frac{2D}{L} v^2 = \frac{4T}{\rho C_L S} - 2g \frac{dh}{d\gamma}$$

or

Let $v^2 = y(x)$ and $\gamma = x$

If $y' + P y = Q$ where P and Q are $f(x)$,

Then

$$y e^{\int P dx} = \int_{\gamma_1}^{\gamma_2} Q e^{\int P dx} dx$$

Here

$$P = \frac{2D}{L}; \quad Q = \frac{4T}{\rho C_L S} - 2g \frac{dh}{d\gamma}$$

Therefore

$$v_{i+1}^2 = e^{\frac{-2D}{L} (\gamma_{i+1} - \gamma_i)} \left[v_i^2 + I_1 - I_2 \right] \quad (6)$$

where

$$I_1 = \frac{4 T B}{\alpha \rho_o C_L S} \int_{\gamma_i}^{\gamma_{i+1}} \frac{e^{2D/L(\gamma - \gamma_i)} d\gamma}{\frac{B}{\alpha} e^{-a h_i} - \cos \gamma_i + \cos \gamma}$$

$$I_2 = \frac{2 g}{\alpha} \int_{\gamma_i}^{\gamma_{i+1}} \frac{e^{2D/L(\gamma - \gamma_i)} \sin \gamma d\gamma}{\frac{B}{\alpha} e^{-a h_i} - \cos \gamma_i + \cos \gamma}$$

CONFIDENTIAL

APPENDIX VII

EVALUATION OF DISTANCE AND VELOCITY IN HORIZONTAL PORTIONS OF FLIGHT

It is desired to evaluate the distance and velocity in the horizontal portions of flight (1-3). Assume that the density is a constant and that gravity is zero. Assume also that the drag due to lift is low and therefore that the drag coefficient is given by

$$C_D = K_o v^{-1}$$

A. FOR POWERED FLIGHT

$$\begin{aligned} -\frac{d}{dt}(mV) &= \text{Drag} - \text{Thrust} \\ &= \frac{1}{2} \rho C_D S v^2 - T \end{aligned}$$

If

$$m = m_o - \dot{m}t$$

then

$$-(\dot{m}V + m\dot{V}) = \frac{1}{2} \rho K_o S V - T$$

Letting

$$K_1 = \frac{1}{2} \rho K_o S$$

$$m\dot{V} + (\dot{m} + K_1)V = T$$

$$\dot{V} + \frac{\dot{m} + K_1}{m_o - \dot{m}t} V = \frac{T}{m_o - \dot{m}t}$$

Now, if

$$y' + P_y = Q$$

Then

$$y e^{\int P dx} = \int Q e^{\int P dx} dx + \text{const.}$$

CONFIDENTIAL

CONFIDENTIAL

Here

$$P = \frac{\dot{m} + K_1}{m_o - \dot{m}t}, \quad V = y, \quad t = x, \quad Q = \frac{T}{m_o - \dot{m}t}$$

$$\int_0^t P dt = (\dot{m} + K_1) \int_0^t \frac{dt}{m_o - \dot{m}t}$$

$$= \ln \left(\frac{m_o}{m_o - \dot{m}t} \right)^{1+K_1/\dot{m}}$$

$$e^{\int P dt} = \left(\frac{m_o}{m_o - \dot{m}t} \right)^{1+K_1/\dot{m}}$$

Inserting the values for the exponential, and Q, the equation for V becomes

$$V_{i+1} = \frac{T}{\dot{m} + K_1} \left[1 - \left(\frac{m_o - \dot{m}t}{m_o} \right)^{1+K_1/\dot{m}} \right] + V_i \left(\frac{m_o - \dot{m}t}{m_o} \right)^{1+K_1/\dot{m}} \quad (1)$$

This equation can be integrated to give distance, s, as a function of time and, when combined with equation 1, s can be gotten as a function of velocity. These two equations follow.

$$s = \left[V_i - \frac{T}{\dot{m} + K_1} \right] \left[\frac{\left(1 - \frac{\dot{m}}{m_o} t \right)^{2+K_1/\dot{m}} - 1}{\left(2 + K_1/\dot{m} \right) \left(-\frac{\dot{m}}{m_o} \right)} \right] + \frac{T t}{\dot{m} + K_1} \quad (2)$$

$$= \frac{-m_o \left(V_{i+1} - \frac{T}{\dot{m} + K_1} \right)^{2 + \frac{K_1}{\dot{m}}} + \frac{K_1}{\dot{m}}}{2\dot{m} + K_1 \left(V_o - \frac{T}{\dot{m} + K_1} \right)^{1 + \frac{K_1}{\dot{m}}} + \frac{K_1}{\dot{m}}} + \frac{m_o}{\dot{m}} \frac{T}{\dot{m} + K_1} \left[1 - \frac{\left(V_{i+1} - \frac{T}{\dot{m} + K_1} \right)^{\frac{\dot{m}}{\dot{m} + K_1}}}{\left(V_i - \frac{T}{\dot{m} + K_1} \right)^{\frac{\dot{m}}{\dot{m} + K_1}}} \right]$$

(3)

CONFIDENTIAL

B. UNPOWERED FLIGHT

From equation 1, with $T = 0 = \dot{m}$, it is possible to get the equation for unpowered flight. Consider the term

$$\left(\frac{m_o - \dot{m}t}{m_o}\right)^{1+\frac{K_1}{\dot{m}}} = \left(1 - \frac{t}{m_o} \dot{m}\right)^{1+K_1/\dot{m}}$$

$$\lim_{\substack{\dot{m} \rightarrow 0 \\ m_o \rightarrow m}} \left(1 - \frac{t}{m_o} \dot{m}\right)^{1+K_1/\dot{m}} = \lim_{\dot{m} \rightarrow 0} \left(1 - \frac{t}{m} \dot{m}\right) \left(1 - \frac{t}{m} \dot{m}\right)^{K_1/\dot{m}}$$

Let $\frac{t}{m} \dot{m} = x$; then as $m \rightarrow 0$, $x \rightarrow 0$

$$\lim_{x \rightarrow 0} (1-x)(1-x)^{\frac{K_1 t}{m} \cdot \frac{1}{x}} = \lim_{x \rightarrow 0} (1-x) \left[\lim_{x \rightarrow 0} (1-x)^{1/x} \right]^{\frac{K_1 t}{m}}$$

But

$$e^{-1} = \lim_{x \rightarrow 0} (1-x)^{1/x}$$

Therefore

$$\lim_{m \rightarrow 0} \left(1 - \frac{t}{m_o} \dot{m}\right)^{1+K_1/\dot{m}} = e^{-\frac{K_1 t}{m}}$$

Hence the equation for unpowered flight is

$$V_{i+1} = V_i e^{-\frac{K_1}{m} (t_{i+1} - t_i)} \quad (4)$$

Again, s can be gotten as a function of velocity and time

$$s_{i \rightarrow i+1} = \frac{m V_i}{K_1} \left(1 - e^{-\frac{K_1}{m} (t_{i+1} - t_i)}\right) \quad (5)$$

$$= \frac{m}{K_1} (V_i - V_{i+1}) \quad (6)$$

CONFIDENTIAL

APPENDIX VIII

DERIVATION OF VELOCITY RELATIONSHIPS DURING INCLINED STRAIGHT FLIGHT

It is desired to determine the velocity as a function of time and distance during the terminal phase of flight. It is desired also to obtain an estimate of the velocity change in this section of flight in order to evaluate the accuracy of the assumption of constant velocity in the determination of the intercept criterion (equation 2 below).

To do this, assume rectilinear flight at some angle, γ , with the horizon. Assume that the drag is given by

$$D = \frac{1}{2} \rho S C_{D_0} V^2$$

where ρ is the density, S the lift area and C_{D_0} is the zero lift drag coefficient and is taken as

$$C_{D_0} = K_0/V$$

Then

$$-m \dot{V} = D + m g \sin \gamma$$

$$- \dot{V} = \frac{\rho S K_0}{2m} V + g \sin \gamma$$

Now

$$\rho = \rho_0 e^{-ah} = \rho_0 e^{-ah_0} e^{-as \sin \gamma}$$

Where ρ_0 is the density at sea level; h is the altitude and s is the distance along the path

$$- \dot{V} = \frac{\rho_0 e^{-ah_0} S K_D}{2m} e^{-as \sin \gamma} V + g \sin \gamma$$

Let

$$G' = \frac{\rho_0 S K_D e^{-ah_0}}{2m} \quad \alpha' = a \sin \gamma \quad (1)$$

$$- \dot{V} = G' e^{-\alpha' s} V + g \sin \gamma$$

CONFIDENTIAL

CONFIDENTIAL

$$- \frac{dV}{dt} = G' e^{-\alpha' s} \frac{ds}{dt} + g \sin \gamma$$

$$- \int_{V_0}^V dV = G' \int_0^s e^{-\alpha' s} ds + g \sin \gamma \int_0^t dt$$

$$- (V - V_0) = \frac{-G'}{\alpha'} (e^{-\alpha' s} - 1) + g \sin \gamma \cdot t$$

$$V = V_0 + \frac{G'}{\alpha'} (e^{-\alpha' s} - 1) - g \sin \gamma t$$

$$= \frac{G'}{\alpha'} e^{-\alpha' s} - g \sin \gamma t + V_0 - \frac{G'}{\alpha'}$$

Let

$$- g \sin \gamma = A \quad V_0 - \frac{G'}{\alpha'} = C \quad (2)$$

$$V = \frac{G'}{\alpha'} e^{-\alpha' s} + A t + C \quad (3)$$

Let

$$A t + C = x$$

Then

$$dt = \frac{1}{A} dx$$

$$\frac{ds}{dt} = A \frac{ds}{dx} = V \frac{G'}{\alpha'} e^{-\alpha' s} + x$$

$$\frac{ds}{dx} = \frac{G'}{A\alpha'} e^{-\alpha' s} + \frac{x}{A}$$

Let

$$u = e^{-\alpha' s} \quad du = -\alpha' e^{-\alpha' s} ds \quad ds = -\frac{1}{\alpha'} \frac{du}{u}$$

Then

$$\frac{ds}{dx} = -\frac{1}{\alpha' u} \frac{du}{dx}$$

CONFIDENTIAL

$$\frac{-1}{a'u} \frac{du}{dx} = \frac{G'}{\Lambda a'} u + \frac{x}{A}$$

$$\frac{du}{dx} = -\frac{G'}{A} u^2 - \frac{uxa'}{A}$$

Let

$$u = y e^{-(a'/2A)x^2} \quad du = e^{-(a'/2A)x^2} \left(dy + \frac{-ya' x dx}{A} \right) = \frac{u}{y} \left(dy - ya' \frac{xdx}{A} \right)$$

$$du = -\frac{G'}{A} u^2 dx - \frac{u a'}{A} xy dx$$

$$\frac{u}{y} \left(dy - \frac{a' xy dx}{A} \right) = -\frac{G'}{A} u^2 dx - \frac{u a' x dx}{A}$$

Cancelling u's and the common second terms

$$\frac{dy}{y} = -\frac{G'}{A} u dx = -\frac{G'}{A} y e^{-(a'/2A)x^2} dx$$

$$\therefore \frac{dy}{y} = -\frac{G'}{A} e^{-(a'/2A)x^2} y^2 dx$$

$$\therefore \frac{-dy}{y^2} = \frac{G'}{A} e^{-(a'/2A)x^2} dx$$

Initial Condit. at $t = 0$, $s = 0$, $x_0 = C$, $u_0 = 1$ $x_0 = e^{(a'/2A)C^2}$

$$\therefore \int_{y_0}^y -\frac{dy}{y^2} = \frac{G'}{A} \int_C^{At+C} e^{-(a'/2A)x^2} dx$$

$$-\frac{1}{y} - e^{-(a'/2A)C^2} = \frac{G'}{A} \int_C^{At+C} e^{-(a'/2A)x^2} dx$$

$$y = e^{(a'/2A)x^2} = e^{-a's} e^{(a'/2A)x^2}$$

$$e^{a's} = e^{(a'/2A)(At+C)^2} \left[e^{-(a'/2A)C^2} + \frac{G'}{A} \int_C^{At+C} e^{-(a'/2A)x^2} dx \right]$$

CONFIDENTIAL

That this is the correct solution can be verified by insertion in the differential equations. Since A is actually negative, let

$$\frac{\alpha'}{2|A|} x^2 = u^2$$

Then the integral becomes

$$\frac{G'}{A} \int_C^{At+C} e^{(\alpha'/2|A|)x^2} dx = G' \frac{\sqrt{2}}{\sqrt{\alpha'|A|}} \int_{\sqrt{\alpha'/2|A|(At+C)}}^{\sqrt{\alpha'/2|A|} C} e^{x^2} dx$$

$$e^{\alpha's} = e^{(\alpha'/2A)(At+C)^2} \left[e^{-(\alpha'/2A)C^2} + G' \frac{\sqrt{2}}{\sqrt{\alpha'|2A|}} \int_{\sqrt{\alpha'/|2A|(At+C)}}^{\sqrt{\alpha'/2|A|} C} e^{x^2} dx \right] \quad (4)$$

Using equations 1, 2 and 4, it is possible to specify s as a function of time, missile and trajectory parameters. From this, one can solve for the velocity decrement, (V-V₀).

To estimate the validity of the constant average velocity assumption, the above procedure was followed. The values used for the various parameters is given below.

$\rho_0 g = 0.0765 \text{ \#/ft}^3$	$k = 40$
$W/S = 20 \text{ \#/ft}^2$	$h_0 = 53,000 \text{ ft.}$
$g = 32.2 \text{ ft/sec}^2$	$\alpha = (22,000 \text{ ft})^{-1}$
$V_0 = 1330 \text{ ft/sec}$	$\gamma = 45^\circ$

Use of equations 1 and 2 yield the following

$$A = -22.8 \text{ ft/sec}^2 \quad \alpha' = (31,000 \text{ ft})^{-1}$$

$$C = 1120 \text{ ft/sec} \quad \alpha'/2A = -(1.41 \times 10^6 \text{ sec}^{-2})^{-1}$$

$$G' = 6.89 \times 10^{-3} \text{ sec}^{-1} \quad C + 10A = 888 \text{ ft/sec}$$

CONFIDENTIAL

With these values and the aid of Jahnke and Emde's "Table of Functions" (p.32) one obtains, as the s corresponding to ten seconds of flight, 12,000 feet. Solving equation 3 gives a velocity at the end of flight of 1030 ft/sec, a velocity decrease of 300 ft/sec. Neglecting drag would give a decrease of 225 ft/sec due to the interchange of kinetic and potential energy.

CONFIDENTIAL

207